



Characterisation of *Bordetella pertussis* virulence mechanisms using engineered human airway tissue models

Charakterisierung der Virulenzmechanismen von *Bordetella pertussis* mit humanen Gewebemodellen der Atemwege.

Dissertation for

Doctoral degree

at the Graduate School of Life Sciences

Julius-Maximilians-Universität Würzburg

Section: Infection and Immunity

Submitted by

David Komla Kessie

from

Accra, Ghana

Würzburg, January 2021



Characterisation of *Bordetella pertussis* virulence mechanisms using engineered human airway tissue model

Charakterisierung der Virulenzmechanismen von *Bordetella pertussis* mit humanen Gewebemodellen der Atemwege

zur Erlangung
des naturwissenschaftlichen Doktorgrades
der *Graduate School of Life Sciences* (GSLS),
Julius-Maximilians-Universität Würzburg
Sektion: Infektion und Immunität

vorgelegt von
David Komla Kessie
aus Accra, Ghana

Würzburg, Januar 2021

Submitted on:

Office stamp

Members of the Thesis Committee

Chairperson	Prof Dr. Markus Sauer,
Primary Supervisor	Prof. Dr. Roy Gross
Supervisor(Second)	Dr. Maria Steinke
Supervisor (Third)	Prof. Dr. Thomas Dandekar
Date of Public Defence	
Date of Receipt of Certificates	

Dedication

This work is dedicated to my Mom, **Peace Dakla** and to the memories of the late Simon S.K. Kessie and Augusta Dakla (geb. Kpokpo)

Summary

Pertussis is a highly contagious acute respiratory disease of humans which is mainly caused by the gram-negative obligate human pathogen *Bordetella pertussis*. Despite the availability and extensive use of vaccines, the disease persists and has shown periodic re-emergence resulting in an estimated 640,000 deaths worldwide in 2014. The pathogen expresses various virulence factors that enable it to modulate the host immune response, allowing it to colonise the ciliated airway mucosa. Many of these factors also directly interfere with host signal transduction systems, causing damage to the ciliated airway mucosa and increase mucous production. Of the many virulence factors of *B. pertussis*, only the tracheal cytotoxin (TCT) is able to recapitulate the pathophysiology of ciliated cell extrusion and blebbing in animal models and in human nasal biopsies. Furthermore, due to the lack of appropriate human models and donor materials, the role of bacterial virulence factors has been extrapolated from studies using animal models infected with either *B. pertussis* or with the closely related species *B. bronchiseptica* which naturally causes respiratory infections in these animals and produces many similar virulence factors. Thus, in the present work, *in vitro* airway mucosa models developed by co-culturing human airway epithelia cells and fibroblasts from the conduction zone of the respiratory tract on a decellularized porcine small intestine submucosa scaffold (SISser®) were used, since these models have a high correlation to native human conducting zone respiratory epithelia. The major aim was to use the engineered airway mucosa models to elucidate the contribution of *B. pertussis* TCT in the pathophysiology of the disease as well as the virulence mechanism of *B. pertussis* in general. TCT and lipopolysaccharide (LPS) either alone or in combination were observed to induce epithelial cell blebbing and necrosis in the *in vitro* airway mucosa model. Additionally, the toxins induced viscous hyper-mucous secretion and significantly disrupted barrier properties of the *in vitro* airway mucosa models. This work also sought to assess the invasion and intracellular survival of *B. pertussis* in the polarised epithelia, which has been critically discussed for many years in the literature. Infection of the models with *B. pertussis* showed that the bacteria can adhere to the models and invade the epithelial cells as early as 6 hours post inoculation. Invasion and intracellular survival assays indicated the bacteria could

invade and persist intracellularly in the epithelial cells for up to 3 days. Due to the novelty of the *in vitro* airway mucosa models, this work also intended to establish a method for isolating individual cells for scRNA-seq after infection with *B. pertussis*. Cold dissociation with *Bacillus licheniformis* subtilisin A was found to be capable of dissociating the cells without inducing a strong fragmentation, a problem which occurs when collagenase and trypsin/EDTA are used. In summary, the present work showed that TCT acts possibly in conjunction with LPS to disrupt the human airway mucosa much like previously shown in the hamster tracheal ring models and thus appears to play an important role during the natural *B. pertussis* infection. Furthermore, we established a method for infecting and isolating infected cells from the airway mucosa models in order to further investigate the effect of *B. pertussis* infection on the different cell populations in the airway by single cell analytics in the future.

Zusammenfassung

Pertussis ist eine hoch ansteckende akute Atemwegserkrankung des Menschen, die durch das gramnegative obligat humanpathogene Bakterium *Bordetella pertussis* verursacht wird. Obwohl seit langer Zeit effektive Impfstoffe verfügbar sind und weltweit eingesetzt werden, stellt die Krankheit nach wie vor ein großes Problem dar und tritt seit einiger Zeit auch in Ländern mit guten Impfraten wieder vermehrt auf. Allein in den letzten 10 Jahren wurden weltweit etwa 24 Millionen Neuinfektionen mit 640,000 Todesfällen pro Jahr gezählt. Die Bakterien exprimieren verschiedene Virulenzfaktoren, die es ihnen ermöglichen, die Immunantwort des Wirts zu modulieren, wodurch sie die Schleimhaut der oberen Atemwege besiedeln können. Viele dieser Faktoren stören auch direkt die Signaltransduktionssysteme der Zellen der oberen Atemwege, was zu einer Schädigung des Flimmerepithels der Atemwege und zu einer starken Erhöhung der Schleimproduktion führt. Von den vielen bekannten Virulenzfaktoren von *B. pertussis* kann soweit bekannt nur das Tracheale Cytotoxin (TCT) die typische Pathophysiologie des Flimmerepithels verursachen, die durch massive Gewebszerstörung gekennzeichnet ist und z.B. das Herauslösen von Epithelzellen aus der Epithelschicht oder die Ausbildung von bläschenförmigen Epithelzellen beinhaltet. Aufgrund des Mangels an geeigneten menschlichen Modellsystemen bzw. an Spendermaterialien wurden die Virulenzeigenschaften des Erregers entweder mit Hilfe von einfachen Zellkultursystemen oder in Tiermodellen untersucht, die keine natürlichen Wirte für *B. pertussis* darstellen. Alternativ hierzu wurden auch Daten, die mit dem eng verwandten tierpathogenen Bakterium *B. bronchiseptica*, das viele aus *B. pertussis* bekannte Virulenzfaktoren produziert, in entsprechenden Tiermodellen erhoben wurden, genutzt, um auf die Virulenzeigenschaften von *B. pertussis* zu schließen. Die vorliegende Arbeit verwendet *In-vitro*-Atemwegsschleimhautmodelle, die durch Co-Kultivierung von menschlichen Atemwegsepithelzellen und Fibroblasten auf einem dezellularisierten Schweine-Dünndarm-Submukosa-Gerüst (SISser®) entwickelt wurden. Die *in-vitro*-Atemwegsschleimhautmodelle weisen eine hohe Korrelation mit nativen menschlichen Epithelien der oberen Atemwege auf. Mithilfe dieser neuartigen Atemwegsschleimhautmodelle sollte der Beitrag von *B. pertussis* TCT zur Pathophysiologie der Krankheit und die Bedeutung von TCT

als relevanter Virulenzfaktor aufgeklärt werden. Es wurde beobachtet, dass TCT und das bakterielle Lipopolysaccharid (LPS) entweder alleine oder in Kombination die Bildung von Epithelzellbläschen und Nekrose in diesen *in-vitro*-Atemwegsschleimhautmodellen induzieren. Zusätzlich induzierten diese Toxine eine viskose Hyperschleimsekretion und störten die Barriereigenschaften der *in-vitro*-Atemwegsschleimhautmodelle signifikant. Zudem wurde in dieser Arbeit versucht, die Invasion und das intrazelluläre Überleben von *B. pertussis* in den polarisierten Epithelien zu bewerten, das in der einschlägigen Fachliteratur kritisch diskutiert wird. Die Infektion der Modelle mit *B. pertussis* zeigte, dass die Bakterien bereits 6 Stunden nach der Inokulation an den Modellen adhären und in diese eindringen können. Invasions- und intrazelluläre Überlebens-tests zeigten, dass die Bakterien bis zu 3 Tage intrazellulär in die Epithelzellen überleben können. Aufgrund der Neuheit der in dieser Arbeit entwickelten *in-vitro*-Atemwegsschleimhautmodelle sollte auch eine Methode zur Isolierung einzelner Zellen für scRNA-seq Analysen nach Infektion mit *B. pertussis* etabliert werden. Dabei wurde festgestellt, dass die Inkubation der Modelle mit Subtilisin A von *Bacillus licheniformis* in der Kälte eine sehr gute Methode darstellt, um die Zellen zu dissoziieren, ohne eine starke Fragmentierung zu induzieren, wie sie unter Verwendung von Kollagenase und Trypsin / EDTA auftritt. Zusammenfassend wird in der vorliegenden Arbeit gezeigt, dass TCT gemeinsam mit LPS eine extrem destruktive Wirkung auf die menschliche Atemwegsschleimhaut besitzt, die der früher gezeigten Wirkung in Tiermodellen stark ähnelt. TCT sollte deshalb tatsächlich als ein wichtiger Virulenzfaktor von *B. pertussis* eingeschätzt werden. Darüber hinaus wurden Methoden zur Infektion und Isolierung von infizierten Zellen aus den Atemwegsschleimhautmodellen entwickelt, um künftig die Auswirkung einer *B. pertussis* Infektion auf die verschiedenen Zellpopulationen in den Atemwegen durch Einzelzellanalytik noch besser erforschen zu können.

Table of Contents

Dedication	iii
Summary	v
Zusammenfassung	vii
Abbreviation	xiv
1. Introduction	1
1.1 Whooping cough disease	1
1.1.1 A brief history	1
1.1.2 The Disease	2
1.1.3 Epidemiology.....	4
1.2 Pathogenesis of <i>B. pertussis</i>	6
1.2.1 Major adhesins	7
1.2.2 Major Toxins.....	9
1.2.3 Some other virulence factors.....	13
1.2.4 Regulation of virulence genes	16
1.3 The human respiratory epithelium	19
1.3.1 The airway epithelium	21
1.4 Host-pathogen interaction during <i>B. pertussis</i> infection	22
1.4.1 Bacteria - host interactions	22
1.4.2 Host defence mechanisms	25
1.5 Experimental models for studying <i>B. pertussis</i>	27
1.6 Aims of the study	29
2 Results	31
2.1 Engineered airway mucosa models show characteristic <i>in vivo</i> airway mucosa features	31
2.2 Airway mucosa models develop tight barrier properties	33
2.3 Interaction of <i>B. pertussis</i> tracheal cytotoxin with human tracheobronchial airway mucosa models.	36
2.3.1 Tracheal cytotoxin disrupts the airway mucosa model.....	36
2.3.2 TCT and LPS synergistically impair mucociliary clearance in the hTBM	37

2.3.3	TCT action leads to loss of barrier function in hTBM	40
2.3.4	TCT elicits iNOS-dependent nitric oxide release from the hTBM.....	42
2.3.5	hTBMs express SLC46A2 transmembrane receptor.....	45
2.3.6	TCT induces inflammatory cytokine expression in hTBM	45
2.4	Single cell RNA-sequencing of <i>B. pertussis</i> infected cells.....	49
2.4.1	Interaction of <i>B. pertussis</i> with airway mucosa models.....	50
2.4.2	Persistence of <i>B. pertussis</i> in engineered airway mucosa models.	52
2.4.3	Detachment of cells from the airway mucosa models.....	54
3	Discussion.....	57
3.1	Establishment and optimization of 3D airway mucosa models.....	58
3.2	The role of TCT in the pathophysiology of <i>B. pertussis</i> infection	62
3.3	Interaction of <i>B. pertussis</i> with the airway mucosa models.....	71
3.3.1	Dissociation of cells for single cell RNA sequencing.....	71
3.3.2	<i>B. pertussis</i> invasion and intracellular survival in airway mucosa models.	74
3.4	Perspectives	77
4	Methods	79
4.1	Donor material and primary cells	79
4.2	Ethical considerations.....	79
4.3	General cell culture methods.....	79
4.3.1	Isolation of cells from biopsies	79
4.3.2	Expansion and passaging of cells.....	80
4.3.3	Thawing and freezing cells.....	81
4.4	Develop and characterization of 3D airway mucosa models.....	81
4.4.1	Decellularization of porcine small intestine serosa (SISser®).....	81
4.4.2	Construction of 3D airway models.....	82
4.4.3	Determination of ciliary beat frequency of the 3D airway models	83
4.4.4	Assessment of mucociliary clearance	84
4.4.5	Transepithelial electrical resistance	84
4.4.6	FITC-Dextran permeability assay	85

4.5	Histology	86
4.5.1	Fixation, paraffin embedding and microtome sectioning	86
4.5.2	Deparaffination and rehydration of the tissue sections	87
4.5.3	Haematoxylin-eosin staining	87
4.5.4	Electron microscopy for ultrastructural analysis	88
4.6	Immunohistology	88
4.6.1	Immunocytochemistry	88
4.6.2	Whole model immunocytochemistry.....	89
4.7	Tracheal cytotoxin experimental design	89
4.7.1	Nitric oxide quantification using Griess test.....	90
4.7.2	Cytometric bead array assay for inflammatory cytokine.....	90
4.8	Propagation of <i>Bordetella pertussis</i>	91
4.8.1	Bacteria culture	91
4.8.2	<i>B. pertussis</i> infectivity assay	92
4.8.3	Invasion assay.....	92
4.8.4	Intracellular survival assay	93
4.9	Molecular biology	93
4.9.1	RNA isolation, cDNA synthesis and Quantitative RT-PCR	93
4.10	Tissue dissociation for single cell RNA sequencing	94
4.11	Immunostaining for FACS analysis	94
5	Chapter 5: Materials	96
5.1	Biological material	96
5.2	Antibodies.....	97
5.3	Composition of Media and solutions	99
5.4	Chemicals, reagents and proteins.....	100
5.5	Technical equipment	105
5.6	Software	108
	References	110
	Appendices	142

Curriculum Vitae	147
List of publications and presentations	150
Affidavit.....	151
Eidesstattliche Erklärung.....	151
Acknowledgements	152

List of Figures

Figure 1-1 Appearance of <i>Bordetella pertussis</i> on Bordet-Gengou medium.	1
Figure 1-2 Stages, progression and presentation of typical pertussis	3
Figure 1-3 Structure of <i>B. pertussis</i> tracheal cytotoxin	11
Figure 1-4 The BvgAS master regulatory system.	18
Figure 1-5 Organisation of the conducting and respiratory airway epithelium.	20
Figure 1-6 Model for <i>Bordetella pertussis</i> interaction with the respiratory epithelium..	23
Figure 2-1 Airway mucosa models show pseudostratified ciliated epithelial layer.....	32
Figure 2-2 Airway mucosa models express characteristic <i>in vivo</i> airway markers.	33
Figure 2-3 Airway mucosa models develop tight junctions.	35
Figure 2-4 Engineered airway mucosa models express organised tight junction markers.	35
Figure 2-5 TCT and LPS cause disruption of the airway mucosa.....	37
Figure 2-6 TCT indirectly induces ciliostasis in human tracheobronchial mucosa models.	38
Figure 2-7 TCT/LPS disrupts displacement of particles after 24 hours in the hTBM. ...	39
Figure 2-8 TCT and LPS impair the barrier function of the hTBM.	41
Figure 2-9 TCT and LPS disrupt tight junction organisation.	42
Figure 2-10 TCT/LPS induces significant NO in completely submerged hTBM.	43
Figure 2-11 TCT and LPS induce expression of iNOS.	44
Figure 2-12 3D human tracheobronchial mucosa models express SLC46A2.	45
Figure 2-13 TCT/LPS induce IL-1 expression in hTBM.	46
Figure 2-14 Inflammatory cytokine gene expression analysis of TCT and LPS.	47
Figure 2-15 Toxin induced inflammatory cytokine secretion into cell culture supernatant.	49
Figure 2-16 Determination of an optimal MOI for infection of engineered airway models.	51
Figure 2-17 <i>B. pertussis</i> adherence to and cell invasion in airway mucosa models....	52
Figure 2-18 Invasion and persistence of <i>B. pertussis</i> in airway mucosa models.....	54
Figure 2-19 Comparison of different fixative methods for LCM.	55

Figure 2-20 Cold dissociation of epithelial cells from 3D models with serine protease.	56
Figure 4-1 Development of 3D airway mucosa models.	83

List of Tables

Table 1-1 Summary of <i>B. pertussis</i> virulence factors and their potential/proposed contribution to pathogenesis.....	15
Table 4-1 Tissue dehydration and paraffin embedding sequence	86
Table 4-2 Tissue deparaffination and rehydration.....	87
Table 4-3 Haematoxylin and Eosin staining	87
Table 5-1 List of Mammalian cells and biological scaffold	96
Table 5-2 List of bacterial strains.....	96
Table 5-3 List of toxins	97
Table 5-4 Oligonucleotides for qPCR.....	97
Table 5-5 Primary antibodies used in this study.....	97
Table 5-6 Secondary antibodies used in this study.....	98
Table 5-7 Composition of cell culture media	99
Table 5-8 Bacterial growth medium.....	99
Table 5-9 List of chemicals.....	100
Table 5-10 Commercial kits.....	102
Table 5-11 Buffers, reagents and solutions used in this work.....	103
Table 5-12 List of equipment.....	105
Table 5-13 List of Disposable material	107
Table 5-14 Softwares used in this work.....	108

Abbreviations

μg - microgram	FITC-Dextran - Fluorescein isothiocyanate-dextran permeability
μm - micrometre	fps – Frames per second
aa – Amino acid	GDP – Guanosine Diphosphate
ACT - Adenylate cyclase toxin	GMP – Guanosine monophosphate
Act-Tub – Acetylated tubulin	GTP – Guanosine triphosphate
ALI – Air-liquid interface	H/E – Haematoxylin/Eosin staining
ANOVA – Analysis of variance	HBEC3-KT - Human bronchial epithelial cell line
aP – Acellular pertussis vaccine	hBM — HBEC3--3KT mucosa models
APC – Antigen presenting cells	hNM – Human nasal mucosa model
BGA – Bordet-Gengou agar	hTBM- Human tracheobronchial mucosa model
Brk – Bordetella serum resistance protein	hTBM: Human tracheobronchial mucosa
BSA - Bovine serum albumin	hTERT – Human telomerase reverse transcriptase
BteA – Bordetella T3SS effector A	Hz - Hertz
Bvg – Bordetella virulence genes	IFN- γ - Interferon gamma
BvgA-P – Phosphorylated response regulator BvgA	IgA – Immunoglobulin A
BvgAS – Bordetella virulence regulatory two component system	IgG – Immunoglobulin G
BvgR – Repressor of Bordetella virulence genes	IgM -Immunoglobulin M
BvgS – Virulence regulatory histidine kinase	IL-1 – Interleukin 1
C4BP – C4 binding protein	IL-10 – Interleukin 10
CBA - Cytometric bead array	IL-16 – Interleukin 16
CBF: Ciliary beat frequency	IL-6 – Interleukin 6
CD11b- Cluster of differentiation 11b (integrin αM)	IL-8 – Interleukin 8
CD18 – Cluster of differentiation 18	kDa - Kilodalton
cDNA - Complementary Deoxynucleic acid	LOS – Lipo-oligosaccharide
CK – Cytokeratin	LPS – <i>E. coli</i> lipopolysaccharide
CR3 – Complement receptor -3	ml - millilitres
CRD - Carbohydrate recognition domain	Muc – Mucin
Ctrl – Mock treated control	NLRP3 – Nucleotide-binding domain and leucine-rich repeat pyrin containing protein-3
DAPI – 4,6 – diaminodino-2-pheynlindole.	NO – Nitric oxide
DGC - diguanylate cyclase	PBS - phosphate buffered saline
DNT – Dermonecrotic toxin	PFA – Paraformaldehyde
EDTA - Ethylenediaminetetraacetic acid	pg - picogram
ELISA – Enzyme linked immunosorbent assay	Prn - Pertactin
FCS - Foetal calf serum	PRR – Pattern recognition receptor
FHA – Filamentous Haemagglutinin	PT - Pertussis toxin
Fim - Fimbriae	RGD – Arginine, Glycine, Aspartate
	Ris – Regulator of intracellular response system
	RNA - Ribonucleic acid
	ROCK - Rho-associated coiled - coil protein kinase
	RT-qPCR – Real time quantitative polymerase chain reaction.

RT: Room temperature
RTX – Repeat in toxin
scRNA-seq – Single cell RNA
sequencing
SEM – Standard error of mean
slgA – Secretory immunoglobulin A
SIS – porcine small intestine
submucosa
SS – Stainer – Scholte
T3SS – Type 3 secretion system
TCS – Two component system
TCT: Tracheal cytotoxin
TEER: Transepithelial electrical
resistance
Th – T helper cell
TLR – Toll-like receptor
TNF α - Tumor necrosis factor alpha
Treg – Regulatory T- cells
vag – Virulence activated genes
vrg – Virulence repressed genes
WHO – World Health Organization
wP – Whole cell pertussis vaccine
ZO-1 – Zona occludens 1

1. Introduction

1.1 Whooping cough disease

1.1.1 A brief history

Pertussis was first mentioned in England in 1540 (Lapin, 1943) and the disease was initially referred to as the “kink” in the British Isles and “kindhoest” in Northern Europe (Holmes, 1940; Cherry, 1999). The first known pertussis epidemic, which occurred in Paris in 1578, was described by Guillaume de Baillou (Cited in Lapin, 1943; 1946). Sydenham was the first to clearly describe the illness and eventually gave it the name pertussis, which means a violent cough (Lapin, 1943). In 1900, Jules Bordet, a Belgian scientist along with Octave Gengou observed the causative organism in the sputum of a 5-month-old child who suffered from pertussis at the time. Although the bacteria appeared to be similar to *Haemophilus influenza*, they considered them as a different species due to their distinct morphological characteristics (Holmes, 1940). Bordet and Gengou eventually successfully isolated the organism in 1906 using a special medium containing glycerine extract of potato, agar and salt mixed with an equal volume of defibrinated rabbit or human blood (Bordet and Gengou, 1906). This medium is still widely used and referred to as the Bordet-Gengou medium (BGA). They published their findings in the *Annales de l’Institut Pasteur* and were the first to develop a vaccine against pertussis although it wasn’t very effective (Holmes, 1940; Lapin, 1943). In their publication, they described the narrow window within which the bacteria could successfully be isolated from patients during disease progression.

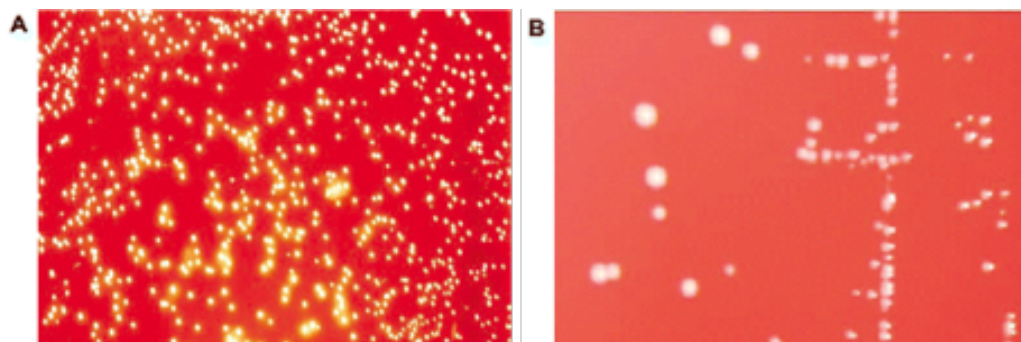


Figure 1-1 Appearance of *Bordetella pertussis* on Bordet-Gengou medium. (A) Freshly collected isolate (B) Subcultured isolate (Reproduced with permission from Guiso, 2009)

Prominent among their observation is the difference in appearance between bacteria isolated from artificial medium and biological samples. They observed the freshly isolated bacteria to be haemolytic and have a greyish glistening appearance reminiscent of mercury drops (**Figure 1-1A**). The subcultured population on the other hand showed a white nonhaemolytic appearance (**Figure 1-1B**). The first isolate was from the expectorate of Bordet's own son, Paul, who had contracted the disease. They also observed that the nonhaemolytic bacteria failed to agglutinate in infected patient serum in contrast to the haemolytic bacteria freshly isolated from the patients (Bordet and Gengou, 1906). This switch between the two apparent forms of the bacteria, called phenotypic variation, was later on reported to occur also in a reversible manner as a response to environmental changes. This reversible switch between the two forms was called phenotypic modulation (Lacey, 1960). Thirty years after the work of Bordet and Gengou, *B. parapertussis* was isolated and identified as a different species which causes a similar but generally much milder illness in humans by Eldering and Kendrick (Eldering and Kendrick, 1938; Eldering et al., 1957). Both species evolved independently from *B. bronchiseptica*, a closely related species causing respiratory infections in various mammals but only rarely in humans (Linz et al., 2016). Endemic and epidemic pertussis outbreaks due to *B. pertussis* have been reported globally in children throughout the last century (Vysoka, 1958; Schneider and Gross, 2001; Nardone et al., 2004; Yeh and Mink, 2006; Hozbor et al., 2009; Leekha et al., 2009; Zhang, 2009; Rohani et al., 2010; Clark, 2014; Hitz et al., 2020; Pham et al., 2020; Zhang et al., 2020)

1.1.2 The Disease

Whooping cough, or pertussis, is a highly contagious disease of the respiratory system. It is caused by members of the genus *Bordetella*. The disease can be life threatening in new-borns, non-vaccinated young children and immunocompromised individuals. Although not fatal in older children, adolescents and adults, it can result in complications such as pneumothorax and rib fractures due to extreme coughing episodes. Effective vaccines have been available and are widely used since the introduction of the whole cell pertussis vaccine (wP) in 1946. The vaccines have helped to greatly reduce the incidence of the disease. However, concerns over reactogenicity led to the replacement of

the wP with less reactogenic acellular pertussis vaccines (aP) since the 1990s. Despite a vaccine coverage of up to 95% worldwide, whooping cough persists and has re-emerged in the last decade (Kilgore et al., 2016). For instance, The WHO estimates about 160 000 pertussis deaths in children below 5 years alone globally in 2014 (Yeung et al., 2017).

Classical pertussis is currently described in three stages; catarrhal, paroxysmal and convalescent, with a duration from between 4 – 8 weeks but it could last much longer (Cherry, 1996). This categorization is based on the classical pertussis as described by Guillaume de Baillou, which has been widely translated with one version reading as follows (Cherry, 1999): “The lung is so irritated by every attempt to expel that which is causing the trouble it neither admits air nor again expels it. The patient is seen to swell up and as if strangled, holds his breath tightly in the middle of his throat”.

Disease progression of pertussis

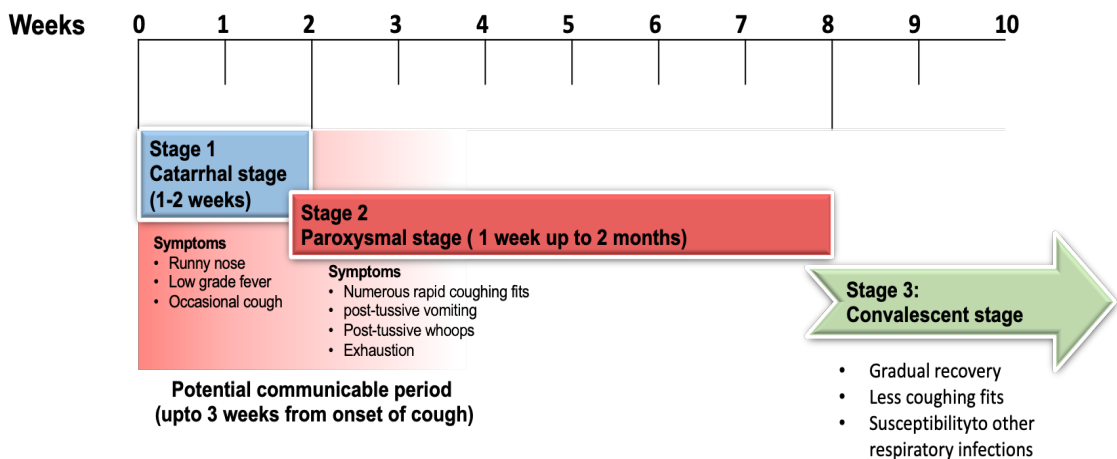


Figure 1-2 Stages, progression and presentation of typical pertussis (Adapted from National Center for Immunization and Respiratory Diseases, 2017).

The catarrhal phase, which begins from the time of contact with the bacteria, is characterized by nonspecific symptoms like the common cold and lasts 5 – 7 days. Symptoms include low grade fever, coryza and mild and occasional coughs (Cherry, 1984). Left untreated, the cough becomes more prominent with coughing fits (paroxysms), post-tussive vomiting and a distinct post-tussive whoop. This stage, referred to as the paroxysmal stage usually lasts between 1-4 weeks but can persist up to 10 weeks. In less severe cases, the disease typically presents with no fever, symptoms of system illness nor pharyngitis (Holt,

1902; Cherry, 1996). The severity of the paroxysms eventually declines, and the cough resembles that due to ordinary bronchitis. The patient then enters the convalescent stage.

The disease can however progress atypically in both infants and adults (Cherry, 1996; 1997). Many of the complications associated with the disease are due to the coughing fits. The force generated during the coughing fits can result in complications such as seizures and encephalopathy, and secondary infections are frequent. The common cause of death from pertussis is the severe leucocytosis linked to pulmonary hypertension (Pierce et al., 2000; Mattoo and Cherry, 2005; Paddock et al., 2008). The severity and complications of the disease decreases with the age of the patient (Cherry, 1996).

1.1.3 Epidemiology

Prior to the introduction of pertussis vaccines, pertussis epidemics were common with peak cycles every 3 – 5 years (Cherry, 2005; 2015). The first vaccine which served as the predecessor to the whole cell pertussis vaccine introduced in 1945 was developed in 1925 (Reviewed in Weston, 2012). The introduction of the whole cell pertussis vaccine (wP), which was combined with diphtheria and tetanus toxoids (DTwP), led to a drastic decrease in the incidence of the disease worldwide (Cherry, 2006; 2015). In the prevaccine era, >93% of the pertussis cases in the USA was reported mainly in children below 10 years (Broome et al., 1981; Cherry et al., 1989; Binkin et al., 1992; Baron et al., 1994; Cherry, 2006). However, since 1987, a shift has been reported in the disease burden to adolescents and adults based on quantitative ELISA tests to determine *B. pertussis* antibodies and antigens in adolescents and adults who presented prolonged cough illnesses (Cherry, 1984; 1997; Cherry et al., 2004; Cherry, 2005).

The wP vaccine was very effective in reducing the incidence of the disease, but due to reported reactogenic effects of the vaccine in children, the concomitant decrease in the readiness of being vaccinated in several countries and the resurgence of pertussis disease, acellular pertussis vaccines (aP) were developed to replace the wP (Hesseltvik and Ericsson, 1954; Winsnes et al., 1985; Kimura and Kuno-Sakai, 1987; Van Savage et al., 1990; Miller et al.,

1992a). These vaccines consisted of purified protective antigens from *B. pertussis*. The efficacy of the aP was demonstrated to be increased with the number of *B. pertussis* components added. The first aP containing filamentous haemagglutinin (FHA) and pertussis toxin (PT) was developed and used in Japan to control pertussis (Kimura and Kuno-Sakai, 1987; Kuno-Sakai and Kimura, 1997; Guiso et al., 2001). aP formulations may also contain additional antigens such as pertactin (Prn) and fimbriae (Fim). Despite the wide coverage of available pertussis vaccines, the disease persists worldwide with reported increases in incidence in some regions. There are still an estimated 24.1 million cases with about 640,000 deaths yearly worldwide due to pertussis (Yeung et al., 2017). Resurgence appears to be independent of the type of vaccine used.

Several factors have been cited to be responsible for the resurgence of pertussis. It should be noted that both the wP and aP protect from development of the disease, but they do not prevent infection and colonisation by the pathogen (Warfel et al., 2014). Furthermore, immunity conferred on individuals does not last forever. Natural infection with *B. pertussis* is estimated to confer an immunity between 6 – 30 years while wP conferred immunity estimated to last between 5 - 13 years (Reviewed in Cherry, 1996; Eberhardt and Siegrist, 2017). In addition, wP and aP stimulate a different kind of T-helper cell response. Natural infections with *B. pertussis* stimulate Th1 and Th17 response while wP vaccination mainly stimulates a Th1 response. The aP vaccine is reported to mainly induce a Th2 type of immunity usually lasting 3 – 5 years (Ausiello et al., 2000; Edwards, 2005; Klein et al., 2012; Warfel et al., 2014). The aP also appears to confer reduced protection to pertussis on individuals compared to the wP. Klein et al. (2013) reported a correlation between increased protection against pertussis in teenagers who received wP compared to teenagers who only received aP within the first two years of their lives. Furthermore, the level of protection was dose-dependent with individuals who received 4 doses of aP about 6 times more likely to encounter a pertussis diagnosis compared to those who received 4 doses of wP (Klein et al., 2012; Klein et al., 2013). Additionally, a study comparing the immunity due to wP and aP in infant baboons showed that aP failed to protect infant baboons against colonization despite stimulating protection against the development of severe pertussis symptoms. The aP cohort were also able to transmit the bacteria to a naïve cohort. The individual baboons that had received

wP but nevertheless suffered from the disease cleared the infection more quickly than those that received the aP (Warfel et al., 2014)

B. pertussis strains worldwide are largely monomorphic but since Mooi et al. (1998) first reported antigen variations between strains used to make vaccines and clinical isolates in the Netherlands, strains not expressing either Prn or PT have been widely reported (Mooi et al., 1999; Fry et al., 2001; Bouchez et al., 2018; Petridou et al., 2018; Barkoff et al., 2019). Such variations were noticed particularly in the conserved regions of the surface antigen Prn and of PT that interact with the immune system (Mooi et al., 1998; Mooi et al., 1999; Barkoff et al., 2019). A strain not expressing PT was found to be less pathogenic and did not cause leucocytosis. This strain was observed to have lost the entire PT operon, while the lack of Prn expression frequently appeared to occur by the disruption of the *prn* gene by an insertion element (Mooi et al., 1998; Mooi et al., 1999). These strains have since then been isolated all over the world with a prevalence of 27 – 50% (Fry et al., 2001; Barkoff et al., 2019; Raeven et al., 2019; Imamura et al., 2020). The odds of being colonised by Prn-deficient strains have been shown to be 2 - 4-fold higher in vaccinated individuals with no differences in clinical symptoms (de Gouw et al., 2014).

Thus, though the acellular vaccines are efficacious and confer immunity to pertussis comparable to the whole cell pertussis vaccine but with less adverse effects, the immunity wanes more quickly and the vaccine fails to protect against colonisation and transmission. The aP vaccine also seems to influence pathogen evolution and may contribute to vaccine evasion.

1.2 Pathogenesis of *B. pertussis*

B. pertussis is usually transmitted between individuals through aerosols or direct contact with contaminated fomites. The organisms attach to the cilia of the airway epithelial cells by means of adhesins such as FHA, Fim and Prn (de Gouw et al., 2011; Fedele et al., 2013; Dorji et al., 2018). The bacteria disrupt the host immune response and bacterial clearance mechanisms by secreting adenylate cyclase toxin (ACT), PT and tracheal cytotoxin (TCT) (Mouallem et al., 1990; Luker et al., 1995; van den Berg et al., 1999; Carbonetti, 2010; Fedele et al., 2017; Dorji et al., 2018; Hasan et al., 2018a; Kessie et al., 2020). The fine-tuned expression of

these and some other virulence factors allows a successful colonization of the respiratory epithelia by the bacteria followed by the development of severe symptoms characteristic of the disease.

1.2.1 Major adhesins

1.2.1.1 Filamentous haemagglutinin

Filamentous haemagglutinin (FHA) is referred to as the major adhesin of *B. pertussis*. The mature FHA is a large protein with a size of 220-kDa (Sato, 1996). It is a surface-associated and secreted protein which facilitates the adherence of the bacteria to the ciliated epithelial cells (Nash and Cotter, 2019). Structurally, FHA is a polypeptide chain folded to form a hairpin loop with an N- and C-terminus head, a tail that contains the RGD motif that mediates binding to the ciliated epithelia and a shaft of a 19-amino-acid residue repeat region (Mazar and Cotter, 2006). FHA is encoded by the *fhaB* gene that is regulated by the BvgAS two-component system as most other virulence factors and is induced under the appropriate environmental conditions to produce a 367-kDa precursor protein, FhaB (Roy and Falkow, 1991; Makhov et al., 1994; Smith et al., 2001; Link et al., 2007). FhaB is transported into the periplasm via the Sec system (Chevalier et al., 2004) where a third of its C-terminal part undergoes proteolytic cleavage by SphB1 to form the mature FHA protein (Coutte et al., 2001). The mature FHA protein is then secreted via a typical two-partner pathway requiring the outer membrane protein FhaC. The secreted FHA, however, remains noncovalently bound to the surface via its N-terminus interacting with FhaC (Mazar and Cotter, 2006). FHA is weakly associated to the surface of the bacteria and is even released in ample amounts which seems counter-intuitive to its function as an adherence molecule (Coutte et al., 2003; Nash and Cotter, 2019). This weak association and eventual release of FHA from the bacterial surfaces is suggested to facilitate the dispersal of bacteria from microcolonies and adherence to new colonization sites in the respiratory tract during an infection (Coutte et al., 2003). The binding of FHA to epithelial cells involves a multidomain interaction between its N-terminal glycosaminoglycan (lectin-like) binding site, the RGD motif (heparin-binding domain) and a carbohydrate recognition domain (CRD) (Mazar and Cotter, 2006). The heparin-binding domain of FHA enables the bacteria to

also bind to nonciliated cells. The RGD motif binds complement receptor type 3 (CR3, $\alpha_m\beta_2$, CD11b/CD18) integrins present on the surface of macrophages (Relman et al., 1990; Ishibashi et al., 2001; Mobberley-Schuman and Weiss, 2005). The binding of FHA to the CR3 is linked to the entry and persistence of *B. pertussis* in phagocytes (Melvin et al., 2015). FHA also binds to the serum protein C4BP, a regulator of complement activation, and inhibits the classical complement activation pathway by preventing the formation of IgG/IgM membrane complex (Berggard et al., 2001; Smith et al., 2001). In addition to its adherence function, FHA also elicits various immunomodulatory effects whose *in vivo* relevance remains to be characterized (Inatsuka et al., 2005; Dirix et al., 2014; Villarino Romero et al., 2016).

1.2.1.2 Fimbriae

B. pertussis fimbriae (fim) are long thin structures composed of one major fimbrial subunit (Fim2 or Fim3) and a minor subunit (FimD) that project from the outer membrane (Geuijen et al., 1996). They are also known as pili or agglutinogens. The major fimbrial subunits are encoded by the genes *fim2*, *fim3* and *fimX*. *fimX* is a pseudogene that is rarely expressed (Geuijen et al., 1996; Smith et al., 2001; Chen et al., 2018). All three genes are subject to phase variation due the insertion or deletion of cytosine residues in a long “C-stretch” region in their promoters (Willems et al., 1990). Each gene can therefore be expressed or not, independent of each other and thus give rise to the two major *B. pertussis* fimbrial serotypes; Serotype 2 and Serotype 3 (Willems et al., 1990; Geuijen et al., 1996; Chen et al., 2018). The major subunits are stacked to form the fimbrial strand while the minor subunit is located at the tip (Hazenbos et al., 1995; Geuijen et al., 1996). The major subunits have been shown to have an affinity for sulphated sugars while FimD forms the major adhesin binding to VLA-5 receptor of monocytes (Hazenbos et al., 1995; Geuijen et al., 1996). The fimbriae have been shown to play a role in the colonisation of the epithelium and to stimulate protective immune response (Gorringe and Vaughan, 2014; Scheller et al., 2015; Guevara et al., 2016)

1.2.1.3 Pertactin

Pertactin (Prn) is a 60-kDa surface exposed autotransporter protein. The *prn* gene encodes a precursor molecule termed p.93 which later undergoes proteolytic maturation after cleavage of the 34 amino acid N-terminal signal sequence and a 30-kDa so-called p.30 fragment from the C-terminus (Charles et al., 1988). The p.30 fragment is suspected to be involved in the export of Prn to the outer membrane (Charles et al., 1994). The secondary structure of Prn reveals two immunodominant regions and an RGD motif similar to FHA (Charles et al., 1991; Hijnen et al., 2004). The exact mechanism by which Prn promotes adherence to host cells still remains unclear. It is however proposed to bind to the integrin moiety since it contains an RGD motif. Prn is thought to be an immunoprotective antigen and is therefore included in many human acellular vaccines although its role in vaccine-based immunoprotection is not clear (Mooi et al., 1998; Guiso et al., 1999; Barkoff et al., 2019). As already mentioned, the use of aP vaccines appears to select for strains deficient in expression of Prn (Wagner et al., 2015; Polak and Lutynska, 2017)

1.2.2 Major Toxins

1.2.2.1 Pertussis toxin

Pertussis toxin (PT) is the only toxin secreted exclusively by *B. pertussis* among the *Bordetellae* (Reviewed in Carbonetti, 2010). It is a 106-kDa hexameric protein belonging to the bacterial A-B toxin superfamily. It is composed of 6 peptide chains encoded by the *ptxA-E* gene (Tamura et al., 1982; Ui et al., 1984; Nomura et al., 1987). Upon synthesis, the toxin is transported across the bacterial membrane by the Ptl type IV secretion system which is encoded by nine genes co-transcribed with the *ptx* genes (Verma and Burns, 2007; Verma et al., 2008). The A-protomer of the toxin consists of the S1 protein encoded by the *ptxA* gene and contains the ADP-ribosylating activity which modulates the activity of certain G-proteins in eukaryotic cells (Hsia et al., 1984; Budnik and Mukhopadhyay, 1993). The A-protomer thus, catalyses the transfer of an ADP-ribose moiety from NAD⁺ to regulatory α -subunits of certain G proteins which, in their active form, inhibit adenylate cyclase activity, inactivate calcium channels and activate potassium channels (Tamura et al., 1982; Ui et al., 1984; Nomura et al., 1987).

The B-oligomer of this A-B toxin contains the receptor binding activity and is comprised of the PtxB, PtxC, PtxE proteins and two copies of the PtxD protein. The N-termini of the PtxB and PtxC contain the lectin-like binding domain which mediates the binding and subsequent entry of the toxin into host cells (Tamura et al., 1982; Ui et al., 1984; Heerze et al., 1992). PT is also reported to facilitate FHA-mediated adhesion to macrophages via its ADP-ribosyltransferase activity (Relman et al., 1990) although this function has been shown to be redundant (Alonso et al., 2001; Carbonetti, 2010). PT is reported to be responsible for the influx of leucocytes, including neutrophils and lymphocytes, into the blood during an infection (Khelef et al., 1994; Paddock et al., 2008; Zlamy, 2016). Despite a plethora of data indicating the importance of PT for the virulence of the bacteria and its protective effect in aP vaccines, the *in vivo* role of this toxin during human infection still remains unclear (Hewlett et al., 2014)

1.2.2.2 Adenylate cyclase toxin

B. pertussis adenylate cyclase toxin (ACT) is a secreted protein belonging to the repeat in toxin (RTX) family which is secreted via a type 1 secretion system. It is a 220-kDa bifunctional protein encoded by the *cyaA* gene and is made up of an adenylate cyclase and a haemolysin subdomain (Pojanapotha et al., 2011; Subrini et al., 2013; Pandit et al., 2015; Novak et al., 2017). The toxin binds and enters targeted cells via the CR3 receptor (Karst et al., 2014; Masin et al., 2015; Osicka et al., 2015) and its enzymatic activity requires stimulation by calmodulin once inside the cells to induce a strong overproduction of cAMP (Karst et al., 2010; Martin et al., 2010; O'Brien et al., 2017; Finley, 2018; Voegele et al., 2018; Angely et al., 2020; Knapp and Benz, 2020). The toxin has been demonstrated to inhibit the proliferation of antigen-dependent T-cells. A major function of ACT appears to be inhibition of chemotactic and phagocytic immune responses (Guermontprez et al., 2001; Dadaglio et al., 2003; Ross et al., 2004; Dunne et al., 2010; Adkins et al., 2014; Fedele et al., 2017) and possibly the induction of apoptosis in some cell types (Ladant and Ullmann, 1999; Boyd et al., 2005; Cheung et al., 2009; Masin et al., 2015; Ahmad et al., 2016).

1.2.2.3 Tracheal cytotoxin

Tracheal cytotoxin (TCT) is a 921Da disaccharide-tetrapeptide belonging to the muramyl peptide family (Goldman et al., 1982; Goldman and Herwaldt, 1985). Thus, unlike the other virulence factors, TCT is no protein, instead it is a peptidoglycan fragment generated and released during the normal peptidoglycan cell wall turnover during the logarithmic growth phase (Goldman and Cookson, 1988; Cloud-Hansen et al., 2006; Johnson et al., 2013). It is formed by all Gram-negative bacteria, but it is normally efficiently recycled via the AmpG permease back into the cytoplasm (Goodell, 1985; Park, 1993; Johnson et al., 2013). *B. pertussis* has a defective AmpG permease which results in inefficient recycling of TCT and consequently the accumulation of the toxin in the periplasm of the bacteria. The toxin is then released into the extracellular space by an unknown mechanism (Rosenthal et al., 1987; Cookson et al., 1989a).

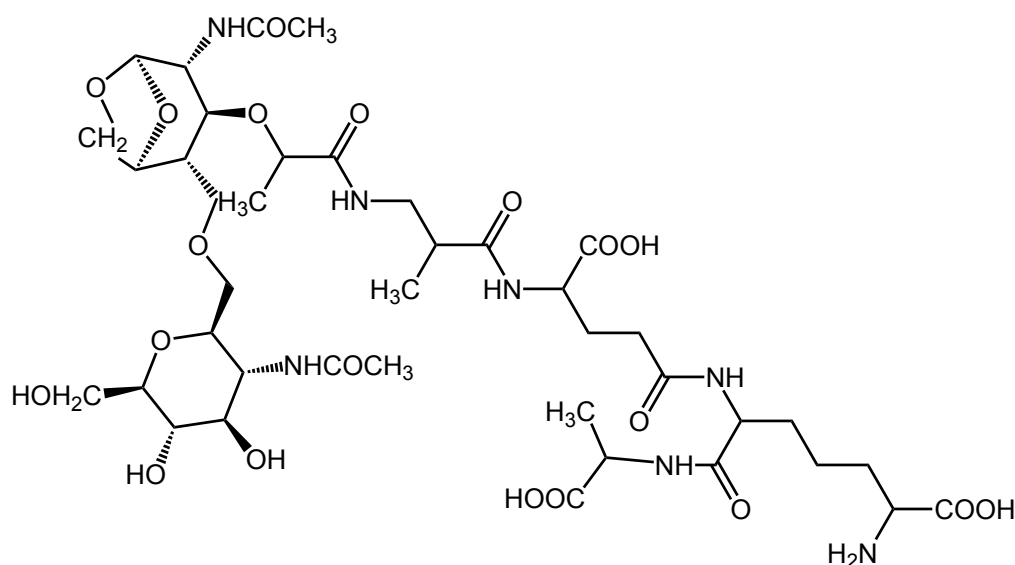


Figure 1-3 Structure of *B. pertussis* tracheal cytotoxin
(Adapted from Goldman and Cookson, 1988)

TCT has been implicated in the disruption of the ciliated epithelia of the airways in both animal models and human nasal brush biopsies (Goldman and Cookson, 1988; Wilson et al., 1991; Luker et al., 1993). The cytotoxicity of the toxin has been attributed to the lactyl tetrapeptide tail of the molecule (Luker et al., 1993; Luker et al., 1995). TCT has previously been reported to indirectly induce cytotoxicity via the induction of interleukin-1 (IL-1). Muramyl peptides are known to interact with cytoplasmic NOD-like receptors to induce the expression of inflammatory cytokines. Paik and colleagues recently showed that the

overexpression of the solute carrier family 46 member 2 (SLC46A2), a member of the thymic stromal cotransporters (TSCOT) in HEK293 cells resulted in an increased sensitivity of the cells to TCT and an upregulation of NOD-1 mediated NF- κ B expression (Paik et al., 2017). This indicates a role of SLC46A2 in the transport of TCT into the cytoplasm of the host cell enabling its interaction with NOD1. IL-1 provokes the expression of the inducible-nitric oxide synthase (iNOS) in hamster tracheal epithelial cells and explants in synergy with lipooligosaccharide (LOS), hence resulting in an increased production of nitric oxide (NO) by nonciliated cells to cytotoxic levels (Heiss et al., 1994; Flak and Goldman, 1996; Flak et al., 2000). The accumulation of the NO to cytotoxic levels can induce the production of high amounts of free radicals in neighbouring epithelial cells which destroy iron-dependent enzymes. However, whether the NO could accumulate to levels in the airway high enough to be toxic to the cells is still debated due to its volatility and strong ventilation occurring in the airways. Furthermore, Magalhaes et al. (2005) reported that human NOD-1 showed reduced sensitivity to TCT compared to murine NOD-1 and suggested that TCT may induce inflammation via an alternate pathway which is yet unknown in humans. Low concentrations of TCT are reported to impair neutrophil function while high concentrations have a cytotoxic effect on neutrophils (Cundell et al., 1994). TCT has also been shown to inhibit DNA synthesis and induce mitochondrial blotting in hamster tracheal explants and epithelial cells (Goldman and Cookson, 1988; Cookson et al., 1989a; Cookson et al., 1989b). Furthermore, TCT has been reported to denude ciliated cells and cause blebbing and necrosis of the epithelial cells of hamster tracheal explants (Luker et al., 1993; Heiss et al., 1994) as reported to be characteristic of infected human tissues (Paddock et al., 2008). Moreover, TCT was described to induce ciliostasis in the airway epithelia and thus to impair the mucociliary clearance mechanism (Wilson et al., 1991)

Skerry et al. (2019) recently reported that mice infected with a TCT-oversecreting *B. pertussis* strain experienced a more severe pulmonary inflammation compared to mice infected with wildtype strain. The group also reported that mice deficient in the peptidoglycan recognition protein 4, a mammalian receptor which induces a stress response upon exposure to bacterial peptidoglycans (Kashyap et al., 2014), experienced the most severe pulmonary inflammation and tissue damage. Thus, although the exact mechanism of these interactions is unknown, these data

indicate an *in vivo* relevance of TCT intoxication at least in mice (Skerry et al., 2019). Due to the observed cytopathologic effect of TCT on ciliated cells and mucociliary clearance of the airways mainly in animal models, TCT is proposed to be involved in the etiology of the cough paroxysms characteristic of pertussis. However, despite the large amount of data available suggesting a potential role of TCT during human disease, the contribution of TCT to *B. pertussis* pathogenesis remains unclear due to the lack of relevant data from human infections.

Interestingly, two other host-associated bacteria, *Vibrio fischeri* and *Neisseria gonorrhoeae*, are also known to release a substantial amount of TCT and related peptidoglycan fragments (Melly et al., 1984; Koropatnick et al., 2004). In the gonococcus, TCT may contribute to virulence by damaging the ciliated epithelium of the human fallopian tubes (Chan and Dillard, 2016), while TCT released by *Vibrio fischeri* has been shown to contribute to tissue re-organization required for the formation of the light organs of juvenile Hawaiian bobtail squids allowing their colonization by the symbiotic and bioluminescent bacteria (Koropatnick et al., 2004).

1.2.3 Some other virulence factors

B. pertussis possesses a type III secretion system (T3SS) which is a nano-injection system consisting of a hollow extracellular needle and a cylindrical basal body embedded in the cell-wall of Gram-negative bacteria (French et al., 2009; Ahuja et al., 2016; Kamanova, 2020). Their main function is the translocation of bacterial effector proteins into host cells which modulate host cell physiology to favour the pathogen. Two such translocated effector proteins are currently known for *B. pertussis*, the BteA protein (also known as BopC) which has a lipid raft targeting domain and BopN with yet unknown function (Dorji et al., 2018; Yahalom et al., 2019). *B. pertussis* T3SS effectors have been shown to promote colonisation, suppress innate and adaptive immunity and enhance the persistence of the bacteria in mice lungs (Fennelly et al., 2008; Kamanova, 2020).

B. pertussis also produces the so-called dermonecrotic toxin (DNT). It is a member of the A-B family of bacterial toxins made of a single chain polypeptide with an N-terminal cell binding and a C-terminal enzymatic domains (Endoh et

al., 1986). It usually localises in the cytoplasm of the bacteria and it is not known to be actively secreted into the extracellular environment (Cowell et al., 1979). However, purified DNT causes necrotic lesions upon subcutaneous injection into mice at low doses. High doses of the toxin are lethal (Iida and Okonogi, 1971; Cowell et al., 1979; Gentry-Weeks et al., 1988; Kerr and Matthews, 2000). DNT catalyses the polyamination or deamination of Rho family GTPases essential for actin skeleton reorganisation, cell motility and cell differentiation (Masuda et al., 2000). DNT irreversibly converts inactive Rho-GDP to the active Rho-GTP resulting in the expression of stress fibres and inhibition of cytokinesis. The toxin also associates with Rho-associated coiled-coil protein kinase (ROCK) to disturb cell differentiation (Masuda et al., 2000; Dorji et al., 2018; Teruya et al., 2020). While there are indications for a role in virulence of DNT for *B. bronchiseptica* (Brockmeier and Lager, 2002), no *in vivo* relevance during *B. pertussis* infection has been reported so far (Teruya et al., 2020)

B. pertussis also exclusively expresses the tracheal colonisation factor (Tcf). It is an autotransporter protein with a size of 60-kDa (Smith et al., 2001). It contains 3 RGD motifs in its N-terminal half with several proline rich regions and appears to contribute to the colonisation of the trachea (Smith and Limbird, 1982). *B. pertussis* also expresses the serum resistance *brk* operon encoding the BrkA and BrkB proteins, which are both required for serum resistance (Fernandez and Weiss, 1994). BrkA contains two RGD motifs and two sulphated glycoconjugate binding sites (Locht, 1999). Mutant strains of *B. pertussis* lacking BrkA show impaired binding to eukaryotic cells *in vitro* and are less virulent in mice compared to wildtype strains (Kerr and Matthews, 2000). BrkA shares about 29% structural homology with Tcf and pertactin. The presence of the two RGD motifs in BrkA suggests they play a role in adherence to host cells during infection. BrkB is predicted to be a cytoplasmic membrane protein as it displays domain homology to various transporters found in *E. coli* and *Mycobacterium leprae* (Fernandez and Weiss, 1994).

The endotoxin of *B. pertussis* is referred to as lipooligosaccharide (LOS) due to the lack of an O-polysaccharide side chain which is replaced by a complex nonrepeating trisaccharide and thus differs from typical lipopolysaccharides (LPS) of other Gram-negative bacteria (Fedele et al., 2008). *B. pertussis* LOS

possesses antigenic and immunomodulating properties (Harvill et al., 2000) and has been reported to act synergistically with TCT to induce cytopathology via the induction of NO in animal models (Flak et al., 2000). *B. pertussis* LOS can also modulate dendritic cell responses as well as a Th17-polarised immune response (Fedele et al., 2008).

Table 1-1 Summary of *B. pertussis* virulence factors and their potential/proposed contribution to pathogenesis

Virulence factor	Proposed role in <i>B. pertussis</i> pathogenesis	Mechanism of action
FHA	Adhesion	Major adhesion molecule which promotes binding to ciliated epithelial cells and macrophages. Promotes bacterial invasion of host cells.
Fim	Adhesion	Colonisation of the epithelium.
Prn	Adhesion	Possesses RGD motif which mediates binding to ciliated epithelial cells and macrophages
PT	Immune evasion, local and systemic toxin effects and adhesion	Inhibits the coupling of G-proteins and thus blocks their signal transduction
ACT	Evasion of host immune response, local and systemic toxin effect	Massive conversion of intracellular ATP to cAMP. Pore formation disrupts cells. Affects immune cell chemotaxis, bacterial phagocytosis and killing.
TCT	Local cytotoxin effects	Disruption of mucociliary clearance via ciliated cell extrusion. Induces hyper-mucous secretion and mitochondrial bloating. Inhibits DNA synthesis
LOS	Local and systemic toxic effects	Dendritic cell response modulation. Synergistic cytotoxic activity with TCT.

T3SS	Translocation of bacterial virulence factors e.g., BteA	Secretion of effector proteins .
Tcf	Adhesion	Tracheal colonization
BrkA	Resistance to killing in serum	Serum resistance factor which confers resistance to complement killing
DNT	Local dermal necrosis and systemic toxic effects(For <i>B. pertussis</i> so far, no in vivo data about virulence function available)	Catalyses polyamination or deamination of Rho family GTPases essential for actin skeleton reorganisation, cell motility and cell differentiation

1.2.4 Regulation of virulence genes

The expression of the most important virulence factors which include several toxins and adhesins as well as several colonisation factors during *B. pertussis* infection is controlled by the master regulatory two-component BvgAS system which was first described by Alison Weiss in 1984 (Weiss and Falkow, 1984). This system is responsible for the regulatory phenomena of phase variation and phenotypic modulation described earlier (Lacey, 1960) and regulates the dynamic expression of the virulence genes in response to extracellular signals in the surrounding environment. Later on, a second two-component system, RisAS, was found to be involved in the control of virulence of *B. pertussis* (Jungnitz et al., 1998)

1.2.4.1 The BvgASR system

B. pertussis virulence factor expression is regulated by the *bvg* locus which was initially referred to as the *vir* locus (Weiss et al., 1984; Stibitz, 1994). The *bvg* locus codes for two components, a 135-kDa BvgS and a 32-kDa BvgA protein (Arico et al., 1989; Miller et al., 1989; Miller et al., 1992b; Uhl and Miller, 1995). BvgS is a so-called hybrid histidine sensor kinase and contains a periplasmic domain, a linker region, a transmitter, a receiver and a histidine phosphotransfer domain, while BvgA is a typical DNA-binding response regulator (Boucher and Stibitz, 1995; Jones et al., 2005). Under laboratory conditions, the BvgAS system is responsive to several environmental cues. Conditions and signals that promote

expression of BvgAS are said to be non-modulating and those that repress BvgAS expression are modulating. The most important modulator of BvgAS seems to be low temperature although the presence of chemicals such as nicotinic acid and sulphate ions are also modulating (Lacey, 1960). *In vivo* relevant signals that cause BvgAS mediated regulation of virulence genes are so far not known. Under non-modulating conditions, the periplasmic domain of the BvgS signals the cytoplasmic transmitter domain to become autophosphorylated at a histidine residue by its kinase activity. The phosphorylated BvgS subsequently activates BvgA by transferring the phosphate to the BvgA receiver domain. The activated BvgA (BvgA-P) then binds to a cis-acting promoter sequence to induce the transcription of the virulence-activated genes (*vag*) (Uhl and Miller, 1994; 1995; 1996a; b). The transcription of the virulence repressed genes (*vrg*) are simultaneously controlled by the BvgA activated phosphodiesterase, BvgR, which regulates the concentration of the second messenger c-di-GMP (Chen and Stibitz, 2019) (Akerley et al., 1992; Moon et al., 2017). The bacteria are said to be in the Bvg⁺ phase under these conditions. *vag* genes have been classified into 3 different temporal classes. Early *vags* such as those encoding FHA and Fim, respond rapidly and are already activated by low concentrations of BvgA-P (Scarlatto et al., 1991). The BvgASR locus itself also belongs to the early genes as it is positively autoregulated, thus providing an additional level of Bvg-induced class-switching (Roy et al., 1990; Roy and Falkow, 1991). Late genes usually encode toxins such as ACT and PT which show relatively slow induction kinetics and require high concentrations of BvgA-P. The BipA encoding gene is the only gene known to belong to the so-called intermediate class of BvgAS regulated genes (Deora et al., 2001). Modulating conditions suppress the phosphorylation of the BvgA by the sensor kinase (de Gouw et al., 2014; Chen and Stibitz, 2019). The inactivation of the BvgAS results in the suppression of the *vags* and expression of the *vrgs* due to the absence of BvgR. Under these conditions, the bacteria display an avirulent phenotype referred to as Bvg⁻ phase (Cotter and Miller, 1994; Yuk et al., 1996; Martinez de Tejada et al., 1998; Kinnear et al., 2001; Veal-Carr and Stibitz, 2005; Chen et al., 2017). As mentioned above, the regulatory system also enables the so-called intermediate phase (Bvgⁱ) under semi modulating conditions (Cotter and Miller, 1997; Deora et al., 2001). The Bvgⁱ phase is characterised by the lack of *vrg* gene

expression, while early virulence factors are fully expressed and the expression of late factors is starting (Deora et al., 2001). So far, only BipA has been identified to be expressed in the Bvgⁱ phase. BipA has significant amino acid similarities with intimin of pathogenic *E. coli* strains and invasins of pathogenic *Yersinia* species (Stockbauer et al., 2001; Deora, 2002; Fuchslocher et al., 2003; Deora, 2004). The BvgAS system is considered to function as a kind of 'rheostat' which enables the survival, persistence and dissemination of the bacterial in diverse host niches by modulating a very fine-tuned transition between the Bvg⁺ Bvg⁻ and Bvgⁱ phases (**Figure 1-4**).

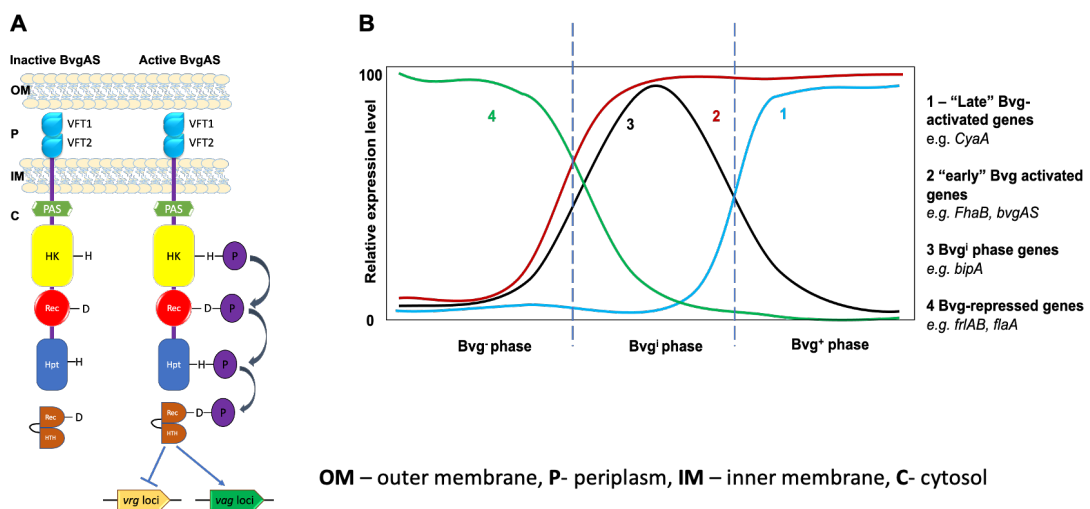


Figure 1-4 The BvgAS master regulatory system.

(A). The sensor kinase (BvgS) is made of venus flytrap (VFT) transmembrane domains, a PAS domain, a histidine kinase domain (HK), a receiver domain (Rec) and a histidine phosphoryl transfer domain (Hpt). The response regulator (BvgA) has an N-terminal Rec and a C-terminal helix-turn-helix (HTH) motif. BvgS becomes active under non-modulating conditions (37°C) and becomes autophosphorylated at a conserved histidine (H) in the HK domain. The phosphoryl group is then sequentially transferred to its Rec domain, followed by phosphotransfer to the Hpt and finally to the Rec domain of BvgA. Activated BvgA (BvgA-P) dimerizes and activates the expression of *vags* and leads to repression of the expression of *vrgs*. Under modulating conditions (e.g., ~25 °C, presence of MgSO₄ or nicotinic acid) BvgS is inactive and remains unphosphorylated resulting in the expression of *vrg* genes. (B) Expression curve of the expression of the four classes of genes and three distinct phenotypes regulated by the BvgAS. Bacteria exhibit the Bvg⁺ phase when BvgAS is fully active. Genes expressed when BvgAS is maximally induced are referred to as "late" Bvg-activated genes (blue curve 1). Genes that are expressed maximally under both Bvg⁺ and Bvgⁱ phase conditions (such as *fhaB*) are referred to as "early" Bvg-activated genes (red curve 2). Genes expressed maximally only under Bvgⁱ phase conditions (such as *bipA*) are presented on curve 3 (Black line). Genes repressed by BvgAS and expressed maximally only at Bvg⁻ phase are represented by curve 4 (green). (Adapted with permission from Deora et al., 2001)

1.2.4.2 The RisAS system

B. pertussis contains a second two-component system, RisAS, involved in virulence regulation in addition to BvgAS system. It was first identified in *B. bronchiseptica* where it functions independently of BvgAS to confer persistence and intracellular survival in eukaryotic cells (Jungnitz et al., 1998; Zimna et al., 2001). It consists of a response regulator (RisA) and a sensor kinase (RisS) encoded by the *risAS* locus (Jungnitz et al., 1998). *B. pertussis* expresses a truncated non-functional RisS sensor but expresses a functional RisA regulator which was shown to be involved in the regulation of *vrg* expression (Stenson et al., 2005). *B. pertussis* RisAS is optimally expressed under non-modulating conditions and promotes the expression of some *vrg* via the activity of RisA (Stenson et al., 2005). Phosphorylation of RisA has recently been shown to be mediated in *B. pertussis* by a non-cooperonic histidine kinase. Its phosphorylation is necessary but not sufficient for *vrg* genes activation and it has been suggested that in *B. pertussis* *vrg* gene expression may ultimately be controlled by the BvgAS regulated BvgR protein (Chen et al., 2017).

1.3 The human respiratory epithelium

The basic function of the human respiratory system is gaseous exchange, which involves the conduction of oxygen from the air to the circulatory system and carbon dioxide out of the body. The development of the respiratory system in humans begins at about 4 weeks of gestation. The nasal sinuses arise as nasal placodes from the ectoderm, the rest of the respiratory system from the larynx to the lungs develop from the endodermal layer (Kim et al., 2004; Edgar et al., 2013). The respiratory system continues to develop into adulthood. The respiratory system can be divided into the conducting zone and the respiratory zone. The conducting zone includes the nasal passage, pharynx, larynx, trachea, bronchi and pulmonary bronchioles (**Figure 1-5**). The main function of the conducting zone is to warm, moisten and remove harmful particles from the air which travels towards the distally located respiratory zone. Most of the conducting zone in healthy individuals is lined with a ciliated pseudostratified columnar epithelium interspersed with mucus-secreting goblet cells as well as serous secreting glands. The epithelial surfaces are lined by a mucus layer that traps

inhaled particles and a low viscous periciliary layer that lubricates the epithelial surface and facilitates the ciliary beating for efficient mucus clearance (Wanner et al., 1996; Knowles and Boucher, 2002). The cilia and the secretions coordinate to form the mucociliary clearance apparatus of the airways. The respiratory zone consists of the respiratory bronchioles, alveolar ducts and the alveolar sacs. The exchange of gases between the lungs and the blood occurs in this zone through the pulmonary arteries. The bronchioles are lined by simple columnar epithelia which transition to the cuboidal in the bronchioles. The alveoli epithelia consist of thin squamous epithelial cells to allow for efficient gaseous exchange (Amador et al., 2020).

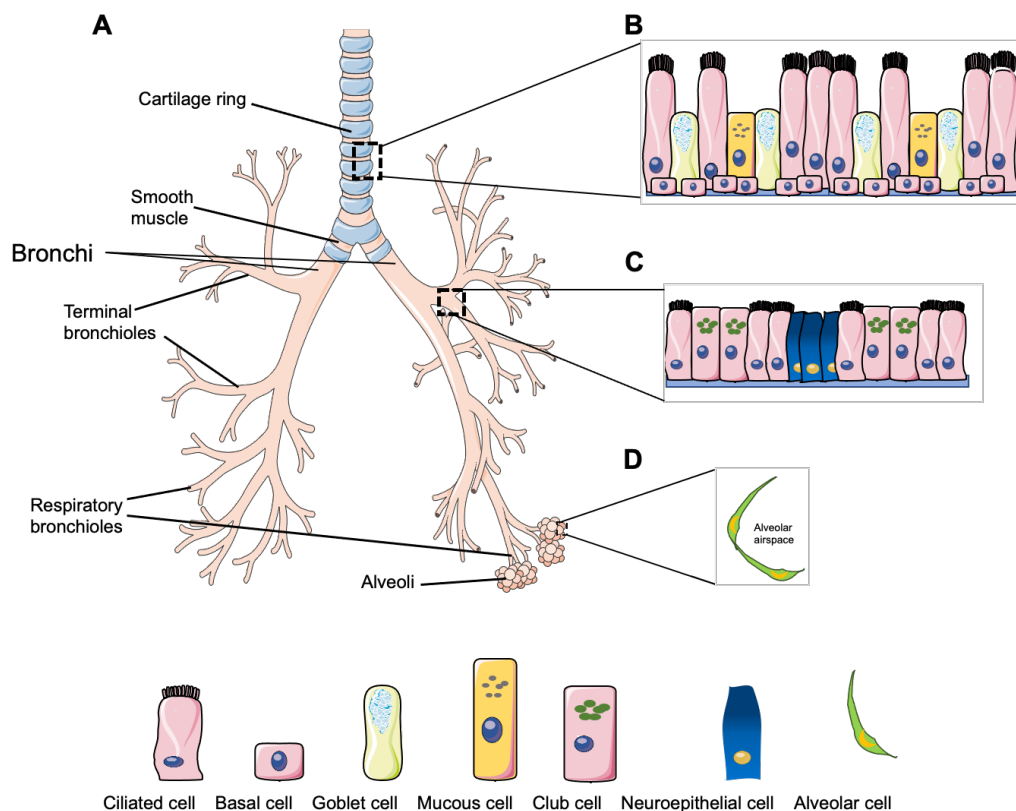


Figure 1-5 Organisation of the conducting and respiratory airway epithelium. **(A)** The human respiratory tract can be divided into the conduction zone and the respiratory zone. The conduction zone consists of the trachea, bronchi and terminal bronchioles and the respiratory zone consists of the respiratory bronchiole and the alveoli. The trachea is kept open by c-shaped cartilaginous rings. **(B)** The mucosa of the trachea and bronchi of the airways consists of a pseudostratified layer of ciliated cells, basal cells as well as secretory cells such as goblet cells which produce mucus. **(C)** The bronchioles are lined by columnar ciliated cells as well as club cells and mucus secreting cells. **(D)** The alveoli are made of alveolar cells with close proximity to capillaries to ensure efficient gaseous exchange (Image adapted from <https://smart.servier.com>).

1.3.1 The airway epithelium

The airway epithelium is made up of a heterogenous cell population that protect underlying structures by forming tight junctions which serve as physical barriers. The products of the secretory cells contain antimicrobial substances such as beta defensins which protect the cells against pathogens (Chong et al., 2008). The secretory and ciliated cells function to protect the lungs against pathogens and particulates inhaled from the environment through the action of mucociliary clearance. The organisation of the airway epithelial cells changes from a pseudostratified columnar arrangement in the trachea to simple columnar in the bronchus and then cuboidal in the bronchioles (Crystal et al., 2008). Eight distinct cell types have been identified in the respiratory epithelia. These have been grouped into three classes based on their ultrastructure, function and biochemical characteristics into basal, ciliated and secretory (Spina, 1998) (**Figure 1-5**).

Ciliated cells form the predominant cell type of the proximal conducting airways. They form about 50% of all the airway epithelial cells (Spina, 1998). On average, each ciliated cell possesses about 300 cilia with numerous mitochondria directly underneath to supply the energy needs to sustain the ciliary motion. The ciliated cells are terminally differentiated elongated columnar cells that make limited contact to the basal membrane (Mercer et al., 1994; Rawlins and Hogan, 2008). Basal cells are very common in the conducting airway epithelium with decreasing number in the terminal bronchioles (Evans and Plopper, 1988). They are electron-dense with low molecular weight cytokeratin. They are firmly attached to the basal membrane and play a major role in the attachment of more superficial cells such as ciliated cells. They are thought to be the primary stem cells of the airway and give rise to the mucous and ciliated epithelia (Evans and Plopper, 1988; Evans et al., 1990). Basal cells are thought to secrete some bioactive molecules such as neural endopeptidases, 15-lipoxygenase products and cytokines (Knight and Holgate, 2003).

The secretory cells found in the respiratory tract include mucous, serous, Club and dense-core granulated cells of the surface epithelia and mucous and serous glands present in the submucosa (Jeffery, 1983; Jeffery and Brain, 1988; Jeffery and Li, 1997). The human trachea is endowed with an estimated 7000 cells/mm² of mucous secreting cells. Most contain acidic high molecular weight

glycoproteins which are secreted into the lumen to trap foreign objects. Production of the right amount and viscoelasticity of mucous is essential for the efficient mucociliary clearance. Certain chemicals, genetic diseases and infections can lead mucous cells hyperplasia and metaplasia (Knight and Holgate, 2003; Moller et al., 2004; Picher et al., 2004; Martinez-Anton et al., 2006; Ovrevik et al., 2015). Mucous secreting cells are thought to be self-renewing and may also differentiate into ciliated epithelia (Evans and Plopper, 1988). Serous cells are similar to mucous secreting cells but tend to contain electron-dense granules. Many contain neutral mucins and nonmucoïd substances such as lipids (Mercer et al., 1994; Jeffery and Li, 1997; Knight and Holgate, 2003).

Club cells are located in the bronchi and bronchioles. They contain electron dense granules and are thought to produce bronchiolar surfactants. They characteristically possess agranular endoplasmic reticulum in the apical cytoplasm and glandular endoplasmic reticulum basally. They can also serve as stem cells for the formation of ciliated and mucous-secreting cells (Hong et al., 2001).

1.4 Host-pathogen interaction during *B. pertussis* infection

1.4.1 Bacteria - host interactions

The colonisation and subsequent disruption and extrusion of the ciliated cells of the respiratory epithelium by *B. pertussis* is well known from a large number of *in vivo* and *in vitro* experiments. In the respiratory tract, the bacteria face the challenge of overcoming the mechanical clearing challenge posed by the mucociliary clearance activity mediated by the beating cilia. Furthermore, competition from resident flora for nutrients and space may pose an additional challenge to the colonisation for *B. pertussis*. The bacteria therefore need to overcome these challenges including an array of host defense mechanisms such as iron sequestration and innate immune response, in order to colonize the respiratory tract. *B. pertussis* has been shown to preferentially adhere to the ciliated epithelial cells although adherence to non-ciliated cells may also occur (Tuomanen and Hendley, 1983; van den Berg et al., 1999; Soane et al., 2000). Animal studies and clinical observations suggest that the virulence mechanism of the bacteria is initiated upon adherence to the airway epithelia via FHA and

fimbriae (Edwards, 2005; Paddock et al., 2008). The bacteria then multiply locally and produce a myriad of virulence factors such as adhesins, immunomodulatory factors and toxins that prevent the rapid clearance of the bacteria from the airways (Akerley et al., 1995; Ladant and Ullmann, 1999; Bassinet et al., 2000; Soane et al., 2000; Mattoo et al., 2001; Anderton et al., 2004; de Gouw et al., 2011; Fedele et al., 2013).

B. pertussis requires iron for a number of essential metabolic processes to survive. *B. pertussis* has accordingly evolved at least three distinct high-affinity transport systems i.e., alcaligin, enterobactin and haem utilization systems, to obtain iron from the low iron concentration environment found in the respiratory mucosa (Brickman and Armstrong, 2002; Reviewed in Dorji et al., 2018). *B. pertussis* also expresses various transporter systems (CorC, GufA) for the uptake of trace metals such as Mg, Mn, Zn, Co and Cu which may play essential roles in bacterial survival and colonisation (Reviewed in Smith et al., 2001). Furthermore, significant host cell damage and lysis during infection frees up intracellular nutrients which may be used by the bacteria.

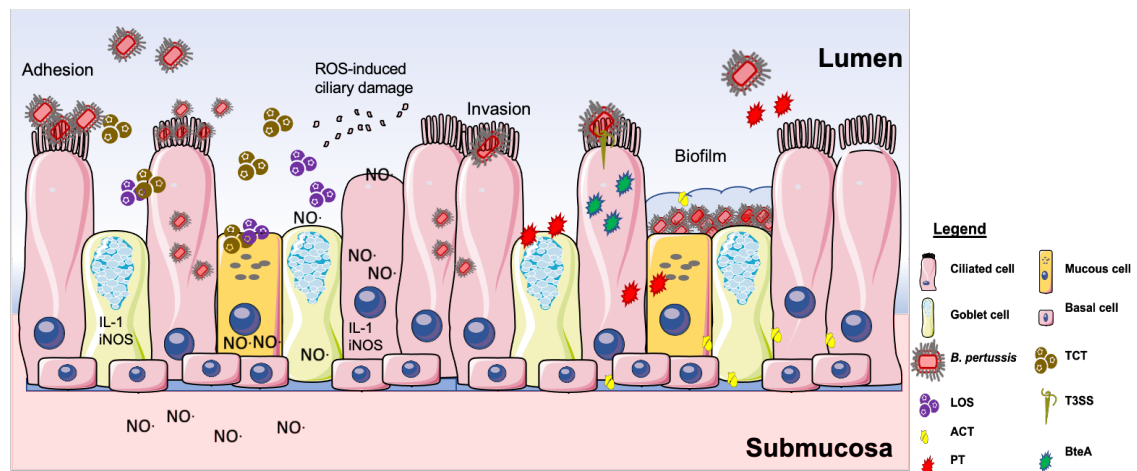


Figure 1-6 Model for *Bordetella pertussis* interaction with the respiratory epithelium. Colonisation of the epithelia by *B. pertussis* is mediated by various virulence factors. Bacteria adhere to ciliated cells via FHA and Fim. TCT and LOS synergistically induce reactive oxygen species via iNOS induced NO which cause ciliary damage. *B. pertussis* can invade epithelial cells and can also form biofilms on the airway mucosa. Cytotoxicity is induced by various virulence factors such as PT, BteA and ACT, which subvert signalling pathways within the cell (Illustration modelled after de Gouw et al., 2011).

The binding of the bacteria to the epithelial cells is mediated predominantly by FHA and fimbriae as mutations in either of these two genes results in reduced adherence to ciliated and nonciliated cells (Geuijen et al., 1996; van den Berg et

al., 1999). The binding of these two adhesins to the respiratory epithelia is dependent on cholesterol rich lipid raft domains in the host cells (Lamberti et al., 2008). These lipid rafts provide clustered signaling proteins and lipid co-factors which serve as important targets for invading bacteria (Lafont and van der Goot, 2005). Other virulence factors such as PT, Prn, ACT, TCT and BteA have also been shown to contribute indirectly to bacterial attachment to the epithelial cells. The cytotoxic effects of these factors may promote adherence by denuding the ciliated cells, thus disrupting the mucociliary clearance mechanism. The disruption of the mucociliary clearance activity results in accumulation of mucus with trapped particles which has been linked to the persistent cough which is characteristic of pertussis. The cellular damage may also expose the basally located receptors to the pathogen that may promote efficient binding of the bacteria.

B. pertussis is considered a classically extracellular pathogen. However, there is growing evidence that *B. pertussis* may possess cell invasive capabilities and an intracellular life cycle. Several of the virulence factors have been reported to contribute to the ability of the bacteria to invade and persist in both primary and immortalized cells lines of epithelial and immune origin (Schipper et al., 1994; Bassinet et al., 2000; Ishibashi et al., 2001; Lamberti et al., 2013; Guevara et al., 2016). FHA has been shown to be essential for *B. pertussis* to invade the epithelial cells via its RGD motif interacting with host cell integrin receptors (Bassinnet et al., 2000; Ishibashi et al., 2001). Prn, Fim and ACT have also been reported to potentially play varying roles in the invasion of host cells by *B. pertussis*. The exact mechanism by which Prn promotes invasion is still not clear but it has been suggested to be mediated by its RGD motif (Bassinnet et al., 2000). The role of ACT in invasion is also not completely understood. However, studies have shown that the deletion of ACT enhanced the uptake of *B. pertussis* by HeLa cells and tracheal epithelial cells (Lee et al., 1990; Bassinet et al., 2000; Zaretzky et al., 2002; Martin et al., 2011; Martin et al., 2015; Angely et al., 2017). The ability of *B. pertussis* to invade cells is also reported to involve interactions with lipid rafts and actin modification of the host cells (Lafont and van der Goot, 2005; Lamberti et al., 2008; French et al., 2009; Hartlova et al., 2010; Lamberti et al., 2010; Lamberti et al., 2013). *B. pertussis* has also been shown to persist in both epithelial cells and immune cells such as neutrophils and macrophages

(Steed et al., 1991; Friedman et al., 1992; Lamberti et al., 2008; Lamberti et al., 2010; Lamberti et al., 2013). The bacteria persist by interfering with phagosome-lysosome fusion and by hiding in nonacidic lysosome-associated membrane-protein-1-negative and cholesterol rich compartments (Lamberti et al., 2013; Karataev et al., 2015). The protein MgtC and the regulatory Ris proteins have also been shown to be essential for intracellular persistence (Jungnitz et al., 1998; Cafiero et al., 2018).

B. pertussis is reported to be capable of biofilm formation. The *B. pertussis* genome is confirmed to possess putative diguanylate cyclase (DGC) - encoding genes and phosphodiesterases, such as BvgR, which are able to synthesize and hydrolyse cyclic di-GMP, a second messenger molecule that has been implicated in biofilm formation (Merkel et al., 1998; Reviewed in de Gouw et al., 2011). Only Bvg⁺ phase bacteria are capable of forming biofilms formation *in vitro* (Mishra et al., 2005). Studies on *B. pertussis* biofilm formation have revealed its regulation by the BvgASR system and that it is promoted by FHA via cell-substrate and inter-bacterial adhesions (Mishra et al., 2005; Conover et al., 2012; Nishikawa et al., 2016). The interaction of ACT with the C-terminus of FHA inhibits biofilm formation (Hoffman et al., 2017; Dorji et al., 2018). Another locus, the *Bordetella bpsABCD* locus encoding enzymes required for the biosynthesis of an exopolysaccharide has been shown to be necessary for the formation of mature biofilms, although it is not required for the initial attachment to artificial surfaces and the respiratory surface *in vivo* (Conover et al., 2012). The *in vivo* relevance of the biofilm formation is not yet clear, but *Bordetella* biofilms have been detected in the nasal cavity of mice and may be a way to evade immune responses and promote colonisation of the respiratory tract (Conover et al., 2011)

1.4.2 Host defence mechanisms

A major challenge to the development of effective vaccines is the elucidation of the mechanisms underlying the host immune response to natural pertussis infection. Upon infection, the respiratory epithelium together with the resident antigen-presenting cells (APC) such as macrophages and dendritic cells form the host innate(mucosal) immune response to the bacteria. The epithelial cells form tight barriers that protect the underlying tissues from the pathogen. The APC are professional immune cells that act as sentinels that sense the presence of

pathogens via pattern recognition receptors (PRRs) and induce inflammation at potential pathogen entry points. These cells express various PRRs such as cell surface toll-like receptors (TLRs), cytosolic NOD-like receptors, C-type lectin receptors and retinoic acid-inducible gene-I-like receptors which recognise pathogen-associated molecular patterns such as LPS (Hippenstiel et al., 2006; Park and Lee, 2013; Wiese et al., 2017). The epithelial cells do not only present a physical barrier but also express PRRs and they are able to independently mount an inflammatory response in response to the presence of pathogens (Knight and Holgate, 2003; Hiemstra et al., 2015). The airway epithelia have been shown to mount an inflammatory response by secreting several proinflammatory cytokines and chemokines such as $\text{TNF}\alpha$, $\text{IFN-}\gamma$ and IL-1, IL-6, IL-8 and IL-16 (Heiss et al., 1993b; Stadnyk, 1994; Maestrelli et al., 1995; Arima et al., 1999; Belcher et al., 2000; Heller et al., 2004).

B. pertussis infection is known to induce a potent IgA response in the nasal cavity within 2 weeks which can persist for several months (Goodman et al., 1981). This secretory IgA (sIgA) inhibits bacterial adherence and promote the clearance of the bacteria from the airway (Solans et al., 2018; Debie et al., 2019). *B. pertussis* LOS activates the TLR4 signalling pathway and as mentioned above, TCT has been shown to induce inflammation by associating with NOD1 receptor in mice (Magalhaes et al., 2005; Paik et al., 2017; Skerry et al., 2019). However, it was recently reported that human NOD1 exhibited a reduced sensitivity towards TCT and it has accordingly been suggested that TCT may be recognized by a yet unknown receptor to induce the reported cytopathology (Magalhaes et al., 2005). TCT oversecreting *B. pertussis* strains have been reported to induce an early inflammatory response in mice which is attenuated by a peptidoglycan recognition protein 4 dependent sphingosine-1-phosphate receptor agonist (Skerry et al., 2019). PT has also been reported to be an agonist that engages TLR2/TLR4 signalling (Fedele et al., 2008; Fedele et al., 2010). In addition to the innate response, colonisation of the respiratory mucosa by *B. pertussis* initiates local chemokine release that results in the recruitment of immune cells. Neutrophils arrive first and this is followed by a wave of natural killer cells, macrophages and lymphocytes (Gillard et al., 2019; Kroes et al., 2019; den Hartog et al., 2020) TCT and PT have been reported to inhibit bacterial clearance by modulating the chemotactic recruitment of neutrophils and phagocytes

(Cundell et al., 1994) which help to clear the airways from the bacteria. Opsonisation of *B. pertussis* has been shown to be important for phagocytic killing (Steed et al., 1991; Hazenbos et al., 1995; Weingart and Weiss, 2000; Lamberti et al., 2010; Hovingh et al., 2018).

Cellular immunity to *B. pertussis* is mostly mediated via CD4⁺ T lymphocytes. Type 1 T-helper cells (Th-1) and interleukin-17(IL-17)-producing T-helper cells (Th-17) cells particularly seem to play an important role in mediating protective immunity (Fedele et al., 2010; Fedele et al., 2011; Higgs et al., 2012; Fedele et al., 2013). However, Th-17 is suspected to contribute to leucocytosis and pulmonary hypertension which causes infant deaths after *B. pertussis* infection (Higgs et al., 2012). Regulatory T-cells (Tregs) have also been identified which help to suppress the immune response by secreting cytokines such as IL-10 and TGF- β in order to re-establish immune homeostasis (Ballke et al., 2016). In summary, the immunity developed by the host seems to be modulated by bacterial virulence factors, which suppress innate effectors, promote Tregs and promote a pro-inflammatory response considered to provide protective functions.

1.5 Experimental models for studying *B. pertussis*

The virulence mechanisms of *B. pertussis* and other obligate human bacterial pathogens have been extensively studied using animal models, organ explants and *in vitro* flat mammalian cell cultures. The animals that have been used for *B. pertussis* studies include mice, hamsters, ferrets, rats, rabbits, dogs and large primates. Such model systems have been used due to the lack of appropriate human models and the difficulty to obtain human donor material. With the exception of baboons (see below), *B. pertussis* does not cause pertussis-like disease in these model animals, and so the close relative *B. bronchiseptica*, a natural pathogen of various mammals including rodents, that produces most of the virulence factors known from *B. pertussis*, was used and the data extrapolated to be applicable to human infections with *B. pertussis*. Although such experiments using 2D tissue cultures and animal experimentation have made important contributions to our understanding basic of functions of *Bordetella* virulence factors and of the disease, the *in vivo* relevance of data for the human infection by principle remains uncertain.

Mice are the most dominant models used in *B. pertussis* studies. Mice models capture the colonisation of the respiratory epithelial but they do not cough, thus cannot spread the bacteria to other mice (Pittman, 1991). Very high numbers of the bacteria are usually inoculated via intraperitoneal injection since the mice can rapidly clear the infection when inoculated intranasally (Pittman et al., 1980). Older mice are resistant to *B. pertussis*, but the suckling mice recapitulate the mortality due to pertussis pneumonia in humans (Pittman et al., 1980; Sato, 1980). Rats are very hard to infect with *B. pertussis*, while rabbits tend to be asymptomatic carriers of the pathogen (Ashworth et al., 1982; Weiss and Hewlett, 1986). The baboon model was recently introduced as it is a close human relative and recapitulates various important aspects of *B. pertussis* pathology (Fernandez, 2012; Naninck et al., 2018; Zimmerman et al., 2018). Baboons have been shown to develop the paroxysmal cough and mucus production associated with *B. pertussis* infection in humans and can transmit the infection from one animal to another (Fernandez, 2012; Warfel et al., 2012). Adult baboons tend to easily develop resistance to pertussis thus requiring experiments with new-borns. Thus, for the moment, baboons appear to be the best animal model for *B. pertussis*, but experimental work with these primates poses ethical problems and is extremely expensive.

Flat cultures of primary human and cancer cell lines have also provided a lot of information about critical virulence mechanisms of the bacteria. However, they lack the complexity typical of native tissues *in vivo* such as polarisation and subsequent differential expression of receptors and secretions. Furthermore, the cancer cell lines tend to possess anomalies atypical of primary cells such as genetic anomalies, cross contamination and mycoplasma cross contamination (Reviewed in Mirabelli et al., 2019). Care must therefore be taken in the interpretation of the data as they may not accurately reflect primary cell response. To overcome the drawbacks of animal models and 2D cell culture models, several studies have attempted to develop *in vitro* 3D human airway models for *B. pertussis* research (Vaughan et al., 2006; Steinke et al., 2014; Hasan et al., 2018a; Lodes et al., 2020).

Choe et al. (2006) first described a method for the development and maintenance of an *in vitro* airway bronchial mucosa models with physiological properties by

co-culturing bronchial epithelial cells and lung fibroblasts on a collagen matrix under airlift conditions. Since then, various airway mucosal models have been developed using both primary and immortalised human airway epithelial cells cultured on collagen matrices under airlift conditions (Vilasaliu et al., 2011; Hamilton et al., 2014; Steinke et al., 2014; Marrazzo et al., 2016; Schweinlin et al., 2017; Yonker et al., 2017; Lodes et al., 2020). These models may provide excellent new tools to study various aspects of the virulence mechanism of *B. pertussis* relevant to humans. Furthermore, immune cells can be implemented in the *in vitro* engineered airway mucosa models to assess the immune interaction during an infection cycle. However, some aspects such as bacterial transmission and development of the persistent cough cannot not be studied in such models.

1.6 Aims of the study

Bordetella pertussis despite being an obligate human pathogen has been studied extensively in rodents and recently in the baboons. Despite providing valuable information on the potential functions of virulence factors and basics of disease development, very little is known about the relevance of these data obtained in animal models during human infection due to interspecies differences. Furthermore, much of the data were obtained by experiments using the closely related species *B. bronchiseptica* for which rodents are a natural host and extrapolated to be possibly valid for *B. pertussis* infection in humans as well. Recent advancements in tissue engineering approaches provides an opportunity to develop complex tissue and organ models using primary human cells to address some of these issues and to prove and evaluate the relevance of data generated in different animal models. Due to their high *in vivo-in vitro* correlation, these 3D tissue models are valuable tools to study bacteria-host interactions without the limitations associated with flat cultures and animal models.

The aim of this study was therefore to investigate the interaction of *B. pertussis* with the human respiratory mucosa using engineered airway mucosa models developed by coculturing airway epithelial cells and fibroblasts on a biological scaffold. Thus, this work focused on the analysis of the activity of virulence factors and the entire bacteria on such human model systems in comparison to previous data obtained in animal models and 2D cell culture systems. In detail, the potential contribution of purified *B. pertussis* tracheal cytotoxin (TCT) to the

cytopathology of infection in the human tracheobronchial mucosa was investigated. This study additionally explored the potential of *B. pertussis* to invade and persist in the human airway epithelia. Both the *in vivo* role of TCT and the potential cell invasive properties of the bacteria are under debate for a long time in the scientific community. Lastly, a method for the dissociation and sorting of the different cell types of the models infected with *B. pertussis* to assess the impact of the infection on ciliated, goblet and basal cells using single cell RNA-sequencing analysis was developed. In essence, this study aimed to assess the suitability of such engineered human airway mucosa models for studies elucidating virulence mechanisms of human pathogens and to further develop methods to use such models to also investigate pathogen-host interactions at the single cell level.

2 Results

2.1 Engineered airway mucosa models show characteristic *in vivo* airway mucosa features

The advent of tissue engineering has led to the development of tissue models with high *in vivo* - *in vitro* correlation. Steinke et al. (2014) developed airway mucosa models by co-culturing primary human airway epithelial cells and skin fibroblasts on a biological scaffold with a high *in-vivo* correlation and demonstrated its possible application for *B. pertussis* infection studies. We adapted this protocol by incorporating human airway fibroblasts isolated from airway biopsies into the models instead of skin fibroblasts and cultured them at an air-liquid interface (ALI). However, the use of primary airway fibroblast at seeding densities described in Steinke et al. (2014) and Schweinlin et al. (2017) resulted in only about 35% differentiation of the tracheobronchial mucosa models. By increasing the number of tracheobronchial fibroblasts to 10^5 cells and the epithelial cells to 3×10^5 cells per 12mm^2 cell crown, the differentiation of the models was improved by more than 50%. As at the preparation of this thesis, differentiation rates of 92% could be achieved. As shown from the H/E staining, the engineered airway mucosa models developed from nasal epithelial cells (hNM) (**Figure 2-1A**) and tracheobronchial epithelial cells (hTBM) (**Figure 2-1B**) differentiated to form pseudostratified ciliated epithelial layers typical of the conducting zone respiratory mucosa. High speed video microscopy also showed the cilia to be functional with synchronous beating. Comparatively, *in vitro* models developed from the immortalised cell line HBEC3-KT (hBM) developed atypical stratified cuboidal epithelia usually without cilia (**Figure 2-1C**) and were therefore not used for further experimentation in this thesis. To determine the ciliary beating frequency of the observed kinocilia, 10 sec high-speed videos of the kinocilia were recorded at 200fps and assessed as described by Lindner et al. (2017). The highest mean ciliary beating frequency of $13.40 \pm 3.55\text{Hz}$ was observed in the hNM and mean CBF of $11.85 \pm 1.95\text{Hz}$ was calculated for the hTBM models (**Figure 2-1D**). The models were also characterised by immunofluorescent staining of typical airway epithelial cell markers such as cytokeratin 5 (CK5) for basal cells, cytokeratin 18 (CK18) for the differentiated epithelial cells and

acetylated tubulin (Act-tub) for the cilia. The models developed goblet cells which secreted Muc5AC and Muc5B positive mucus which are typical components of the airway mucosa as shown in **Figure 2-2**. The fibroblasts were immunostained with vimentin to show their location in the matrix. Models developed from the HBEC3-KT cell lines varied from the primary cell models by possessing predominantly CK5-positive basal cells (**Figure 2-2C**) with CK14-positive differentiated cells. They also did not express the ciliated cell marker acetylated tubulin which could be clearly seen in the airway models developed from the primary nasal (**Figure 2-2B**) and tracheobronchial cells (**Figure 2-2A**). Also observed in the hBM is a scant population of both Muc5AC and Muc5B- positive cells as well as CK18 compared to the primary cell models. Upon differentiation, the airway mucosa models can be maintained under airlift conditions up to 120 days with media change every second day. Due to the high fidelity of both hNM and hTBM to recapitulate typical features of the native airway mucosa, they were utilised further for infection experiments.

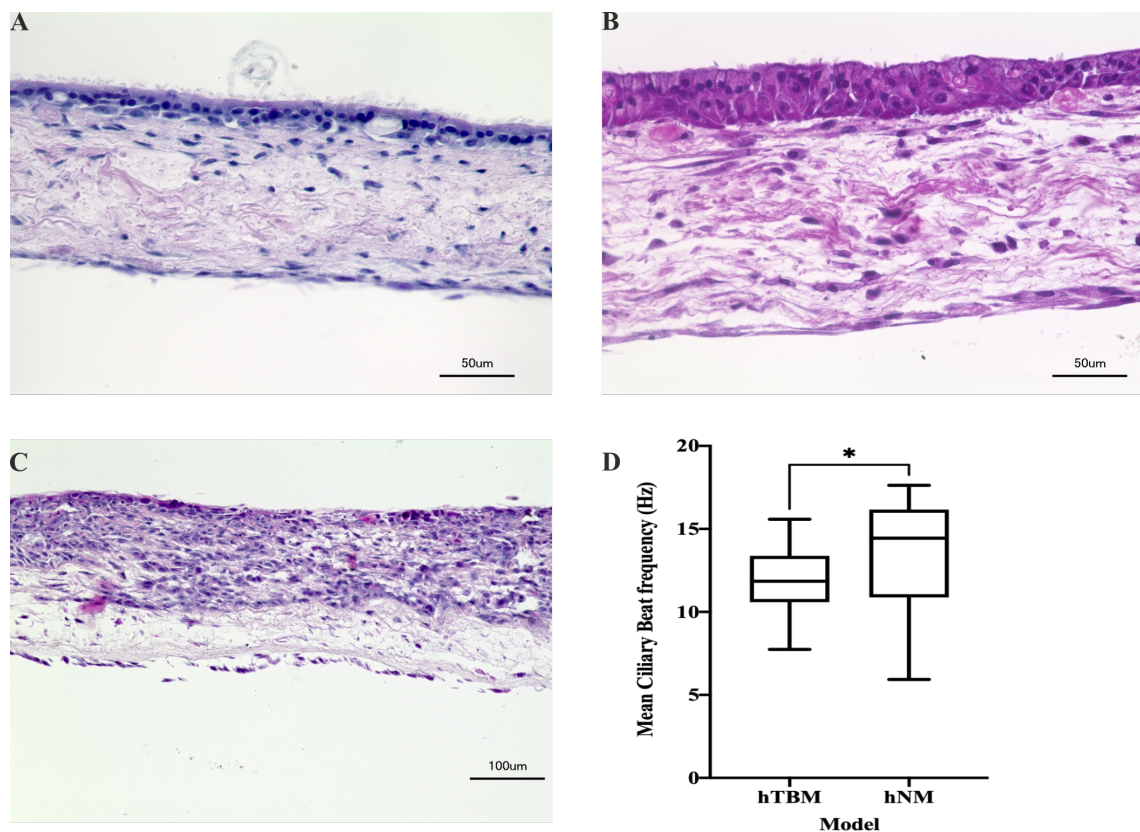


Figure 2-1 Airway mucosa models show pseudostratified ciliated epithelial layer. Human airway fibroblasts were cocultured with primary nasal epithelial cells (**A**), primary tracheobronchial epithelial cells (**B**) and the immortalised cell line HBEC3-KT (**C**) on SIS scaffold under airlift conditions for 21-28 days. The models were fixed with 4% PFA at RT for 2 hours and paraffin embedded. 5µm sections of the paraffin embedded models

were cut, deparaffinated and stained with Haematoxylin and Eosin. The hTBM and hNM developed a pseudostratified epithelial layer with cilia that project from the surface of the pseudostratified epithelia while the hBM do not possess cilia. **(D)** Ciliary beating frequency (CBF) of the kinocilia observed under high-speed video microscopy was accessed using Fourier fast transform analysis. The mean CBF was significantly higher in hNM compared to hTBM. Box plot represents the range (\pm SD) of the ciliary beating frequency of kinocilia of at least 6 different hNM and hTBM. Asterisk (*) denotes significance by Student's *t* test (* p <0.05)

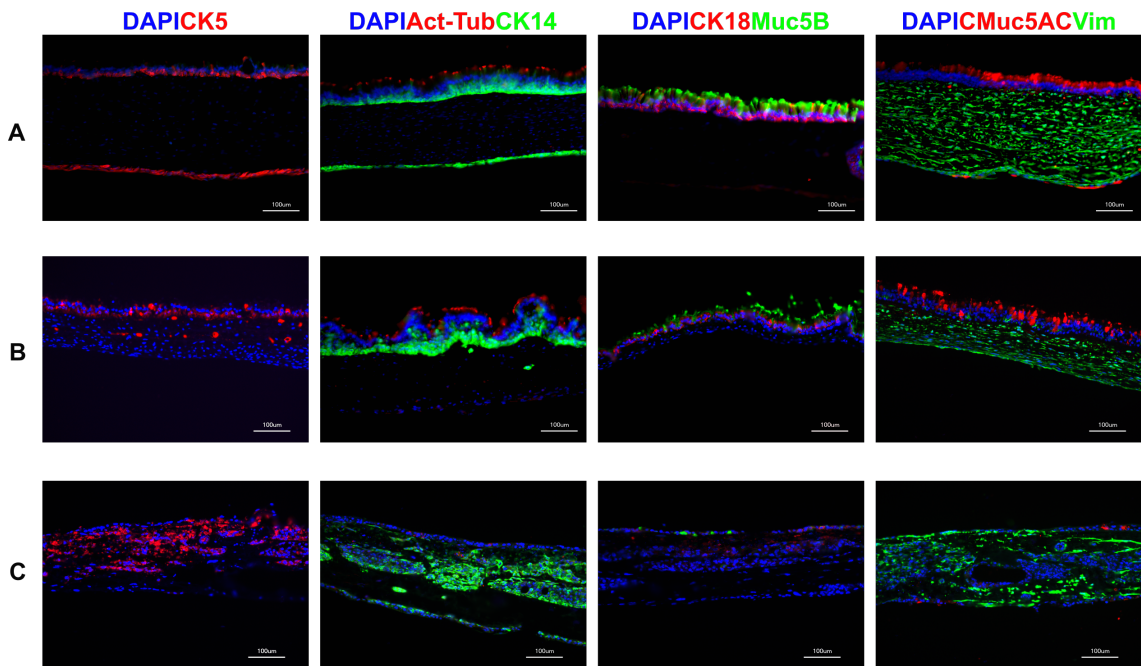


Figure 2-2 Airway mucosa models express characteristic *in vivo* airway markers. Paraffin sections (5 μ m) of 21-28-day old airway mucosa models were made and characterised by immunostaining for characteristic airway features. Human tracheobronchial mucosa models **(A)** and nasal mucosa (hNM) models **(B)** possess characteristic airway epithelial cells such as CK5-positive basal cells, cilia (Act -Tubulin) and Muc5AC- and Muc5B-positive goblet cells and secreted mucins. The epithelial cell layer also expresses the epithelia markers CK14 and CK18. **(C)** The hBM possess CK5-positive basal cells, Muc5B and Muc5AC positive mucin and are also positive for CK14. They show reduced expression of CK18 and ciliated cell acetylated tubulins. **Scale bar:** 100 μ m

2.2 Airway mucosa models develop tight barrier properties

Epithelia tend to develop various junctional complexes which allow them to form tight physical barriers such as tight junctions, adherens junctions as well as communicate through gap junctions and desmosomes. These junctional complexes protect the underlying tissues from infectious agents and foreign particles. Tight junction formation is also used as a measure of maturity of many *in vitro* barrier models. The development of the tight junctions in our engineered airway mucosa models was measured noninvasively once a week for 21 days

under air-liquid interface (ALI) to assess the progress of the models. The transepithelial electrical resistance (TEER) of the airway models was measured noninvasively using chopstick electrodes. As shown in **Figure 2-3**, the highest TEER values were recorded after 21 days under airlift conditions for all three models. Interestingly, while the *in vitro* mucosa models developed from primary cells showed a dramatic increase in TEER over the 21 days under airlift, the TEER of the hBMs developed gradually and reached a mean of $28.85 \pm 0.60 \Omega\text{cm}^2$ on day 21. The hNM averaged a TEER of $25.94 \pm 1.77 \Omega\text{cm}^2$ from the 4th day under airlift to $64.43 \pm 9.71 \Omega\text{cm}^2$ at day 21. In the hTBM, TEER values of $25.80 \pm 1.46 \Omega\text{cm}^2$ and $53.78 \pm 7.43 \Omega\text{cm}^2$ were recorded on day 4 and 21 respectively. The TEER did not vary significantly between day 4 and 11 as well as between day 11 and day 18. Conversely, statistically significant variations were obtained for TEER of hTBM measured on day 4 and day 18 ($p=0.0179$) and 21 ($p<0.0001$) as well as between day 11 and day 21 ($p=0.0047$). The development of the TEER in the hNM was very interesting as it showed a sudden burst from day 18 to day 21. The variation in TEER recorded on day 4 was not statistically significant when compared to TEER recorded on day 11 and day 18 in the hNM. However, the TEER on day 21 showed a statistically significant variation when compared to day 4 ($p<0.0001$), day 11 ($p<0.0001$) and day 18 ($p=0.0019$). Comparatively, the TEER did not vary significantly between the different models after 11 days. However, TEER recorded in hTBM significantly varied from TEER recorded in hBM on day 18. Both hTBM and hNM had a significantly higher TEER on day 21 compared to the hBM (**Figure 2-3**).

The organisation of the tight junction was also assessed by immunostaining of the models for ZO-1 and E-cadherin expression after 24 hours. As shown in the confocal microscopy images in **Figure 2-4**, all three models express the tight junction marker ZO-1 and the junctional protein E-cadherin which are typical of the airway. However, while hTBM and hNM showed organised expression with the typical honeycomb configuration, the hBM did not exhibit this typical pattern. Taken together, the TEER and organisation of the tight junction in hTBM and hNM indicate that the models are able to develop a functional physical barrier between the luminal surface of the epithelia and the submucosal compartments.

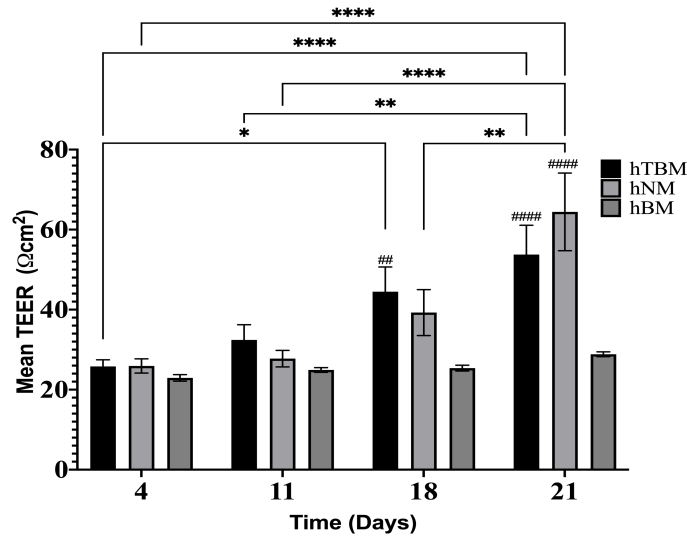


Figure 2-3 Airway mucosa models develop tight junctions.

The develop of a tight barrier by the models was determined noninvasively by measuring the transepithelial electrical resistance (TEER) on days 4, 11, 18 and 21 after airlift. The TEER of the seeded SIS scaffolds was estimated by normalising to an unseeded SIS scaffold mounted on a cell crown. The TEER of the hTBM and hNM increased weekly from days 4 through to day 21. The TEER of the hBM increased gradually and reached a maximum TEER at day 21. The data represents means (\pm SEM) of at least 12 models from 3 independent experiments. Asterisks (*) indicate within model TEER statistical significance measured on the different days (* p <0.05, ** p <0.01, *** p <0.005, **** p <0.0001). # indicates the statistical significance of the TEER between the different models (## p <0.01, #### p <0.0001). Non-significant statistical comparisons are not annotated.

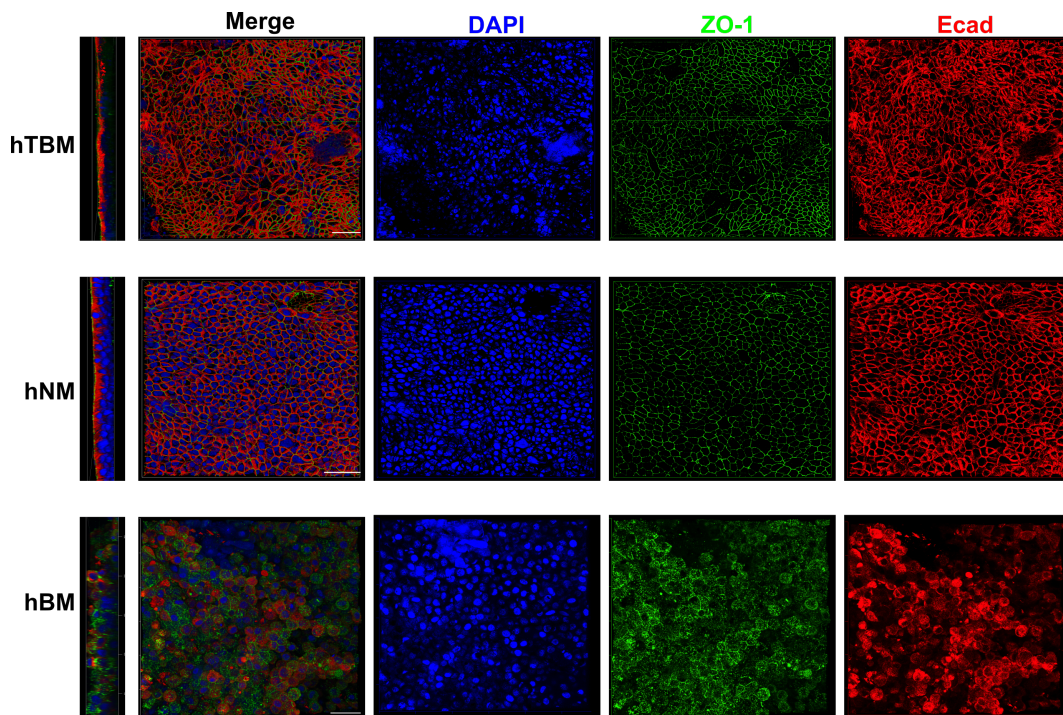


Figure 2-4 Engineered airway mucosa models express organised tight junction markers. Mature engineered airway mucosa models were fixed in 4%PFA overnight at 4°C and the whole model was immunostained with an anti-ZO-1 and anti-E-cadherin antibody. A

z-stack image of the models was captured using a laser scanning confocal microscope through 25µm and reconstructed. The hTBM and hNM show nicely organised tight junctions with the typical honeycomb structure while the hBM show less organised honeycomb ZO-1 and E-cadherin expression patterns. **Scale bar:** 50µm

2.3 Interaction of *B. pertussis* tracheal cytotoxin with human tracheobronchial airway mucosa models.

2.3.1 Tracheal cytotoxin disrupts the airway mucosa model

Tracheal cytotoxin (TCT) alone and in conjunction with LPS has been implicated in the cytopathology of *B. pertussis* by inducing blebbing and epithelial cell extrusion based on data using hamster tracheal ring explants (Goldman et al., 1982; Heiss et al., 1993a) and human nasal biopsies (Wilson et al., 1991) and to impair the mucociliary clearance machinery. To determine if TCT can induce similar effects on the human airway *in vitro*, hTBM were incubated for 24 hours with 3µM TCT and/or 100ng/ml LPS from the apical compartment. However, unlike in previous studies where the explanted tissues were incubated completely submerged in the toxin solution, the toxins were added from the luminal side of the hTBM to mimic the direction of contact during natural infection. The basal compartment was filled with fresh mixed medium without the toxins. The hTBM were incubated with the toxins for 24 hours and fixed with 4% paraformaldehyde (PFA) overnight at 4°C. The hTBM were then paraffin embedded and 5µm sections stained with haematoxylin/eosin (H/E) for histological analysis. As shown in **Figure 2-5A**, extruded cells (black arrowheads) could already be observed from models incubated with TCT in combination with LPS (TCT/LPS) for 24 hours from the H/E staining of the paraffin sections. The extrusion of cells from hTBM incubated with either TCT or LPS alone could not be observed in the H/E staining. The hTBM were further analysed using electron microscopy after the 24 hours incubation with the toxins. As shown in **Figure 2-5B**, ultrastructural scanning electron micrographs showed extrusion of the epithelial cells in the hTBM treated with either TCT or LPS alone as well as in combination. Mock control treated models remained intact and did not show epithelial cell extrusion. The combination of TCT and LPS appeared to cause a more severe damage to the hTBM compared to either toxin alone (**Figure 2-5B**). Further analysis of the airway mucosa models using transmission electron microscopy (TEM) showed

that the cellular blebbing and extrusion was not restricted to only the ciliated cells but also occurred in the non-ciliated cells (**Figure 2-5C**). Also evident from **Figure 2-5B** is the denuding of ciliated cells (blue arrows) in the hTBM that were incubated with TCT/LPS for 24 hours. Taken together, the data suggest that TCT and LPS severely disrupt the airway epithelia after 24 hours incubation.

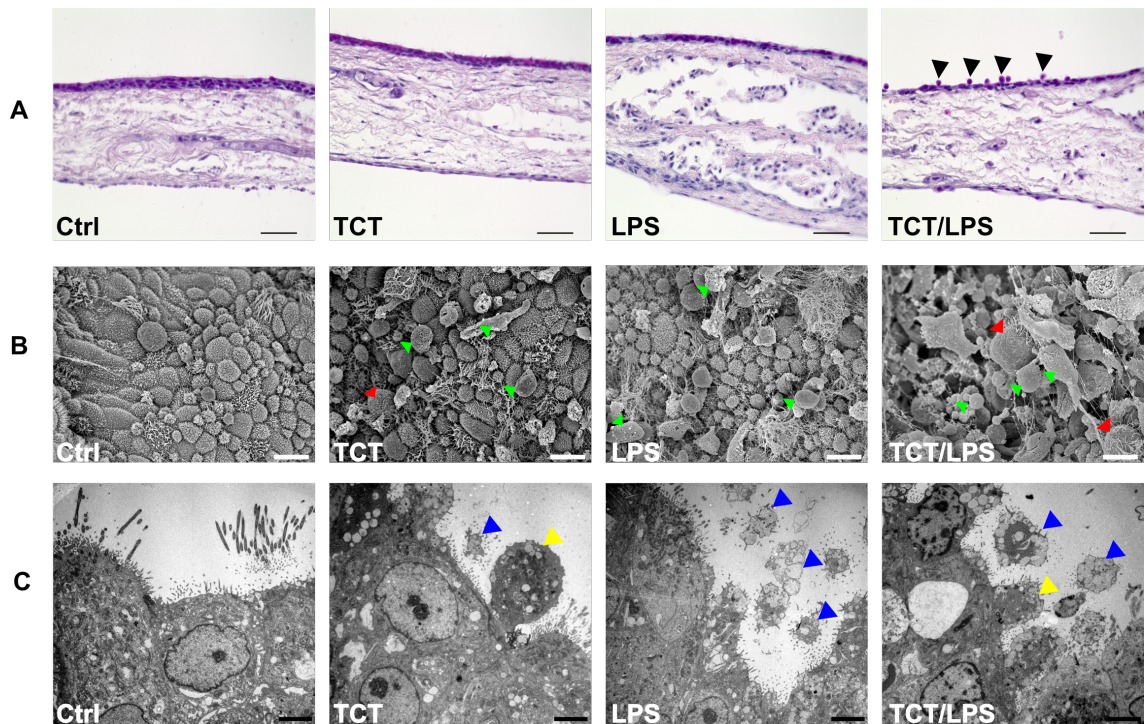


Figure 2-5 TCT and LPS cause disruption of the airway mucosa. hTBM were developed and incubated for 24 hours with either 3 μ M TCT, 100ng/ml LPS or a combination of both (TCT/LPS) from the luminal side. A mock treated control was also set up by incubating with fresh mixed medium. **(A)** H/E staining of formalin fixed and paraffin embedded sections showing extrusion of cells from 24-hours TCT/LPS treated hTBM. Black arrowheads indicate extruded cells. **Scale bar: 50 μ m.** **(B)** Scanning electron micrographs of human tracheobronchial mucosa models showing extrusion of epithelial cells after 24 hours of toxin treatment. Green and red arrowheads indicate extruded ciliated cells and non-ciliated cells respectively. **Scale bar: 10 μ m.** **(C)** Transmission electron micrographs showing the pinching effect of incubating the human tracheobronchial mucosa models with TCT and LPS under submerged conditions for 24 hours. Blue arrowheads indicated denuded ciliated cells that have been extruded from the epithelia. Yellow arrowhead indicates a nonciliated cells undergoing blebbing. **Scale bar: 2 μ m** (Adapted from Kessie et al., 2020)

2.3.2 TCT and LPS synergistically impair mucociliary clearance in the hTBM

One major pathophysiology of pertussis is the dysfunction of the mucociliary clearance apparatus due to the high mucus production and denuding of ciliated cells. Only TCT, among the many virulence factors of *B. pertussis*, has been able

to recapitulate this pathophysiology in either animal models or explanted human tissue (Reviewed in de Gouw et al., 2011). Previous observations from TCT treated hamster tracheal explants reported ciliostasis due to the toxin (Goldman and Cookson, 1988; Luker et al., 1993). To determine if TCT could induce ciliostasis in the hTBM, the ciliary beating frequency (CBF) of the hTBM was determined by assessing high speed videos before and 24 hours after toxin addition as described by Lindner et al. (2017). From **Figure 2-6A**, the incubation of the hTBM with either TCT or LPS alone or in combination resulted in minor declines in the CBF which were not statistically significant compared to mock treated controls. Since the method of CBF assessment involved selecting viable cells with beating cilia, the effect of the toxin was further analysed by generating a frequency-dependent heat map of the beating cilia. As shown in **Figure 2-6C**, incubation of the hTBM with TCT and TCT/LPS resulted in loss of ciliated cells. However, intact ciliated cells still showed cilia beating with an average frequency above the physiological minimum of 7Hz reported for the tracheobronchial ciliated cells (Clary-Meinesz et al., 1997). Taken together, the data indicate that TCT and TCT/LPS indirectly induce ciliostasis by causing loss of ciliated cells.

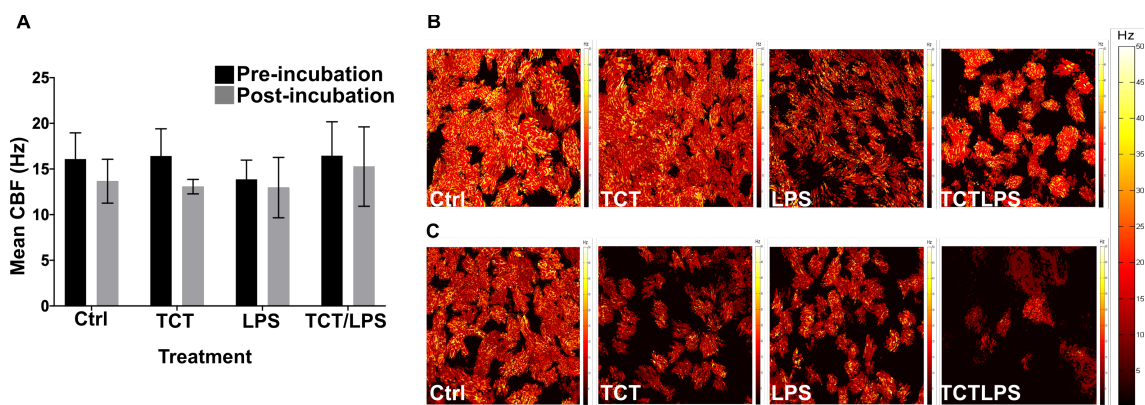


Figure 2-6 TCT indirectly induces ciliostasis in human tracheobronchial mucosa models. **(A)** Histogram of the mean ciliary beat frequency of the hTBM before and after 24 hours of toxin incubation. Data represents means (bars) and standard errors of 3 independent experiments. **(B)** Representative heatmaps of ciliary beating frequency of hTBM generated from high-speed videos recorded before addition of toxins. **(C)** Representative heatmaps of ciliary beating frequency after incubation with the toxins. (Adapted from Kessie et al., 2020)

To further assess if the observed loss of ciliated cells resulted in a defect in the particle transport efficiency of the hTBM, a particle transport assay was performed pre- and post-toxin incubation using dynabeads and analysed using Image pro®- v.10. To analyse the particle transport ability of hTBM, 15 seconds

long high-speed videos of the particles were recorded at 200fps. 100 frames which correspond to 1 second were extracted and analysed to determine the displacement of the particles. As seen from **Figure 2-7A-H**, the hTBM incubated with TCT and LPS alone showed particle displacement before and after the treatment. However, models treated with TCT/LPS despite the observed ciliary beating did not cause a displacement in the particles. The particles seem to oscillate around a fixed point (**Figure 2-7H, P**). The hTBM treated with TCT/LPS were also observed to possess a lot of cellular debris and showed hyper mucus production which seem to trap the dynabeads, thus preventing them from being displaced. Taken together, the loss of ciliated cells, the extensive deposition of cellular debris and the hyper mucus production may cause a disruption in the mucociliary clearance mechanism in TCT/LPS treated hTBM, thus suggesting a potential role of this phenomenon during *in vivo* infection.

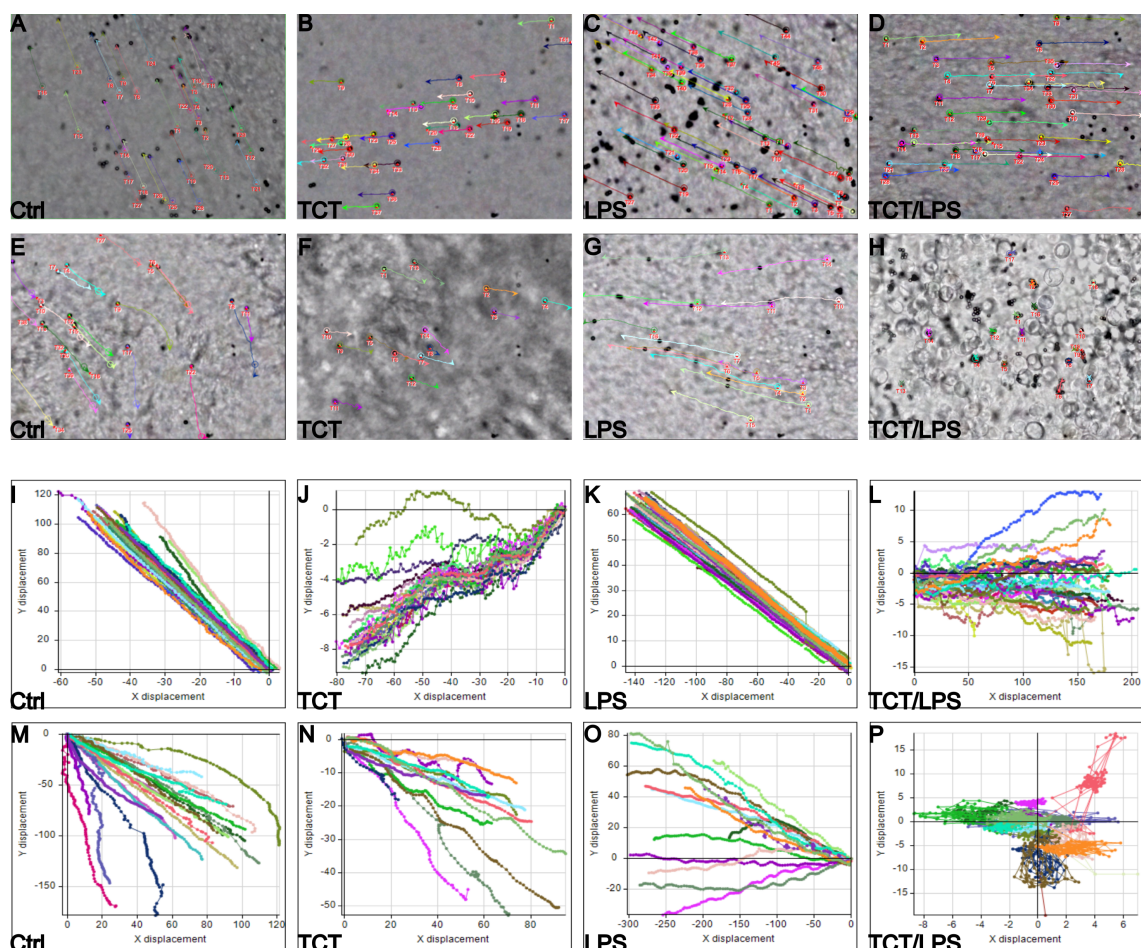


Figure 2-7 TCT/LPS disrupts displacement of particles after 24 hours in the hTBM. The disruption of the mucociliary clearance ability of the hTBM post toxin treatment was assessed using the particle transport assay. (**A-D**) Particle movement line graphs derived from highspeed videos of particle transport or pre-treatment hTBM. (**E-H**) Particle line graphs of highspeed videos of 24 hours toxin treated hTBM. The direction

of particle displacement is indicated by the coloured lines with arrowheads. Graphs show the particle displacement from the different toxin treated models. **(I-L)** Displacement of tracked particles before addition of toxins. **(M-P)** Particle displacement of 24 hours toxin treated hTBM over 100 frames. Mock treated as well as hTBM treated with TCT and LPS alone were able to clear the particles after the 24 hours treatment. A strong effect on particle movement was seen only in TCT/LPS treated hTBM where the particles oscillate around their point of origin in TCT/LPS treated hTBM. (Adapted from Kessie et al., 2020)

2.3.3 TCT action leads to loss of barrier function in hTBM

To best of our knowledge, the effect of TCT/LPS on the tight junction organization of the airway mucosa has not previously been described. Due to tight junction proteins being apically located (Reviewed by Zihni et al., 2016), it was hypothesized that the observed toxin induced blebbing and epithelial cell extrusion may concomitantly affect the tight junctions. Thus, the tight junction organization and function were assessed by measuring the transepithelial electrical resistance (TEER) and FITC-Dextran permeability of the hTBM before and after incubation with the toxins. In addition, the models were also immunostained for the tight junction markers ZO-1 and the adherens junction marker E-cadherin. As shown **Figure 2-8A**, mock treating of the hTBM with its apical side covered with media for 24 hours already caused a 48.06% decline in the TEER. Treatment of the hTBM with TCT alone induced a statistically insignificant further decline of 8.55% in TEER compared to 24 hours mock treated hTBM. LPS alone induced a significant decline of 64.04% in the TEER after the 24 hours incubation period. hTBM incubated with TCT/LPS experienced the most significant decline of 79.44% in TEER. Thus, the decline in TEER caused by the combination of TCT and LPS varied significantly compared to hTBM treated with either toxins alone or mock treated. TEER is a highly sensitive parameter and even minor disruptions in the tight junctions are known to cause very significant effects, therefore, the barrier integrity of the models was further assessed with the FITC-Dextran permeability assay. Interestingly, although the TEER for mock treated models under submerged conditions was already significantly reduced after the 24 hours incubation period, the models did not experience a higher permeability to FITC-Dextran after the same incubation period. Similarly, the LPS treated hTBM did not show a significant increase in FITC-Dextran permeability. However, the hTBMs treated with TCT alone or with TCT/LPS showed significant decreases in their barrier integrity. TCT/LPS treatment particularly induced a very

significant increase in the permeability of the models to the FITC-Dextran as shown in **Figure 2-8B**.

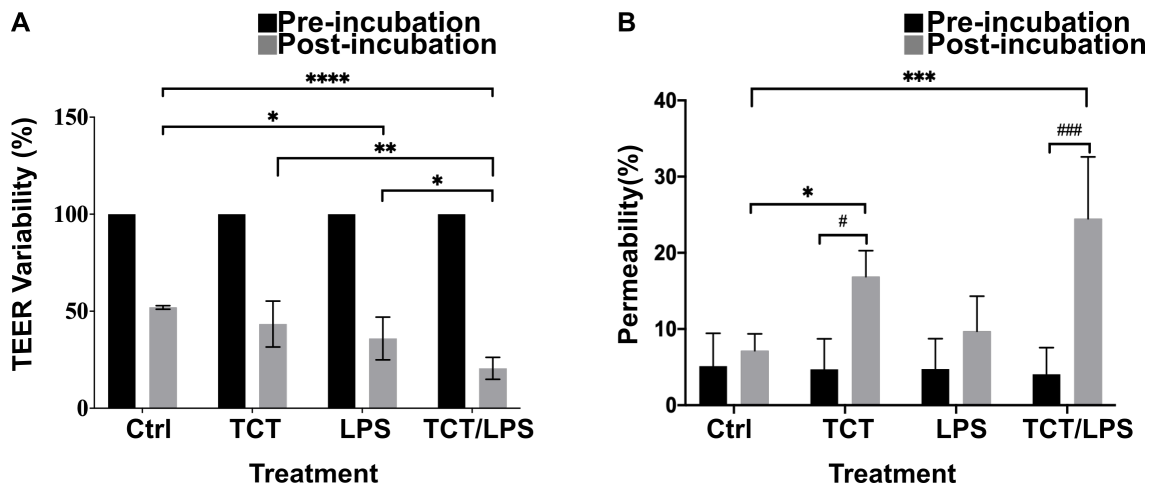


Figure 2-8 TCT and LPS impair the barrier function of the hTBM. **(A)** The TEER of the hTBM treated with TCT, LPS and TCT/LPS as well as mock treated controls were measured before and 24-hours after incubation. The variability in TEER was measured relative to pre-incubation TEER and expressed as a percentage. Submerged conditions alone already caused a significant decrease in TEER in all treatment groups. Models incubated with TCT/LPS and LPS alone had the most significant effect on TEER variability after 24 hours. Asterisks represent statistical significance of barrier integrity after 24 hours between the different treatment groups tested by Tukey’s two-way ANOVA (* $p \leq 0.05$ ** $p \leq 0.01$ *** $p < 0.0005$, **** $p < 0.0001$). **(B)** The permeability (%) of the hTBM to 4-kDa FITC-Dextran was determined before and after 24 hours toxin incubation. The statistical significance of the permeability of the hTBM within the same treatment groups before and after toxin treatment was also tested (# $p \leq 0.05$, ### $p \leq 0.005$). The graphs represent mean permeability (SEM) of 3 independent experiments. (Reproduced with permission from Kessie et al., 2020)

The disruptive effect of the TCT and LPS on the tight junctions was additionally assessed by immunostaining for junctional complex proteins ZO-1 and E-cadherin. As shown in **Figure 2-9A**, incubation of the hTBM with the luminal surface covered with media led to minor disruptions in the ZO-1 and E-cadherin expression pattern (arrowheads). The expression of ZO-1 and E-cadherin by the mock treated hTBM showed disruptions of the typical honeycomb structure. Compared to the mock control however, TCT and LPS either alone or in combination had a much more dramatic effect on the organisation of the two junctional proteins. These observations are in line with the observed decreases in the TEER values post toxin incubation.

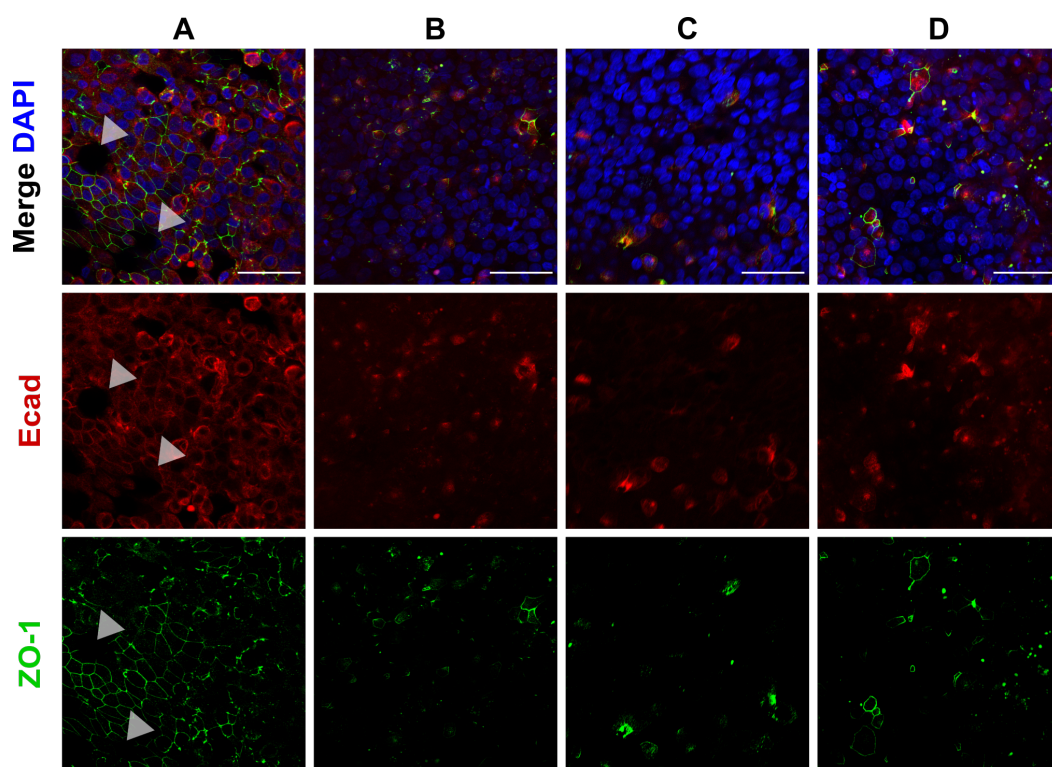


Figure 2-9 TCT and LPS disrupt tight junction organisation.

24 hours treated hTBM were fixed with 4% PFA and the whole model was immunostained for ZO-1 and E-cadherin. **(A)** Mock treated hTBM maintained the tight junction organisation of ZO-1 and E-cadherin after 24 hours. Areas of tight junction disruption are indicated by white arrow heads. hTBM incubated with TCT **(B)**, LPS **(C)**, and TCT/LPS **(D)** showing complete loss of ZO-1 and E-cadherin expression and organisation after 24 hours. **Scale bar:** 50 μ m (Reproduced with permission from Kessie et al., 2020)

2.3.4 TCT elicits iNOS-dependent nitric oxide release from the hTBM

Previous reports based on animal models have implicated nitric oxide (NO) in the disruptive effect of TCT on the airway epithelia (Heiss et al., 1993a; Heiss et al., 1994; Flak and Goldman, 1996; Abramson et al., 2001). To determine if the toxins induced significant levels of NO, the hTBM were incubated with the toxins as previously described and the apical and basal supernatants were analysed for dissolved nitric oxide. **Figure 2-10A** shows the results of the dissolved NO concentration in the supernatants collected from the apical and basal compartments from apically treated hTBM. NO measured in media from the apical compartment was volume corrected to remove the bias due to the media volume differences in the apical and basal compartment. The dissolved NO in the basal compartment was significantly ($p < 0.0001$) higher when compared to the volume corrected apical concentrations for all treatment groups. However, the concentration of the dissolved NO did not vary significantly when comparing

media from the different toxin treatments in either the apical or basal compartments. In further tests, the hTBM were removed from the cell crowns and incubated completely submerged in 1ml each of 3 μ M TCT, 100ng/ml LPS and TCT/LPS for 24 hours. A mock control of fresh warm mix medium without any toxin was also set up. 100 μ l of the supernatants from the different treatment groups was collected and the NO concentration determined using the Griess test. The results of the Griess test were subjected to an ordinary one-way ANOVA to determine if the different treatments induced significant release of NO after the 24 hours incubation (**Figure 2-10B**). Interestingly, the models incubated completely submerged in TCT/LPS showed a statically significant release of NO compared to mock treated hTBM. As shown in **Figure 2-10B**, the hTBM treated with either TCT alone ($p=0.1242$) or LPS alone ($p=0.2475$) did not induce significant levels of NO in the supernatant although they consistently showed a tendency towards increased NO production. Finally, the potential effect of ventilation on the NO concentration was investigated, since there is a possibility that NO may not be able to accumulate to concentrations which may be toxic to the airway epithelial cells *in vivo* due to high ventilation occurring in the human respiratory tract. Thus, to deduce the effect of ventilation on the concentration of NO that dissolved in the supernatants, the models were vented periodically by opening the lid of the plate under a flow hood. As shown in **Figure 2-10C**, ventilation did not have any significant effect on the concentration of NO in the supernatants.

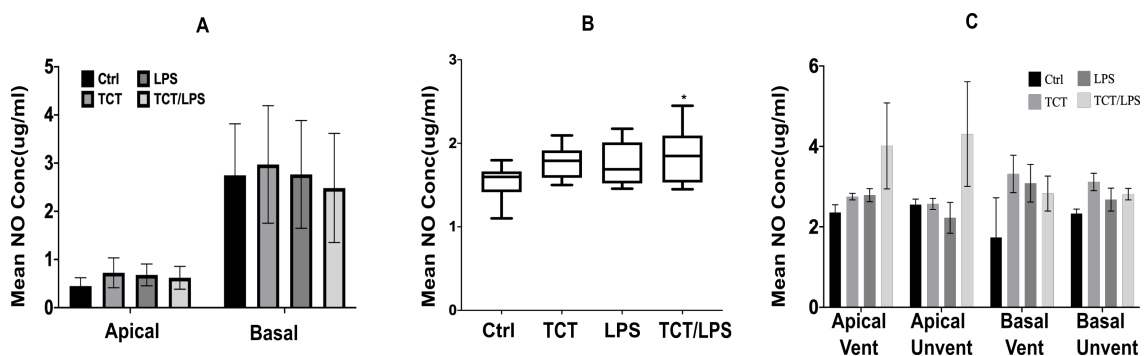


Figure 2-10 TCT/LPS induces significant NO in completely submerged hTBM. Mature hTBM were incubated with 3 μ M TCT, 100ng/ml LPS, a combination of TCT/LPS and a mock control of mixed media without any toxin. 50 μ l of the supernatants were used to determine the mean nitric oxide concentration using the Griess test in hTBM with apically applied toxins. **(A)** The mean NO in the apical compartment was divided by a factor of 5 to remove bias due to media volume differences in the apical and basal compartments. The graph represents mean NO \pm SEM (Error bars) of 6 independent experiments. **(B)** The boxplot represents mean NO in supernatants from hTBM

completely submerged in fresh media, 3 μ M TCT, 100ng/ml LPS and TCT/LPS. An ordinary one-way ANOVA followed by Tukey's post-hoc analysis yielded a statistically significant difference in TCT/LPS treated hTBM compared to control (n=3) (*p= 0.0174). (C) Comparison of NO from apically treated hTBM either ventilated or unventilated to mimic the *in vivo* situation in the airway. Bar chart represents mean \pm SEM of at least three independent experiments performed in duplicate. (Adapted from Kessie et al., 2020)

To determine if the apparent toxin mediated NO expression was due to the inducible nitric oxide synthase, the treated hTBM were fixed in 4% PFA and analysed by immunostaining with anti-iNOS specific antibodies which do not cross-react with the constitutive and endothelial nitric oxide synthases also present in the tissues. The models were immunostained without sectioning. Additionally, the hTBM were counterstained with the epithelial cell marker CK18. Confocal microscopy of the immunostained models showed that both TCT and LPS alone as well as in combination induced an increased expression of the iNOS in the hTBM compared to the mock treated controls (**Figure 2-11**), thus further supporting the notion of toxin induced NO production in the hTBM.

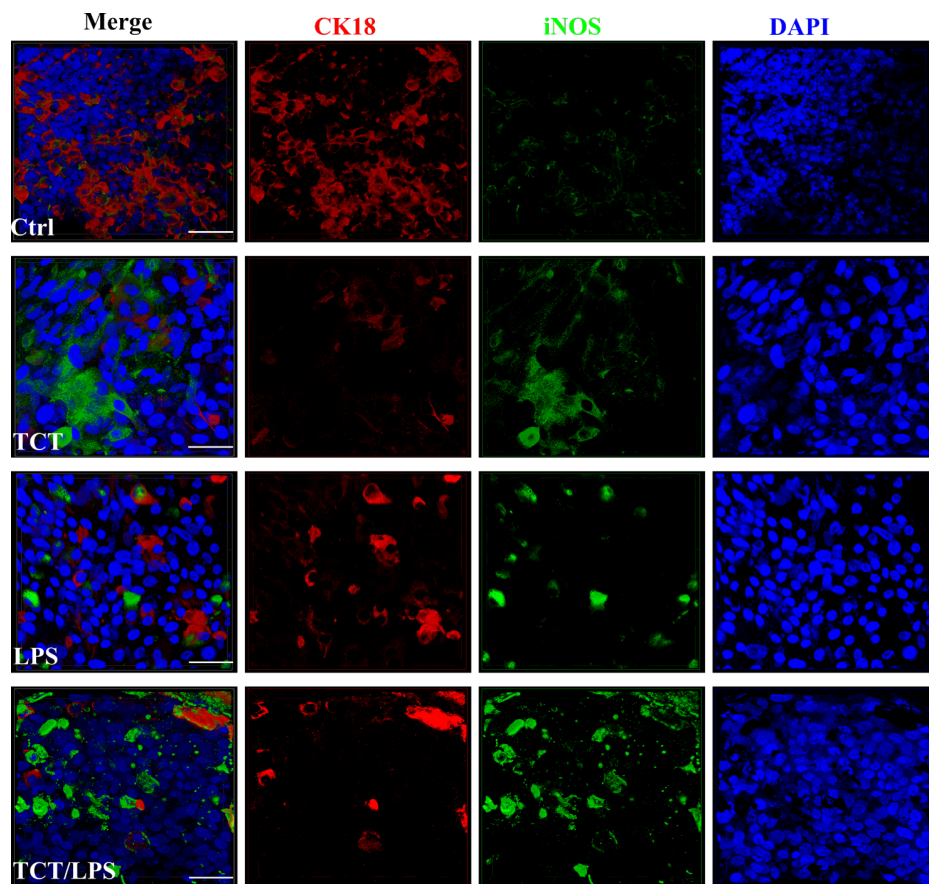


Figure 2-11 TCT and LPS induce expression of iNOS.

24 hours toxin treated hTBM were fixed and the whole models were immunostained with anti-iNOS specific antibody. The models were counterstained with the epithelial cell marker CK18. Compared to mock treated controls, TCT and LPS alone as well as in

combination induced a higher expression of iNOS in the hTBM. iNOS expression did not colocalise with CK18-positive cells. **Scale bar:** 50µm (Reproduced with permission from Kessie et al., 2020)

2.3.5 hTBMs express SLC46A2 transmembrane receptor

The induction of inflammation by the muramyl peptides such as TCT has previously been shown to be mediated by cytoplasmic NOD-like receptors (Strober et al., 2006). This interaction requires the translocation of the muramyl peptides from the extracellular space into the cytoplasm by transmembrane transporter proteins. Paik et al. (2017) recently reported that the thymic stromal cotransporter homolog which is encoded by the Solute Carrier Family 46 Member 2 gene (*SLC46A2*) facilitated TCT interaction with NOD1. To assess if the hTBM indeed expressed this transporter, the models were fixed in 4% PFA and paraffin embedded. 5µm sections of the paraffin embedded tissues were then immunostained for SLC46A2. As shown in **Figure 2-12**, the hTBM expressed the SLC46A2 transporters in the epithelial layer.

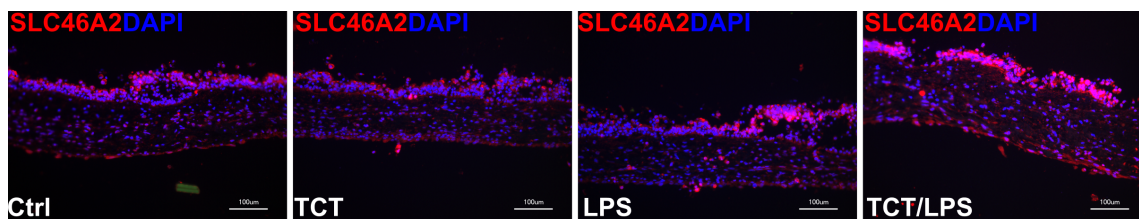


Figure 2-12 3D human tracheobronchial mucosa models express SLC46A2. hTBM were developed as previously described. 24-hours toxin and mock control treated hTBM were fixed in 4% PFA for 2 hours at RT and embedded with paraffin. 5µm sections of the paraffin embedded hTBM were cut, deparaffinated and immunostained for the transmembrane transporter SLC46A2 (red dots). **Scale bar:** 100µm. (Reproduced with permission from Kessie et al., 2020)

2.3.6 TCT induces inflammatory cytokine expression in hTBM

The disruptive effect of TCT in the pathology of pertussis has been linked to the induction of proinflammatory cytokines, especially to interleukin 1 (Flak et al., 2000). Exogenously added IL-1 has been shown to induce a similar response in epithelial cells as TCT (Heiss et al., 1993b; Kim et al., 2015). IL-1 is therefore implicated as an intermediary in the disruptive effect of TCT on the respiratory mucosa in hamster tracheal epithelial cells (Heiss et al., 1993b). It therefore remains to be demonstrated that TCT can induce IL-1 independently *in vivo* in humans as well. To assess the ability of TCT to induce IL-1, the toxin treated

hTBM were fixed with 4% PFA on the cell crown overnight at 4°C. The whole model was then blocked with 5% BSA containing 0.1% TritonX-100 and immunostained for IL-1 α and IL-1 β . Analysis of the immunostained hTBM with confocal microscopy showed that TCT and LPS either alone or in combination are able to induce a clear increase in the expression of both IL-1 α and IL-1 β after 24 hours (**Figure 2-13**).

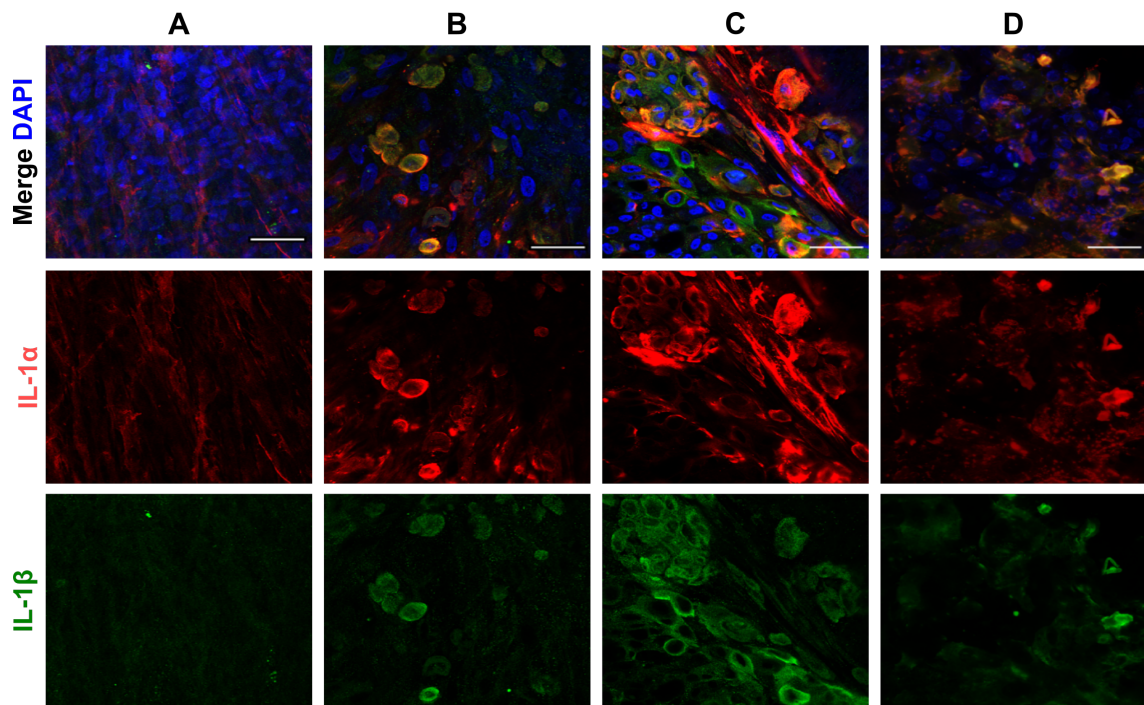


Figure 2-13 TCT/LPS induce IL-1 expression in hTBM.

hTBM were treated as previously described with 3 μ M TCT, 100ng/ml LPS and TCT/LPS for 24 hours. The hTBM were fixed overnight at 4°C, washed with cold PBS and the whole models were decorated with anti-IL-1 α and anti-IL-1 β antibodies. The models were counterstained with fluorescently conjugated secondary antibodies and analysed using a laser scanning confocal microscope. Compared to mock treated controls (**A**), the hTBM treated with TCT(**B**) and LPS (**C**) alone and TCT/LPS (**D**) clearly show a higher expression of both IL-1 α and IL-1 β after 24 hours. **Scale bar:** 50 μ m (Reproduced with permission from Kessie et al., 2020)

To prove whether the induction of these cytokines by the toxins was also detectable on the transcriptional level, the expression of their genes was measured on the mRNA level by RT-qPCR. For this purpose, the tissues were lysed, and total RNA was isolated from the 24 hours treated hTBM. The relative gene expression analysis showed a 2-fold increase in the *IL-1 α* expression due to TCT alone and the TCT/LPS combination (**Figure 2-14A**). *IL-1 β* expression however seemed to be suppressed by the combination of TCT and LPS after 24 hours incubation compared to the mock treated controls. Statistical comparison

using an ordinary one-way ANOVA followed by a post hoc Tukey multiple comparison yielded statistically insignificant differences of the *IL-1 α* and *IL-1 β* expression data (**Figure 2-14 A, B**). To determine if the toxins induced the expression of other inflammatory cytokines in the hTBM, the induction of the proinflammatory cytokine *IL6*, and the anti-inflammatory cytokine *IL10* were also assessed at the mRNA level. As displayed on **Figure 2-14C**, TCT and LPS alone appeared to downregulate the expression of *IL6* after 24 hours. However, the combination of TCT and LPS showed a tendency towards *IL6* upregulation compared to mock treated controls. Compared to either toxin alone, TCT/LPS showed statistically significant upregulation of *IL6* in the hTBM after 24 hours (**Figure 2-14C**). Either toxins alone or in combination did not seem to significantly impact the induction of *IL10* from the hTBM compared to the mock treated controls after 24 hours (**Figure 2-14**).

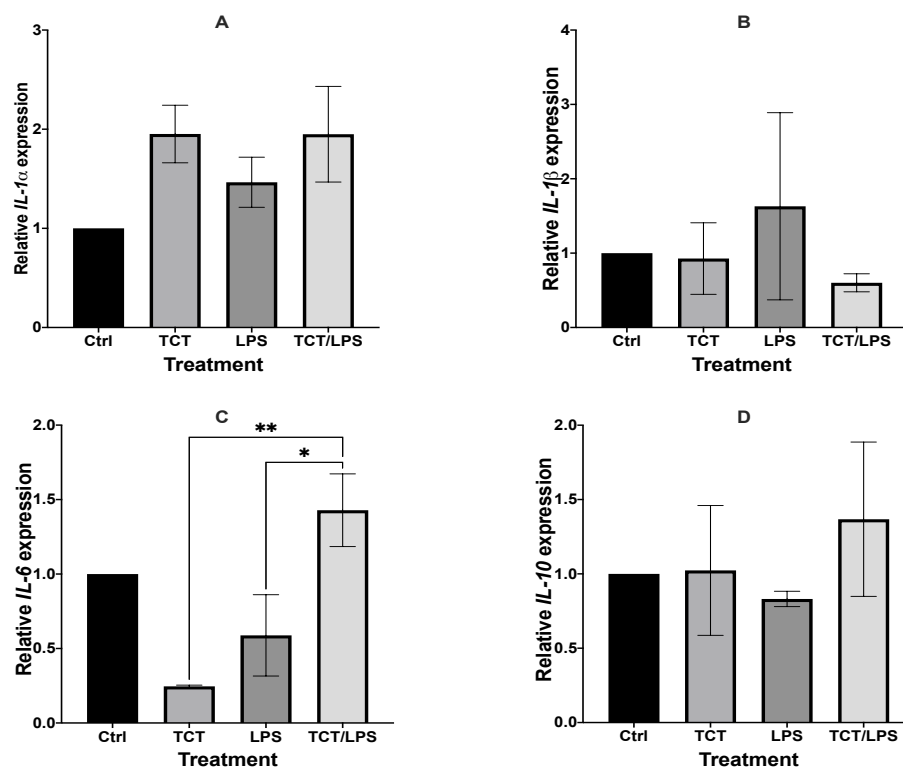


Figure 2-14 Inflammatory cytokine gene expression analysis of TCT and LPS.

The relative gene expression of *IL-1 α* , *IL-1 β* , *IL-6* and *IL-10* of hTBM treated with 3 μ M TCT, 100ng/ml LPS and TCT/LPS for 24 hours was measure after total RNA extraction using RT-qPCR. The inflammatory cytokine gene expression was normalised to *GAPDH* expression. (**A**) TCT and TCT/LPS showed a 2-fold relative increase of *IL-1 α* gene expression after 24 hours compared to controls, while LPS alone induced a 1.5-fold change. However, these data did not prove to be statistically significant. (**B**) TCT and LPS alone had insignificant effect on the *IL-1 β* expression fold change after 24 hours incubation. The combination of TCT/LPS seem to suppress the expression of *IL-1 β* after

24 hours, although again not significant statistically. **(C)** TCT alone and LPS had a suppressive effect on *IL-6* expression in the hTBM after 24 hours but this effect was statistically not significant compared to mock control. Instead, the combination of TCT/LPS induced a significant increase of *IL-6* expression when compared to mock control. TCT/LPS induced a significant *IL-6* expression compared to models treated with TCT and LPS alone after 24 hours. **(D)** Toxin treated models did not induce significant relative expression of *IL-10* compared to mock treated controls. Data presented represent means (bar) and standard error (error bars) of 3 independent experiments performed in duplicates. The expression fold change was submitted to an ordinary one-way analysis of variance and a Tukey's post-hoc test for multiple comparisons at a confidence interval of 95% (^{ns} $p>0.05$, $p<0.05$, $**p<0.01$). (Reproduced with permission from Kessie et al., 2020)

Since the cytokine expression data at the transcriptional level were mostly statistically insignificant at 24 hours, the effect of the toxins on inflammatory cytokine expression and secretion into the supernatant was additionally assessed using the cytometric bead array (CBA). The CBA data did not show statistically significant increase in the $IL-1\beta$ expression in the hTBM treated with either toxins alone or in combination. Despite these statistically insignificant results, the toxins appear to induce an apically directed secretion of $IL-1\beta$ (**Figure 2-15A**). Similarly, either toxin alone or in combination did not significantly induce the release of $IL-8$ from the hTBM after 24 hours into the supernatant. The combination of TCT/LPS however showed a strong tendency ($p=0,0563$) to provoke $IL8$ secretion into the apical compartment (**Figure 2-15C**). As shown in **Figure 2-15B**, incubation of the hTBM with TCT alone and in combination with LPS showed an at least 10-fold increase in $IL-6$ secretion into the supernatants from the basal compartments compared to mock treated hTBM. A significant increase in the expression of the inhibitory $IL-10$ was observed in TCT/LPS treated models (**Figure 2-15D**). Taken together, although partially statistically not significant, the data indicate that TCT and LPS may modulate the expression of proinflammatory cytokines besides $IL-1$ as well as other proinflammatory cytokines in the airway epithelial cells.

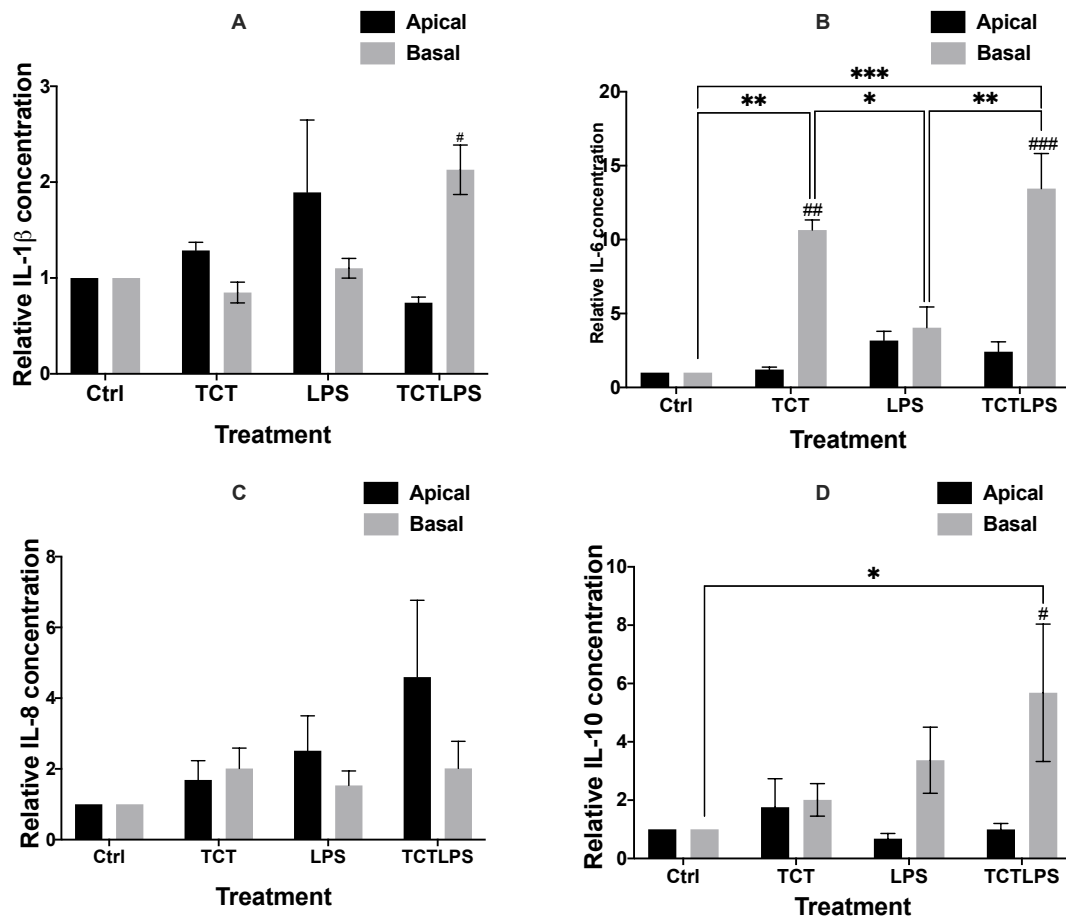


Figure 2-15 Toxin induced inflammatory cytokine secretion into cell culture supernatant. The cell culture supernatants from the apical and basal compartments were analysed for secreted IL-1 β (A), IL-6 (B), IL-8 (C), IL-10(D) post toxin treatment. The concentrations (pg/ml) from the different treatment groups were normalized to the mock treated hTBM to eliminate donor variations and expressed as relative concentration. Data represents means \pm SEM of at least 3 independent experiments performed in duplicate. * shows statistical significance between the different treatment groups (* p <0.05, ** p <0.01, *** p <0.001) and # indicates statistically significant difference between apical and basal compartment of the same treatment group (## p <0.01, #### p <0.0005). All comparisons that did not show statistical significance do not carry any annotations on them. (Reproduced with permission from Kessie et al., 2020)

2.4 Single cell RNA-sequencing of *B pertussis* infected cells

Single cell RNA-sequencing (scRNA-seq) has so far mostly been performed with intracellular bacteria and their infected host cells but not with extracellular adherent bacteria. This is due to the relative ease of isolating cells infected with bacteria typically expressing a fluorescent marker by cell sorting. *Bordetellae* are classically considered extracellular pathogens although invasive forms have been reported. In addition, the methods available to dissociate tissues into single cell suspension required for scRNA-seq also result in the separation of the bacteria which are only adherent to their host cells. There is therefore the need

to establish a method to reproducibly infect and isolate bacteria associated cells from the models in order to analyse the transcriptome of the different cell populations by single cell analytics. To achieve this, the engineered airway mucosa models were infected with *B. pertussis* to determine the optimum multiplicity of infection and to assess whether the epithelial cells in the models can be invaded by bacteria.

2.4.1 Interaction of *B. pertussis* with airway mucosa models

Bordetella pertussis interacts preferentially with the ciliated cells of the airway mucosa cells where they can form microcolonies. The bacteria may even form biofilms and may also adhere to nonciliated cells such as the mucus producing goblet cells (de Gouw et al., 2011; Cattelan et al., 2017). The number of epithelial cells in the models was estimated to be between 8×10^5 - 10^6 cells on a 1.2cm^2 area cell crown. The number of adherent *B. pertussis* on ciliated cells varies with the density of inoculum (Tuomanen and Hendley, 1983). Previous studies with *B. pertussis* frequently utilised a very high multiplicity of infection (MOI) of 100 -150 which may not reflect the natural situation. To determine an appropriate MOI at which optimum adherence is observed after 6 hours, the models were inoculated with *B. pertussis* Tohama 1 diluted to an OD_{600} of 0.1, 0.01 and 0.001 corresponding to MOI 100, MOI 10 and MOI 1 respectively in mixed medium. As shown in Figure 2-16, the number of cell-associated bacteria recovered after 6 hours did not vary significantly between cells inoculated at MOI 100 and MOI 10. However, 2.62% of the initial inoculum was recovered from models inoculated at MOI 10 compared to 0.26% from those inoculated at MOI 100. The number of adherent *B. pertussis* to the models therefore seemed to be optimal at MOI 10 after 6 hours. Further infection experiments with the models were therefore performed with an MOI of 10.

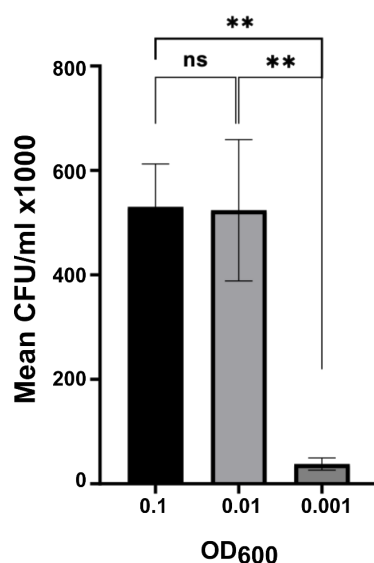


Figure 2-16 Determination of an optimal MOI for infection of engineered airway models. Human tracheobronchial mucosa models were inoculated for 6 hours with *B. pertussis* Tohama 1 wildtype at OD600 of 0.1, 0.01, 0.001 which are respectively equivalent to MOI 100, MOI10 and MOI 1. The graph represents the means (SE) of three independent experiments performed in duplicate. * represents statistical significance using Tukey's one-way ANOVA (^{ns}p= not significant, **p< 0.01).

The adherence of *B. pertussis* to nasal brush biopsies has previously been reported to vary with the length of ciliated cell exposure to the bacteria showing a plateau at 3 hours when inoculated with bacteria, however using a large excess of bacteria (MOI 20000) (Tuomanen and Hendley, 1983). To determine if a similar phenomenon would occur in the engineered airway mucosa models, the models developed by co-culturing primary tracheobronchial fibroblasts with either primary tracheobronchial epithelial cells (hTBM) or the HBEC3-KT immortalised tracheobronchial cell line (hBM) were inoculated at a MOI of 10 for 6 hours and 24 hours. Adherent as well as intracellular bacteria were assessed at 6 hours and 24 hours post infection. A student's *t-test* showed that significantly more adherent bacteria ($p < 0.0001$) were recovered from the hTBM compared to the hBM 6 hours post infection. As summarised in **Figure 2-17A**, 2.70×10^5 cfu/ml representing 1.3% of the inoculated bacteria were recovered from the hTBM while only 2.5×10^2 cfu/ml representing 0.001250% of the inoculated bacteria were recovered from the hBM. However, the number of adherent bacteria was nearly identical between hTBM and hBM 24 hours post infection with 4.16% and 4.02% of the inoculated bacteria recovered respectively. The cell invasiveness of the bacteria was also assessed using the gentamicin protection assay with hTBM and hBM inoculated at MOI 10 at 6 - and 24 - hours post infection. Interestingly, as shown in **Figure**

2-17B, intracellular *B. pertussis* were already observed 6 hours post infection in the hTBM but not in hBM and 970 ± 156 cfu/ml representing 0.0005% of initial inoculum were recovered from the hTBM. Surprisingly, much higher numbers of intracellular bacteria were recovered from both hTBM and hBM 24-hours post infection with about twice as many intracellular bacteria found in the hTBM (0.203%) as compared to 0.100% of the initial inoculum in the hBM. Taken together, the data indicate that cilia may be critical for early adherence and subsequent invasion of the airway epithelia.

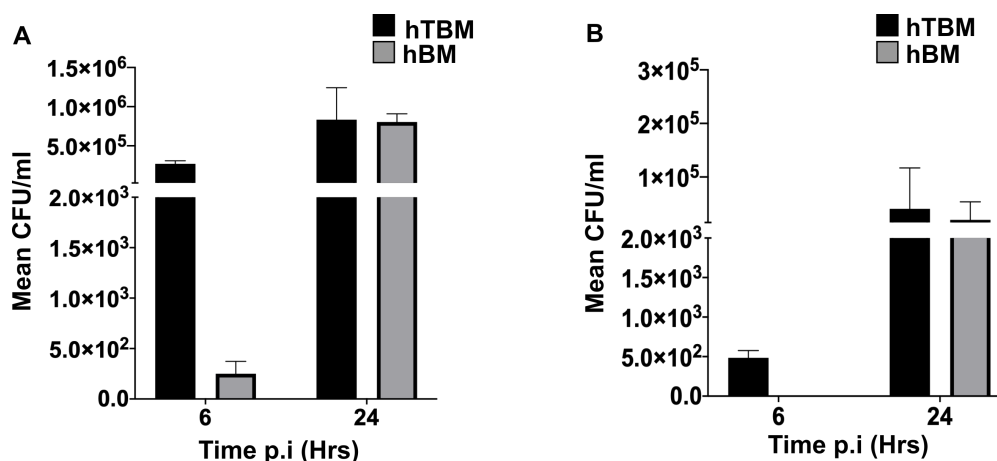


Figure 2-17 *B. pertussis* adherence to and cell invasion in airway mucosa models. Airway mucosa models developed from primary tracheobronchial epithelial cells (hTBM) and immortalized HBEC3-KT cells (hBM) were infected with *B. pertussis* wildtype at a relative MOI10. **(A)** Comparison of the number of adherent bacteria as obtained by counting the colony forming units after 6 hours and 24 hours post infection in primary and immortalised airway epithelial cell models. **(B)** Results of the gentamicin protection assay performed at 6 hours and 24 hours post infection. Graphs represent means \pm SE of 3 independent experiments performed in duplicate.

2.4.2 Persistence of *B. pertussis* in engineered airway mucosa models.

Previous studies have shown that *B. pertussis* is able to invade and persist in both professional and nonprofessional immune cells for 24 hours (Schipper et al., 1994; Lamberti et al., 2013; Fedele et al., 2017; Cafiero et al., 2018). Long-term studies using monocultures of immortalised epithelial cell lines such as HeLA, Caco-2 and A549 have reported intracellular persistence of *B. pertussis* for up to 4 days (Schipper et al., 1994). The ability of *B. pertussis* to invade the epithelial cells of the models and its intracellular survival potential were assessed with the polymyxin B protection assay. When the models were inoculated with bacteria at MOI10 for 6 hours, the intracellular bacteria were completely cleared 24 hours after polymyxin B treatment. Hence, intracellular survival assays were performed

with the models inoculated at MOI50 for 24 hours to ensure optimal invasion prior to polymyxin B treatment. To achieve this, the models were incubated with *B. pertussis* at MOI of 50 for 24 hours and washed to remove non-adherent bacteria before incubating with 100µg/ml polymyxin B for 2 hours to kill the extracellular bacteria. The models were subsequently incubated for a further 7 days with only 10µg/ml polymyxin B to avoid intracellular killing of the bacteria. As shown in **Figure 2-18A**, both the hTBM and hNM showed significantly high susceptibility to invasion by *B. pertussis* compared to hBM after 24 hours. However, the number of viable bacteria declined rapidly after a further 24 hours and no viable bacteria were detected after 72 hours anymore, indicating the bacteria are unable to survive intracellularly for a prolonged time (**Figure 2-18A**). A control experiment was also set up by infecting hTBM as described above and after initial killing of extracellular bacteria with 100µg/ml polymyxin B, the hTBM was thoroughly washed with PBS and cultured for up to 7 days without polymyxin B to ensure that the drug did not interfere with intracellular survival in the previous experiments. The shedding of viable bacteria into the apical compartment was assessed daily for the 7 days by washing the apical compartment with 100µl PBS and plating it on BGA. Interestingly, no growth was observed on the BGA plates from samples throughout the 7 days without polymyxin B treatment. To determine the intracellular localisation of the *B. pertussis*, hTBM models were infected with a GFP expressing *B. pertussis* *Tohama 1* strain and treated with polymyxin B as previously described for 5 days since in the previous experiments, no viable bacteria were obtained after 5 days. The hTBM was then fixed with 4% PFA overnight at 4°C. A whole mount staining with the late endosomal/lysosomal marker LAMP1 was performed together with the epithelial cell marker pan-cytokeratin to determine the intracellular localisation of bacteria. As shown in **Figure 2-18B** some of the intracellular bacteria colocalised with LAMP1-positive domains. However, a subpopulation of the intracellular bacteria seemed to be located outside LAMP1-positive endosomal domains in the hTBM up to 48 hours after polymyxin B treatment as previously described for *in vitro* A549 infected with *B. pertussis* by Lamberti et al. (2013).

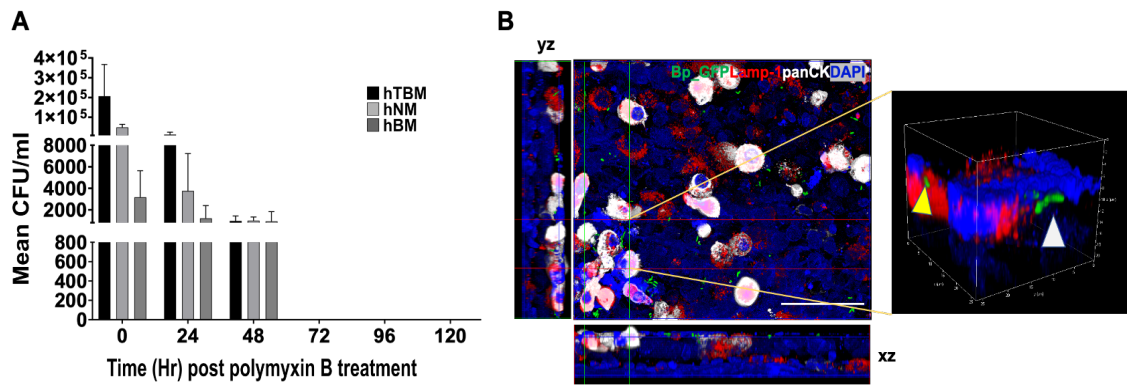


Figure 2-18 Invasion and persistence of *B. pertussis* in airway mucosa models. **(A)** Airway mucosa models were developed and infected with *B. pertussis* (MOI=50) for 24 hours, washed to remove nonadherent bacteria and treated with 100 μ g/ml polymyxin B to kill extracellular bacteria. The models were then incubated for a further 5 days with 10 μ g/ml polymyxin B. The mean (SE) of viable intracellular *B. pertussis* at the various time points was determined from at least three independent experiments performed. **(B)** Mature hTBM were also inoculated with Bp_TH1_GFP as previously described. A polymyxin B protection assay was performed and the whole model was immunostained with the epithelial cell marker and late endosomal marker LAMP1. The image shows intracellular *B. pertussis* (green) localised in acidic LAMP1 positive endosomes (yellow arrowhead) as well as in nonacidic compartments (white arrowhead) in hTBM after 48 hours polymyxin B treatment. **Scale bar:** 50 μ m

2.4.3 Detachment of cells from the airway mucosa models

As shown above, both adherent and intracellular *B. pertussis* were observed in the hTBM after 6 hours, hence, attempts were made to establish a protocol to reliably separate the bacteria-associated cells from bystanders by using the laser-capture microdissection (LCM). This method required the samples to be snap-frozen in order to preserve the RNA and sectioned prior to the dissection. However, the tissues became extremely distorted and the epithelial morphology could not be distinguished anymore after snap-freezing (**Figure 2-19**). Fixing the tissue models with ice cold methanol prior to snap freezing did not solve the distortion problem. Foley et al. (2019) recently published a method for scRNA-seq of formalin fixed paraffin embedded (FFPE) samples using the smart-3seq method. However, formalin covalently modifies nucleic acid bases and cleaves RNA strands. This was avoided by fixing the tissue with Methacarn (60% methanol, 30% chloroform, 10% glacial acetic acid) which is known to preserve RNA better than formalin. However, due to strong autofluorescence of the models and the difficulty in locating bacteria-associated cells from the 10 μ m sections, the use of LCM to capture bacteria associated host cells was near impossible.

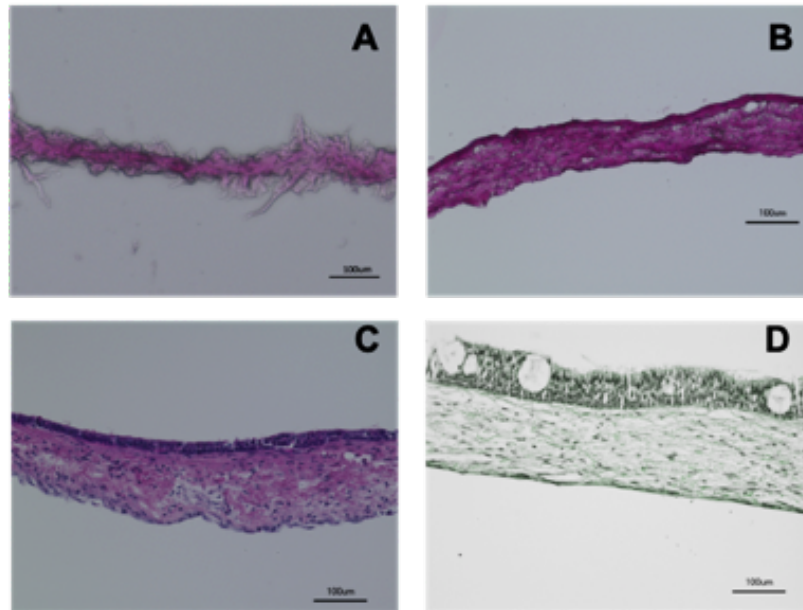


Figure 2-19 Comparison of different fixative methods for LCM.

Different fixative methods were used to determine the most appropriate method to preserve the epithelial architecture for laser capture micro-dissections (LCM). hTBM were developed as previously described, fixed and 10µm sections were cut and stained with haematoxylin and eosin. **(A)** Unfixed tissue models became extremely distorted upon snap-freezing. **(B)** Methanol fixed tissues did not maintain the epithelial architecture after snap-freezing. **(C)** Methacarn fixed paraffin embedded tissues maintained the architecture of the epithelia. **(D)** Tissue models were strongly auto-fluorescent in the GFP channel thus making the identification of bacteria associated epithelial cells impossible in the sections. **Scale bar: 100µm**

An alternate method to detach the cells from the scaffold with trypsin resulted in cell fragmentation while adding noise to the transcriptome of the cells. Therefore, a cold dissociation method using *Bacillus licheniformis* subtilisin A protease was used as described by O'Flanagan et al. (2019) but without the addition of EDTA. Using trypan blue, we observed a very high viability of up to 90% with little fragmentation using the cold dissociation method compared to warm dissociation with trypsin/EDTA. As shown in **Figure 2-20**, 78.8% of the cells were confirmed to express the epithelial cell marker panCK. Due to the high viability of the dissociated cells, the use of cold dissociation with the *B. licheniformis* subtilisin A serine protease seems to be the best suited method for dissociation of cells from the 3D tissue models for transcriptome analysis using scRNA-seq.

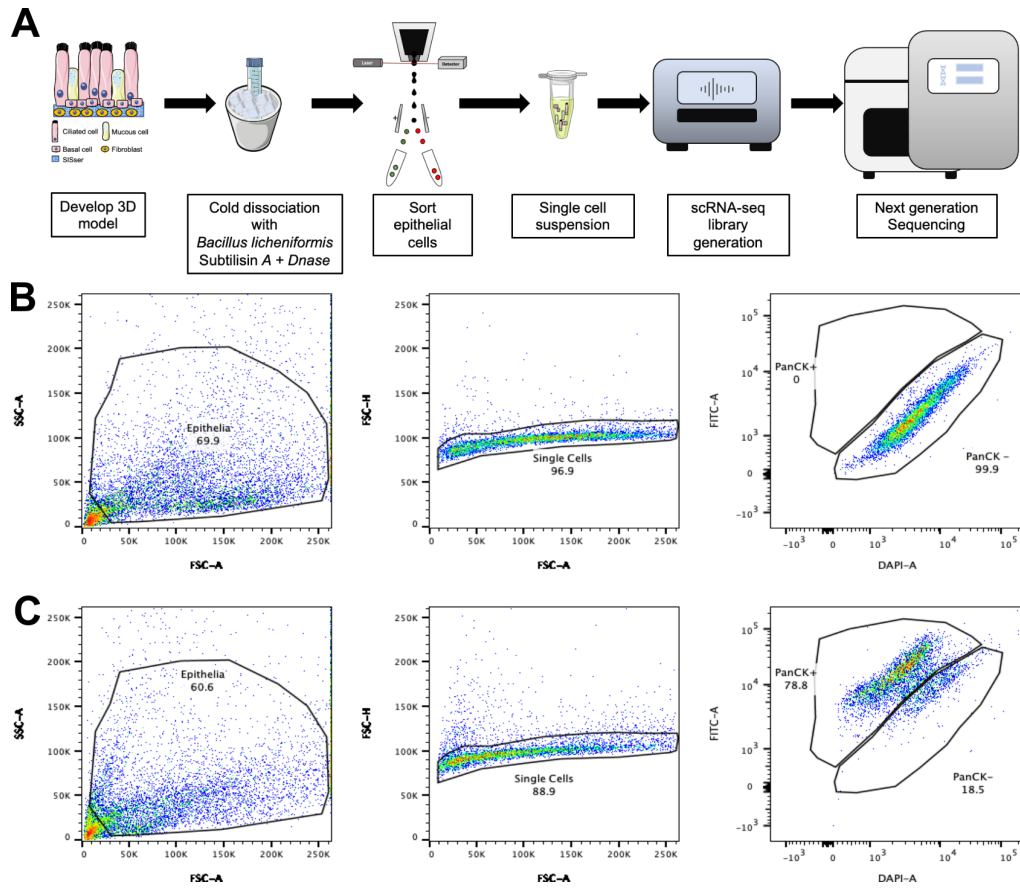


Figure 2-20 Cold dissociation of epithelial cells from 3D models with serine protease. (A) Airway mucosa models are developed by co-culturing human tracheobronchial epithelial cells and fibroblasts at ALI for 21 days. Mature models are removed from cell crown and incubated with 10mg/ml *B. licheniformis* subtilisin A protease on ice for 30 minutes. DNase was added to the solution. The dissociated cells were passed through a 4 μ m cell sieve and the epithelial cells were sorted using BD FACS Aria III. scRNA-seq libraries were then prepared from the single cell suspension for NGS sequencing. Dissociated cells were stained with panCK and Epcam (C) and sorted to determine the proportion of the cells that were epithelial cells by comparing them to the unstained population (B).

3 Discussion

Bordetella pertussis causes the whooping cough disease in humans. It is an obligate human pathogen with no known animal reservoir. Thus, in the past, experimental models of pertussis had to rely mainly on laboratory animals, organ cultures from animal tissues, epithelial cell lines and 2-dimensional human cell culture models (Wilson et al., 1991; van den Akker, 1997; van den Berg et al., 1999; Ishibashi et al., 2001; Gueirard et al., 2005; Magalhaes et al., 2005; Lamberti et al., 2013). Despite providing important information about the interaction of *B. pertussis* with the respiratory mucosa, animal models may not be appropriate due to interspecies differences (Reviewed in Jansen et al., 2020) while flat cultures lack the complexity of tissues. Furthermore, much of the information about the basics of virulence properties was gathered using the closely related species *B. bronchiseptica* which expresses most of the virulence factors known from *B. pertussis* and which causes respiratory infections in various mammals including rodents, dogs and pigs. Furthermore, the use of immortalised and cancer cell lines in 2-dimensional culture has the drawback of lacking the architecture and polarisation of the airway mucosa *in vivo*. The advent of tissue engineering has enabled the development of true-to-form human tissues for *in vitro* studies with results directly translatable to humans (Bonassar and Vacanti, 1998; Mertsching et al., 2005; Alaribe et al., 2016; Schweinlin et al., 2016; Schweinlin et al., 2017; Heydarian et al., 2019; Linkous et al., 2019). To engineer various human tissues, cells isolated from donor material, or immortalised or cancer cell lines are seeded on biocompatible scaffolds in appropriate media for a number of days or weeks before they differentiate properly and reach maturity. Under the appropriate conditions, these cell models develop polarity and show high *in vivo*-*in vitro* correlation. This thesis uses the human airway mucosa models based on those published by Schweinlin et al. (2017) to study the interaction of *B. pertussis* with the human airway epithelia. These models do not only provide the opportunity for studies using model systems closely resembling the *in vivo* situation, but they also allow for the generation of data that may be directly relevant in humans.

3.1 Establishment and optimization of 3D airway mucosa models.

The airway epithelial surface of the entire respiratory tract is constantly exposed to particulates, gaseous material as well as microbes including pathogens which are potentially harmful. The epithelial lining and the submucosal glands of the conducting airways play an important role in the prevention and removal of foreign substances from reaching the lungs as well as the submucosal tissues. Mucociliary clearance forms the primary defence mechanism of the airway, however, other mechanisms such as coughing, anatomical barriers, aerodynamic changes and immune mechanisms are also employed to keep the lungs clean and functional. To act as a barrier capable of protecting the underlying tissues, the airways possess various adaptations such as ciliated and secretory cells which perform various functions. The beating cilia provide the force necessary to move foreign materials trapped by the mucus layer in the respiratory tract towards the mouth for expulsion. For the development of such a mucociliary clearing apparatus in *in vitro* airway models, culturing the cells at an air-liquid interface is a critical condition (Pezzulo et al., 2011). Furthermore, to study how various respiratory pathogens such as *B. pertussis* and *Haemophilus influenzae* interact with the airways, it is critical to ensure that the models express the characteristic features of the airways such as ciliated cells which cover at least 60% of the conducting airway epithelial surface (Lodes et al., 2020) and beat with a ciliary beating frequency (CBF) of a minimum of about 7Hz (Dresdner and Wong, 1985; Clary-Meinesz et al., 1997; Chilvers and O'Callaghan, 2000; Nikolaizik et al., 2020). In the case of *B. pertussis*, the expression of cilia is also critical for the initial attachment to and colonization of the airway mucosa (Tuomanen and Hendley, 1983). Aside the airlift conditions, co-culturing the epithelial cells with fibroblasts has been shown to greatly improve the differentiation and polarisation of the epithelial cells in 3D cultures compared to monocultures of epithelial cells (Steinke et al., 2014; Heydarian et al., 2019). Thus, the models used in this study were developed by seeding human airway epithelial cells and fibroblasts on a SISser scaffold. The SISser is derived from a section of decellularized porcine small intestine based on the BioVaSc® technology (Mertsching et al., 2005). In contrast to the BioVaSc® however, the mucosa and vascular network is scraped off and then decellularized leaving a clear collagen matrix on which the cells are

seeded to generate the 3D *in vitro* airway mucosa models. Previous studies have relied on collagen coated synthetic Transwell inserts (Lin et al., 2007; Fedele et al., 2011; Yonker et al., 2017). The SISser therefore serves as a natural substitute to collagen-coated polyethylene membrane inserts that are usually used for air-liquid interface culture of airway models. Furthermore, the SISser also provides a layer of dense collagen fibres which provides a flexible, stable and natural environment for three-dimensional cell culture (Schweinlin et al., 2016).

The generation of the models was based on the so-called co-culture method described by Steinke et al. (2014) in which skin fibroblasts were cocultured with airway epithelial cells. However, the models in this study were developed by combining primary human airway epithelial cells and fibroblasts isolated from tracheobronchial or nasal biopsies. As shown in the **Figure 2-1**, co-culturing of primary epithelial cells and fibroblasts isolated from nasal and tracheobronchial biopsies developed the typical airway mucosa features such as cilia and secretory cells, which did not develop when an immortalised cell line was used. The addition of fibroblasts to the respiratory epithelia cells has been shown to improve the differentiation of the epithelia compared to monocultures of epithelial cells as they secrete important modulating and signalling factors that promote robust differentiation of the epithelial layer (Steinke et al., 2014; Schweinlin et al., 2017; Derakhshani et al., 2019; Heydarian et al., 2019; Lodes et al., 2020). Nonetheless, the use of primary epithelial cells for the development of 3D models is limited by the number of replications and availability of donor material. In addition, one should consider that the use of primary cells from different donors may pose problems in the interpretation of results due to genetic variability of the respective donor materials. Primary epithelial cells can usually only be used to passage 3 in complex 3D models. Several attempts have therefore been made to overcome these limits by using for example viral oncoproteins to immortalise primary cells to extend their replication beyond 12 regenerations (Reddel et al., 1988; Coursen et al., 1997). These cells however usually became malignant after several passages. The HBEC3-KT is an immortalised primary human bronchial epithelial cell line developed by insertion of the human telomerase (hTERT) and mouse cyclin dependent kinase 4 (CD4) with a retroviral construct (Ramirez et al., 2004) and hence it does not become malignant after several passages. Several immortalised human airway epithelial cell lines such VA10 (Hasan et al.,

2018a), BEAS-2B (Watkins et al., 1997; Belcher et al., 2000; Qiu et al., 2013), CALU-3 (Pezzulo et al., 2011; Audry et al., 2019) have also been developed and cultured at ALI to study various bacterial pathogens of the airways. Despite these immortalised cell lines circumventing the limited replication of primary epithelial cells, these cells in general do not appear to fully recapitulate the *in vivo* characteristics of the airway when cultured under airlift conditions *in vitro*. For example, the BEAS-2B cells do not form tight junctions, CALU-3 and VA10 cells do not develop cilia despite showing polarisation (Reviewed in Hasan et al., 2018b). The VA10 cells especially did not show polarisation and did not develop any of the *in vivo* airway characteristics when cultured on the SISser (Lodes et al., 2020). The hBM as shown in **Figure 2-1C** possess a stratified epithelial layer which, however, only produced cilia in less than 10% of the models. On occasions when cilia were produced, they showed asynchronous beating and covered less than 5% of the model surface (Lodes et al., 2020). Both cell types however produced mucins when cultured on the SISser (Lodes et al., 2020).

The arrangement of the different cell types in the airways is also critical for their function. The CK5-positive basal cells were located close to the basal membrane in the hNM and hTBM while they seemed to be diffused in the hBM models. The basal cells are stem cells of the adult airways and they differentiate to give rise to the other cell types. They also play a crucial role in the repair of the airway epithelia after injury. They tend to be located basally relative to the ciliated and mucus producing cells, hence their name, and they tend to attach firmly to the basement membrane (Evans et al., 1990). The pseudostratified nature of the epithelia ensures that all the cells have direct contact with the basement membrane. Furthermore, the polarisation of the cells ensures that there is a differential expression of receptors and other structures apically and basally. The expression of pattern recognition factors such as the toll-like receptors for early detection of bacterial molecular patterns tend to be located apically (Park and Lee, 2013; Wiese et al., 2017). Additionally, polarisation plays an essential role in the secretion of mucins and various antimicrobials that serve as the first line of defence of the airways (Hiemstra et al., 2015; Zhang et al., 2016; Audry et al., 2019) The ciliated cells with their apically located cilia in the engineered primary airway epithelial models showed coordinated and synchronized beating with CBF within the normal range of 7.1 – 15Hz (Rutland et al., 1982; Veale et al., 1993;

Clary-Meinesz et al., 1997; Nikolaizik et al., 2020). The hBM on the other hand hardly produced functional cilia, instead to a certain extent, micro-cilia could be observed which did not seem to beat synchronously.

In the course of this thesis, the differentiation of the models was further improved by doubling the number of fibroblast from about 4,000 cells/mm² to around 8,000 cells/mm² and increasing the number of epithelial cells from about 20,000 cells/mm² to 25,000 cells/mm². This increased cell numbers resulted in a differentiation rate > 90% in passage 1 and 2 primary epithelial cells and about 70% differentiation in passage 3 epithelial cells. The addition of such high cell numbers to the scaffold occasionally caused rapid degradation of the scaffold in some of the models resulting in the development of holes that disrupted the ALI. However, this occurred rarely and was observed in less than 5% of all the models developed. This observed degradation of the scaffold may be dependent on the batch of porcine SIS, duration of the culture and donor. Donor material in which the turnover of the cells was observed to be very high usually caused the development of these wholes after 21 days. The number of cells seeded on the SIS scaffold therefore seems to be critical for the efficient differentiation and maturation of the 3D airway mucosa models.

One function of the airway mucosa is to serve as a physical barrier to block the entry of pathogens and other foreign objects. This requires the development of junctional complexes such as tight junctions, adherens junctions and gap junctions between the cells of the epithelia. As shown in **Figure 2-3**, the models generated from primary donor materials developed apparently intact tight junctions. TEER measurement provides a non-invasive method to monitor the development of tight junctions in *in vitro* barrier models. The engineered primary airway mucosa models showed highly organised tight junctions with average TEER values of $53.78 \pm 7.43 \Omega \text{cm}^2$ in the hTBM and $64.43 \pm 9.7 \Omega \text{cm}^2$ in hNM. Previous studies reported very high TEER values of between 700 - 3000 Ωcm^2 in normal human bronchial epithelial cells cultured on collagen- and fibronectin-coated Transwell membrane inserts for 15 days under airlift conditions (Yoo et al., 2003; Lin et al., 2007; Pezzulo et al., 2011). The reason for the observed low TEER values recorded in the hTBM and hNM are not clear but factors such as temperature, pH and type of media can strongly impact the measured TEER

values (Randell et al., 1992; Clary-Meinesz et al., 1998; Yoo et al., 2003; Lin et al., 2007; Nikolaizik et al., 2020). Furthermore, the TEER values reported from previous studies were measured from airway epithelial cells grown on specially coated plastic Transwell® inserts. It is still unclear whether the TEERs recorded in this thesis or the very high TEERs reported in ALI cultures of primary cells on coated Transwell inserts represent the *in vivo* situation as to our knowledge such data are not available. However, the differences between the TEER values may be due to substantial differences in scaffolds used. The SISser has previously been characterised to express collagen types I, II, IV and VI as well the ECM glycoproteins elastin, laminin and fibronectin (Shi and Ronfard, 2013). There is therefore no need for the addition of artificial ECM components such as fibronectin, collagen and retinoic acid, which is a prerequisite for the plastic Transwell ALI cultures.

Taken together, the engineered primary human airway mucosa models possess the physiological characteristic features found *in vivo*. They therefore were used in this thesis as the *in vitro* tool to assess the interaction of *B. pertussis* and its toxins with the respiratory epithelia.

3.2 The role of TCT in the pathophysiology of *B. pertussis* infection

The role of tracheal cytotoxin (TCT) in the pathophysiology of *B. pertussis* has been extensively studied and reported using hamster tracheal explants and cultured epithelial cells (Goldman et al., 1982; Goldman and Herwaldt, 1985; Heiss et al., 1993a; Flak et al., 2000). However, due to the lack of appropriate human models and the scarcity of human donor tissue, the role of TCT in the pathology of pertussis in human is still debated. This work therefore sought to assess the potential impact of TCT in *B. pertussis* pathology using airway mucosa models developed from primary human tracheobronchial epithelial cells co-cultured with fibroblasts due their *high in vivo - in vitro* correlation as outlined above.

In order to assess the effect of TCT, the matured hTBM were incubated from the luminal side with 3µM TCT, 100ng LPS or a combination of TCT and LPS for 24 hours. The amount of toxin applied was based on previous observations from the literature that reported cytotoxicity of the toxins at these concentrations (Heiss et

al., 1994; Flak and Goldman, 1999; Flak et al., 2000) The hTBM were apically incubated with the toxins in order to mimic the direction of contact in a natural infection. A mock control was also set up by incubating the hTBM with fresh mixed media for the same period. Necrotizing bronchitis and blebbing of the respiratory epithelia resulting in denuding of the ciliated cells was found to characterise severe and fatal pertussis cases of infants (Paddock et al., 2008). None of the many virulence factors of the *B. pertussis* except TCT have been able to recapitulate this pathology in animal models. Ultrastructural analysis of 24-hour treated hTBM correlated with previous results obtained using hamster tracheal ring explants (Goldman et al., 1982; Goldman and Herwaldt, 1985; Luker et al., 1993; Flak et al., 2000) and human nasal brush biopsies (Wilson et al., 1991). TCT was previously reported to act synergistically with LPS to induce a much more severe blebbing effect of ciliated cells (Flak and Goldman, 1999; Flak et al., 2000). As shown in **Figure 2-5**, incubation of the hTBM with the toxins for 24 hours caused membrane rupture and deposits of cellular debris typical of necrotic cells. Interestingly however, unlike in the hamster model, the cytotoxic effect of the TCT and LPS was not limited to ciliated cells alone. Both ciliated and nonciliated cells in the hTBMs used in this study were observed to experience the blebbing and necrosis due to the toxin. This was in sharp contrast to studies in hamster models which reported blebbing effects only in ciliated cells but not in nonciliated cells such as the goblet cells (Goldman and Cookson, 1988; Cookson et al., 1989a; Heiss et al., 1994). On the other hand, the data reported here are in agreement with Wilson et al. (1991) who described similar observations of equal cytoplasmic blebbing and cellular extrusion of ciliated and non-ciliated cells in human nasal biopsies after TCT treatment. This observed difference between the hamster models and human models may be ascribed to interspecies differences in response to the toxin and thus highlight the fact that data obtained in animal models may require further proof using human models. Also, the effect of the toxin may be more prominent in ciliated cells since they require more energy to maintain ciliary beating. Furthermore, since the ciliated cells generate the force that clears the airways of particles trapped in the mucous, the toxin may be an evolutionary adaptation to disrupt the ciliary clearance function, thus, enhancing bacterial adherence and colonisation of the airway epithelia. Additionally, ciliated and club cells may express relatively more SLC46A2

transporters compared to nonciliated cells (Berglund et al., 2008) such as goblet cells thus facilitating a more efficient uptake of TCT by these cell types.

The expression of iNOS has previously been reported to be indicative of airway inflammation (Folkerts et al., 2001). Apart from its own cytotoxicity, elevated levels of NO also induce the production of other free radicals such as superoxide anions which have additional toxic effects such as the inhibition of iron-containing enzymes essential for mitochondrial respiration, thus leading to a reduction in the available cellular energy (Tomita et al., 2001). Cytokine-dependent release of NO has previously been reported in hamster tracheal ring explants to mediate the strong disruptive effect of TCT/LPS intoxication (Heiss et al., 1993a; Heiss et al., 1994; Flak and Goldman, 1996; 1999; Flak et al., 2000). In fact, the toxin induced NO has been shown to inhibit DNA synthesis and to induce mitochondrial damage in hamster tracheal epithelial cells (Flak et al., 2000). The severe damage reported in the ciliated cells due to TCT and LPS may therefore be due to their high energy demands to maintain ciliary beating as suggested above. Immunofluorescent staining of the inducible nitric oxide synthase (iNOS) as shown in **Figure 2-11** and Western blot analysis (data not shown) indicate that the NO released upon intoxication of the hTBM was in fact mediated by this enzyme. The respiratory epithelia are known to express constitutive NO-synthases which generate picomolar amounts of NO for intracellular and extracellular signalling (Watkins et al., 1997; Lee et al., 2003). iNOS, on the other hand, induces and sustains high levels of NO known to have the potential to induce cytotoxic effects on tissues (Yamaoka et al., 2002). An increased expression of iNOS as well as consistent increases in NO in supernatants was observed in the hTBM treated with TCT and TCT/LPS despite the differences not being statistically significant. The results described here overall corroborate observations from these early hamster tracheal ring experiments on upregulation of iNOS expression by TCT and LPS. However, since at least part of the data was statistically not significant, this conclusion, although very likely, requires further experimental proof. The use of primary cells and the associated strong donor-to-donor response may be a major reason for the statistical problems with these data. Also, the diffusivity and low solubility of NO in media which is dependent on the pH and ionicity (Zacharia and Deen, 2005) may be a contributing factor. It is also important to note that NO has an extremely short

half-life which is in the range of seconds under physiological conditions (Gaston et al., 1994), thus only the accumulated nitrite over time could be determined. However, a significant increase of NO was measured in the supernatants of hTBM incubated completely submerged in TCT/LPS containing medium (**Figure 2-10**). Therefore, the volume of fluid covering the hTBM and the method of toxin application may also contribute to the observed differences between hTBM incubated with toxins apically or completely submerged. It is also worth mentioning that in the case of the experiments with the hTBM completely submerged in toxin containing medium, the models were developed from cells derived from a single donor, thus eliminating donor-to-donor response differences. It should also be noted that the concentration of NO measured from both methods of toxin application did not show a strong variation (mean= 2 μ M). The statistical issues encountered with these experiments can be addressed in the future by increasing the number of models or using more sensitive methods to quantify both the nitrite and NO released upon intoxication of the models. Other methods that use the quantification of the conversion rate of L-arginine to L-citrulline can be combined with NO measurements in order to determine the total nitrite turnover. Although the data presented here are not entirely conclusive, all together they support the data obtained in the hamster tracheal ring explants and strongly indicate that TCT triggered NO induction by iNOS may be relevant in the human system and may be a major factor contributing to tissue destruction during natural *B. pertussis* infection.

A major effect of TCT previously reported using hamster tracheal explants is the induction of ciliostasis. Ciliostasis can be define as the slowing and/or complete loss of ciliary activity in ciliated cells. 1 μ M TCT is reported to cause a complete halt of ciliary activity after 96 hours while concentrations of 3 μ m TCT achieved this feat in 48 -72 hours (Cookson et al., 1989a; Luker et al., 1993; Heiss et al., 1994). Interestingly, the analysis of the ciliary beat frequenting (CBF) as summarised in **Figure 2-6** showed minimal reduction in all treatment groups with the CBF remaining above the minimum physiological frequency of 7.1 Hz (Katz et al., 1987; Veale et al., 1993; Sanderson and Dirksen, 1995; Clary-Meinesz et al., 1997; Sedaghat et al., 2016). This observation is in marked contrast to the reported observations in the hamster tracheal model after 24 hours. It should however be noted that only intact cells with functioning beating cilia were utilized

for the assessment of the CBF. This method may therefore introduce a bias since we observed large areas of the TCT/LPS treated hTBMs without any beating movement as shown by the dark areas in the heatmap generated from the high-speed videos of beating cilia after toxin incubation (**Figure 2-6**). The observed maintenance of the CBF above the physiological frequency even in toxin treated hTBM may be due to the high levels of NO they produced, which according to previous studies may upregulate the CBF (Jain et al., 1993; Jiao et al., 2011). Correlations between NO concentration and the CBF have been reported in disease conditions such as airway inflammation, Kartagener's syndrome and infections that result in reduced NO in exhaled air (Jain et al., 1993; Li et al., 2000; Wang et al., 2000). Furthermore, there was an observed increase in viscous mucus secretion especially in TCT/LPS treated hTBMs. These results corroborate previous observations by Wilson et al. (1991) who reported that *B. pertussis* culture filtrates did not significantly affect the CBF of human nasal biopsies after 4 hours incubation but resulted in loss of ciliation by killing and extrusion of ciliated cells. Anderton et al. (2004) however reported early significant effects on ciliary-mediated bead clearance using dog trachea organs infected with virulent *B. bronchiseptica* and suggested that ciliostasis may have occurred although tissue damage appeared to be quite minimal. Interestingly, despite the observed normal CBF in toxin treated models, particle transport analysis showed models treated with a combination of TCT/LPS lost the ability to displace the microbead particles, while little effect on microbead transport was observed after administration of the single toxins (**Figure 2-7**). After administration of TCT/LPS, the microbeads seem to be trapped in the viscous mucus and to oscillate around the point of origin. Thus, according to the data presented in this thesis, TCT and LPS seem to indirectly disrupt ciliary function by affecting epithelial cell viability and inducing hyper viscosity in the airway mucus which traps cellular debris and thereby inhibits their clearance. The CBF of the ciliated cells and the amount and viscosity of the mucus combine to form the mucociliary clearance escalator which is employed by the airways to remove foreign objects. Furthermore, as discussed below, the toxin induced expression of inflammatory cytokines can alter the mucociliary clearance mechanism in the airway by corrupting the mucociliary clearance apparatus (Rhee et al., 1999; Heijink et al., 2020). In conclusion, there appears to be a coordinated disruption

of a variety of features by the toxins which together impair the function of the mucociliary clearance mechanism in the airways and thus contribute to pathogenicity of *B. pertussis*.

The observed blebbing and necrosis induced by TCT and LPS may lead to disruption of the tight junctions which tend to be formed at the apical borders of cells (Vllasaliu et al., 2011; Kojima et al., 2013; Zihni et al., 2016). As postulated, incubation of the hTBM with the different toxins resulted in loss of tight junction organisation as well as function as determined using FITC-Dextran permeability assays and TEER measurements (**Figure 2-8**). TCT and LPS alone and in combination severely affected the organisation of the junctional proteins ZO-1 and E-cadherin with TCT/LPS in combination causing an increased permeability to the FITC-Dextran. TEER on the other hand is more sensitive to minor disruptions in barrier integrity and is severely affected by parameters such as temperature, medium composition and cell passage number (Srinivasan et al., 2015). The hTBM did not particularly tolerate their luminal surface being covered with media as even the mock treated controls were observed to experience a ~47% decline in the TEER within 24 hours under submerged conditions. Taken together, the immunofluorescence staining of the ZO-1 and E-cadherin, the TEER measurements and the data obtained by the FITC-Dextran permeability assays indicate that at least the combined presence of TCT and LPS resulted in a significant disruption in the tight barrier developed by the hTBM and thus caused an exposure of the submucosal tissues. The observed disruption of the tight junctions is likely attributable to the increased NO productions in the toxin treated hTBM which is known to inhibit the synthesis of tight junction associated proteins such as occludin, claudins, ZO-1 and ZO-3 (Zech et al., 1998; Han et al., 2003; Kobayashi et al., 2020). Furthermore, inflammatory cytokines have also been shown to regulate the organisation of tight junction in the airway. (Zech et al., 1998; Coyne et al., 2002; Han et al., 2003; Capaldo and Nusrat, 2009; Petecchia et al., 2012; Kojima et al., 2013; Heijink et al., 2020).

The cytotoxicity of TCT in combination with LPS has been linked to the induction of IL-1 in hamster tracheal epithelial cells (Dinarello and Krueger, 1986; Heiss et al., 1993b). Previous reports have demonstrated a correlation between IL-1 stimulation and inhibition of cell proliferation (Heiss et al., 1993b) as well as pyrogenic effects of muramyl peptides (Dinarello et al., 1978; Dinarello and

Krueger, 1986; Dinarello, 1989). The induction of inflammation by muramyl peptides such as TCT, is mediated by the cytoplasmic nucleotide-binding oligomerisation domain-like receptor 1 (NOD-1). NOD-like receptor mediated induction of inflammation is mediated by the transcription factor NF- κ B (Kobayashi et al., 2002; van Heel et al., 2005; Strober et al., 2006; Kufer, 2008; Moreno et al., 2010; Paik et al., 2017). The transmembrane transport of TCT into the cytoplasm required for its interaction with NOD-1 is reported to be mediated by the SLC46A2 protein (Paik et al., 2017). As shown in **Figure 2-12**, the hTBM in fact express this transporter protein in the epithelial layer. LPS induction of inflammation is mediated by the Toll-like receptor 4 (Park and Lee, 2013; Debie et al., 2019). These two pathways independently induce the phosphorylation and subsequent nuclear localization of NF- κ B. The relatively high concentration of pro-inflammatory cytokines observed in the hTBM intoxicated with a combination of TCT and LPS may therefore be due to the simultaneous induction of NF- κ B by the convergence of these two pathways, thus sustaining the inflammatory response. IL-1 α tends to be induced early during the inflammatory response and acts as a transcription factor which promotes the expression of chemokines such as IL8 or initiate inflammatory signal transduction by binding to its membrane receptor (Kunkel et al., 1991; Werman et al., 2004). The observed low and statistically insignificant upregulation of IL-1 α and IL-1 β levels in the hTBM treated with TCT and LPS for 24 hours may be due to their early activation kinetics and short half-life (Turner et al., 1989; Werman et al., 2004). Thus, a more detailed analysis of the expression kinetics of these cytokines may be worthwhile to be performed in future experiments using these *in vitro* 3D airway mucosa models. However, once induced, these two cytokines can induce and maintain the expression of other pro-inflammatory cytokines. Furthermore, the apparently reduced sensitivity of human NOD-1 versus mouse NOD-1 to TCT as reported by Magalhaes et al. (2005) may also be a contributing factor to the observed low IL-1 expression levels. Additionally, precursor IL-1 α and precursor IL-1 β can persist intracellularly for up to 24 hours until they are processed into their active forms by caspase-1 or the nucleotide-binding domain and leucine-rich repeat pyrin containing protein-3 (NLRP3) (Dinarello, 2018). The observed discrepancy between the transcription data of the interleukin-1 genes determined by RT-qPCR and the immunostaining of the interleukin-1 could be attributed to

either posttranslational regulation or the differences in the half-life of the precursor proteins and their transcripts since the antibodies used for immunostaining do not discriminate between the precursor and active forms of the cytokines. Upon caspase-1 mediated cleavage, IL-1 β is secreted into the extracellular space (Monie, 2017) where it may contribute to the observed loss of the barrier function as shown in **Figure 2-8A** (Hermanns et al., 2004). The observed significant two-fold increase in the secretion of the IL-1 β into the basal compartment of the TCT/LPS treated hTBM may induce basal cell migration to repair the damage due to the toxins as IL-1 β is reported to induce cellular migration and differentiation in damaged airway mucosa (Cooper et al., 2001; White et al., 2008). Furthermore, secreted IL-1 β also promotes IL-6 expression (Mizutani et al., 1989), a cytokine that was significantly upregulated in TCT and TCT/LPS treated hTBMs as discussed below.

IL-6 is a pleiotropic cytokine usually expressed by antigen presenting cells, but it can also be produced by various non-hematopoietic cells such as the epithelial cells. IL-6 is known to promote antibody production and CD4 T-cell activation which also occurs during natural infection with *B. pertussis* (Mizutani et al., 1989; Ben-Baruch et al., 1995; Higgs et al., 2012). The observed significant secretion of IL-6 into the basal compartment of the toxin treated hTBMs may be an attempt to promote basal cell differentiation as IL-6 has also been reported to promote the differentiation of basal cells into ciliated cells via the STAT3/*Foxj1* signalling pathway (Tadokoro et al., 2014). The observed significant IL-6 expression in the TCT and LPS treated hTBM may also contribute to the increased barrier permeability as shown in **Figure 2-8** via ZO-1 misslocalization, actin structure remodelling and increased actin contractibility as reported for endothelial cells (Desai et al., 2002). The significant levels of IL-6 induced by TCT and LPS as shown in this study corroborate the recent report by Skerry et al. (2019) that, TCT-hypersecreting *B. pertussis* strains induced an increased expression of IL-6 in mice which also presented a significantly enhanced pulmonary inflammatory pathology compared to wildtype strains. Due to the ability of TCT to induce significant levels of IL-6, which is an important modulator of CD4 T-cell receptor function, there was a proposal for its inclusion in the aP vaccine formulation (Dienz and Rincon, 2009).

IL-8 was secreted at a remarkably high concentrations (pg/ml) by the toxin treated hTBM as well as mock treated controls. IL-8 is a potent chemoattractant and stimulator of neutrophil accumulation in the respiratory system (Kunkel et al., 1991; Teran et al., 1997; Yoon et al., 2010). The stimulation of IL-8 expression from the epithelial cells is dependent on the expression of IL-1 (Kunkel et al., 1991; Yoon et al., 2010). Mock treated control hTBM were observed to secrete a very high amount of IL-8 observed statistical insignificance of IL8 expressed by the intoxicated hTBM compared to mock treated controls may be attributed to the lack of neutrophils in the models which secretes more IL-8 and thus sustains the inflammatory reaction upon induction (Cassatella et al., 1992; Park et al., 1998; Yoon et al., 2010). The ability of TCT to induce significant IL-6 levels, which is an important modulator of CD4 T-cell effector function, makes for a good argument for its inclusion in aP (Dienz and Rincon, 2009).

On the other hand, IL-10 concentration was found to be significantly increased in particular after TCT/LPS intoxication (**Figure 2-15**). IL-10 serves as an inhibitory cytokine which down modulates the inflammatory response. It therefore functions to reduce the damaging effect on the epithelia caused by inflammation (Cassatella et al., 1993). Furthermore, IL-10 has been shown to promote the formation and organisation of tight junctions by promoting localisation of the tight junction proteins to the membrane (Madsen et al., 1997; Capaldo and Nusrat, 2009). It should however be noted that despite the significant 5-fold difference in IL-10 secreted by TCT/LPS treated hTBM compared to controls, the actual concentration of 4.10pg/ml was very low. In fact, this concentration is extremely dwarfed when compared to the concentrations of the proinflammatory IL-6 (63969.40pg/ml) and IL-8 (125748.83pg/ml) measured in the basal compartment of the TCT/LPS treated hTBM. Thus, in conclusion, TCT and LPS seem to upregulate the expression of proinflammatory cytokines while the expression of the anti-inflammatory cytokine IL10 is kept at a minimal level. Furthermore, inflammatory cytokines can alter the mucociliary clearance mechanism in the airway by corrupting the mucociliary clearance apparatus as described above.

Taken together, the disruption of the tight junctions, the induction of necrosis and of epithelial cell extrusion strongly suggest that TCT and LPS play a role in the colonisation of the human airway epithelia by *B pertussis* and thus confirm several previous observations made with hamster tracheal explants. However,

interesting differences were noted between the animal and human derived models regarding the cell types affected by the toxins and the mechanism of their interference with the mucociliary clearance mechanism. The destruction of the airway epithelia induced by TCT and LPS may occur early during the *B. pertussis* infection to aid colonisation and metabolite acquisition. The tissue disruption may also grant access to the basolateral side to other toxins such as the adenylate cyclase toxin (ACT) to induce further epithelial cytopathology. The loss of ciliated cells and viscous hyper-mucus secretion probably has a strong detrimental effect on the mucociliary clearance mechanism which suggests that TCT may even contribute to the induction of the coughing reflex that is characteristic of whooping cough.

3.3 Interaction of *B. pertussis* with the airway mucosa models

3.3.1 Dissociation of cells for single cell RNA sequencing

Single cell RNA-sequencing (scRNA-seq) technologies have empowered the interrogation of pathogen-host interactions at a resolution which cannot be achieved with bulk sequencing methods. However, due to its sensitivity, small changes in gene expression can be amplified by technical and biological noise which may dramatically influence the interpretation of the biological data (Stegle et al., 2015; Potter, 2018). Efforts must therefore be made during sample handling as well as bioinformatic analysis to ensure minimal experimental noise and optimal data filtration. While scRNA-seq has been widely used to characterize the interaction of intracellular bacteria and their host cells due to the ease of isolating single infected cells, to the best of our knowledge, there are currently no reports of the use of scRNA-seq technology to analyse the transcriptome of extracellularly adherent bacteria such as *B. pertussis* and their host cells. This thesis, therefore, aimed to develop a method for isolating such bacteria-associated cells from the 3D airway mucosa models for scRNA-seq analysis.

Previous studies have demonstrated that *B. pertussis* adhered to epithelial cells as early as 3 hours post infection (Tuomanen and Hendley, 1983; Lamberti et al., 2013; Guevara et al., 2016). Tissue necrosis and epithelial cell blebbing were reported as early as 6 hours after infection of native tracheobronchial biopsies

with *B. pertussis* (Steinke et al., 2014). The pathogen has been shown to preferentially adhere to the ciliary tuft during infection (Tuomanen and Hendley, 1983; Mattoo et al., 2001). The adhesion to the ciliary tuft is mediated by various bacterial proteins including FHA, Fim, Prn and PT (Soane et al., 2000; de Gouw et al., 2011). The observed differences in bacteria adherence between the hTBM and hBM 6 hours post infection shown in **Figure 2-17** may likely be due to the lack of cilia in the hBM, since Lodes et al. (2020) showed that the HBEC3-KT do not consistently differentiate to form ciliated epithelia which normally should cover at least 60% of the model surface. Furthermore, when cilia are expressed in the hBM models, they tend to be defective as they either do not beat or their CBF is below the physiological rate. However, the strong increase in the number of adherent bacteria to the epithelia of the hBM at a later timepoint may be due to less specific interactions of bacterial adhesins with these cells or by adhesion mediated by other bacterial factors. Focus on the dissociation of the models for scRNA-seq was therefore placed on the hTBM since they more accurately recapitulate adhesion and invasive behaviour of the bacteria as previously reported in the literature.

Currently available techniques for scRNA-seq require single cell suspensions to be passed through microfluidic or microwell platforms which require solid tissues to be enzymatically and mechanically disrupted to generate single cell suspensions. The laser capture microdissection (LCM) allows for the targeted excision of single cells from a variety of samples and thus appears to be the method of choice to analyse cells inoculated with extracellularly adherent bacteria such as *B. pertussis*. This method, however, requires that the tissues to be very thinly sectioned (7-15 μ m) to ensure optimum results. Sample preparation is therefore very critical, thus methods that offer excellent preservation of RNA, DNA and proteins, such as snap-freezing, should be employed for optimal downstream analysis. Here it is shown that due to the limited extracellular matrix secreted by the 3D models coupled with their less compact nature, the epithelial architecture was lost when the tissues were snap-frozen in OCT (**Figure 2-19A**). However, successful dissection of cells with extracellularly adherent bacteria requires accurately identifying the cells prior to laser dissection. Formalin-fixed paraffin-embedded (FFPE) tissues maintain their morphology very well, but formalin creates cross-links between proteins and nucleic acids and between

different proteins(Liu, 2010). Methacarn is known to be an excellent molecular fixative that maintains nucleic acid integrity similar to fresh-frozen tissue and concurrently preserves the morphology of the tissue as shown in **Figure 2-19C** (Shibutani et al., 2000). However, as shown in **Figure 2-19B**, snap-freezing the airway mucosa models after Methacarn fixation resulted in the distortion of the epithelial layer. Application of this method also required using very high numbers of bacteria, but bacteria-associated cells could not easily be identified due to the very strong autofluorescence of the tissues. This method is therefore very cumbersome, and the extended period required to section cells from the samples will introduce a lot of experimental noise into the transcriptome.

To overcome the challenges of using the LCM, the serine protease subtilisin A was used to digest the tissue models in order to isolate the epithelial cells. Subtilisin A, isolated from the Himalayan glacier-resident bacterium *B. licheniformis*, has been shown to be suitable for dissociation of non-malignant renal tissues at 4 - 6°C provoking only a low level of artifacts in scRNA-seq data (Adam et al., 2017). Trypsinisation and tissue digestion with collagenase requires tissues to be maintained at 37°C, a temperature at which the cells are also physiologically active. The transcriptional machinery remains active at 37°C and extended incubation will introduce gene expression artifacts. O'Flanagan et al. (2019) recently reported when using 10x chromium scRNA-seq that, dissociation of solid tumours (breast and ovarian) with collagenase and trypsin resulted in the upregulation of multiple canonical stress-related genes and heat shock proteins. Furthermore, attempts during this thesis to dissociate the tissue models with trypsin resulted in cell fragmentation. By using the cold dissociation with subtilisin A, there was less cell fragmentation and viable cells with intact beating cilia were observed. Furthermore, cells dissociated using the cold active subtilisin A have been shown to maintain their surface proteins and yield large cell populations when FACS-sorted as compared to warm dissociation using collagenase and trypsin (Adam et al., 2017; O'Flanagan et al., 2019). Taken together, cold dissociation with the cold active *B. licheniformis* subtilisin A seems to provide an appropriate method for the detachment of the epithelial cells for downstream transcriptome analysis using scRNA-seq technology and may be used to perform single cell transcriptomics with *B. pertussis* infected tissue models.

3.3.2 *B. pertussis* invasion and intracellular survival in airway mucosa models.

Bordetella pertussis is classically considered an extracellular pathogen. There is a mounting evidence, however, mainly based on infection assays in flat cell cultures, that *B. pertussis* is capable of invasion and eventual intracellular survival in eukaryotic cells (Steed et al., 1991; Friedman et al., 1992; Masure, 1993; Bassinet et al., 2000; Higgs et al., 2012; Lamberti et al., 2013; Martin et al., 2015). Previous studies to assess the intracellular survival capability of *B. pertussis* have mainly relied on 2D cell cultures which lack the complexity of the 3D environment encountered by the pathogen *in vivo*. Thus, this study utilized the engineered airway mucosa models, which have been shown in earlier chapters to closely replicate native airway mucosa, to survey the epithelial cell invasion and intracellularly survival of *B. pertussis*. Adhesion to host cells is essential for the subsequent invasion of the host cells by pathogenic bacteria (Hazebos et al., 1995; van den Berg et al., 1999). Invasion of respiratory epithelial cells by *B. pertussis* occurs already after 3 hours inoculation *in vitro* (Bassinnet et al., 2000; Gueirard et al., 2005; Lamberti et al., 2013). Similarly, observations during this thesis also indicate that cell invasion already occurs after 4 hours of infection of the primary cell model (hTBM). The invasion and intracellular survival of *B. pertussis* in non-phagocytic cells has previously been reported to be mediated by both bacterial factors and host cell surface components such as integrins (Bassinnet et al., 2000; Isberg et al., 2000; Ishibashi et al., 2001; Hartlova et al., 2010). Studies that assessed the invasion and survival of the *B. pertussis* in professional phagocytic cells such as macrophages and neutrophils showed that opsonisation is required for efficient killing of the bacteria (Steed et al., 1991; Lamberti et al., 2008). The results presented here indicated that only a very small proportion of bacteria are able to successfully invade the epithelial cells as early as 6 hours after infection, but surprisingly this number increased greatly after 24 hours followed by a complete clearance of viable bacteria during the next two days. Lamberti et al. (2013) suggested invasion of host cells by *B. pertussis* could proceed for at least 24 hours after initial attachment in respiratory epithelial cells *in vitro*. The observed increase in invasion after 24 hours in the models could therefore be temporal, as prolonged incubation of the models with the bacteria

permitted increased bacterial adherence and subsequent invasion as shown in **Figure 2-17**. Furthermore, the bacteria could undergo limited proliferation intracellularly as reported by Lamberti et al. (2010) in macrophages, thus, contributing to the observed significant numbers in invasive bacteria after 24 hours. The invasion of tracheal epithelial cells by *B. pertussis* has been shown by Bassinet et al. (2000) to be mediated by adhesins mainly through FHA. The promotion of invasion by FHA is reported to be through the interaction of its RGD motif with the host cell $\alpha 5\beta 1$ integrin (Ishibashi et al., 2001). Lipid rafts have been shown to mediate the internalisation and eventual trafficking of various pathogens including *Bordetella* to nonacidic subcellular compartments (Lafont and van der Goot, 2005; French et al., 2009; Bumba et al., 2010; Hartlova et al., 2010; Lamberti et al., 2013). This lipid raft domains act as cluster domains which mediate the entry and evasion of intracellular killing of *B. pertussis* into epithelial cells through tyrosine kinase activity (Lamberti et al., 2008; Lamberti et al., 2010; Lamberti et al., 2013).

B. pertussis has previously been reported to survive inside macrophages from the examination of biopsies from infants and children with confirmed cases of *B. pertussis* pneumonia (Bromberg et al., 1991; Paddock et al., 2008). *B. pertussis* has been shown to remain viable inside nonacidic compartments within immune cells where they seem to be able to replicate as well suggesting its potential of a facultative intracellular lifestyle, at least in certain cell types (Friedman et al., 1992; Lamberti et al., 2008; Lamberti et al., 2010). Potential intracellular niches of these pathogens during infection have been a matter of debate for many years, since the bacteria can only be isolated very early after the onset of the disease while the symptoms last for many weeks. As shown in **Figure 2-18B** the a subpopulation of the intracellular bacteria apparently did not colocalise acidic compartments such as the late endosomal LAMP1 compartments 48 hours after polymyxin B treatment. In fact, *B. pertussis* has been described to be able to evade intracellular killing by remaining in nonacidic compartments (Lamberti et al., 2008; Lamberti et al., 2010). Furthermore, secreted adenylate cyclase toxin (ACT) is reported to generate an ACT-cloud around the bacteria to promote its internalisation via a clathrin-independent, caveolae - dependent entry pathway that ensures the bacteria are sorted into sphingomyelin and cholesterol rich nonacidic endosomes (Martin et al., 2011; Martin et al., 2015). The data shown

in **Figure 2-18B** are in line with these earlier findings, since with some exceptions, most of the bacteria were not found to be associated with LAMP1 expressing late acidic lysosomal compartments up to 48 hours after polymyxin B treatment. However, no viable bacteria were observed in the airway models 72 hours after polymyxin B treatment, indicating a complete eradication of the intracellular bacteria at later timepoints. Thus, due to the controversial relevance of cell invasion by *B. pertussis*, scRNA-seq analysis should first be performed with cells with adherent bacteria despite the required more complex technical issues. Moreover, due to the relatively small number of invading bacteria and their limited intracellular survival capacity, the data presented here raise some doubts about an *in vivo* role of bacterial invasion and intracellular survival in well-structured epithelia. Nevertheless, the preliminary data generated in this study should to be investigated further using mutant strains of the bacteria and microscopy methods such as confocal microscopy and electron microscopy. Furthermore, *B. pertussis* engineered to express different molecular flags in acidic and nonacidic compartments can also be combined with live imaging techniques to confirm some of the observations from this preliminary study.

3.4 Perspectives

Throughout the course of this work, attempts were made to assess the impact of *Bordetella pertussis* infection on the respiratory epithelial by using *in vitro* airway mucosa models developed from the co-culture of primary human airway epithelial cells and fibroblasts. These 3D co-culture airway models provide relevant model systems that could contribute to our understanding of the virulence mechanisms of *B. pertussis* at an early stage of infection in order to improve upon the available vaccines. However, since the models in their current state do not include immune cells, the role of the innate immune cells such as neutrophils and dendritic cells, which infiltrate the airway mucosa and act as sentinels *in vivo* during the pathogenesis of the disease cannot be assessed. Thus, in the future, the models should be improved by the implementation of immune cells isolated from the blood to the model systems. Peripheral blood mononuclear cells can be isolated from donor blood and differentiated into dendritic cells, macrophages and neutrophils. These cells can then be added to the fully differentiated airway mucosa models and will surely provide valuable data on the interaction between these cells, the nonprofessional immune epithelial cells and the bacteria. However, a delicate balance of the three types of media i.e., AECGM for airway epithelial cells, FGM for fibroblasts and RPMI for immune cells will be needed to ensure the optimum condition for the maintenance of all cell types, thus, requiring significant but worthwhile efforts for their development. The model systems can also be developed further by adding an endothelial cell layer to the basal compartment. Combining the different cell populations under dynamic culture conditions will allow for a comprehensive analysis of how systemic infections with *Bordetella* as well as other respiratory bacteria and viruses occur.

In this study, *E. coli* LPS was used instead of *B. pertussis* LOS in order to make comparable analysis with the data previously generated using hamster tracheal explants. However, despite the differences in the structure of LOS and LPS, they have been shown to have very similar biological activity in terms of lethal toxicity in animal studies (Watanabe et al., 1990; Flak et al., 2000). Although the biological activity of LPS and LOS is very similar, in the long term it may be interesting to compare the cytopathology of LOS/TCT in order to unravel potential differences in their effects on the airway cells in comparison to data shown here

using LPS. Furthermore, the role of inflammatory cytokines in the host cell response to TCT/LPS needs to be investigated further to overcome the statistical problems encountered during this study which are probably posed by the use of primary cells derived from different donors.

It will be interesting to elucidate the effect *B. pertussis* wildtype strains and certain mutants in virulence genes have on the tissue models and on different cell populations present in the airway mucosa and to understand their responses to their infection and communication with each other. The combination of the cold dissociation method with subtilisin A and FACS will enable the separation of single cells infected with extracellular adherent *B. pertussis* and will thus facilitate the use of scRNA-seq analysis to assess the differential expression of various genes in the different cell populations i.e., ciliated cells, goblet cells and basal cells. This can be achieved by sorting the different cell populations using conjugated-antibodies to separate the different cells populations based on surface markers prior to scRNA-seq library preparation. Furthermore, a temporal analysis of differentially expressed genes between by-stander and bacteria associated cells can be assessed with Smart-3seq scRNA-seq technology. If successful, this can be taken further by performing transcriptome analysis of bacteria invaded cells compared to non-invaded cells to further evaluate the uncertain relevance of cell invasion by *B. pertussis*.

In conclusion, the combination of these new technologies of tissue engineering and single cell transcriptomics will provide entirely new insights into the interaction of *B. pertussis* with airway epithelia and may pave the way for the development of not only improved vaccines but also medicines which can interfere with the dangerous symptoms of whooping cough.

4 Methods

4.1 Donor material and primary cells

Primary tracheobronchial epithelial cells and fibroblasts were isolated from tracheobronchial biopsies obtained from donors between the ages of 25 to 85 years undergoing selective bronchial/lung resections at the Department of Thoracic and Cardiovascular Surgery at the University Clinic of Wuerzburg and the Department of Thoracic Surgery, Otto-von-Guericke University of Magdeburg. Primary nasal epithelial cells and fibroblasts were isolated from nasal biopsies obtained from donors between the ages of 20 to 80 from the Department of Otorhinolaryngology, Plastic, Aesthetic and Reconstructive Head and Neck Surgery of the University Hospital Würzburg. Informed consent was obtained from patients prior to surgery.

4.2 Ethical considerations

The use of the primary materials in this study was approved by the institutional ethics committee of the Julius-Maximilians-University of Wuerzburg (vote 182/10, 179/17) and Otto-von-Guericke University Magdeburg (vote 163/17).

4.3 General cell culture methods

4.3.1 Isolation of cells from biopsies

To isolate primary airway epithelial, the biopsies were rinsed vigorously twice in cold DPBS to remove blood cells and other loose debris. Isolation of the primary cells was done within 48 hours from the time the biopsy is resected from the donor. For tracheobronchial epithelia cells, the circular biopsy was cut on opposing sides to expose the epithelial layer. This is however not necessary for the nasal biopsies. Using sterile forceps, the epithelial layer was peeled and placed in 10cm cell culture dishes. The pieces were incubated overnight in 2mL airway epithelial cell growth medium (AECGM), which is enough to cover the pieces and allow adhesion in a humidified incubator at 37°C and 5% CO₂. The next day, 3ml AECGM is added to the plate and the pieces are cultured for 7 days with media change on the 4th day. The epithelial cells were observed to grow out of the pieces on the plate. Fibroblasts were isolated from these same pieces on

the 8th day. The pieces are gently removed from the cell culture plate and placed in new 10cm plates. They are rehashed with a scalpel, suspended in 500U/ml collagenase and incubated for 15 minutes at 37°C. The collagenase is aspirated, and the pieces washed once with fibroblast growth medium (FGM). The pieces were resuspended in 3ml FGM and transferred into 10cm cell culture plates. They were then incubated overnight at 37°C and 5% CO₂ in a humidified incubator. The media is topped up to 5mL the following day and the pieces were cultured for 7 days with media change on the 4th day. Isolated cells were either expanded further for the development of the 3D airway mucosa models or freeze-stored for later use. All media used for the isolation of the cells contained 0.1mg/ml Streptomycin, 100U/ml penicillin and 0.25ug/ml amphotericin B.

4.3.2 Expansion and passaging of cells

The isolated airway epithelia cells were cultured in AECGM. Cells were either expanded immediately after isolation or retrieved from frozen-storage for expansion. Primary airway epithelial cells (Passage 0) were seeded at a density of 5×10^5 cells in a T75 cell culture flask. Airway fibroblasts (Passage 0) were seeded at a density of 10^6 cells in T75 cell culture flasks. The cells were passaged at a confluency of approximately 80-90% at a ratio of 1:2 T75 flask. To passage the cells, the media was aspirated, and the cells washed with DPBS to remove residual media and serum. The epithelial cells were incubated for 10 minutes with DPBS/EDTA to aid their detachment from the flask. The cells were then incubated with 1% Trypsin/EDTA solution at 37°C and 5% CO₂ for 3-5 minutes. Fibroblasts were detached from the cell culture flask by incubating with 0.1% Trypsin/EDTA for 5 minutes. The flasks were retrieved from the incubator, gently tapped on the side and viewed under the microscope to confirm detachment of the cells. The trypsin/EDTA was inactivated with FCS. The cell suspension is pipetted into 15mL falcon tubes and centrifuged at 1000rpm for 5 minutes at room temperature (RT). The supernatant was aspirated, and the cell pellet resuspended in the appropriate media for the cells and reseeded in new flasks at a density of 1:2 or seeded on SIS-scaffolds. The primary airway epithelial cells were used until passage 3 and the fibroblasts until passage 9 for the development of the 3D airway mucosa models.

4.3.3 Thawing and freezing cells

Cells were either seeded onto new culture flasks, discarded or frozen for later use upon passaging. Cells were frozen in freezing media containing 90% FCS and 10% DMSO. DMSO serves as a cryoprotectant. It is however toxic to cells and the procedure was done quickly to minimize cell exposure. The cells were resuspended in the cell-freezing medium to approximately 10^6 cells/ml and transferred into cryovials. The cryovials were placed into Cryo 1°C freezing containers filled with isopropanol and placed in a -80°C freezer. The isopropanol and the freezing container prevent ice crystal formation within the cells due to rapid cooling by ensuring a gradual cooling of approximately -1°C/min. The frozen cells were transferred from freezing containers the following day into cryoboxes at -80°C or the gas phase of liquid nitrogen.

Cryovials of airway epithelial cells and fibroblasts were retrieved from the liquid nitrogen tank and transferred to the cell culture lab on ice. The vials were placed in a water bath prewarmed to 37°C and retrieved when a small piece of ice remains in the vial. The cells were transferred into 15ml falcon tubes containing 1ml of the appropriate media and centrifuged at 1000rpm for 5 minutes at RT. The supernatant was aspirated, the cell pellet is resuspended in 1ml of the appropriate medium and transferred into cell culture flasks for expansion.

4.4 Develop and characterization of 3D airway mucosa models

4.4.1 Decellularization of porcine small intestine serosa (SISser®)

Small intestinal submucosal (SIS) scaffolds were produced from 1.5- to 2-m long segment of porcine jejunum explanted from 17 to 20 kg “deutsche Landschwein” breed of piglets. Animal experiments were performed according to the German law and institutional guidelines approved by the Ethics Committee of the District of Unterfranken, Würzburg, Germany (approval number: 55.2-2532-2-256). Care of all the piglets followed the guide for care and use of laboratory animals published by the National Institutes of Health (NIH publication no. 85–23, revised 1996) after approval from our institutional animal protection board. The piglets were obtained from the pig breeder (Niedermayer, Germany) and explanted as described previously (Pusch et al., 2011, Schweinlin et al., 2017). The piglets were sacrificed at the Centre for Experimental Molecular Medicine (ZEMM,

Wuerzburg). The piglets were injected with heparin and sacrificed with anaesthesia overdose prior to the explantation of the small intestine. The jejunal segments were stored in PBS containing 1% (v/v) gentamycin at 4°C and transported to the Chair of Tissue Engineering and Regenerative Medicine (Wuerzburg) for decellularization. The small intestine was cut into 10cm segments and the mucosa of the segments was scraped off with forceps prior to decellularization to produce the SISser scaffold used in this work. The decellularization method employed to produce the cell-free SIS scaffolds relies on the use of sodium deoxycholate, which causes complete lyses and nucleic acid degradation of the cells (Moll et al., 2013). The SIS was then sterilized with gamma radiation. The whole decellularization process was completed in 7 days.

4.4.2 Construction of 3D airway models

The development of the 3D airway mucosa models was adapted from the method previously described by Steinke et al. (2014). To develop the airway mucosa models, the tubular SISser was retrieved from PBS and cut on one side using a sterile scalpel. The SISser was then opened up using two forceps and the serous membrane removed by pulling it to one side. The SISser scaffold is cut into about 1.5cm² size and fixed between two metal rings (cell crowns). The construct is then incubated for 2 hours with FGM in the apical and basal compartments of either a 6-well or 12-well plate depending on the size. The construct is then seeded with 10⁵ fibroblasts and incubated overnight. Subsequently, 3.0x10⁵ airway epithelial cells are seeded from the apical compartment of the construct. The FGM in the basal compartment is aspirated and replaced with a mix of FGM and AECGM at a 1:1 ratio (mixed medium). The setup was incubated under submerged conditions for two days and then airlifted by aspirating the media from the apical compartment. The setup was cultured under airlift conditions for 21 – 28 days and considered mature when beating cilia was observed with high-speed video microscopy.

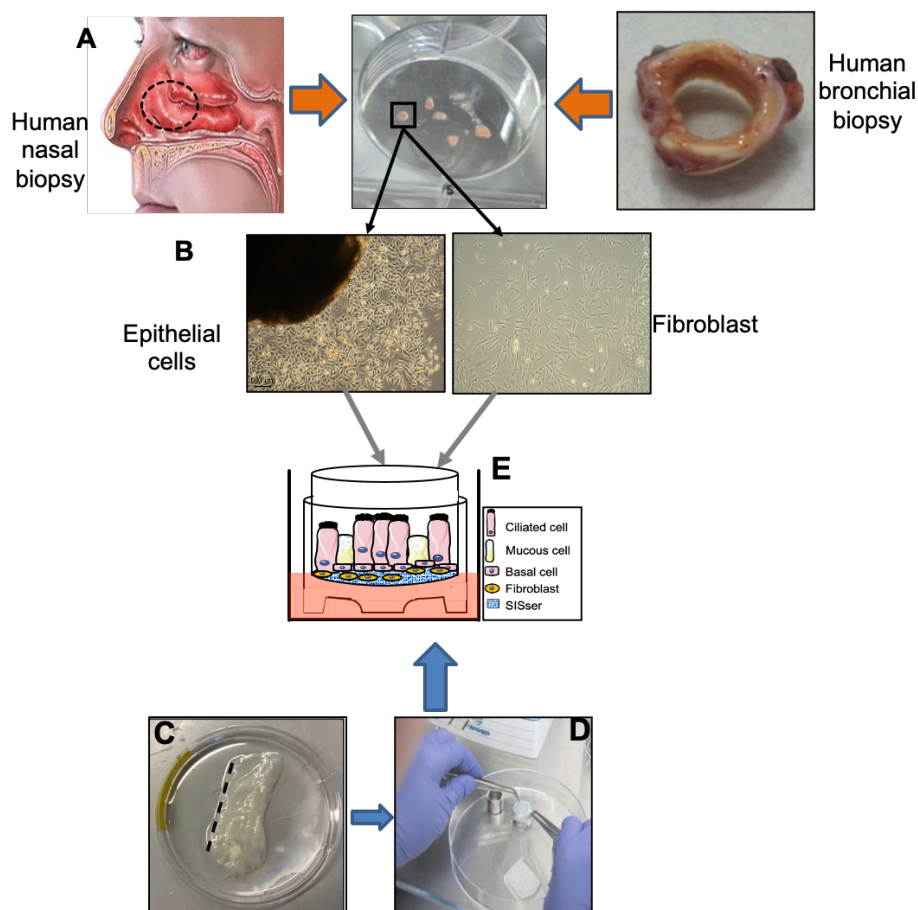


Figure 4-1 Development of 3D airway mucosa models.

Respiratory epithelial cells were isolated by peeling the epithelial layer from the biopsy material (A) with the aid of sterile forceps and culturing them with AECGM until epithelial cells are observed to grow out (~7 days) into the cell culture plates. The pieces were then digested with collagenase, washed and cultured in FGM to isolate fibroblasts (B). Isolated cells were expanded for another 7 days to obtain enough cells. Tubular SIS scaffold were cut on one side, the serosa is pulled away (C) and the SISser scaffold is then fixed between the cell crowns (D). The cell crown was placed in a well plate and seeded sequentially with the fibroblasts and then epithelial cells. The set is cultured submerged for 3 days and then under airlift conditions for 21 – 28 days (E).

4.4.3 Determination of ciliary beat frequency of the 3D airway models

To determine the ciliary beat frequency, the airway mucosa models were transferred from the cell crowns onto silicon coated Delta T dishes and held in place with insect pinning needles. The airway mucosa models were then covered with 1ml of mixed media and mounted on the microscope stage for viewing. The temperature of the mixed medium was maintained at 37°C throughout the recording of the videos with a Biopetechs Delta T5 μ -Environmental culture dish controller set to 38°C. 10 seconds long high-speed videos of beating cilia were recorded at 100fps with a Nikon Eclipse 80i microscope equipped with a water immersion Achromplan 40x/0.80W objective. The mean ciliary beat frequency

(CBF) was calculated from at least 10 randomly selected ciliated cells in each movie. The CBF was determined by the Fourier transformation of grey level changes over time with a MATLAB script developed by Prof. Dr. Peter König (Lindner et al., 2017). For the determination of the change in CBF after incubation with the toxins, high-speed videos were recorded before and 24 hours after the addition of the toxins as described above. At least 5 different areas of each model were selected, and movies of cilia motion was recorded at 640 X 480 pixels and analyzed as earlier described.

4.4.4 Assessment of mucociliary clearance

The mucociliary clearance mechanism was assessed using a particle transport assay. The hTBM were transferred from the cell crown onto silicon coated Delta T-dishes and fixed in place as described above. The models were then washed with prewarmed sterile PBS and covered with 1ml fresh mixed medium. The temperature was maintained at 37⁰C throughout the recording of the videos with a Biopetechs Delta T5 μ -Environmental culture dish controller. DynabeadsTM Protein G were suspended in fresh mixed medium and added to a final concentration of 15ug/ml. Using a 20x/0.5W water immersion objective, 15-second-long high-speed video recordings of the beads were made at 200fps. The videos were then analyzed with Image-Pro [®] Premier software to determine the displacement of the beads. At least 10 particles were tracked over 100 frames to determine their displacement for all the models.

4.4.5 Transepithelial electrical resistance

The transepithelial electrical resistance (TEER), which is a measure of the tight junction organization, was taken on days 4, 11, 18 and 21 after models were airlifted. Models used in the determination of the TEER were developed using plastic cell crowns with an area of 0.33cm². The TEER was determined using the EVOM2 electrical Volt-ohmmeter with STX2 chopstick electrodes. Prior to the measurement of the TEER, the electrodes were sterilized in 70% ethanol for 10 minutes, washed in DPBS and preconditioned in the appropriate prewarmed mixed media for another 10 minutes. The models were prepared by washing the epithelial side with prewarmed sterile DPBS. 1.5ml and 300 μ l of prewarmed fresh mixed media was then pipetted into the basal and apical compartments

respectively. The electrical resistance across the membrane of the airway models was measured with the short arm of the electrode in the apical compartment and the long arm in the basal compartment. The electrical resistance was measured from three different locations of the model close to the edges and the mean taken as the resistance of the cell crown. Three measurements from unseeded SISser mounted on a cell crown were also taken as blank. The TEER of the airway mucosa models was obtained by normalising the measured resistances to the resistance obtained from the blanks. The TEER was then determined using the formula

$$(Mean\ Tissue\ Resistance - Blank\ Resistance) * Area\ of\ tissue\ model$$

The TEER was expressed as ohm.mm² (Ω mm²). The TEER of the hTBM in the toxin experiment was similarly determined before and after toxin treatment. The TEER measured post toxin treatment of the hTBM was then expressed as a percentage relative to the pre-intoxication TEER for the different treatment groups.

4.4.6 FITC-Dextran permeability assay

The ability of the airway models to form a tight barrier was further analyzed using the FITC-dextran permeability assay. The permeability assay was performed with a 4-kDa fluorescein isothiocyanate-dextran (FITC-Dextran) compound dissolved in mixed media. Briefly, the lyophilized FITC-Dextran was dissolved in cell culture medium to a final concentration of 0.25mg/ml and sterile-filtered through a 0.2 μ m mesh. The airway models were washed with sterile PBS and 2ml fresh mixed medium was added to the basal compartment. 500 μ l of the FITC-Dextran solution was added to the apical compartment and incubated at 37°C for 30 minutes. 200 μ l of the media from the basal compartment were collected after the 30 minutes incubation into 96 well plates and analyzed in a TECAN reader (Absorbance 490nm, emission 525nm). The mean absorbance from the different models was normalized to a cell-free SIS scaffold mounted on a cell crown. The permeability of the models to FITC-Dextran was expressed as a percentage after normalization with the cell-free SIS scaffold.

4.5 Histology

4.5.1 Fixation, paraffin embedding and microtome sectioning

The models were initially washed with PBS to remove remaining media after aspiration. The apical and basal compartments were filled with 500ul and 3ml of 4% PFA respectively and left in the dark for 2 hours at RT. The models were then removed from the cell crowns, excess scaffold cut away and transferred into embedding cassettes lined with filter paper. The embedding cassettes were consequently transferred to the water compartment of the automated spin tissue processor. The embedding process was as follows:

Table 4-1 Tissue dehydration and paraffin embedding sequence

Step	Solution	Time (h)
Washing out fixative	Distilled water	2
Ethanol dehydration	50% EtOH	1
	70% EtOH	1
	80% EtOH	1
	96% EtOH	1
	Isopropyl I	1
	Isopropyl I	1
Alcohol removal	Isopropyl/xylene (1:2)	1
	Xylene I	1
	Xylene II	1
Paraffin infiltration	Paraffin I	1.5
	Paraffin II	1.5

The paraffin infiltrated models were removed from the embedding cassettes and paraffin blocks were made using rectangular molds. The blocks were cooled on a cooling plate at 4°C and 5µm thin sections were made on a microtome onto glass slides for histology and immunostaining. The thin sections were air dried overnight at 37°C in a hot air dryer.

4.5.2 Deparaffination and rehydration of the tissue sections

Prior to histology and immunostaining, the paraffin embedded sections were deparaffinized and rehydrated according to the following protocol:

Table 4-2 Tissue deparaffination and rehydration

100% Xylene I	10 minutes
100% Xylene II	10 minutes
96% EtOH I	1 minute
96 % EtOH II	1 minute
70% EtOH	1 minute
50% EtOH	1 minute
Distilled water	5 minutes
PBS	-

4.5.3 Haematoxylin-eosin staining

Prior to performing a haematoxylin-eosin staining, the 5 μ m paraffin sections were deparaffinated and rehydrated as described in table 4-2 above. The samples were imaged on the BZ9000 microscope.

Table 4-3 Haematoxylin and Eosin staining

Solution	Time (min)	Process
Haematoxylin	3	Staining Basophilic structures
De-ionized Water	Until solution is clear	Rinsing
Eosin	3	Staining Acidophilic Structures
De-ionized Water	Until solution is clear	Rinsing
Ethanol 70 %	1	Dehydration
Ethanol 96 %	2	Clearing
Isopropyl I	5	Dehydration
Isopropyl II	5	Clearing

Xylene I	5	Clearing
Xylene II	5	

4.5.4 Electron microscopy for ultrastructural analysis

For ultrastructural analysis using electron microscopy, the models were washed with cold PBS three times, removed from the cell crowns and excess scaffold removed with a scalpel. The models were then fixed overnight at 4°C with either 2.5% glutaraldehyde (50mM cacodylate, [pH7.2], 50mM KCl and 2.5% MgCl₂) for Transmission Electron Microscopy (TEM) or in 6.5% glutaraldehyde for Scanning Electron Microscopy (SEM). The fixed models were then transported on ice to the Imaging Core Facility at the Biocentre of the University of Wuerzburg for further processing as previously described by Spiliotis et al. (2008). The mounted images were examined on the JEOL JEM-2100 TEM or the JEOL JSM-7500F SEM.

4.6 Immunohistology

4.6.1 Immunocytochemistry

The treatment of the tissues for paraffin embedding leads to the formation of protein crosslinks that mask target antigens, usually resulting in a weak or false negative staining. The thin paraffin sections were unmasked in a sodium-citrate buffer or EDTA buffer depending on the antibody as recommended by the manufacturer. The slides were immersed in the appropriate buffer in a curvette in a steam chamber for 20 minutes. The curvette was retrieved and allowed to cool for 10 minutes and then placed under running distilled water for 5 minutes prior to immunostaining. The slides were briefly stored in PBS before immunostaining. The sections were covered with blocking solution containing 0.01% TritonX-100 and incubated for 1hr at RT. This ensured permeabilization as well as blocking of unspecific binding sites for the fluorophore coupled secondary antibodies. The primary antibodies were diluted in the antibody dilution solution, pipetted over the sections and incubated overnight at 4°C in a dark humidified chamber. The slides were recovered the next day, washed three times in PBS containing 0.05% Tween-20 followed by secondary antibodies incubation for 1 hr at RT. The slides were washed again three times, covered with

Fluoromount® G+ DAPI and covered with coverslips to prevent drying. Negative controls (slides without primary antibodies) were also prepared to control for specificity of the primary antibodies. The samples were imaged using either a TCS SP5/SP8 laser scanning confocal microscope.

4.6.2 Whole model immunocytochemistry

In order to detect the areas of bacteria adhesion, whole model mounts which do not require paraffin embedding and subsequent antigen recovery were performed. Furthermore, the agitation of the models during the paraffin embedding process led to the loss of adherent bacteria. For whole model staining, the airway mucosa models were fixed with 4% PFA overnight at 4°C. The models were removed from the cell crown and washed three times with PBS to remove traces of 4% PFA. Blocking solution containing 0.01% TritonX-100 is pipetted into the apical compartment of the cell crown and incubated for 1 hr at RT. The blocking solution was removed, and the primary antibodies diluted in antibody dilution solution containing 0.01% TritonX-100 are added and incubated overnight at 4°C in a dark humidified chamber. The following day, the models were washed three times with PBS containing 0.5% Tween-20 on a shaker for 7 minutes each. Secondary antibodies were added and incubated for 1 hr at RT. The models were washed three times again, removed from the cell crowns and mounted with FluoromountG + DAPI on glass slides after cutting away the excess SIS-scaffold. On occasion, the models were removed from the cell crowns and cut into sections for multiple staining procedures. The immunostained models were mounted with the luminal surface towards the coverslip. A Z-stack image was made through 25µm of the mounted models with the TCS SP8 confocal microscope using the 60x oil immersion objective lens or 40x objective lens. 3D images were reconstructed using the Leica LAS-X software.

4.7 Tracheal cytotoxin experimental design

The fully differentiated hTBM were washed 3x with fresh mixed medium to wash away some of the mucus prior to incubation with the toxins. The models were transferred into 12-well plates with 1ml of fresh mixed medium in the basal compartment. 300µl each of 3µM TCT, 100ng/ml LPS (*Escherichia coli* 026: B6) or a mixture of TCT and LPS (TCT/LPS) in mixed medium was pipetted into the

apical compartment and the setup was incubated for 24 hours in a humidified incubator at 37°C and 5% CO₂. A mock control of freshly prepared mixed media without any toxin was also setup under the same conditions as above. To determine the effect of ventilation, the hTBM were placed for 30 minutes under the flow hood with the well plate open. This was repeated after every 2 hours of incubation for 12 hours. The supernatants from the apical and basal compartment were analyzed for NO production using the Griess test.

4.7.1 Nitric oxide quantification using Griess test

The amount of nitric oxide dissolved in the supernatants in the apical and basal compartments after incubation with the toxins was measured using Griess reagent test kit. The test was performed according to the kit manufacturer's instructions. Briefly, 50 µl of the culture supernatant from the apical and basal compartments were pipetted into 95-well plates. 50µl of the Sulphanilamide solution was added to the supernatants and incubated in the dark for 10 minutes at RT. Using a multistep pipette, 50µl of the NED solution was added to the wells and incubated for 10 minutes in the dark at RT. Absorbance was measured at 548nm using a TECAN infinite M200 microplate reader. The concentration of nitrite in the supernatants was determined by extrapolating from a standard curve. The supernatants from at least 3 independent experiments were used to determine the amount of nitric oxide (NO) released upon toxin incubation.

4.7.2 Cytometric bead array assay for inflammatory cytokine

The concentration of secreted inflammatory cytokines in the cell culture supernatant of toxin treated and mock treated control hTBM was determined using the BD cytometric bead array (CBA) kit. The CBA kit enables the simultaneous quantification of up to 6 inflammatory cytokines (IL-1 β , IL-6, IL-8, IL-10, TNF, IL-12p70) in 12.5µl sample. 50µl of cell culture supernatants were collected from the apical and basal compartments of 24-hour toxin treated airway models in 0.5ml Eppendorf tubes. The supernatants were centrifuged at 12000rpm at 4°C for 60 seconds to sediment the cellular debris and the upper media transferred into fresh Eppendorf tubes. Samples were frozen at -80°C until they were analyzed. For this study, IL-1 β , IL-6, IL-8 and IL-10 in the cell culture supernatants were quantified. Each bead was vortexed and 2µl of each of the

cytokine beads was mixed together and then mixed with 12.5µl of each sample in a 96 well conical bottom plate. 2µl of the human inflammatory cytokine PE detection reagent was added to the assay wells. The plate was placed on a shaker and mixed at 1100rpm for 5 minutes. The plate was then incubated for 3hrs in the dark at RT. 200µl of wash buffer was added to the plate and centrifuged at 800rpm for 5 minutes. The plate was quickly flipped upside down to remove the liquid and the beads were resuspended in 200µl wash buffer. The cytokine capture beads were assessed using a BD Accuri™ C6 Plus flow cytometer. The cytokines were quantified using the FCAP Array™ software version 3.0. A 1:50 dilution of the supernatants was done to lower the IL-6 and IL-8 levels to within the limits of detection of the kit. The inflammatory cytokine concentrations from the treatment groups were normalized to control concentrations and expressed as relative concentrations to eliminate donor response variations.

4.8 Propagation of *Bordetella pertussis*

4.8.1 Bacteria culture

B. pertussis is very fastidious, requiring specific conditions for its culture and maintenance. Stocks of *B. pertussis* freeze-stored in 15% glycerine at -80°C were retrieved from cold storage in ice boxes and streaked onto Bordet-Gengou agarose (BGA) plates with sterile inoculation loops under a cell culture flow hood. The plate was incubated at 37°C for 2 days and re-streaked onto fresh BGA plates and incubated overnight. The bacteria were transferred from the BGA plate into 5ml of 1xStainer-Scholte (1xSS) medium with an inoculation loop and incubated overnight on an elliptical shaker. The liquid culture was retrieved from the incubator and the optical density of the liquid culture was determined at 600nm to determine bacterial growth. The bacterial culture was diluted to an OD₆₀₀ of 0.2 in 5ml of fresh 1xSS and incubated with shaking until the culture reached an OD₆₀₀ of between 0.8-1.0 for infection. The bacteria were then resuspended in fresh mammalian cell culture media without antibiotics to the appropriate OD for infecting the airway mucosa models.

4.8.2 *B. pertussis* infectivity assay

The bacteria were cultured as described above and resuspended in prewarmed fresh mixed medium without antibiotics for infection of the engineered airway mucosa models. The airway mucosa models were also developed as described earlier. The airway mucosa models were then washed twice with prewarmed sterile PBS and the basal compartment filled with 1ml fresh medium without antibiotics. The bacterial suspension was then added to the apical compartment and incubated in a humidified incubator at 37°C and 5% CO₂. Adherence of the bacteria to the airway mucosa cells was determined at 6 hours or 24 hours post infection. Nonadherent bacteria were washed off with prewarmed sterile PBS and the models were incubated with 200µl of 1% saponin for 30 minutes at 37°C to lyse the cells. The lysate was transferred into 1.5ml Eppendorf tubes containing 800µl warm DPBS and the mixture was homogenized by gently pipetting up and down. Serial 10-fold dilutions of the adhered bacterial suspension (usually 10⁻¹ to 10⁻⁵) were made with sterile PBS and 100µl of the suspension plated onto BGA plates. The BGA plates were then incubated at 37°C for 48 hours. The colonies on the BGA plates were counted and expressed as colony forming units/ml (cfu/ml). The number of adherent bacteria was determined from three independent experiments performed in duplicate.

4.8.3 Invasion assay

The polymyxin B protection assay was used to assess invasion of the airway epithelial cells by *B. pertussis*. The bacteria were cultivated and the 3D airway mucosa models were infected as described for infectivity assay above. The supernatants were aspirated and the models were washed 3x with sterile PBS to remove nonadherent bacteria. The extracellular bacteria were killed by incubating the infected models with fresh mixed media containing 100µg/ml polymyxin B for 2 hours. The models were washed again 2x with sterile PBS and incubated with 1% saponin for 30 minutes to lyse the cells. Serial 10-fold dilutions of the lysate were made, plated on BGA and incubated for 48 hours at 37°C. The colonies were counted and expressed as colony forming units/ml (cfu/ml). Three independent experiments performed in duplicate were used for the invasion assay.

4.8.4 Intracellular survival assay

The polymyxin B protection assay was used to assess the intracellular survival of the bacteria in the airway epithelial cells. Mature 3D airway mucosa models were infected as described above at a MOI of 50 for 24 hours. The models were then washed 3x with sterile PBS to remove all non-adherent bacteria. The extracellular bacteria were killed by incubating the models with mixed media containing 100µg/ml polymyxin B in the apical and basal compartments for 2 hours. Intracellular bacteria were estimated 24-hours post inoculation as for invasion assay. The models were washed once with sterile PBS and then cultured with mixed media containing 10µg/ml polymyxin B over 7 days with CFU determined every day by lysing the cells with 1% saponin. Serial 10-fold dilutions of the bacterial suspension were plated on BGA plates and the cfu calculated after 2 days of incubation at 37°C. For confocal imaging, the models were inoculated with GFP-expressing *B. pertussis*, washed 3x with sterile PBS and fixed with 4%PFA overnight at 4°C. The whole models were then immunostained with anti-LAMP1 and anti-panCK and z-stacks images through 25µm were made on TCS SP5 microscope. The 3D images were reconstructed using a Leica LAS-X.

4.9 Molecular biology

4.9.1 RNA isolation, cDNA synthesis and Quantitative RT-PCR

For the isolation of total RNA, the airway mucosa models were lysed with ceramic beads by agitating for 2 minutes at 50rpm in lysis buffer containing β-Mercaptoethanol. Total RNA was isolated using the Qiagen RNA isolation kit according to the manufacturer's instruction and the RNA eluted with 14µl nuclease free water. Isolated total-RNA quality and quantity was determined using TECAN infinite M200 microplate reader. 1µg of the total RNA was transcribed to cDNA with iScript™ cDNA synthesis kit. The relative expression of target genes was quantified with the SSOFast™ EvaGreen® Supermix on the Sens Quest CFX96 real time PCR thermocycler. The GAPDH gene was used as reference in all the quantitative RT-PCR experiments. Primers were designed using Primer3 and were used at a final concentration of 500nM. A 3-cycle amplification method was performed with cycling conditions as follows: (i) initial

denaturation at 95°C 3 min, followed by 40 cycles of (ii) denaturation at 95°C for 10 s, (iii) primer annealing at 65°C for 30 s and (iv) stabilization, elongation and fluorescence detection at 72°C for 30 s. The gene expression fold change was calculated using the $2^{(-\Delta\Delta CT)}$ Livak threshold cycle (C_T) method (Livak and Schmittgen, 2001).

4.10 Tissue dissociation for single cell RNA sequencing

To assess the proportion of the different cell types in the airway mucosa models, a serine protease enzyme, Subtilisin A, isolated from *Bacillus licheniformis* was used. A stock solution of 100mg/ml of the Subtilisin A enzyme was prepared by dissolving the powdered content in nuclease free water and 100µl stocks were aliquoted and stored at -20°C. To dissociate the epithelial cells from the SISser scaffold, the models were washed 3x with cold sterile PBS. The models were then removed from the cell crown and excess scaffold was removed. The models were then placed in 10cm cell culture plates and cut into at least 6 smaller pieces with a scalpel to improve exposure of the models to the enzyme. The pieces were transferred into 15ml Eppendorf tubes and incubated with 1ml of 10mg/ml *B. licheniformis* subtilisin A supplemented with 100units/ml DNase 1 in DPBS with magnesium and calcium. The tubes containing the tissue suspension was incubated for 30 minutes on ice with trituration every 10 minutes with a 5ml pipette. The dissociated cells were passed through a 40µm cell strainer to remove large pieces of the scaffold. The cell suspension was then washed twice in DPBS containing 5% FCS, pelleted and resuspended in DPBS containing 5% FCS for staining and later FACS sorted. 10µl of the cell suspension was then mixed with 10µl of trypan blue and counted using the haemocytometer to determine the cell viability as well as total cell count.

4.11 Immunostaining for FACS analysis

The airway mucosa models were dissociated as described above. The pelleted cells were then resuspended in 100µl of 5% FCS in PBS. The cell suspension was incubated on ice for 15 min to block the nonspecific antigen binding. 2µl of PerCP-Cy5.5 conjugated to Epcam was added to the cell suspension and incubated for 15 min on ice. Fixation and permeabilization of the cells were performed using the BD FIX and PERM® kit according to manufacturer

instructions. Briefly, 100 μ l of Reagent A was added to the cell suspension and incubated in the dark on ice for 15 minutes. The cells were then washed once in 3ml of PBS containing 5% FCS and centrifuged for 5 minutes at 1200rpm. The supernatant was aspirated, and the cells resuspended in 100 μ l of reagent B. 2 μ l of FITC-conjugated panCK was added, vortexed and incubated on ice for 20 minutes. Similarly, the isotype controls for both antibodies were added at the same concentrations as above. The cells were washed again with 3ml blocking solution and centrifuged. The supernatant was aspirated, and the pellets resuspended in 1%FCS/PBS for sorting and analysis. The cells were then passed through a 0.4 μ m filter into FACS tubes and sorted with a BD FACS Aria III.

5 Chapter 5: Materials

5.1 Biological material

Table 5-1 List of Mammalian cells and biological scaffold

Cell	Description	Media	Source
HTEC	Primary human tracheobronchial epithelia cells	AECGM	Tracheobronchial biopsy from 15 male and 13 female donors aged between 30 – 80 years
HNEC	Primary human nasal epithelial cells	AECGM	Nasal biopsy from 6 male donors and 5 female donors aged between 17 and 75 years
HBF	Primary human tracheobronchial fibroblasts	FGM	Tracheobronchial biopsy isolated from 6 male and 5 female donors aged between 30 – 80 years.
nFb	Primary human nasal fibroblast	FGM	Nasal biopsy from 3 female and 2 male donors aged between 17 and 50 years.
HBEC3-KT	Immortalised primary bronchial epithelial cells	KSFM	American Type Culture Collection (ATCC)
SISser	Porcine-derived small intestine serosa		Decellularizing explanted small intestines from pig

Table 5-2 List of bacterial strains

Species	Description	Company/provider
Bp_TH1	Wildtype B. pertussis Tohama I strain	
Bp_GFP	Wildtype B. pertussis Tohama I strain carrying GFP plasmid. Kanamycin resistant	Sebo Lab, Prague
Bp_347	Avirulent strain of B. pertussis	

Table 5-3 List of toxins

Toxin	Origin	Company/Provider
LPS	<i>Escherichia coli</i> 026: B6	Sigma Aldrich, USA
Tracheal Cytotoxin	<i>B. pertussis</i> TH1	William Evan Goldman, USA

Table 5-4 Oligonucleotides for qPCR

Target	Strand	Sequence
<i>IL-1α</i>	sense	CTTAGTGCCGTGAGTTTCCC
<i>IL-1α</i>	antisense	TGTGACTGCCCAAGATGAAG
<i>IL-1β</i>	sense	AAGCCCTTGCTGTAGTGGTG
<i>IL-1β</i>	antisense	GAAGCTGATGGCCCTAAACA
<i>IL-6</i>	sense	CATTTGTGGTTGGGTCAGG
<i>IL-6</i>	antisense	AGTGAGGAACAAGCCAGAGC
<i>IL-10</i>	sense	CTCATGGCTTTGTAGATGCCT
<i>IL-10</i>	antisense	GCTGTCATCGATTTCTTCCC
<i>GAPDH</i>	sense	TGACGCTGGGGCTGGCATTG
<i>GAPDH</i>	antisense	GCTCTTGCTGGGGCTGGTGG

5.2 Antibodies

Table 5-5 Primary antibodies used in this study

Target	Host	Dilution	Company (catalog)
IL1- α	Rabbit polyclonal	1:100	Abcam, UK (Ab7632)
IL-1 β	Mouse monoclonal	1:100	Thermo Scientific, GER (M421B)
SLC46A2	Rabbit Polyclonal	1:500	Thermo scientific, GER (PA5-31389)
iNOS	Rabbit polyclonal	1:500	Thermo Scientific , GER (PA3-030A)
Ck 18	Mouse monoclonal	1:100	Agilent, USA (M7010)
Ck 14	Rabbit polyclonal	1:1000	Sigma-Aldrich, GER (HPA023040)

Ck 5/6	Mouse monoclonal	1:200	Agilent, USA (M7237)
Muc5AC	Mouse monoclonal	1:100	Sigma-Aldrich, GER (HPA008246)
Muc5B	Rabbit polyclonal	1:100	Thermo Scientific, GER (MA1-38223)
Act-tubulin	Mouse monoclonal	1:1000	Sigma-Aldrich, GER (T8328)
ZO-1	Rabbit polyclonal	1:1000	Proteintech, UK (21773-1-AP)
E-cadherin	Mouse monoclonal	1:100	BD Biosciences , GER (610181)
Vimentin	Rabbit monoclonal	1:1000	Abcam, UK (Ab92547)
LAMP-1	Rabbit polyclonal	1:1000	Sigma-Aldrich , GER (L1418)
Pan-Ck	Mouse monoclonal	1:2000	Sigma-Aldrich, GER (C 2562)
Epcam_PerCP_ Cy5.5	Mouse monoclonal	1:100	BD Biosciences, GER (347199)
Pancytokeratin_FITC	Mouse polyclonal	1:100	Abcam, UK (ab11214)

Table 5-6 Secondary antibodies used in this study

Antibody	Dye	Dilution	Host	Manufacturer	Cat. no.
Anti-mouse	AF 555	1:400	Donkey	Invitrogen, GER	A-31570
Anti-mouse	AF 647	1:400	Donkey	Invitrogen, GER	A-31571
Anti-rabbit	AF 555	1:400	Donkey	Invitrogen, GER	A-31572
Anti-rabbit	AF 647	1:400	Donkey	Invitrogen, GER	A-31573
Anti-mouse	AF488	1:400	Donkey	Invitrogen, GER	A-21202
Anti-rabbit	AF488	1:400	Donkey	Invitrogen, GER	A-21206

5.3 Composition of Media and solutions

Table 5-7 Composition of cell culture media

Medium	Components	Supplier/Catalog
Airway epithelial cell growth basal medium	Basal medium Supplements (I,II,III)	PELOBiotech, GER (PB-MH-350-0099)
Fibroblast growth medium (FGM)	DMEM (Glutamax) 10% (v/v) FCS	Thermo-Scientific, GER (31966047) Sigma-Aldrich, GER
Freezing medium	90% (v/v) FCS 10% (v/v) DMSO	Sigma-Aldrich, GER Sigma-Aldrich, GER (41639)
Keratinocyte Serum Free Medium (Defined)	Basal medium Supplement	Thermo-Scientific, GER (10744019)

Table 5-8 Bacterial growth medium

Medium	Ingredients
5xStainer-Scholte (1 L Solution, pH7.6)	5.35g Sodium Glutamate 1.2g L-Proline 12.5g Potassium dihydrogenphosphate (KH ₂ PO ₄) 1g Potassium Chloride (KCl) 0.5g Magnesium Chloride hexahydrate (MgCl ₂ .6H ₂ O) 7.5g Tris base
CaCl ₂ solution	0.13 g Calcium chloride dihydrate (CaCl ₂ .2H ₂ O) in 10 ml dH ₂ O
Casamino acid solution	5 g Casamino acid in 50ml dH ₂ O
Cyclodextrin solution	2.5 g Cyclodextrin in 50 ml 62.5 mM NaOH
100xSS (50ml)	<i>Solution I (45 ml dH₂O)</i> 50 mg Iron (II) sulphate heptahydrate (FeSO ₄ .7H ₂ O) 100 mg L-Ascorbic acid 4 mg Nicotinic acid

	100 mg Glutathione <u>Solution II (5 ml dH₂O)</u> 200 g L-Cystine 500 µl 32% HCl <i>Mix solution I and II and sterile filter</i>
1xSS (1 L solution)	2 ml CaCl ₂ solution 200 ml 5xSS solution 10 ml 100xSS 10 ml Casamino acid solution 10 ml Cyclodextrin solution
Bordet-Gengou agar (1 L solution)	30 g Bordet-Gengou base (agar) 8 ml Glycerin 15% (v.v) defibrinated sheep blood

5.4 Chemicals, reagents and proteins

Table 5-9 List of chemicals

Chemical/Solution	Producer	Catalog No
β-Mercaptoethanol	Sigma-Aldrich, GER	8057400250
Albumin fraction V (BSA)	Carl Roth, GER	90604-29-8
Ammonium persulphate	Sigma-Aldrich, GER	A3678
Antibody Diluent	DCS Innovative Diagnostik-Systeme, GER	AL120R500
Bromophenol blue	Sigma-Aldrich, GER	1.08122
Calcium chloride	VWR, GER	1.02391.1000
Calcium chloride dihydrate	Sigma-Aldrich, GER	21102
Chloroform	Carl Roth	7331.2
Citric acid	VWR, GER	1.00244.1000
Deoxycholic acid sodium salt	Carl Roth, GER	3484.2
Descosept® AF	Dr. Schumacher GmbH, GER	00-311-050
Dexamethasone	Sigma-Aldrich, GER	D4902
Difco Bordet Gengou Agar Base	BD Bioscience, GER	248200
Dimethyl sulfoxide (DMSO)	Sigma-Aldrich, GER	D2438-50ML

DNase I	Sigma-Aldrich, GER	D5025-15KU
Dulbecco's Modified Eagle Medium, high glucose, GlutaMAX™ (DMEM)	Gibco® Life Tech™, GER	10564011
Dulbecco's Phosphate Buffered Saline (PBS with Mg and Ca)	Sigma-Aldrich, GER	D8662
Dulbecco's Phosphate Buffered Saline (PBS without Mg and Ca)	Sigma-Aldrich, GER	D8537
Entellan®	Merck, GER	1079600500
Eosin 1 % aqueous solution	Morphisto GmbH, GER	10177.01000
Ethanol 96%, denatured	Carl Roth, GER	T171.4
Ethanol, absolute	Carl Roth, GER	9065.4
Ethylenediaminetetraacetic acid (EDTA)	Sigma-Aldrich, GER	E5134-1KG
Fetal Calf Serum	PAN Biotech, GER	P30-3306
Fluoromount-G™ +DAPI	Southern Biotech, USA	SBA-0100-20
Formaldehyde	Carl Roth, GER	P087.3
Glutaraldehyde	Sigma-Aldrich, GER	G5882
Glutathione	Sigma-Aldrich, GER	G4251
Glycerin	Carl Roth, GER	3783.2
Glycine	Carl Roth, GER	3908.3
Haematoxylin Solution acidic	Morphisto GmbH, GER	10231.01000
Hydrochloric acid (1M)	Carl Roth, GER	K025.1
Incidin® plus	Ecolab, GER	3011520
Isopropyl	Carl Roth, GER	2316.5
Kanamycin sulphate	Carl Roth, GER	T832.2
L- Cystine	Sigma-Aldrich, GER	168149
L-Ascorbic acid	Sigma-Aldrich, GER	A92902
L-Proline	Sigma-Aldrich, GER	81709
Magnesium Chloride hexahydrate	Carl Roth, GER	HN03.1
Methanol	Sigma-Aldrich, GER	32213-2,5L
Methyl-β-cyclodextrin	Sigma-Aldrich, GER	C4555-1G
Nicotinic acid	Sigma-Aldrich, GER	N4126

Paraffin	Carl Roth, GER	6642.6
Polymyxin B Sulphate	Sigma-Aldrich, GER	P4932
Potassium Chloride	Carl Roth, GER	5346.2
Potassium dihydrogenphosphate	Carl Roth, GER	3904.1
Skimmed milk powder	Carl Roth, GER	T145.2
Sodium cacodylate trihydrate	Sigma-Aldrich, GER	C0250
Sodium chloride	Carl Roth, GER	HN00.3
Sodium chloride	Carl Roth, GER	HNOO.3
Sodium dodecyl sulfate	Carl Roth, GER	CN30.3
Sodium Glutamate	Sigma-Aldrich, GER	1446600
Sodium hydroxide	Sigma-Aldrich, GER	S8045
Sodium pyruvate (100 mM)	Invitrogen, GER	11360-039
Subtilisin A	Sigma-Aldrich, GER	P5380
TissueTek® O.C.T.™	Sakura, GER	4586
Tris base	Sigma-Aldrich, GER	T6066-5kg
Triton™ X-100	Sigma-Aldrich, GER	X100-1L
Trypan blue, 0.4 %	Sigma-Aldrich, GER	T8154-100ml
Trypsin 0,5% 10x	Invitrogen, GER	15400-054
Tween®-20	Sigma-Aldrich, GER	P7949-500ml
Xylene (>98 %)	Carl Roth, GER	9713.3

Table 5-10 Commercial kits

Kit	Description	Company/Ref
RNeasy Mini Kit	Total RNA isolation from mammalian and bacterial cells	Qiagen, GER (74104)
Griess Reagent	Griess reagent for quantifying dissolved nitric oxide in cell culture supernatant	Promega, USA (G2930)
Bradford assay	Kit for quantifying protein	Sigma-Aldrich, GER (B6916)

Cytometric Bead array	Bead-based kit for quantifying inflammatory cytokine	BD Biosciences, GER (551811)
Fix and Perm® Cell Permeabilization	Fixative and permeabilization kit for FACS	Life technologies, GER (GAS003)
RNase-free DNase Set	DNase for DNA digestion during RNA isolation	Qiagen, GER (79254)

Table 5-11 Buffers, reagents and solutions used in this work

Solution/buffer	Ingredients
Blocking solution (IF)	5% (w/v) Bovine Serum albumin 1x Phosphate buffered saline
Methacarn	60% (v/v) Methanol 30% (v/v) Chloroform 10% (v/v) Acetic acid
Citrate buffer (pH6.0)	4.2g/l Citric acid monohydrate 1.76g/l Sodium hydroxide pellets in deionized water
Tris EDTA (pH9)	10mM Tris base 1mM EDTA
Mounting solution	Fluoromount G + DAPI
Permeabilization solution	0.01% (v/v) TritonX-100 in 5% BSA/PBS
Washing buffer (PBS-T)	10% (v/v) PBS stock 0.5% (v/v) Tween-20 In demineralized water
Antibody diluent	5% (w/v) BSA in PBS-solution
Radioimmunoprecipitation assay (RIPA) buffer	50 mM Tris base pH7.5 150mM NaCl 1mM EDTA 1% (v/v) TritonX-100 1% (v/v) Sodium-deoxycholate
SDS upper PAGE buffer (250ml)	0.5M Tris Base pH6.8 0.4% (v/v) SDS

SDS lower PAGE buffer (250ml)	1.5M Tri base pH 8.8 0.4% (v/v) SDS
40%APS (WB)	4g Ammonium persulphate 10 ml sterile water
Upper PAGE gel solution	0.5 M Tris base 0.4% SDS
5X Laemmli for PAGE	340mM Tri base 10% SDS 30% (v/v) Glycerin 6mg Bromophenol blue 5% (v/v) β -Mercaptoethanol
10x SDS-PAGE running buffer	250mM Tris 1.9mM Glycin 1.5% SDS
1X SDS-PAGE running buffer (1L)	100ml 10x SDS-PAGE 900ml Distilled water
5x Transfer Buffer	960mM Glycin 125mM Tris Base
1x Transfer buffer (1L)	200ml 5x Transfer Buffer 800ml distilled water
10x TBS (pH7.6)	250mM Tris Base 1.5mM NaCl
Blocking solution (WB)	5% (w/v) skimmed milk powder in TBST
Blocking solution (FACS)	95% (v/v) DPBS without calcium and magnesium 5% (v/v) FCS
FACS Buffer	94,6% (v/v) DPBS without calcium and magnesium 1% (v/v) FCS 0,4% (v/v) EDTA
Cell dissociation solution in 1ml DPBS with Mg and Ca	10mg/ml <i>B. licheniformis</i> Subtilisin A 100units/ml DNase1
Fixative for TEM	50mM Sodium Cacodylate (pH7.2)

	50mM KCl 2.5% MgCl ₂ 2.5% glutaraldehyde
Fixative for SEM	50mM Cacodylate (pH7.2) 50mM KCl 2.5% MgCl ₂ 6.5% Glutaraldehyde
Polymyxin B stock	Polymyxin Sulphate powder (10mg/ml) in sterile water
Kanamycin stock	Kanamycin powder (30mg/ml) in sterile water

5.5 Technical equipment

Table 5-12 List of equipment

Device	Manufacturer
Accu-jet pipettor	Brand, GER
Analytical Balance	Kern & Sohn, GER
Aspiration Device: VacuBoy	Integra Biosciences, GER
Autoclaves: DX-45 Bench-top Autoclave Steam sterilizer (Varioklav) Technoclav	Systec GmbH, GER HP-Medizintechnik, GER Integra Biosciences AG, GER
Biological safety cabinet NU-425-600 E	Nuaire, USA
Blocking Station	Leica, GER
Cell incubator: 37 °C, 5 % CO ₂	Heraeus, GER
Centrifuges: Centrifuge 5417R Multifuge X12 Multifuge X1R Pico 17 Rotilabo	Eppendorf, GER Thermo Fisher Scientific, GER Thermo Fisher Scientific, GER Thermo Fisher Scientific, GER Carl Roth, GER
Cold storage room, 4 °C	Genheimer, GER
Cooling plate	Leica, GER

Cryostat (Leica CM3050 S)	Leica, GER
Dalsa Motion Traveller highspeed video camera	Imaging Solutions GmbH, GER
Delta T Dishes	Biotech Inc, USA
Delta T5 μ -Environment controller	Biotech Inc, USA
Digital camera	Canon, GER
Drying oven	Memmert, GER
Embedding cassette printer VCP-5001	Vogel Medizintechnik, GER
Embedding center	Thermo Fisher Scientific, GER
Flow Cytometer Accuri C6 Aria III	BD Biosciences, USA BD Biosciences, USA
Freezer -20°C: Comfort	Liebherr, GER
Freezer -80°C: HFU586 Basic	Heraeus Med, GER
Freezing container: Mr. Frosty™	VWR, GER
Fume hood	Prutscher Laboratory Systems, AT
Genie 2 Vortex	Carl Roth, GER
Ice machine AF-80	Scotsman, IT
Immersion thermostat for water bath	Lauda, GER
Laboratory dish washer	Miele, GER
Liquid nitrogen storage tank MVE 815 P190	German-cryo, GER
Magnetic stirrer and heater 720-HPS	VWR, GER
Tecan Infinite® Microplate reader M200	Tecan, GER
Microscopes: Bright field (Axio Lab.A1) Nikon 80i Confocal (SP8) Confocal (SP5) Fluorescence (BZ-9000)	Carl Zeiss Microscopy GmbH, GER Nikon GmbH, GER Leica, GER Leica, GER Keyence, GER

JEM-2100 TEM	JOEL, JP
JSM-7599F SEM	JOEL, JP
Millicel® ERS-2 Volt-Ohmmeter	Merck, GER
Multichannel pipette plus	Eppendorf, GER
Multistep pipette	Brand, GER
Neubauer cell counting chamber (haemocytometer)	Marienfeld GmbH & Co. KG, GER
Orbital shaker (KM-2 Akku)	Edmund Bühler GmbH, GER
Peristaltic pump	Ismatec, GER
pH meter	Mettler Toledo, GER
Pipette plugger	Bellco Glass, GER
Refrigerator (MedLine)	Liebherr, GER
Rocking platform shaker	VWR, GER
Slide printer VSP-5001	Vogel Medizintechnik, GER
Sliding microtome (Leica SM2010R)	Leica, GER
NanoDrop 1000	Thermo Scientific, USA
Steamer (MultiGourmet)	Braun, GER
Thermostat	Eppendorf, GER
Tissue floatation bath (GFL1052)	GFL, GER
Water purification system (MilliQ®)	Merck-Millipore, GER

Table 5-13 List of Disposable material

Disposable material	Source
Cell culture flasks (25cm ² , 75cm ² , 150cm ²)	Techno Plastik Products AG, CH Corning, GER
Cell culture multiwell plates (6 well, 12 well, 24 well, 96 well)	Techno Plastik Products AG, CH Greiner, GER
Cell scrapers	Sarstedt, GER
Centrifuge tubes (15ml; 50ml)	Greiner Bio-One, GER
Combitips Plus (0.5 ml, 1ml, 2.5 ml, 5 ml)	Eppendorf, GER
Cover slips for object slides (24x60 mm)	Menzel-Gläser, GER
Cover slips (round, Ø 12 mm)	Marienfeld GmbH & Co KG, GER
Cryo tubes (1.8 ml)	Nunc, GER

Disposable microtome blades (type S35)	pfm medical, GER
Disposable pipettes (5 ml, 10 ml, 25 ml, 50 ml)	Greiner Bio-One, GER
Disposal bags	Hartenstein, GER
Embedding cassettes	Klinipath, GER
Embedding filter paper	Labonord, GER
Medical gloves, nitrile	Medline, GER)
Microscope slides: Uncoated Polylysine™	Menzel, GER Langenbrinck, GER
Paper towel	IGEFA, GER
Parafilm® M	Carl Roth, GER
Petri Dishes: 145 x 20mm	Greiner Bio-One, GER
Pipette tips (0.5-10µl, 10-100µl, 100-1000µl)	Eppendorf, GER
Reaction tubes (0.5ml, 1.5ml, 2ml)	Sarstedt, GER
Scalpel blades, rounded	Bayha, GER
Sterile filter (pore size:0.2µm)	Sartorius Stedium Biotech, GER
Syringes (20ml, 50ml)	BD Biosciences, GER
Weighing dish	Hartenstein, GER
Whatman filter paper	Hartenstein, GER
Aluminium foil	Carl Roth GmbH, GER
Ceramic beads for tissue lysis (S5310.0100)	Genaxxon, GER
Insect pinning needles	Ento Sphinx, CZ
5ml FACS tubes	Sigma-Aldrich, GER
Cell Strainer (40µm, 70µm)	Sigma-Aldrich, GER

5.6 Software

Table 5-14 Softwares used in this work

Software	Company
ChemDraw ® V 19.1 for Mac	Perkin Elmer Infomatics, UK
Endnote™ v20 for MacOS	Clarivate™, Australia

FCAP array™ v3.0 for Windows	BD Biosciences, USA
FIJI for MacOS	NIH, USA
Graphpad™ Prism V 8	Graphpad Software, USA
Image Pro ® Premier 10	Media cybernetics, USA
Inkscape for MacOS	Inkscape, USA
LASX for Windows	Leica Microsystems, GER
MacOS BigSur v11.1	Apple Inc, USA
Matlab® V2011a/b	Mathworks, USA
Microsoft Office 365 for MacOS	Microsoft, USA
Motion Traveller ® for Windows	Imaging Solutions GmbH, GER

References

- Abramson, S.B., Amin, A.R., Clancy, R.M., and Attur, M. (2001). The role of nitric oxide in tissue destruction. *Best Pract Res Clin Rheumatol* 15(5), 831-845. doi: 10.1053/berh.2001.0196.
- Adam, M., Potter, A.S., and Potter, S.S. (2017). Psychrophilic proteases dramatically reduce single-cell RNA-seq artifacts: a molecular atlas of kidney development. *Development* 144(19), 3625-3632. doi: 10.1242/dev.151142.
- Adkins, I., Kamanova, J., Kocourkova, A., Svedova, M., Tomala, J., Janova, H., et al. (2014). Bordetella adenylate cyclase toxin differentially modulates toll-like receptor-stimulated activation, migration and T cell stimulatory capacity of dendritic cells. *PLoS One* 9(8), e104064. doi: 10.1371/journal.pone.0104064.
- Ahmad, J.N., Cerny, O., Linhartova, I., Masin, J., Osicka, R., and Sebo, P. (2016). cAMP signalling of Bordetella adenylate cyclase toxin through the SHP-1 phosphatase activates the BimEL-Bax pro-apoptotic cascade in phagocytes. *Cell Microbiol* 18(3), 384-398. doi: 10.1111/cmi.12519.
- Ahuja, U., Shokeen, B., Cheng, N., Cho, Y., Blum, C., Coppola, G., et al. (2016). Differential regulation of type III secretion and virulence genes in Bordetella pertussis and Bordetella bronchiseptica by a secreted anti-sigma factor. *Proc Natl Acad Sci U S A* 113(9), 2341-2348. doi: 10.1073/pnas.1600320113.
- Akerley, B.J., Cotter, P.A., and Miller, J.F. (1995). Ectopic expression of the flagellar regulon alters development of the Bordetella-host interaction. *Cell* 80(4), 611-620. doi: 10.1016/0092-8674(95)90515-4.
- Akerley, B.J., Monack, D.M., Falkow, S., and Miller, J.F. (1992). The bvgAS locus negatively controls motility and synthesis of flagella in Bordetella bronchiseptica. *J Bacteriol* 174(3), 980-990. doi: 10.1128/jb.174.3.980-990.1992.
- Alaribe, F.N., Manoto, S.L., and Motaung, S.C.K.M. (2016). Scaffolds from biomaterials: advantages and limitations in bone and tissue engineering. *Biologia* 71(4). doi: 10.1515/biolog-2016-0056.
- Alonso, S., Pethe, K., Mielcarek, N., Raze, D., and Locht, C. (2001). Role of ADP-ribosyltransferase activity of pertussis toxin in toxin-adhesin redundancy with filamentous hemagglutinin during Bordetella pertussis infection. *Infect Immun* 69(10), 6038-6043. doi: 10.1128/IAI.69.10.6038-6043.2001.
- Amador, C., Weber, C., and Varacallo, M. (2020). "Anatomy, Thorax, Bronchial," in *StatPearls*. (Treasure Island (FL)).
- Anderton, T.L., Maskell, D.J., and Preston, A. (2004). Ciliostasis is a key early event during colonization of canine tracheal tissue by Bordetella bronchiseptica. *Microbiology (Reading)* 150(Pt 9), 2843-2855. doi: 10.1099/mic.0.27283-0.
- Angely, C., Ladant, D., Planus, E., Louis, B., Filoche, M., Chenal, A., et al. (2020). Functional and structural consequences of epithelial cell invasion by

- Bordetella pertussis* adenylate cyclase toxin. *PLoS One* 15(5), e0228606. doi: 10.1371/journal.pone.0228606.
- Angely, C., Nguyen, N.M., Andre Dias, S., Planus, E., Pelle, G., Louis, B., et al. (2017). Exposure to *Bordetella pertussis* adenylate cyclase toxin affects integrin-mediated adhesion and mechanics in alveolar epithelial cells. *Biol Cell* 109(8), 293-311. doi: 10.1111/boc.201600082.
- Arico, B., Miller, J.F., Roy, C., Stibitz, S., Monack, D., Falkow, S., et al. (1989). Sequences required for expression of *Bordetella pertussis* virulence factors share homology with prokaryotic signal transduction proteins. *Proc Natl Acad Sci U S A* 86(17), 6671-6675. doi: 10.1073/pnas.86.17.6671.
- Arima, M., Plitt, J., Stellato, C., Bickel, C., Motojima, S., Makino, S., et al. (1999). Expression of interleukin-16 by human epithelial cells. Inhibition by dexamethasone. *Am J Respir Cell Mol Biol* 21(6), 684-692. doi: 10.1165/ajrcmb.21.6.3671.
- Ashworth, L.A., Irons, L.I., and Dowsett, A.B. (1982). Antigenic relationship between serotype-specific agglutinogen and fimbriae of *Bordetella pertussis*. *Infect Immun* 37(3), 1278-1281. doi: 10.1128/IAI.37.3.1278-1281.1982.
- Audry, M., Robbe-Masselot, C., Barnier, J.P., Gachet, B., Saubamea, B., Schmitt, A., et al. (2019). Airway Mucus Restricts *Neisseria meningitidis* Away from Nasopharyngeal Epithelial Cells and Protects the Mucosa from Inflammation. *mSphere* 4(6). doi: 10.1128/mSphere.00494-19.
- Ausiello, C.M., Lande, R., Urbani, F., Di Carlo, B., Stefanelli, P., Salmaso, S., et al. (2000). Cell-mediated immunity and antibody responses to *Bordetella pertussis* antigens in children with a history of pertussis infection and in recipients of an acellular pertussis vaccine. *J Infect Dis* 181(6), 1989-1995. doi: 10.1086/315509.
- Ballke, C., Gran, E., Baekkevold, E.S., and Jahnsen, F.L. (2016). Characterization of Regulatory T-Cell Markers in CD4+ T Cells of the Upper Airway Mucosa. *PLoS One* 11(2), e0148826. doi: 10.1371/journal.pone.0148826.
- Barkoff, A.M., Mertsola, J., Pierard, D., Dalby, T., Hoegh, S.V., Guillot, S., et al. (2019). Pertactin-deficient *Bordetella pertussis* isolates: evidence of increased circulation in Europe, 1998 to 2015. *Euro Surveill* 24(7). doi: 10.2807/1560-7917.ES.2019.24.7.1700832.
- Baron, S., Begue, P., and Grimprel, E. (1994). [Epidemiology of pertussis in industrialized countries]. *Sante* 4(3), 195-200.
- Bassinat, L., Gueirard, P., Maitre, B., Housset, B., Gounon, P., and Guiso, N. (2000). Role of adhesins and toxins in invasion of human tracheal epithelial cells by *Bordetella pertussis*. *Infect Immun* 68(4), 1934-1941. doi: 10.1128/iai.68.4.1934-1941.2000.
- Belcher, C.E., Drenkow, J., Kehoe, B., Gingeras, T.R., McNamara, N., Lemjabbar, H., et al. (2000). The transcriptional responses of respiratory epithelial cells to *Bordetella pertussis* reveal host defensive and pathogen counter-defensive strategies. *Proc Natl Acad Sci U S A* 97(25), 13847-13852. doi: 10.1073/pnas.230262797.

- Ben-Baruch, A., Michiel, D.F., and Oppenheim, J.J. (1995). Signals and receptors involved in recruitment of inflammatory cells. *J Biol Chem* 270(20), 11703-11706. doi: 10.1074/jbc.270.20.11703.
- Berggard, K., Lindahl, G., Dahlback, B., and Blom, A.M. (2001). Bordetella pertussis binds to human C4b-binding protein (C4BP) at a site similar to that used by the natural ligand C4b. *Eur J Immunol* 31(9), 2771-2780. doi: 10.1002/1521-4141(200109)31:9<2771::aid-immu2771>3.0.co;2-0.
- Berglund, L., Bjorling, E., Oksvold, P., Fagerberg, L., Asplund, A., Szigyarto, C.A., et al. (2008). A gene-centric Human Protein Atlas for expression profiles based on antibodies. *Mol Cell Proteomics* 7(10), 2019-2027. doi: 10.1074/mcp.R800013-MCP200.
- Binkin, N.J., Salmaso, S., Tozzi, A.E., Scuderi, G., Greco, D., and Greco, D. (1992). Epidemiology of pertussis in a developed country with low vaccination coverage: the Italian experience. *Pediatr Infect Dis J* 11(8), 653-661.
- Bonassar, L.J., and Vacanti, C.A. (1998). Tissue engineering: the first decade and beyond. *J Cell Biochem Suppl* 30-31, 297-303.
- Bordet, J., and Gengou, O. (1906). Le microbe de la coqueluche. *Ann Inst Pasteur* 20, 48-68.
- Boucher, P.E., and Stibitz, S. (1995). Synergistic binding of RNA polymerase and BvgA phosphate to the pertussis toxin promoter of Bordetella pertussis. *J Bacteriol* 177(22), 6486-6491. doi: 10.1128/jb.177.22.6486-6491.1995.
- Bouchez, V., Guglielmini, J., Dazas, M., Landier, A., Toubiana, J., Guillot, S., et al. (2018). Genomic Sequencing of Bordetella pertussis for Epidemiology and Global Surveillance of Whooping Cough. *Emerg Infect Dis* 24(6), 988-994. doi: 10.3201/eid2406.171464.
- Boyd, A.P., Ross, P.J., Conroy, H., Mahon, N., Lavelle, E.C., and Mills, K.H. (2005). Bordetella pertussis adenylate cyclase toxin modulates innate and adaptive immune responses: distinct roles for acylation and enzymatic activity in immunomodulation and cell death. *J Immunol* 175(2), 730-738.
- Brickman, T.J., and Armstrong, S.K. (2002). Alcaligin siderophore production by Bordetella bronchiseptica strain RB50 is not repressed by the BvgAS virulence control system. *J Bacteriol* 184(24), 7055-7057. doi: 10.1128/jb.184.24.7055-7057.2002.
- Brockmeier, S.L., and Lager, K.M. (2002). Experimental airborne transmission of porcine reproductive and respiratory syndrome virus and Bordetella bronchiseptica. *Vet Microbiol* 89(4), 267-275. doi: 10.1016/s0378-1135(02)00204-3.
- Bromberg, K., Tannis, G., and Steiner, P. (1991). Detection of Bordetella pertussis associated with the alveolar macrophages of children with human immunodeficiency virus infection. *Infect Immun* 59(12), 4715-4719. doi: 10.1128/IAI.59.12.4715-4719.1991.
- Broome, C.V., Preblud, S.R., Bruner, B., McGowan, J.E., Hayes, P.S., Harris, P.P., et al. (1981). Epidemiology of pertussis, Atlanta, 1977. *J Pediatr* 98(3), 362-367. doi: 10.1016/s0022-3476(81)80696-8.

- Budnik, L.T., and Mukhopadhyay, A.K. (1993). Pertussis toxin can distinguish the augmentary effect elicited by epidermal growth factor from that of phorbol ester on luteal adenylate cyclase activity. *Endocrinology* 133(1), 265-270. doi: 10.1210/endo.133.1.8319575.
- Bumba, L., Masin, J., Fiser, R., and Sebo, P. (2010). Bordetella adenylate cyclase toxin mobilizes its beta2 integrin receptor into lipid rafts to accomplish translocation across target cell membrane in two steps. *PLoS Pathog* 6(5), e1000901. doi: 10.1371/journal.ppat.1000901.
- Cafiero, J.H., Lamberti, Y.A., Surmann, K., Vecerek, B., and Rodriguez, M.E. (2018). A Bordetella pertussis MgtC homolog plays a role in the intracellular survival. *PLoS One* 13(8), e0203204. doi: 10.1371/journal.pone.0203204.
- Capaldo, C.T., and Nusrat, A. (2009). Cytokine regulation of tight junctions. *Biochim Biophys Acta* 1788(4), 864-871. doi: 10.1016/j.bbame.2008.08.027.
- Carbonetti, N.H. (2010). Pertussis toxin and adenylate cyclase toxin: key virulence factors of Bordetella pertussis and cell biology tools. *Future Microbiol* 5(3), 455-469. doi: 10.2217/fmb.09.133.
- Cassatella, M.A., Bazzoni, F., Ceska, M., Ferro, I., Baggiolini, M., and Berton, G. (1992). IL-8 production by human polymorphonuclear leukocytes. The chemoattractant formyl-methionyl-leucyl-phenylalanine induces the gene expression and release of IL-8 through a pertussis toxin-sensitive pathway. *J Immunol* 148(10), 3216-3220.
- Cassatella, M.A., Meda, L., Bonora, S., Ceska, M., and Constantin, G. (1993). Interleukin 10 (IL-10) inhibits the release of proinflammatory cytokines from human polymorphonuclear leukocytes. Evidence for an autocrine role of tumor necrosis factor and IL-1 beta in mediating the production of IL-8 triggered by lipopolysaccharide. *J Exp Med* 178(6), 2207-2211. doi: 10.1084/jem.178.6.2207.
- Cattelan, N., Jennings-Gee, J., Dubey, P., Yantorno, O.M., and Deora, R. (2017). Hyperbiofilm Formation by Bordetella pertussis Strains Correlates with Enhanced Virulence Traits. *Infect Immun* 85(12). doi: 10.1128/IAI.00373-17.
- Chan, J.M., and Dillard, J.P. (2016). Neisseria gonorrhoeae Crippled Its Peptidoglycan Fragment Permease To Facilitate Toxic Peptidoglycan Monomer Release. *J Bacteriol* 198(21), 3029-3040. doi: 10.1128/JB.00437-16.
- Charles, I., Fairweather, N., Pickard, D., Beesley, J., Anderson, R., Dougan, G., et al. (1994). Expression of the Bordetella pertussis P.69 pertactin adhesin in Escherichia coli: fate of the carboxy-terminal domain. *Microbiology (Reading)* 140 (Pt 12), 3301-3308. doi: 10.1099/13500872-140-12-3301.
- Charles, I.G., Dougan, G., Pickard, D., Charfield, S., Smith, M., Novotny, P., et al. (1988). Molecular cloning and analysis of P. 69, a vir-controlled protein from Bordetella pertussis. *Tokai J Exp Clin Med* 13 Suppl, 227-234.
- Charles, I.G., Li, J.L., Roberts, M., Beesley, K., Romanos, M., Pickard, D.J., et al. (1991). Identification and characterization of a protective

- immunodominant B cell epitope of pertactin (P.69) from *Bordetella pertussis*. *Eur J Immunol* 21(5), 1147-1153. doi: 10.1002/eji.1830210509.
- Chen, Q., Lee, G., Craig, C., Ng, V., Carlson, P.E., Jr., Hinton, D.M., et al. (2018). A Novel Bvg-Repressed Promoter Causes vrg-Like Transcription of fim3 but Does Not Result in the Production of Serotype 3 Fimbriae in Bvg(-) Mode *Bordetella pertussis*. *J Bacteriol* 200(20). doi: 10.1128/JB.00175-18.
- Chen, Q., Ng, V., Warfel, J.M., Merkel, T.J., and Stibitz, S. (2017). Activation of Bvg-Repressed Genes in *Bordetella pertussis* by RisA Requires Cross Talk from Noncooperonic Histidine Kinase Risk. *J Bacteriol* 199(22). doi: 10.1128/JB.00475-17.
- Chen, Q., and Stibitz, S. (2019). The BvgASR virulence regulon of *Bordetella pertussis*. *Curr Opin Microbiol* 47, 74-81. doi: 10.1016/j.mib.2019.01.002.
- Cherry, J.D. (1984). The epidemiology of pertussis and pertussis immunization in the United Kingdom and the United States: a comparative study. *Curr Probl Pediatr* 14(2), 1-78. doi: 10.1016/0045-9380(84)90016-1.
- Cherry, J.D. (1996). Historical review of pertussis and the classical vaccine. *J Infect Dis* 174 Suppl 3, S259-263. doi: 10.1093/infdis/174.supplement_3.s259.
- Cherry, J.D. (1997). The role of *Bordetella pertussis* infections in adults in the epidemiology of pertussis. *Dev Biol Stand* 89, 181-186.
- Cherry, J.D. (1999). Pertussis in the preantibiotic and prevaccine era, with emphasis on adult pertussis. *Clin Infect Dis* 28 Suppl 2, S107-111. doi: 10.1086/515057.
- Cherry, J.D. (2005). The epidemiology of pertussis: a comparison of the epidemiology of the disease pertussis with the epidemiology of *Bordetella pertussis* infection. *Pediatrics* 115(5), 1422-1427. doi: 10.1542/peds.2004-2648.
- Cherry, J.D. (2006). Epidemiology of pertussis. *Pediatr Infect Dis J* 25(4), 361-362. doi: 10.1097/01.inf.0000210478.60841.69.
- Cherry, J.D. (2015). The history of Pertussis(Whooping cough).
- Cherry, J.D., Baraff, L.J., and Hewlett, E. (1989). The past, present, and future of pertussis. The role of adults in epidemiology and future control. *West J Med* 150(3), 319-328.
- Cherry, J.D., Xing, D.X., Newland, P., Patel, K., Heininger, U., and Corbel, M.J. (2004). Determination of serum antibody to *Bordetella pertussis* adenylate cyclase toxin in vaccinated and unvaccinated children and in children and adults with pertussis. *Clin Infect Dis* 38(4), 502-507. doi: 10.1086/381204.
- Cheung, G.Y., Kelly, S.M., Jess, T.J., Prior, S., Price, N.C., Parton, R., et al. (2009). Functional and structural studies on different forms of the adenylate cyclase toxin of *Bordetella pertussis*. *Microb Pathog* 46(1), 36-42. doi: 10.1016/j.micpath.2008.10.005.
- Chevalier, N., Moser, M., Koch, H.G., Schimz, K.L., Willery, E., Loch, C., et al. (2004). Membrane targeting of a bacterial virulence factor harbouring an extended signal peptide. *J Mol Microbiol Biotechnol* 8(1), 7-18. doi: 10.1159/000082076.

- Chilvers, M.A., and O'Callaghan, C. (2000). Analysis of ciliary beat pattern and beat frequency using digital high speed imaging: comparison with the photomultiplier and photodiode methods. *Thorax* 55(4), 314-317. doi: 10.1136/thorax.55.4.314.
- Choe, M.M., Tomei, A.A., and Swartz, M.A. (2006). Physiological 3D tissue model of the airway wall and mucosa. *Nat Protoc* 1(1), 357-362. doi: 10.1038/nprot.2006.54.
- Chong, K.T., Thangavel, R.R., and Tang, X. (2008). Enhanced expression of murine beta-defensins (MBD-1, -2, -3, and -4) in upper and lower airway mucosa of influenza virus infected mice. *Virology* 380(1), 136-143. doi: 10.1016/j.virol.2008.07.024.
- Clark, T.A. (2014). Changing pertussis epidemiology: everything old is new again. *J Infect Dis* 209(7), 978-981. doi: 10.1093/infdis/jiu001.
- Clary-Meinesz, C., Mouroux, J., Cosson, J., Huitorel, P., and Blaive, B. (1998). Influence of external pH on ciliary beat frequency in human bronchi and bronchioles. *Eur Respir J* 11(2), 330-333. doi: 10.1183/09031936.98.11020330.
- Clary-Meinesz, C., Mouroux, J., Huitorel, P., Cosson, J., Schoevaert, D., and Blaive, B. (1997). Ciliary beat frequency in human bronchi and bronchioles. *Chest* 111(3), 692-697. doi: 10.1378/chest.111.3.692.
- Cloud-Hansen, K.A., Peterson, S.B., Stabb, E.V., Goldman, W.E., McFall-Ngai, M.J., and Handelsman, J. (2006). Breaching the great wall: peptidoglycan and microbial interactions. *Nat Rev Microbiol* 4(9), 710-716. doi: 10.1038/nrmicro1486.
- Conover, M.S., Mishra, M., and Deora, R. (2011). Extracellular DNA is essential for maintaining *Bordetella* biofilm integrity on abiotic surfaces and in the upper respiratory tract of mice. *PLoS One* 6(2), e16861. doi: 10.1371/journal.pone.0016861.
- Conover, M.S., Redfern, C.J., Ganguly, T., Sukumar, N., Sloan, G., Mishra, M., et al. (2012). BpsR modulates *Bordetella* biofilm formation by negatively regulating the expression of the Bps polysaccharide. *J Bacteriol* 194(2), 233-242. doi: 10.1128/JB.06020-11.
- Cookson, B.T., Cho, H.L., Herwaldt, L.A., and Goldman, W.E. (1989a). Biological activities and chemical composition of purified tracheal cytotoxin of *Bordetella pertussis*. *Infect Immun* 57(7), 2223-2229. doi: 10.1128/IAI.57.7.2223-2229.1989.
- Cookson, B.T., Tyler, A.N., and Goldman, W.E. (1989b). Primary structure of the peptidoglycan-derived tracheal cytotoxin of *Bordetella pertussis*. *Biochemistry* 28(4), 1744-1749. doi: 10.1021/bi00430a048.
- Cooper, P., Potter, S., Mueck, B., Yousefi, S., and Jarai, G. (2001). Identification of genes induced by inflammatory cytokines in airway epithelium. *Am J Physiol Lung Cell Mol Physiol* 280(5), L841-852. doi: 10.1152/ajplung.2001.280.5.L841.
- Cotter, P.A., and Miller, J.F. (1994). BvgAS-mediated signal transduction: analysis of phase-locked regulatory mutants of *Bordetella bronchiseptica*

- in a rabbit model. *Infect Immun* 62(8), 3381-3390. doi: 10.1128/IAI.62.8.3381-3390.1994.
- Cotter, P.A., and Miller, J.F. (1997). A mutation in the *Bordetella bronchiseptica* *bvgS* gene results in reduced virulence and increased resistance to starvation, and identifies a new class of Bvg-regulated antigens. *Mol Microbiol* 24(4), 671-685. doi: 10.1046/j.1365-2958.1997.3821741.x.
- Coursen, J.D., Bennett, W.P., Gollahon, L., Shay, J.W., and Harris, C.C. (1997). Genomic instability and telomerase activity in human bronchial epithelial cells during immortalization by human papillomavirus-16 E6 and E7 genes. *Exp Cell Res* 235(1), 245-253. doi: 10.1006/excr.1997.3670.
- Coutte, L., Alonso, S., Reveneau, N., Willery, E., Quatannens, B., Locht, C., et al. (2003). Role of adhesin release for mucosal colonization by a bacterial pathogen. *J Exp Med* 197(6), 735-742. doi: 10.1084/jem.20021153.
- Coutte, L., Antoine, R., Drobecq, H., Locht, C., and Jacob-Dubuisson, F. (2001). Subtilisin-like autotransporter serves as maturation protease in a bacterial secretion pathway. *EMBO J* 20(18), 5040-5048. doi: 10.1093/emboj/20.18.5040.
- Cowell, J.L., Hewlett, E.L., and Manclark, C.R. (1979). Intracellular localization of the dermonecrotic toxin of *Bordetella pertussis*. *Infect Immun* 25(3), 896-901. doi: 10.1128/IAI.25.3.896-901.1979.
- Coyne, C.B., Vanhook, M.K., Gambling, T.M., Carson, J.L., Boucher, R.C., and Johnson, L.G. (2002). Regulation of airway tight junctions by proinflammatory cytokines. *Mol Biol Cell* 13(9), 3218-3234. doi: 10.1091/mbc.e02-03-0134.
- Crystal, R.G., Randell, S.H., Engelhardt, J.F., Voynow, J., and Sunday, M.E. (2008). Airway epithelial cells: current concepts and challenges. *Proc Am Thorac Soc* 5(7), 772-777. doi: 10.1513/pats.200805-041HR.
- Cundell, D.R., Kanthakumar, K., Taylor, G.W., Goldman, W.E., Flak, T., Cole, P.J., et al. (1994). Effect of tracheal cytotoxin from *Bordetella pertussis* on human neutrophil function in vitro. *Infect Immun* 62(2), 639-643. doi: 10.1128/IAI.62.2.639-643.1994.
- Dadaglio, G., Morel, S., Bauche, C., Moukrim, Z., Lemonnier, F.A., Van Den Eynde, B.J., et al. (2003). Recombinant adenylate cyclase toxin of *Bordetella pertussis* induces cytotoxic T lymphocyte responses against HLA*0201-restricted melanoma epitopes. *Int Immunol* 15(12), 1423-1430.
- de Gouw, D., Diavatopoulos, D.A., Bootsma, H.J., Hermans, P.W., and Mooi, F.R. (2011). Pertussis: a matter of immune modulation. *FEMS Microbiol Rev* 35(3), 441-474. doi: 10.1111/j.1574-6976.2010.00257.x.
- de Gouw, D., Hermans, P.W., Bootsma, H.J., Zomer, A., Heuvelman, K., Diavatopoulos, D.A., et al. (2014). Differentially expressed genes in *Bordetella pertussis* strains belonging to a lineage which recently spread globally. *PLoS One* 9(1), e84523. doi: 10.1371/journal.pone.0084523.
- Debrie, A.S., Mielcarek, N., Lecher, S., Roux, X., Sirard, J.C., and Locht, C. (2019). Early Protection against Pertussis Induced by Live Attenuated *Bordetella pertussis* BPZE1 Depends on TLR4. *J Immunol* 203(12), 3293-3300. doi: 10.4049/jimmunol.1901102.

- den Hartog, G., Schijf, M.A., Berbers, G.A.M., van der Klis, F.R.M., and Buisman, A.M. (2020). Bordetella pertussis induces IFN-gamma production by NK cells resulting in chemo-attraction by respiratory epithelial cells. *J Infect Dis*. doi: 10.1093/infdis/jiaa140.
- Deora, R. (2002). Differential regulation of the Bordetella bipA gene: distinct roles for different BvgA binding sites. *J Bacteriol* 184(24), 6942-6951. doi: 10.1128/jb.184.24.6942-6951.2002.
- Deora, R. (2004). Multiple mechanisms of bipA gene regulation by the Bordetella BvgAS phosphorelay system. *Trends Microbiol* 12(2), 63-65. doi: 10.1016/j.tim.2003.12.004.
- Deora, R., Bootsma, H.J., Miller, J.F., and Cotter, P.A. (2001). Diversity in the Bordetella virulence regulon: transcriptional control of a Bvg-intermediate phase gene. *Mol Microbiol* 40(3), 669-683. doi: 10.1046/j.1365-2958.2001.02415.x.
- Derakhshani, S., Kurz, A., Japtok, L., Schumacher, F., Pilgram, L., Steinke, M., et al. (2019). Measles Virus Infection Fosters Dendritic Cell Motility in a 3D Environment to Enhance Transmission to Target Cells in the Respiratory Epithelium. *Front Immunol* 10, 1294. doi: 10.3389/fimmu.2019.01294.
- Desai, T.R., Leeper, N.J., Hynes, K.L., and Gewertz, B.L. (2002). Interleukin-6 causes endothelial barrier dysfunction via the protein kinase C pathway. *J Surg Res* 104(2), 118-123. doi: 10.1006/jsre.2002.6415.
- Dienz, O., and Rincon, M. (2009). The effects of IL-6 on CD4 T cell responses. *Clin Immunol* 130(1), 27-33. doi: 10.1016/j.clim.2008.08.018.
- Dinarello, C.A. (1989). "Interleukin-1 and Its Biologically Related Cytokines.", 153-205.
- Dinarello, C.A. (2018). Overview of the IL-1 family in innate inflammation and acquired immunity. *Immunol Rev* 281(1), 8-27. doi: 10.1111/imr.12621.
- Dinarello, C.A., Elin, R.J., Chedid, L., and Wolff, S.M. (1978). The pyrogenicity of the synthetic adjuvant muramyl dipeptide and two structural analogues. *J Infect Dis* 138(6), 760-767. doi: 10.1093/infdis/138.6.760.
- Dinarello, C.A., and Krueger, J.M. (1986). Induction of interleukin 1 by synthetic and naturally occurring muramyl peptides. *Fed Proc* 45(11), 2545-2548.
- Dirix, V., Mielcarek, N., Debrie, A.S., Willery, E., Alonso, S., Versheure, V., et al. (2014). Human dendritic cell maturation and cytokine secretion upon stimulation with Bordetella pertussis filamentous haemagglutinin. *Microbes Infect* 16(7), 562-570. doi: 10.1016/j.micinf.2014.04.003.
- Dorji, D., Mooi, F., Yantorno, O., Deora, R., Graham, R.M., and Mukkur, T.K. (2018). Bordetella Pertussis virulence factors in the continuing evolution of whooping cough vaccines for improved performance. *Med Microbiol Immunol* 207(1), 3-26. doi: 10.1007/s00430-017-0524-z.
- Dresdner, R.D., and Wong, L.B. (1985). Measurement of ciliary beat frequency using high-speed video microscopy. *ISA Trans* 24(1), 33-38.
- Dunne, A., Ross, P.J., Pospisilova, E., Masin, J., Meaney, A., Sutton, C.E., et al. (2010). Inflammasome activation by adenylate cyclase toxin directs Th17

- responses and protection against *Bordetella pertussis*. *J Immunol* 185(3), 1711-1719. doi: 10.4049/jimmunol.1000105.
- Eberhardt, C.S., and Siegrist, C.A. (2017). What Is Wrong with Pertussis Vaccine Immunity? Inducing and Recalling Vaccine-Specific Immunity. *Cold Spring Harb Perspect Biol* 9(12). doi: 10.1101/cshperspect.a029629.
- Edgar, R., Mazor, Y., Rinon, A., Blumenthal, J., Golan, Y., Buzhor, E., et al. (2013). LifeMap Discovery: the embryonic development, stem cells, and regenerative medicine research portal. *PLoS One* 8(7), e66629. doi: 10.1371/journal.pone.0066629.
- Edwards, K.M. (2005). Overview of pertussis: focus on epidemiology, sources of infection, and long term protection after infant vaccination. *Pediatr Infect Dis J* 24(6 Suppl), S104-108. doi: 10.1097/01.inf.0000166154.47013.47.
- Eldering, G., Hornbeck, C., and Baker, J. (1957). Serological study of *Bordetella pertussis* and related species. *J Bacteriol* 74(2), 133-136. doi: 10.1128/JB.74.2.133-136.1957.
- Eldering, G., and Kendrick, P. (1938). *Bacillus Para-Pertussis*: A Species Resembling Both *Bacillus Pertussis* and *Bacillus Bronchisepticus* but Identical with Neither. *J Bacteriol* 35(6), 561-572. doi: 10.1128/JB.35.6.561-572.1938.
- Endoh, M., Amitani, M., and Nakase, Y. (1986). Purification and characterization of heat-labile toxin from *Bordetella bronchiseptica*. *Microbiol Immunol* 30(7), 659-673. doi: 10.1111/j.1348-0421.1986.tb02992.x.
- Evans, M.J., Cox, R.A., Shami, S.G., and Plopper, C.G. (1990). Junctional adhesion mechanisms in airway basal cells. *Am J Respir Cell Mol Biol* 3(4), 341-347. doi: 10.1165/ajrcmb/3.4.341.
- Evans, M.J., and Plopper, C.G. (1988). The role of basal cells in adhesion of columnar epithelium to airway basement membrane. *Am Rev Respir Dis* 138(2), 481-483. doi: 10.1164/ajrccm/138.2.481.
- Fedele, G., Bianco, M., and Ausiello, C.M. (2013). The virulence factors of *Bordetella pertussis*: talented modulators of host immune response. *Arch Immunol Ther Exp (Warsz)* 61(6), 445-457. doi: 10.1007/s00005-013-0242-1.
- Fedele, G., Bianco, M., Debie, A.S., Locht, C., and Ausiello, C.M. (2011). Attenuated *Bordetella pertussis* vaccine candidate BPZE1 promotes human dendritic cell CCL21-induced migration and drives a Th1/Th17 response. *J Immunol* 186(9), 5388-5396. doi: 10.4049/jimmunol.1003765.
- Fedele, G., Nasso, M., Spensieri, F., Palazzo, R., Frasca, L., Watanabe, M., et al. (2008). Lipopolysaccharides from *Bordetella pertussis* and *Bordetella parapertussis* differently modulate human dendritic cell functions resulting in divergent prevalence of Th17-polarized responses. *J Immunol* 181(1), 208-216. doi: 10.4049/jimmunol.181.1.208.
- Fedele, G., Schiavoni, I., Adkins, I., Klimova, N., and Sebo, P. (2017). Invasion of Dendritic Cells, Macrophages and Neutrophils by the *Bordetella Adenylate Cyclase Toxin*: A Subversive Move to Fool Host Immunity. *Toxins (Basel)* 9(10). doi: 10.3390/toxins9100293.

- Fedele, G., Spensieri, F., Palazzo, R., Nasso, M., Cheung, G.Y., Coote, J.G., et al. (2010). Bordetella pertussis commits human dendritic cells to promote a Th1/Th17 response through the activity of adenylate cyclase toxin and MAPK-pathways. *PLoS One* 5(1), e8734. doi: 10.1371/journal.pone.0008734.
- Fennelly, N.K., Sisti, F., Higgins, S.C., Ross, P.J., van der Heide, H., Mooi, F.R., et al. (2008). Bordetella pertussis expresses a functional type III secretion system that subverts protective innate and adaptive immune responses. *Infect Immun* 76(3), 1257-1266. doi: 10.1128/IAI.00836-07.
- Fernandez, R.C. (2012). Airborne transmission of Bordetella pertussis demonstrated in a baboon model of whooping cough. *J Infect Dis* 206(6), 808-810. doi: 10.1093/infdis/jis444.
- Fernandez, R.C., and Weiss, A.A. (1994). Cloning and sequencing of a Bordetella pertussis serum resistance locus. *Infect Immun* 62(11), 4727-4738. doi: 10.1128/IAI.62.11.4727-4738.1994.
- Finley, N.L. (2018). Revealing how an adenylate cyclase toxin uses bait and switch tactics in its activation. *PLoS Biol* 16(2), e2005356. doi: 10.1371/journal.pbio.2005356.
- Flak, T.A., and Goldman, W.E. (1996). Autotoxicity of nitric oxide in airway disease. *Am J Respir Crit Care Med* 154(4 Pt 2), S202-206. doi: 10.1164/ajrccm/154.4_Pt_2.S202.
- Flak, T.A., and Goldman, W.E. (1999). Signalling and cellular specificity of airway nitric oxide production in pertussis. *Cell Microbiol* 1(1), 51-60. doi: 10.1046/j.1462-5822.1999.00004.x.
- Flak, T.A., Heiss, L.N., Engle, J.T., and Goldman, W.E. (2000). Synergistic epithelial responses to endotoxin and a naturally occurring muramyl peptide. *Infect Immun* 68(3), 1235-1242. doi: 10.1128/iai.68.3.1235-1242.2000.
- Foley, J.W., Zhu, C., Jolivet, P., Zhu, S.X., Lu, P., Meaney, M.J., et al. (2019). Gene expression profiling of single cells from archival tissue with laser-capture microdissection and Smart-3SEQ. *Genome Res* 29(11), 1816-1825. doi: 10.1101/gr.234807.118.
- Folkerts, G., Kloek, J., Muijsers, R.B., and Nijkamp, F.P. (2001). Reactive nitrogen and oxygen species in airway inflammation. *Eur J Pharmacol* 429(1-3), 251-262. doi: 10.1016/s0014-2999(01)01324-3.
- French, C.T., Panina, E.M., Yeh, S.H., Griffith, N., Arambula, D.G., and Miller, J.F. (2009). The Bordetella type III secretion system effector BteA contains a conserved N-terminal motif that guides bacterial virulence factors to lipid rafts. *Cell Microbiol* 11(12), 1735-1749. doi: 10.1111/j.1462-5822.2009.01361.x.
- Friedman, R.L., Nordensson, K., Wilson, L., Akporiaye, E.T., and Yocum, D.E. (1992). Uptake and intracellular survival of Bordetella pertussis in human macrophages. *Infect Immun* 60(11), 4578-4585. doi: 10.1128/IAI.60.11.4578-4585.1992.
- Fry, N.K., Neal, S., Harrison, T.G., Miller, E., Matthews, R., and George, R.C. (2001). Genotypic variation in the Bordetella pertussis virulence factors

- pertactin and pertussis toxin in historical and recent clinical isolates in the United Kingdom. *Infect Immun* 69(9), 5520-5528. doi: 10.1128/iai.69.9.5520-5528.2001.
- Fuchslocher, B., Millar, L.L., and Cotter, P.A. (2003). Comparison of *bipA* alleles within and across *Bordetella* species. *Infect Immun* 71(6), 3043-3052. doi: 10.1128/iai.71.6.3043-3052.2003.
- Gaston, B., Drazen, J.M., Loscalzo, J., and Stamler, J.S. (1994). The biology of nitrogen oxides in the airways. *Am J Respir Crit Care Med* 149(2 Pt 1), 538-551. doi: 10.1164/ajrccm.149.2.7508323.
- Gentry-Weeks, C.R., Cookson, B.T., Goldman, W.E., Rimler, R.B., Porter, S.B., and Curtiss, R., 3rd (1988). Dermonecrotic toxin and tracheal cytotoxin, putative virulence factors of *Bordetella avium*. *Infect Immun* 56(7), 1698-1707. doi: 10.1128/IAI.56.7.1698-1707.1988.
- Geuijen, C.A., Willems, R.J., and Mooi, F.R. (1996). The major fimbrial subunit of *Bordetella pertussis* binds to sulfated sugars. *Infect Immun* 64(7), 2657-2665. doi: 10.1128/IAI.64.7.2657-2665.1996.
- Gillard, J., van Schuppen, E., and Diavatopoulos, D.A. (2019). Functional Programming of Innate Immune Cells in Response to *Bordetella pertussis* Infection and Vaccination. *Adv Exp Med Biol* 1183, 53-80. doi: 10.1007/5584_2019_404.
- Goldman, W.E., and Cookson, B.T. (1988). Structure and functions of the *Bordetella* tracheal cytotoxin. *Tokai J Exp Clin Med* 13 Suppl, 187-191.
- Goldman, W.E., and Herwaldt, L.A. (1985). *Bordetella pertussis* tracheal cytotoxin. *Dev Biol Stand* 61, 103-111.
- Goldman, W.E., Klapper, D.G., and Baseman, J.B. (1982). Detection, isolation, and analysis of a released *Bordetella pertussis* product toxic to cultured tracheal cells. *Infect Immun* 36(2), 782-794. doi: 10.1128/IAI.36.2.782-794.1982.
- Goodell, E.W. (1985). Recycling of murein by *Escherichia coli*. *J Bacteriol* 163(1), 305-310. doi: 10.1128/JB.163.1.305-310.1985.
- Goodman, Y.E., Wort, A.J., and Jackson, F.L. (1981). Enzyme-linked immunosorbent assay for detection of pertussis immunoglobulin A in nasopharyngeal secretions as an indicator of recent infection. *J Clin Microbiol* 13(2), 286-292. doi: 10.1128/JCM.13.2.286-292.1981.
- Gorringe, A.R., and Vaughan, T.E. (2014). *Bordetella pertussis* fimbriae (Fim): relevance for vaccines. *Expert Rev Vaccines* 13(10), 1205-1214. doi: 10.1586/14760584.2014.930667.
- Gueirard, P., Bassinet, L., Bonne, I., Prevost, M.C., and Guiso, N. (2005). Ultrastructural analysis of the interactions between *Bordetella pertussis*, *Bordetella parapertussis* and *Bordetella bronchiseptica* and human tracheal epithelial cells. *Microb Pathog* 38(1), 41-46. doi: 10.1016/j.micpath.2004.08.003.
- Guermonprez, P., Khelef, N., Blouin, E., Rieu, P., Ricciardi-Castagnoli, P., Guiso, N., et al. (2001). The adenylate cyclase toxin of *Bordetella pertussis* binds

- to target cells via the alpha(M)beta(2) integrin (CD11b/CD18). *J Exp Med* 193(9), 1035-1044.
- Guevara, C., Zhang, C., Gaddy, J.A., Iqbal, J., Guerra, J., Greenberg, D.P., et al. (2016). Highly differentiated human airway epithelial cells: a model to study host cell-parasite interactions in pertussis. *Infect Dis (Lond)* 48(3), 177-188. doi: 10.3109/23744235.2015.1100323.
- Guiso, N. (2009). Bordetella pertussis and pertussis vaccines. *Clin Infect Dis* 49(10), 1565-1569. doi: 10.1086/644733.
- Guiso, N., Boursaux-Eude, C., Weber, C., Hausman, S.Z., Sato, H., Iwaki, M., et al. (2001). Analysis of Bordetella pertussis isolates collected in Japan before and after introduction of acellular pertussis vaccines. *Vaccine* 19(23-24), 3248-3252. doi: 10.1016/s0264-410x(01)00013-5.
- Guiso, N., Capiou, C., Carletti, G., Poolman, J., and Hauser, P. (1999). Intranasal murine model of Bordetella pertussis infection. I. Prediction of protection in human infants by acellular vaccines. *Vaccine* 17(19), 2366-2376. doi: 10.1016/s0264-410x(99)00037-7.
- Hamilton, N., Bullock, A.J., Macneil, S., Janes, S.M., and Birchall, M. (2014). Tissue engineering airway mucosa: a systematic review. *Laryngoscope* 124(4), 961-968. doi: 10.1002/lary.24469.
- Han, X., Fink, M.P., and Delude, R.L. (2003). Proinflammatory cytokines cause NO*-dependent and -independent changes in expression and localization of tight junction proteins in intestinal epithelial cells. *Shock* 19(3), 229-237. doi: 10.1097/00024382-200303000-00006.
- Hartlova, A., Cervený, L., Hubalek, M., Krocova, Z., and Stulik, J. (2010). Membrane rafts: a potential gateway for bacterial entry into host cells. *Microbiol Immunol* 54(4), 237-245. doi: 10.1111/j.1348-0421.2010.00198.x.
- Harvill, E.T., Preston, A., Cotter, P.A., Allen, A.G., Maskell, D.J., and Miller, J.F. (2000). Multiple roles for Bordetella lipopolysaccharide molecules during respiratory tract infection. *Infect Immun* 68(12), 6720-6728. doi: 10.1128/iai.68.12.6720-6728.2000.
- Hasan, S., Kulkarni, N.N., Asbjarnarson, A., Linhartova, I., Osicka, R., Sebo, P., et al. (2018a). Bordetella pertussis Adenylate Cyclase Toxin Disrupts Functional Integrity of Bronchial Epithelial Layers. *Infect Immun* 86(3). doi: 10.1128/IAI.00445-17.
- Hasan, S., Sebo, P., and Osicka, R. (2018b). A guide to polarized airway epithelial models for studies of host-pathogen interactions. *FEBS J* 285(23), 4343-4358. doi: 10.1111/febs.14582.
- Hazenbos, W.L., Geuijen, C.A., van den Berg, B.M., Mooi, F.R., and van Furth, R. (1995). Bordetella pertussis fimbriae bind to human monocytes via the minor fimbrial subunit FimD. *J Infect Dis* 171(4), 924-929. doi: 10.1093/infdis/171.4.924.
- Heerze, L.D., Chong, P.C., and Armstrong, G.D. (1992). Investigation of the lectin-like binding domains in pertussis toxin using synthetic peptide sequences. Identification of a sialic acid binding site in the S2 subunit of the toxin. *J Biol Chem* 267(36), 25810-25815.

- Heijink, I.H., Kuchibhotla, V.N.S., Roffel, M.P., Maes, T., Knight, D.A., Sayers, I., et al. (2020). Epithelial cell dysfunction, a major driver of asthma development. *Allergy* 75(8), 1902-1917. doi: 10.1111/all.14421.
- Heiss, L.N., Flak, T.A., Lancaster, J.R., Jr., McDaniel, M.L., and Goldman, W.E. (1993a). Nitric oxide mediates Bordetella pertussis tracheal cytotoxin damage to the respiratory epithelium. *Infect Agents Dis* 2(4), 173-177.
- Heiss, L.N., Lancaster, J.R., Jr., Corbett, J.A., and Goldman, W.E. (1994). Epithelial autotoxicity of nitric oxide: role in the respiratory cytopathology of pertussis. *Proc Natl Acad Sci U S A* 91(1), 267-270. doi: 10.1073/pnas.91.1.267.
- Heiss, L.N., Moser, S.A., Unanue, E.R., and Goldman, W.E. (1993b). Interleukin-1 is linked to the respiratory epithelial cytopathology of pertussis. *Infect Immun* 61(8), 3123-3128. doi: 10.1128/IAI.61.8.3123-3128.1993.
- Heller, N.M., Matsukura, S., Georas, S.N., Boothby, M.R., Rothman, P.B., Stellato, C., et al. (2004). Interferon-gamma inhibits STAT6 signal transduction and gene expression in human airway epithelial cells. *Am J Respir Cell Mol Biol* 31(5), 573-582. doi: 10.1165/rcmb.2004-0195OC.
- Hermanns, M.I., Unger, R.E., Kehe, K., Peters, K., and Kirkpatrick, C.J. (2004). Lung epithelial cell lines in coculture with human pulmonary microvascular endothelial cells: development of an alveolo-capillary barrier in vitro. *Lab Invest* 84(6), 736-752. doi: 10.1038/labinvest.3700081.
- Hesselvik, L., and Ericsson, H. (1954). Active basal immunity and its application to epidemiology. IV. Initial pain in diphtheria-tetanus-pertussis vaccination. *Acta Paediatr* 43(1), 22-26. doi: 10.1111/j.1651-2227.1954.tb03994.x.
- Hewlett, E.L., Burns, D.L., Cotter, P.A., Harvill, E.T., Merkel, T.J., Quinn, C.P., et al. (2014). Pertussis pathogenesis--what we know and what we don't know. *J Infect Dis* 209(7), 982-985. doi: 10.1093/infdis/jit639.
- Heydarian, M., Yang, T., Schweinlin, M., Steinke, M., Walles, H., Rudel, T., et al. (2019). Biomimetic Human Tissue Model for Long-Term Study of Neisseria gonorrhoeae Infection. *Front Microbiol* 10, 1740. doi: 10.3389/fmicb.2019.01740.
- Hiemstra, P.S., McCray, P.B., Jr., and Bals, R. (2015). The innate immune function of airway epithelial cells in inflammatory lung disease. *Eur Respir J* 45(4), 1150-1162. doi: 10.1183/09031936.00141514.
- Higgs, R., Higgins, S.C., Ross, P.J., and Mills, K.H. (2012). Immunity to the respiratory pathogen Bordetella pertussis. *Mucosal Immunol* 5(5), 485-500. doi: 10.1038/mi.2012.54.
- Hijnen, M., Mooi, F.R., van Gageldonk, P.G., Hoogerhout, P., King, A.J., and Berbers, G.A. (2004). Epitope structure of the Bordetella pertussis protein P.69 pertactin, a major vaccine component and protective antigen. *Infect Immun* 72(7), 3716-3723. doi: 10.1128/IAI.72.7.3716-3723.2004.
- Hippenstiel, S., Opitz, B., Schmeck, B., and Suttrop, N. (2006). Lung epithelium as a sentinel and effector system in pneumonia--molecular mechanisms of pathogen recognition and signal transduction. *Respir Res* 7, 97. doi: 10.1186/1465-9921-7-97.

- Hitz, D.A., Tewald, F., and Eggers, M. (2020). Seasonal *Bordetella pertussis* pattern in the period from 2008 to 2018 in Germany. *BMC Infect Dis* 20(1), 474. doi: 10.1186/s12879-020-05199-w.
- Hoffman, C., Eby, J., Gray, M., Heath Damron, F., Melvin, J., Cotter, P., et al. (2017). *Bordetella* adenylate cyclase toxin interacts with filamentous haemagglutinin to inhibit biofilm formation in vitro. *Mol Microbiol* 103(2), 214-228. doi: 10.1111/mmi.13551.
- Holmes, W.H. (1940). "Whooping-cough, or pertussis. ," in *In: Bascillary and rickettsial infections: acute and chronic. A textbook. Black death to white plague.* (New York: Macmillan).
- Holt, L.E. (1902). "The diseases of infancy and childhood: for the use of students and practitioners of medicine.." (New York: D. Appleton), 985 -996.
- Hong, K.U., Reynolds, S.D., Giangreco, A., Hurley, C.M., and Stripp, B.R. (2001). Clara cell secretory protein-expressing cells of the airway neuroepithelial body microenvironment include a label-retaining subset and are critical for epithelial renewal after progenitor cell depletion. *Am J Respir Cell Mol Biol* 24(6), 671-681. doi: 10.1165/ajrcmb.24.6.4498.
- Hovingh, E.S., Kuipers, B., Bonacic Marinovic, A.A., Jan Hamstra, H., Hijdra, D., Mughini Gras, L., et al. (2018). Detection of opsonizing antibodies directed against a recently circulating *Bordetella pertussis* strain in paired plasma samples from symptomatic and recovered pertussis patients. *Sci Rep* 8(1), 12039. doi: 10.1038/s41598-018-30558-8.
- Hozbor, D., Mooi, F., Flores, D., Weltman, G., Bottero, D., Fossati, S., et al. (2009). Pertussis epidemiology in Argentina: trends over 2004-2007. *J Infect* 59(4), 225-231. doi: 10.1016/j.jinf.2009.07.014.
- Hsia, J.A., Moss, J., Hewlett, E.L., and Vaughan, M. (1984). Requirement for both cholera toxin and pertussis toxin to obtain maximal activation of adenylate cyclase in cultured cells. *Biochem Biophys Res Commun* 119(3), 1068-1074.
- Iida, T., and Okonogi, T. (1971). Lethality of *Bordetella pertussis* in mice. *J Med Microbiol* 4(1), 51-61. doi: 10.1099/00222615-4-1-51.
- Imamura, T., Shoji, K., Kono, N., Kubota, M., Nishimura, N., Ishiguro, A., et al. (2020). Allele frequencies of *Bordetella pertussis* virulence-associated genes identified from pediatric patients with severe respiratory infections. *J Infect Chemother* 26(7), 765-768. doi: 10.1016/j.jiac.2020.02.016.
- Inatsuka, C.S., Julio, S.M., and Cotter, P.A. (2005). *Bordetella* filamentous hemagglutinin plays a critical role in immunomodulation, suggesting a mechanism for host specificity. *Proc Natl Acad Sci U S A* 102(51), 18578-18583. doi: 10.1073/pnas.0507910102.
- Isberg, R.R., Hamburger, Z., and Dersch, P. (2000). Signaling and invasion-promoted uptake via integrin receptors. *Microbes Infect* 2(7), 793-801. doi: 10.1016/s1286-4579(00)90364-2.
- Ishibashi, Y., Relman, D.A., and Nishikawa, A. (2001). Invasion of human respiratory epithelial cells by *Bordetella pertussis*: possible role for a filamentous hemagglutinin Arg-Gly-Asp sequence and alpha5beta1 integrin. *Microb Pathog* 30(5), 279-288. doi: 10.1006/mpat.2001.0432.

- Jain, B., Rubinstein, I., Robbins, R.A., Leise, K.L., and Sisson, J.H. (1993). Modulation of airway epithelial cell ciliary beat frequency by nitric oxide. *Biochem Biophys Res Commun* 191(1), 83-88. doi: 10.1006/bbrc.1993.1187.
- Jansen, K., Pou Casellas, C., Groenink, L., Wever, K.E., and Masereeuw, R. (2020). Humans are animals, but are animals human enough? A systematic review and meta-analysis on interspecies differences in renal drug clearance. *Drug Discov Today* 25(4), 706-717. doi: 10.1016/j.drudis.2020.01.018.
- Jeffery, P.K. (1983). Morphologic features of airway surface epithelial cells and glands. *Am Rev Respir Dis* 128(2 Pt 2), S14-20. doi: 10.1164/arrd.1983.128.2P2.S14.
- Jeffery, P.K., and Brain, A.P. (1988). Surface morphology of human airway mucosa: normal, carcinoma or cystic fibrosis. *Scanning Microsc* 2(1), 553-560.
- Jeffery, P.K., and Li, D. (1997). Airway mucosa: secretory cells, mucus and mucin genes. *Eur Respir J* 10(7), 1655-1662. doi: 10.1183/09031936.97.10071655.
- Jiao, J., Wang, H., Lou, W., Jin, S., Fan, E., Li, Y., et al. (2011). Regulation of ciliary beat frequency by the nitric oxide signaling pathway in mouse nasal and tracheal epithelial cells. *Exp Cell Res* 317(17), 2548-2553. doi: 10.1016/j.yexcr.2011.07.007.
- Johnson, J.W., Fisher, J.F., and Mobashery, S. (2013). Bacterial cell-wall recycling. *Ann N Y Acad Sci* 1277, 54-75. doi: 10.1111/j.1749-6632.2012.06813.x.
- Jones, A.M., Boucher, P.E., Williams, C.L., Stibitz, S., and Cotter, P.A. (2005). Role of BvgA phosphorylation and DNA binding affinity in control of Bvg-mediated phenotypic phase transition in *Bordetella pertussis*. *Mol Microbiol* 58(3), 700-713. doi: 10.1111/j.1365-2958.2005.04875.x.
- Jungnitz, H., West, N.P., Walker, M.J., Chhatwal, G.S., and Guzman, C.A. (1998). A second two-component regulatory system of *Bordetella bronchiseptica* required for bacterial resistance to oxidative stress, production of acid phosphatase, and in vivo persistence. *Infect Immun* 66(10), 4640-4650. doi: 10.1128/IAI.66.10.4640-4650.1998.
- Kamanova, J. (2020). *Bordetella* Type III Secretion Injectosome and Effector Proteins. *Front Cell Infect Microbiol* 10, 466. doi: 10.3389/fcimb.2020.00466.
- Karataev, G.I., Sinyashina, L.N., Medkova, A.Y., and Semin, E.G. (2015). [Persistence of *Bordetella Pertussis* Bacteria and a Possible Mechanism of Its Formation]. *Zh Mikrobiol Epidemiol Immunobiol* (6), 114-121.
- Karst, J.C., Ntsogo Enguene, V.Y., Cannella, S.E., Subrini, O., Hessel, A., Debard, S., et al. (2014). Calcium, acylation, and molecular confinement favor folding of *Bordetella pertussis* adenylate cyclase CyaA toxin into a monomeric and cytotoxic form. *J Biol Chem* 289(44), 30702-30716. doi: 10.1074/jbc.M114.580852.

- Karst, J.C., Sotomayor Perez, A.C., Guijarro, J.I., Raynal, B., Chenal, A., and Ladant, D. (2010). Calmodulin-induced conformational and hydrodynamic changes in the catalytic domain of *Bordetella pertussis* adenylate cyclase toxin. *Biochemistry* 49(2), 318-328. doi: 10.1021/bi9016389.
- Kashyap, D.R., Rompca, A., Gaballa, A., Helmann, J.D., Chan, J., Chang, C.J., et al. (2014). Peptidoglycan recognition proteins kill bacteria by inducing oxidative, thiol, and metal stress. *PLoS Pathog* 10(7), e1004280. doi: 10.1371/journal.ppat.1004280.
- Katz, I., Zwas, T., Baum, G.L., Aharonson, E., and Belfer, B. (1987). Ciliary beat frequency and mucociliary clearance. What is the relationship? *Chest* 92(3), 491-493. doi: 10.1378/chest.92.3.491.
- Kerr, J.R., and Matthews, R.C. (2000). *Bordetella pertussis* infection: pathogenesis, diagnosis, management, and the role of protective immunity. *Eur J Clin Microbiol Infect Dis* 19(2), 77-88. doi: 10.1007/s100960050435.
- Kessie, D.K., Lodes, N., Oberwinkler, H., Goldman, W.E., Walles, T., Steinke, M., et al. (2020). Activity of Tracheal Cytotoxin of *Bordetella pertussis* in a Human Tracheobronchial 3D Tissue Model. *Front Cell Infect Microbiol* 10, 614994. doi: 10.3389/fcimb.2020.614994.
- Khelef, N., Bachelet, C.M., Vargaftig, B.B., and Guiso, N. (1994). Characterization of murine lung inflammation after infection with parental *Bordetella pertussis* and mutants deficient in adhesins or toxins. *Infect Immun* 62(7), 2893-2900. doi: 10.1128/IAI.62.7.2893-2900.1994.
- Kilgore, P.E., Salim, A.M., Zervos, M.J., and Schmitt, H.J. (2016). Pertussis: Microbiology, Disease, Treatment, and Prevention. *Clin Microbiol Rev* 29(3), 449-486. doi: 10.1128/CMR.00083-15.
- Kim, C.H., Park, H.W., Kim, K., and Yoon, J.H. (2004). Early development of the nose in human embryos: a stereomicroscopic and histologic analysis. *Laryngoscope* 114(10), 1791-1800. doi: 10.1097/00005537-200410000-00022.
- Kim, K.Y., Lee, G., Yoon, M., Cho, E.H., Park, C.S., and Kim, M.G. (2015). Expression Analyses Revealed Thymic Stromal Co-Transporter/Slc46A2 Is in Stem Cell Populations and Is a Putative Tumor Suppressor. *Mol Cells* 38(6), 548-561. doi: 10.14348/molcells.2015.0044.
- Kimura, M., and Kuno-Sakai, H. (1987). Experiences with acellular pertussis vaccine in Japan and epidemiology of pertussis. *Tokai J Exp Clin Med* 12(5-6), 263-273.
- Kinnear, S.M., Marques, R.R., and Carbonetti, N.H. (2001). Differential regulation of Bvg-activated virulence factors plays a role in *Bordetella pertussis* pathogenicity. *Infect Immun* 69(4), 1983-1993. doi: 10.1128/IAI.69.4.1983-1993.2001.
- Klein, N.P., Bartlett, J., Fireman, B., Rowhani-Rahbar, A., and Baxter, R. (2013). Comparative effectiveness of acellular versus whole-cell pertussis vaccines in teenagers. *Pediatrics* 131(6), e1716-1722. doi: 10.1542/peds.2012-3836.

- Klein, N.P., Bartlett, J., Rowhani-Rahbar, A., Fireman, B., and Baxter, R. (2012). Waning protection after fifth dose of acellular pertussis vaccine in children. *N Engl J Med* 367(11), 1012-1019. doi: 10.1056/NEJMoa1200850.
- Knapp, O., and Benz, R. (2020). Membrane Activity and Channel Formation of the Adenylate Cyclase Toxin (CyaA) of *Bordetella pertussis* in Lipid Bilayer Membranes. *Toxins (Basel)* 12(3). doi: 10.3390/toxins12030169.
- Knight, D.A., and Holgate, S.T. (2003). The airway epithelium: structural and functional properties in health and disease. *Respirology* 8(4), 432-446. doi: 10.1046/j.1440-1843.2003.00493.x.
- Knowles, M.R., and Boucher, R.C. (2002). Mucus clearance as a primary innate defense mechanism for mammalian airways. *J Clin Invest* 109(5), 571-577. doi: 10.1172/JCI15217.
- Kobayashi, K., Inohara, N., Hernandez, L.D., Galan, J.E., Nunez, G., Janeway, C.A., et al. (2002). RICK/Rip2/CARDIAK mediates signalling for receptors of the innate and adaptive immune systems. *Nature* 416(6877), 194-199. doi: 10.1038/416194a.
- Kobayashi, M., Shu, S., Marunaka, K., Matsunaga, T., and Ikari, A. (2020). Weak Ultraviolet B Enhances the Mislocalization of Claudin-1 Mediated by Nitric Oxide and Peroxynitrite Production in Human Keratinocyte-Derived HaCaT Cells. *Int J Mol Sci* 21(19). doi: 10.3390/ijms21197138.
- Kojima, T., Go, M., Takano, K., Kurose, M., Ohkuni, T., Koizumi, J., et al. (2013). Regulation of tight junctions in upper airway epithelium. *Biomed Res Int* 2013, 947072. doi: 10.1155/2013/947072.
- Koropatnick, T.A., Engle, J.T., Apicella, M.A., Stabb, E.V., Goldman, W.E., and McFall-Ngai, M.J. (2004). Microbial factor-mediated development in a host-bacterial mutualism. *Science* 306(5699), 1186-1188. doi: 10.1126/science.1102218.
- Kroes, M.M., Mariman, R., Hijdra, D., Hamstra, H.J., van Boxtel, K., van Putten, J.P.M., et al. (2019). Activation of Human NK Cells by *Bordetella pertussis* Requires Inflammasome Activation in Macrophages. *Front Immunol* 10, 2030. doi: 10.3389/fimmu.2019.02030.
- Kufer, T.A. (2008). Signal transduction pathways used by NLR-type innate immune receptors. *Mol Biosyst* 4(5), 380-386. doi: 10.1039/b718948f.
- Kunkel, S.L., Standiford, T., Kasahara, K., and Strieter, R.M. (1991). Interleukin-8 (IL-8): the major neutrophil chemotactic factor in the lung. *Exp Lung Res* 17(1), 17-23. doi: 10.3109/01902149109063278.
- Kuno-Sakai, H., and Kimura, M. (1997). Epidemiology of pertussis and use of acellular pertussis vaccines in Japan. *Dev Biol Stand* 89, 331-332.
- Lacey, B.W. (1960). Antigenic modulation of *Bordetella pertussis*. *J Hyg (Lond)* 58, 57-93. doi: 10.1017/s0022172400038134.
- Ladant, D., and Ullmann, A. (1999). *Bordetella pertussis* adenylate cyclase: a toxin with multiple talents. *Trends Microbiol* 7(4), 172-176.
- Lafont, F., and van der Goot, F.G. (2005). Bacterial invasion via lipid rafts. *Cell Microbiol* 7(5), 613-620. doi: 10.1111/j.1462-5822.2005.00515.x.

- Lamberti, Y., Gorgojo, J., Massillo, C., and Rodriguez, M.E. (2013). Bordetella pertussis entry into respiratory epithelial cells and intracellular survival. *Pathog Dis* 69(3), 194-204. doi: 10.1111/2049-632X.12072.
- Lamberti, Y., Perez Vidakovics, M.L., van der Pol, L.W., and Rodriguez, M.E. (2008). Cholesterol-rich domains are involved in Bordetella pertussis phagocytosis and intracellular survival in neutrophils. *Microb Pathog* 44(6), 501-511. doi: 10.1016/j.micpath.2008.01.002.
- Lamberti, Y.A., Hayes, J.A., Perez Vidakovics, M.L., Harvill, E.T., and Rodriguez, M.E. (2010). Intracellular trafficking of Bordetella pertussis in human macrophages. *Infect Immun* 78(3), 907-913. doi: 10.1128/IAI.01031-09.
- Lapin, J.H. (1943). *Whooping Cough*. Springfield, IL: Charles C Thomas Publisher.
- Lapin, J.H. (1946). Immunization against whooping cough. *J Pediatr* 29, 90-94. doi: 10.1016/s0022-3476(46)80243-9.
- Lee, C.K., Roberts, A.L., Finn, T.M., Knapp, S., and Mekalanos, J.J. (1990). A new assay for invasion of HeLa 229 cells by Bordetella pertussis: effects of inhibitors, phenotypic modulation, and genetic alterations. *Infect Immun* 58(8), 2516-2522. doi: 10.1128/IAI.58.8.2516-2522.1990.
- Lee, S.K., Park, H.S., Lim, H.E., Kim, S.S., Nahm, D.H., Lee, Y.M., et al. (2003). Localization of inducible nitric oxide synthase and endothelial constitutive nitric oxide synthase in airway mucosa of toluene diisocyanate-induced asthma. *Allergy Asthma Proc* 24(4), 275-280.
- Leekha, S., Thompson, R.L., and Sampathkumar, P. (2009). Epidemiology and control of pertussis outbreaks in a tertiary care center and the resource consumption associated with these outbreaks. *Infect Control Hosp Epidemiol* 30(5), 467-473. doi: 10.1086/596774.
- Li, D., Shirakami, G., Zhan, X., and Johns, R.A. (2000). Regulation of ciliary beat frequency by the nitric oxide-cyclic guanosine monophosphate signaling pathway in rat airway epithelial cells. *Am J Respir Cell Mol Biol* 23(2), 175-181. doi: 10.1165/ajrcmb.23.2.4022.
- Lin, H., Li, H., Cho, H.J., Bian, S., Roh, H.J., Lee, M.K., et al. (2007). Air-liquid interface (ALI) culture of human bronchial epithelial cell monolayers as an in vitro model for airway drug transport studies. *J Pharm Sci* 96(2), 341-350. doi: 10.1002/jps.20803.
- Lindner, K., Strobele, M., Schlick, S., Webering, S., Jenckel, A., Kopf, J., et al. (2017). Biological effects of carbon black nanoparticles are changed by surface coating with polycyclic aromatic hydrocarbons. *Part Fibre Toxicol* 14(1), 8. doi: 10.1186/s12989-017-0189-1.
- Link, S., Schmitt, K., Beier, D., and Gross, R. (2007). Identification and regulation of expression of a gene encoding a filamentous hemagglutinin-related protein in Bordetella holmesii. *BMC Microbiol* 7, 100. doi: 10.1186/1471-2180-7-100.
- Linkous, A., Balamatsias, D., Snuderl, M., Edwards, L., Miyaguchi, K., Milner, T., et al. (2019). Modeling Patient-Derived Glioblastoma with Cerebral Organoids. *Cell Rep* 26(12), 3203-3211 e3205. doi: 10.1016/j.celrep.2019.02.063.

- Linz, B., Ivanov, Y.V., Preston, A., Brinkac, L., Parkhill, J., Kim, M., et al. (2016). Acquisition and loss of virulence-associated factors during genome evolution and speciation in three clades of *Bordetella* species. *BMC Genomics* 17(1), 767. doi: 10.1186/s12864-016-3112-5.
- Liu, A. (2010). Laser capture microdissection in the tissue biorepository. *J Biomol Tech* 21(3), 120-125.
- Livak, K.J., and Schmittgen, T.D. (2001). Analysis of relative gene expression data using real-time quantitative PCR and the 2^{(-Delta Delta C(T))} Method. *Methods* 25(4), 402-408. doi: 10.1006/meth.2001.1262.
- Locht, C. (1999). Molecular aspects of *Bordetella pertussis* pathogenesis. *Int Microbiol* 2(3), 137-144.
- Lodes, N., Seidensticker, K., Perniss, A., Nietzer, S., Oberwinkler, H., May, T., et al. (2020). Investigation on Ciliary Functionality of Different Airway Epithelial Cell Lines in Three-Dimensional Cell Culture. *Tissue Eng Part A* 26(7-8), 432-440. doi: 10.1089/ten.TEA.2019.0188.
- Luker, K.E., Collier, J.L., Kolodziej, E.W., Marshall, G.R., and Goldman, W.E. (1993). *Bordetella pertussis* tracheal cytotoxin and other muramyl peptides: distinct structure-activity relationships for respiratory epithelial cytopathology. *Proc Natl Acad Sci U S A* 90(6), 2365-2369. doi: 10.1073/pnas.90.6.2365.
- Luker, K.E., Tyler, A.N., Marshall, G.R., and Goldman, W.E. (1995). Tracheal cytotoxin structural requirements for respiratory epithelial damage in pertussis. *Mol Microbiol* 16(4), 733-743. doi: 10.1111/j.1365-2958.1995.tb02434.x.
- Madsen, K.L., Lewis, S.A., Tavernini, M.M., Hibbard, J., and Fedorak, R.N. (1997). Interleukin 10 prevents cytokine-induced disruption of T84 monolayer barrier integrity and limits chloride secretion. *Gastroenterology* 113(1), 151-159. doi: 10.1016/s0016-5085(97)70090-8.
- Maestrelli, P., di Stefano, A., Occari, P., Turato, G., Milani, G., Pivrotto, F., et al. (1995). Cytokines in the airway mucosa of subjects with asthma induced by toluene diisocyanate. *Am J Respir Crit Care Med* 151(3 Pt 1), 607-612. doi: 10.1164/ajrccm.151.3.7533600.
- Magalhaes, J.G., Philpott, D.J., Nahori, M.A., Jehanno, M., Fritz, J., Le Bourhis, L., et al. (2005). Murine Nod1 but not its human orthologue mediates innate immune detection of tracheal cytotoxin. *EMBO Rep* 6(12), 1201-1207. doi: 10.1038/sj.embor.7400552.
- Makhov, A.M., Hannah, J.H., Brennan, M.J., Trus, B.L., Kocsis, E., Conway, J.F., et al. (1994). Filamentous hemagglutinin of *Bordetella pertussis*. A bacterial adhesin formed as a 50-nm monomeric rigid rod based on a 19-residue repeat motif rich in beta strands and turns. *J Mol Biol* 241(1), 110-124. doi: 10.1006/jmbi.1994.1478.
- Marrazzo, P., Maccari, S., Taddei, A., Bevan, L., Telford, J., Soriani, M., et al. (2016). 3D Reconstruction of the Human Airway Mucosa In Vitro as an Experimental Model to Study NTHi Infections. *PLoS One* 11(4), e0153985. doi: 10.1371/journal.pone.0153985.

- Martin, C., Etxaniz, A., Uribe, K.B., Etxebarria, A., Gonzalez-Bullon, D., Arlucea, J., et al. (2015). Adenylate Cyclase Toxin promotes bacterial internalisation into non phagocytic cells. *Sci Rep* 5, 13774. doi: 10.1038/srep13774.
- Martin, C., Gomez-Bilbao, G., and Ostolaza, H. (2010). Bordetella adenylate cyclase toxin promotes calcium entry into both CD11b+ and CD11b- cells through cAMP-dependent L-type-like calcium channels. *J Biol Chem* 285(1), 357-364. doi: 10.1074/jbc.M109.003491.
- Martin, C., Uribe, K.B., Gomez-Bilbao, G., and Ostolaza, H. (2011). Adenylate cyclase toxin promotes internalisation of integrins and raft components and decreases macrophage adhesion capacity. *PLoS One* 6(2), e17383. doi: 10.1371/journal.pone.0017383.
- Martinez de Tejada, G., Cotter, P.A., Heininger, U., Camilli, A., Akerley, B.J., Mekalanos, J.J., et al. (1998). Neither the Bvg- phase nor the vrg6 locus of Bordetella pertussis is required for respiratory infection in mice. *Infect Immun* 66(6), 2762-2768. doi: 10.1128/IAI.66.6.2762-2768.1998.
- Martinez-Anton, A., Debolos, C., Garrido, M., Roca-Ferrer, J., Barranco, C., Alobid, I., et al. (2006). Mucin genes have different expression patterns in healthy and diseased upper airway mucosa. *Clin Exp Allergy* 36(4), 448-457. doi: 10.1111/j.1365-2222.2006.02451.x.
- Masin, J., Osicka, R., Bumba, L., and Sebo, P. (2015). Bordetella adenylate cyclase toxin: a unique combination of a pore-forming moiety with a cell-invading adenylate cyclase enzyme. *Pathog Dis* 73(8), ftv075. doi: 10.1093/femspd/ftv075.
- Masuda, M., Betancourt, L., Matsuzawa, T., Kashimoto, T., Takao, T., Shimonishi, Y., et al. (2000). Activation of rho through a cross-link with polyamines catalyzed by Bordetella dermonecrotizing toxin. *EMBO J* 19(4), 521-530. doi: 10.1093/emboj/19.4.521.
- Masure, H.R. (1993). The adenylate cyclase toxin contributes to the survival of Bordetella pertussis within human macrophages. *Microb Pathog* 14(4), 253-260. doi: 10.1006/mpat.1993.1025.
- Mattoo, S., and Cherry, J.D. (2005). Molecular pathogenesis, epidemiology, and clinical manifestations of respiratory infections due to Bordetella pertussis and other Bordetella subspecies. *Clin Microbiol Rev* 18(2), 326-382. doi: 10.1128/CMR.18.2.326-382.2005.
- Mattoo, S., Foreman-Wykert, A.K., Cotter, P.A., and Miller, J.F. (2001). Mechanisms of Bordetella pathogenesis. *Front Biosci* 6, E168-186. doi: 10.2741/mattoo.
- Mazar, J., and Cotter, P.A. (2006). Topology and maturation of filamentous haemagglutinin suggest a new model for two-partner secretion. *Mol Microbiol* 62(3), 641-654. doi: 10.1111/j.1365-2958.2006.05392.x.
- Melly, M.A., McGee, Z.A., and Rosenthal, R.S. (1984). Ability of monomeric peptidoglycan fragments from Neisseria gonorrhoeae to damage human fallopian-tube mucosa. *J Infect Dis* 149(3), 378-386. doi: 10.1093/infdis/149.3.378.

- Melvin, J.A., Scheller, E.V., Noel, C.R., and Cotter, P.A. (2015). New Insight into Filamentous Hemagglutinin Secretion Reveals a Role for Full-Length FhaB in *Bordetella* Virulence. *mBio* 6(4). doi: 10.1128/mBio.01189-15.
- Mercer, R.R., Russell, M.L., Roggli, V.L., and Crapo, J.D. (1994). Cell number and distribution in human and rat airways. *Am J Respir Cell Mol Biol* 10(6), 613-624. doi: 10.1165/ajrcmb.10.6.8003339.
- Merkel, T.J., Stibitz, S., Keith, J.M., Leef, M., and Shahin, R. (1998). Contribution of regulation by the *bvg* locus to respiratory infection of mice by *Bordetella pertussis*. *Infect Immun* 66(9), 4367-4373.
- Mertsching, H., Walles, T., Hofmann, M., Schanz, J., and Knapp, W.H. (2005). Engineering of a vascularized scaffold for artificial tissue and organ generation. *Biomaterials* 26(33), 6610-6617. doi: 10.1016/j.biomaterials.2005.04.048.
- Miller, E., Vurdien, J.E., and White, J.M. (1992a). The epidemiology of pertussis in England and Wales. *Commun Dis Rep CDR Rev* 2(13), R152-154.
- Miller, J.F., Johnson, S.A., Black, W.J., Beattie, D.T., Mekalanos, J.J., and Falkow, S. (1992b). Constitutive sensory transduction mutations in the *Bordetella pertussis* *bvgS* gene. *J Bacteriol* 174(3), 970-979. doi: 10.1128/jb.174.3.970-979.1992.
- Miller, J.F., Roy, C.R., and Falkow, S. (1989). Analysis of *Bordetella pertussis* virulence gene regulation by use of transcriptional fusions in *Escherichia coli*. *J Bacteriol* 171(11), 6345-6348. doi: 10.1128/jb.171.11.6345-6348.1989.
- Mirabelli, P., Coppola, L., and Salvatore, M. (2019). Cancer Cell Lines Are Useful Model Systems for Medical Research. *Cancers (Basel)* 11(8). doi: 10.3390/cancers11081098.
- Mishra, M., Parise, G., Jackson, K.D., Wozniak, D.J., and Deora, R. (2005). The BvgAS signal transduction system regulates biofilm development in *Bordetella*. *J Bacteriol* 187(4), 1474-1484. doi: 10.1128/JB.187.4.1474-1484.2005.
- Mizutani, H., May, L.T., Sehgal, P.B., and Kupper, T.S. (1989). Synergistic interactions of IL-1 and IL-6 in T cell activation. Mitogen but not antigen receptor-induced proliferation of a cloned T helper cell line is enhanced by exogenous IL-6. *J Immunol* 143(3), 896-901.
- Mobberley-Schuman, P.S., and Weiss, A.A. (2005). Influence of CR3 (CD11b/CD18) expression on phagocytosis of *Bordetella pertussis* by human neutrophils. *Infect Immun* 73(11), 7317-7323. doi: 10.1128/IAI.73.11.7317-7323.2005.
- Moll, C., Reboredo, J., Schwarz, T., Appelt, A., Schurlein, S., Walles, H., et al. (2013). Tissue engineering of a human 3D in vitro tumor test system. *J Vis Exp* (78). doi: 10.3791/50460.
- Moller, W., Haussinger, K., Winkler-Heil, R., Stahlhofen, W., Meyer, T., Hofmann, W., et al. (2004). Mucociliary and long-term particle clearance in the airways of healthy nonsmoker subjects. *J Appl Physiol (1985)* 97(6), 2200-2206. doi: 10.1152/jappphysiol.00970.2003.

- Monie, T.P. (2017). The Canonical Inflammasome: A Macromolecular Complex Driving Inflammation. *Subcell Biochem* 83, 43-73. doi: 10.1007/978-3-319-46503-6_2.
- Mooi, F.R., He, Q., van Oirschot, H., and Mertsola, J. (1999). Variation in the Bordetella pertussis virulence factors pertussis toxin and pertactin in vaccine strains and clinical isolates in Finland. *Infect Immun* 67(6), 3133-3134. doi: 10.1128/IAI.67.6.3133-3134.1999.
- Mooi, F.R., van Oirschot, H., Heuvelman, K., van der Heide, H.G., Gaastra, W., and Willems, R.J. (1998). Polymorphism in the Bordetella pertussis virulence factors P.69/pertactin and pertussis toxin in The Netherlands: temporal trends and evidence for vaccine-driven evolution. *Infect Immun* 66(2), 670-675. doi: 10.1128/IAI.66.2.670-675.1998.
- Moon, K., Bonocora, R.P., Kim, D.D., Chen, Q., Wade, J.T., Stibitz, S., et al. (2017). The BvgAS Regulon of Bordetella pertussis. *mBio* 8(5). doi: 10.1128/mBio.01526-17.
- Moreno, L., McMaster, S.K., Gatheral, T., Bailey, L.K., Harrington, L.S., Cartwright, N., et al. (2010). Nucleotide oligomerization domain 1 is a dominant pathway for NOS2 induction in vascular smooth muscle cells: comparison with Toll-like receptor 4 responses in macrophages. *Br J Pharmacol* 160(8), 1997-2007. doi: 10.1111/j.1476-5381.2010.00814.x.
- Mouallem, M., Farfel, Z., and Hanski, E. (1990). Bordetella pertussis adenylate cyclase toxin: intoxication of host cells by bacterial invasion. *Infect Immun* 58(11), 3759-3764.
- Naninck, T., Coutte, L., Mayet, C., Contreras, V., Loch, C., Le Grand, R., et al. (2018). In vivo imaging of bacterial colonization of the lower respiratory tract in a baboon model of Bordetella pertussis infection and transmission. *Sci Rep* 8(1), 12297. doi: 10.1038/s41598-018-30896-7.
- Nardone, A., Pebody, R.G., Maple, P.A., Andrews, N., Gay, N.J., and Miller, E. (2004). Sero-epidemiology of Bordetella pertussis in England and Wales. *Vaccine* 22(9-10), 1314-1319. doi: 10.1016/j.vaccine.2003.08.039.
- Nash, Z.M., and Cotter, P.A. (2019). Regulated, sequential processing by multiple proteases is required for proper maturation and release of Bordetella filamentous hemagglutinin. *Mol Microbiol* 112(3), 820-836. doi: 10.1111/mmi.14318.
- National Center for Immunization and Respiratory Diseases, N.C.I.R.D. (2017). *Pertussis (Whooping cough)* [Online]. Centers for Disease Control. Available: <https://www.cdc.gov/pertussis/about/signs-symptoms.html> [Accessed 25.05 2020].
- Nikolaizik, W., Hahn, J., Bauck, M., and Weber, S. (2020). Comparison of ciliary beat frequencies at different temperatures in young adults. *ERJ Open Res* 6(4). doi: 10.1183/23120541.00477-2020.
- Nishikawa, S., Shinzawa, N., Nakamura, K., Ishigaki, K., Abe, H., and Horiguchi, Y. (2016). The bvg-repressed gene brtA, encoding biofilm-associated surface adhesin, is expressed during host infection by Bordetella bronchiseptica. *Microbiol Immunol* 60(2), 93-105. doi: 10.1111/1348-0421.12356.

- Nomura, Y., Kawata, K., Kitamura, Y., and Watanabe, H. (1987). Effects of pertussis toxin on the alpha 2-adrenoceptor-inhibitory GTP-binding protein-adenylate cyclase system in rat brain: pharmacological and neurochemical studies. *Eur J Pharmacol* 134(2), 123-129.
- Novak, J., Cerny, O., Osickova, A., Linhartova, I., Masin, J., Bumba, L., et al. (2017). Structure-Function Relationships Underlying the Capacity of Bordetella Adenylate Cyclase Toxin to Disarm Host Phagocytes. *Toxins (Basel)* 9(10). doi: 10.3390/toxins9100300.
- O'Brien, D.P., Durand, D., Voegelé, A., Hourdel, V., Davi, M., Chamot-Rooke, J., et al. (2017). Calmodulin fishing with a structurally disordered bait triggers CyaA catalysis. *PLoS Biol* 15(12), e2004486. doi: 10.1371/journal.pbio.2004486.
- O'Flanagan, C.H., Campbell, K.R., Zhang, A.W., Kabeer, F., Lim, J.L.P., Biele, J., et al. (2019). Dissociation of solid tumor tissues with cold active protease for single-cell RNA-seq minimizes conserved collagenase-associated stress responses. *Genome Biol* 20(1), 210. doi: 10.1186/s13059-019-1830-0.
- Osicka, R., Osickova, A., Hasan, S., Bumba, L., Cerny, J., and Sebo, P. (2015). Bordetella adenylate cyclase toxin is a unique ligand of the integrin complement receptor 3. *Elife* 4, e10766. doi: 10.7554/eLife.10766.
- Ovrevik, J., Refsnes, M., Lag, M., Holme, J.A., and Schwarze, P.E. (2015). Activation of Proinflammatory Responses in Cells of the Airway Mucosa by Particulate Matter: Oxidant- and Non-Oxidant-Mediated Triggering Mechanisms. *Biomolecules* 5(3), 1399-1440. doi: 10.3390/biom5031399.
- Paddock, C.D., Sanden, G.N., Cherry, J.D., Gal, A.A., Langston, C., Tatti, K.M., et al. (2008). Pathology and pathogenesis of fatal Bordetella pertussis infection in infants. *Clin Infect Dis* 47(3), 328-338. doi: 10.1086/589753.
- Paik, D., Monahan, A., Caffrey, D.R., Elling, R., Goldman, W.E., and Silverman, N. (2017). SLC46 Family Transporters Facilitate Cytosolic Innate Immune Recognition of Monomeric Peptidoglycans. *J Immunol* 199(1), 263-270. doi: 10.4049/jimmunol.1600409.
- Pandit, R.A., Meetum, K., Suvarnapunya, K., Katzenmeier, G., Chaicumpa, W., and Angsuthanasombat, C. (2015). Isolated CyaA-RTX subdomain from Bordetella pertussis: Structural and functional implications for its interaction with target erythrocyte membranes. *Biochem Biophys Res Commun* 466(1), 76-81. doi: 10.1016/j.bbrc.2015.08.110.
- Park, B.S., and Lee, J.O. (2013). Recognition of lipopolysaccharide pattern by TLR4 complexes. *Exp Mol Med* 45, e66. doi: 10.1038/emm.2013.97.
- Park, H.S., Jung, K.S., Hwang, S.C., Nahm, D.H., and Yim, H.E. (1998). Neutrophil infiltration and release of IL-8 in airway mucosa from subjects with grain dust-induced occupational asthma. *Clin Exp Allergy* 28(6), 724-730. doi: 10.1046/j.1365-2222.1998.00299.x.
- Park, J.T. (1993). Turnover and recycling of the murein sacculus in oligopeptide permease-negative strains of Escherichia coli: indirect evidence for an alternative permease system and for a monolayered sacculus. *J Bacteriol* 175(1), 7-11. doi: 10.1128/jb.175.1.7-11.1993.

- Petecchia, L., Sabatini, F., Usai, C., Caci, E., Varesio, L., and Rossi, G.A. (2012). Cytokines induce tight junction disassembly in airway cells via an EGFR-dependent MAPK/ERK1/2-pathway. *Lab Invest* 92(8), 1140-1148. doi: 10.1038/labinvest.2012.67.
- Petridou, E., Jensen, C.B., Arvanitidis, A., Giannaki-Psinaki, M., Michos, A., Krogfelt, K.A., et al. (2018). Molecular epidemiology of *Bordetella pertussis* in Greece, 2010-2015. *J Med Microbiol* 67(3), 400-407. doi: 10.1099/jmm.0.000688.
- Pezzulo, A.A., Starner, T.D., Scheetz, T.E., Traver, G.L., Tilley, A.E., Harvey, B.G., et al. (2011). The air-liquid interface and use of primary cell cultures are important to recapitulate the transcriptional profile of in vivo airway epithelia. *Am J Physiol Lung Cell Mol Physiol* 300(1), L25-31. doi: 10.1152/ajplung.00256.2010.
- Pham, N.T.H., Le, N.D.T., Le, N.K., Nguyen, K.D., Larsson, M., Olson, L., et al. (2020). Pertussis epidemiology and effect of vaccination among diagnosed children at Vietnam, 2015-2018. *Acta Paediatr.* doi: 10.1111/apa.15259.
- Picher, M., Burch, L.H., and Boucher, R.C. (2004). Metabolism of P2 receptor agonists in human airways: implications for mucociliary clearance and cystic fibrosis. *J Biol Chem* 279(19), 20234-20241. doi: 10.1074/jbc.M400305200.
- Pierce, C., Klein, N., and Peters, M. (2000). Is leukocytosis a predictor of mortality in severe pertussis infection? *Intensive Care Med* 26(10), 1512-1514. doi: 10.1007/s001340000587.
- Pittman, M. (1991). History of the development of pertussis vaccine. *Dev Biol Stand* 73, 13-29.
- Pittman, M., Furman, B.L., and Wardlaw, A.C. (1980). *Bordetella pertussis* respiratory tract infection in the mouse: pathophysiological responses. *J Infect Dis* 142(1), 56-66. doi: 10.1093/infdis/142.1.56.
- Pojanapotha, P., Thamwiriyasati, N., Powthongchin, B., Katzenmeier, G., and Angsuthanasombat, C. (2011). *Bordetella pertussis* CyaA-RTX subdomain requires calcium ions for structural stability against proteolytic degradation. *Protein Expr Purif* 75(2), 127-132. doi: 10.1016/j.pep.2010.07.012.
- Polak, M., and Lutynska, A. (2017). The importance of *Bordetella pertussis* strains which do not produce virulence factors in the epidemiology of pertussis. *Postepy Hig Med Dosw (Online)* 71(0), 367-379. doi: 10.5604/01.3001.0010.3821.
- Potter, S.S. (2018). Single-cell RNA sequencing for the study of development, physiology and disease. *Nat Rev Nephrol* 14(8), 479-492. doi: 10.1038/s41581-018-0021-7.
- Qiu, H.N., Wong, C.K., Chu, I.M., Hu, S., and Lam, C.W. (2013). Muramyl dipeptide mediated activation of human bronchial epithelial cells interacting with basophils: a novel mechanism of airway inflammation. *Clin Exp Immunol* 172(1), 81-94. doi: 10.1111/cei.12031.

- Raeven, R.H.M., van der Maas, L., Pennings, J.L.A., Fuursted, K., Jorgensen, C.S., van Riet, E., et al. (2019). Antibody Specificity Following a Recent *Bordetella pertussis* Infection in Adolescence Is Correlated With the Pertussis Vaccine Received in Childhood. *Front Immunol* 10, 1364. doi: 10.3389/fimmu.2019.01364.
- Ramirez, R.D., Sheridan, S., Girard, L., Sato, M., Kim, Y., Pollack, J., et al. (2004). immortalization of human bronchial epithelial cells in the absence of viral oncoproteins. *Cancer Res* 64(24), 9027-9034. doi: 10.1158/0008-5472.CAN-04-3703.
- Randell, T., Yli-Hankala, A., Valli, H., and Lindgren, L. (1992). Topical anaesthesia of the nasal mucosa for fibreoptic airway endoscopy. *Br J Anaesth* 68(2), 164-167. doi: 10.1093/bja/68.2.164.
- Rawlins, E.L., and Hogan, B.L. (2008). Ciliated epithelial cell lifespan in the mouse trachea and lung. *Am J Physiol Lung Cell Mol Physiol* 295(1), L231-234. doi: 10.1152/ajplung.90209.2008.
- Reddel, R.R., Ke, Y., Gerwin, B.I., McMenamin, M.G., Lechner, J.F., Su, R.T., et al. (1988). Transformation of human bronchial epithelial cells by infection with SV40 or adenovirus-12 SV40 hybrid virus, or transfection via strontium phosphate coprecipitation with a plasmid containing SV40 early region genes. *Cancer Res* 48(7), 1904-1909.
- Relman, D., Tuomanen, E., Falkow, S., Golenbock, D.T., Saukkonen, K., and Wright, S.D. (1990). Recognition of a bacterial adhesion by an integrin: macrophage CR3 (alpha M beta 2, CD11b/CD18) binds filamentous hemagglutinin of *Bordetella pertussis*. *Cell* 61(7), 1375-1382. doi: 10.1016/0092-8674(90)90701-f.
- Rhee, C.S., Hong, S.K., Min, Y.G., Lee, C.H., Lee, K.S., Ahn, S.H., et al. (1999). Effects of IL-1 beta, TNF-alpha, and TGF-beta on ciliary beat frequency of human nasal ciliated epithelial cells in vitro. *Am J Rhinol* 13(1), 27-30. doi: 10.2500/105065899781389920.
- Rohani, P., Zhong, X., and King, A.A. (2010). Contact network structure explains the changing epidemiology of pertussis. *Science* 330(6006), 982-985. doi: 10.1126/science.1194134.
- Rosenthal, R.S., Nogami, W., Cookson, B.T., Goldman, W.E., and Folkening, W.J. (1987). Major fragment of soluble peptidoglycan released from growing *Bordetella pertussis* is tracheal cytotoxin. *Infect Immun* 55(9), 2117-2120. doi: 10.1128/IAI.55.9.2117-2120.1987.
- Ross, P.J., Lavelle, E.C., Mills, K.H., and Boyd, A.P. (2004). Adenylate cyclase toxin from *Bordetella pertussis* synergizes with lipopolysaccharide to promote innate interleukin-10 production and enhances the induction of Th2 and regulatory T cells. *Infect Immun* 72(3), 1568-1579.
- Roy, C.R., and Falkow, S. (1991). Identification of *Bordetella pertussis* regulatory sequences required for transcriptional activation of the *fhaB* gene and autoregulation of the *bvgAS* operon. *J Bacteriol* 173(7), 2385-2392. doi: 10.1128/jb.173.7.2385-2392.1991.

- Roy, C.R., Miller, J.F., and Falkow, S. (1990). Autogenous regulation of the *Bordetella pertussis* bvgABC operon. *Proc Natl Acad Sci U S A* 87(10), 3763-3767. doi: 10.1073/pnas.87.10.3763.
- Rutland, J., Griffin, W.M., and Cole, P.J. (1982). Human ciliary beat frequency in epithelium from intrathoracic and extrathoracic airways. *Am Rev Respir Dis* 125(1), 100-105. doi: 10.1164/arrd.1982.125.1.100.
- Sanderson, M.J., and Dirksen, E.R. (1995). Quantification of ciliary beat frequency and metachrony by high-speed digital video. *Methods Cell Biol* 47, 289-297. doi: 10.1016/s0091-679x(08)60822-5.
- Sato, H. (1996). [Virulence factors of *Bordetella pertussis*]. *Nihon Saikingaku Zasshi* 51(3), 737-744. doi: 10.3412/jsb.51.737.
- Sato, T. (1980). Effect of nasal mucosa irritation on airway resistance. *Auris Nasus Larynx* 7(1), 39-50. doi: 10.1016/s0385-8146(80)80012-5.
- Scarlato, V., Arico, B., Prugnola, A., and Rappuoli, R. (1991). Sequential activation and environmental regulation of virulence genes in *Bordetella pertussis*. *EMBO J* 10(12), 3971-3975.
- Scheller, E.V., Melvin, J.A., Sheets, A.J., and Cotter, P.A. (2015). Cooperative roles for fimbria and filamentous hemagglutinin in *Bordetella* adherence and immune modulation. *mBio* 6(3), e00500-00515. doi: 10.1128/mBio.00500-15.
- Schipper, H., Krohne, G.F., and Gross, R. (1994). Epithelial cell invasion and survival of *Bordetella bronchiseptica*. *Infect Immun* 62(7), 3008-3011. doi: 10.1128/IAI.62.7.3008-3011.1994.
- Schneider, B., and Gross, R. (2001). *Bordetella pertussis*: increasing problems with a well-known pathogen and its relatives. *Contrib Microbiol* 8, 123-136. doi: 10.1159/000060407.
- Schweinlin, M., Rossi, A., Lodes, N., Lotz, C., Hackenberg, S., Steinke, M., et al. (2017). Human barrier models for the in vitro assessment of drug delivery. *Drug Deliv Transl Res* 7(2), 217-227. doi: 10.1007/s13346-016-0316-9.
- Schweinlin, M., Wilhelm, S., Schwedhelm, I., Hansmann, J., Rietscher, R., Jurowich, C., et al. (2016). Development of an Advanced Primary Human In Vitro Model of the Small Intestine. *Tissue Eng Part C Methods* 22(9), 873-883. doi: 10.1089/ten.TEC.2016.0101.
- Sedaghat, M.H., Shahmardan, M.M., Norouzi, M., and Heydari, M. (2016). Effect of Cilia Beat Frequency on Muco-ciliary Clearance. *J Biomed Phys Eng* 6(4), 265-278.
- Shi, L., and Ronfard, V. (2013). Biochemical and biomechanical characterization of porcine small intestinal submucosa (SIS): a mini review. *Int J Burns Trauma* 3(4), 173-179.
- Shibutani, M., Uneyama, C., Miyazaki, K., Toyoda, K., and Hirose, M. (2000). Methacarn fixation: a novel tool for analysis of gene expressions in paraffin-embedded tissue specimens. *Lab Invest* 80(2), 199-208. doi: 10.1038/labinvest.3780023.
- Skerry, C., Goldman, W.E., and Carbonetti, N.H. (2019). Peptidoglycan Recognition Protein 4 Suppresses Early Inflammatory Responses to

- Bordetella pertussis* and Contributes to Sphingosine-1-Phosphate Receptor Agonist-Mediated Disease Attenuation. *Infect Immun* 87(2). doi: 10.1128/IAI.00601-18.
- Smith, A.M., Guzman, C.A., and Walker, M.J. (2001). The virulence factors of *Bordetella pertussis*: a matter of control. *FEMS Microbiol Rev* 25(3), 309-333. doi: 10.1111/j.1574-6976.2001.tb00580.x.
- Smith, S.K., and Limbird, L.E. (1982). Evidence that human platelet alpha-adrenergic receptors coupled to inhibition of adenylate cyclase are not associated with the subunit of adenylate cyclase ADP-ribosylated by cholera toxin. *J Biol Chem* 257(17), 10471-10478.
- Soane, M.C., Jackson, A., Maskell, D., Allen, A., Keig, P., Dewar, A., et al. (2000). Interaction of *Bordetella pertussis* with human respiratory mucosa in vitro. *Respir Med* 94(8), 791-799. doi: 10.1053/rmed.2000.0823.
- Solans, L., Debie, A.S., Borkner, L., Aguilo, N., Thiriard, A., Coutte, L., et al. (2018). IL-17-dependent SIgA-mediated protection against nasal *Bordetella pertussis* infection by live attenuated BPZE1 vaccine. *Mucosal Immunol* 11(6), 1753-1762. doi: 10.1038/s41385-018-0073-9.
- Spiliotis, M., Lechner, S., Tappe, D., Scheller, C., Krohne, G., and Brehm, K. (2008). Transient transfection of *Echinococcus multilocularis* primary cells and complete in vitro regeneration of metacystode vesicles. *Int J Parasitol* 38(8-9), 1025-1039. doi: 10.1016/j.ijpara.2007.11.002.
- Spina, D. (1998). Epithelium smooth muscle regulation and interactions. *Am J Respir Crit Care Med* 158(5 Pt 3), S141-145. doi: 10.1164/ajrccm.158.supplement_2.13tac100a.
- Srinivasan, B., Kolli, A.R., Esch, M.B., Abaci, H.E., Shuler, M.L., and Hickman, J.J. (2015). TEER measurement techniques for in vitro barrier model systems. *J Lab Autom* 20(2), 107-126. doi: 10.1177/2211068214561025.
- Stadnyk, A.W. (1994). Cytokine production by epithelial cells. *FASEB J* 8(13), 1041-1047. doi: 10.1096/fasebj.8.13.7926369.
- Steed, L.L., Setareh, M., and Friedman, R.L. (1991). Intracellular survival of virulent *Bordetella pertussis* in human polymorphonuclear leukocytes. *J Leukoc Biol* 50(4), 321-330. doi: 10.1002/jlb.50.4.321.
- Stegle, O., Teichmann, S.A., and Marioni, J.C. (2015). Computational and analytical challenges in single-cell transcriptomics. *Nat Rev Genet* 16(3), 133-145. doi: 10.1038/nrg3833.
- Steinke, M., Gross, R., Walles, H., Gangnus, R., Schutze, K., and Walles, T. (2014). An engineered 3D human airway mucosa model based on an SIS scaffold. *Biomaterials* 35(26), 7355-7362. doi: 10.1016/j.biomaterials.2014.05.031.
- Stenson, T.H., Allen, A.G., Al-Meer, J.A., Maskell, D., and Pepler, M.S. (2005). *Bordetella pertussis* *risA*, but not *risS*, is required for maximal expression of Bvg-repressed genes. *Infect Immun* 73(9), 5995-6004. doi: 10.1128/IAI.73.9.5995-6004.2005.

- Stibitz, S. (1994). Mutations in the *bvgA* gene of *Bordetella pertussis* that differentially affect regulation of virulence determinants. *J Bacteriol* 176(18), 5615-5621. doi: 10.1128/jb.176.18.5615-5621.1994.
- Stockbauer, K.E., Fuchslocher, B., Miller, J.F., and Cotter, P.A. (2001). Identification and characterization of BipA, a *Bordetella Bvg*-intermediate phase protein. *Mol Microbiol* 39(1), 65-78. doi: 10.1046/j.1365-2958.2001.02191.x.
- Strober, W., Murray, P.J., Kitani, A., and Watanabe, T. (2006). Signalling pathways and molecular interactions of NOD1 and NOD2. *Nat Rev Immunol* 6(1), 9-20. doi: 10.1038/nri1747.
- Subrini, O., Sotomayor-Perez, A.C., Hessel, A., Spiczka-Karst, J., Selwa, E., Sapay, N., et al. (2013). Characterization of a membrane-active peptide from the *Bordetella pertussis* CyaA toxin. *J Biol Chem* 288(45), 32585-32598. doi: 10.1074/jbc.M113.508838.
- Tadokoro, T., Wang, Y., Barak, L.S., Bai, Y., Randell, S.H., and Hogan, B.L. (2014). IL-6/STAT3 promotes regeneration of airway ciliated cells from basal stem cells. *Proc Natl Acad Sci U S A* 111(35), E3641-3649. doi: 10.1073/pnas.1409781111.
- Tamura, M., Nogimori, K., Murai, S., Yajima, M., Ito, K., Katada, T., et al. (1982). Subunit structure of islet-activating protein, pertussis toxin, in conformity with the A-B model. *Biochemistry* 21(22), 5516-5522. doi: 10.1021/bi00265a021.
- Teran, L.M., Johnston, S.L., Schroder, J.M., Church, M.K., and Holgate, S.T. (1997). Role of nasal interleukin-8 in neutrophil recruitment and activation in children with virus-induced asthma. *Am J Respir Crit Care Med* 155(4), 1362-1366. doi: 10.1164/ajrccm.155.4.9105080.
- Teruya, S., Hiramatsu, Y., Nakamura, K., Fukui-Miyazaki, A., Tsukamoto, K., Shinoda, N., et al. (2020). *Bordetella* Dermonecrotic Toxin Is a Neurotropic Virulence Factor That Uses CaV3.1 as the Cell Surface Receptor. *mBio* 11(2). doi: 10.1128/mBio.03146-19.
- Tomita, M., Sato, E.F., Nishikawa, M., Yamano, Y., and Inoue, M. (2001). Nitric oxide regulates mitochondrial respiration and functions of articular chondrocytes. *Arthritis Rheum* 44(1), 96-104. doi: 10.1002/1529-0131(200101)44:1<96::AID-ANR13>3.0.CO;2-#.
- Tuomanen, E.I., and Hendley, J.O. (1983). Adherence of *Bordetella pertussis* to human respiratory epithelial cells. *J Infect Dis* 148(1), 125-130. doi: 10.1093/infdis/148.1.125.
- Turner, M., Chantry, D., Buchan, G., Barrett, K., and Feldmann, M. (1989). Regulation of expression of human IL-1 alpha and IL-1 beta genes. *J Immunol* 143(11), 3556-3561.
- Uhl, M.A., and Miller, J.F. (1994). Autophosphorylation and phosphotransfer in the *Bordetella pertussis* BvgAS signal transduction cascade. *Proc Natl Acad Sci U S A* 91(3), 1163-1167. doi: 10.1073/pnas.91.3.1163.
- Uhl, M.A., and Miller, J.F. (1995). BvgAS is sufficient for activation of the *Bordetella pertussis* ptx locus in *Escherichia coli*. *J Bacteriol* 177(22), 6477-6485. doi: 10.1128/jb.177.22.6477-6485.1995.

- Uhl, M.A., and Miller, J.F. (1996a). Central role of the BvgS receiver as a phosphorylated intermediate in a complex two-component phosphorelay. *J Biol Chem* 271(52), 33176-33180. doi: 10.1074/jbc.271.52.33176.
- Uhl, M.A., and Miller, J.F. (1996b). Integration of multiple domains in a two-component sensor protein: the *Bordetella pertussis* BvgAS phosphorelay. *EMBO J* 15(5), 1028-1036.
- Ui, M., Katada, T., Murayama, T., Kurose, H., Yajima, M., Tamura, M., et al. (1984). Islet-activating protein, pertussis toxin: a specific uncoupler of receptor-mediated inhibition of adenylate cyclase. *Adv Cyclic Nucleotide Protein Phosphorylation Res* 17, 145-151.
- van den Akker, W.M. (1997). *Bordetella bronchiseptica* has a BvgAS-controlled cytotoxic effect upon interaction with epithelial cells. *FEMS Microbiol Lett* 156(2), 239-244. doi: 10.1111/j.1574-6968.1997.tb12734.x.
- van den Berg, B.M., Beekhuizen, H., Willems, R.J., Mooi, F.R., and van Furth, R. (1999). Role of *Bordetella pertussis* virulence factors in adherence to epithelial cell lines derived from the human respiratory tract. *Infect Immun* 67(3), 1056-1062. doi: 10.1128/IAI.67.3.1056-1062.1999.
- van Heel, D.A., Ghosh, S., Hunt, K.A., Mathew, C.G., Forbes, A., Jewell, D.P., et al. (2005). Synergy between TLR9 and NOD2 innate immune responses is lost in genetic Crohn's disease. *Gut* 54(11), 1553-1557. doi: 10.1136/gut.2005.065888.
- Van Savage, J., Decker, M.D., Edwards, K.M., Sell, S.H., and Karzon, D.T. (1990). Natural history of pertussis antibody in the infant and effect on vaccine response. *J Infect Dis* 161(3), 487-492. doi: 10.1093/infdis/161.3.487.
- Vaughan, M.B., Ramirez, R.D., Wright, W.E., Minna, J.D., and Shay, J.W. (2006). A three-dimensional model of differentiation of immortalized human bronchial epithelial cells. *Differentiation* 74(4), 141-148. doi: 10.1111/j.1432-0436.2006.00069.x.
- Veal-Carr, W.L., and Stibitz, S. (2005). Demonstration of differential virulence gene promoter activation in vivo in *Bordetella pertussis* using RIVET. *Mol Microbiol* 55(3), 788-798. doi: 10.1111/j.1365-2958.2004.04418.x.
- Veale, D., Rodgers, A.D., Griffiths, C.J., Ashcroft, T., and Gibson, G.J. (1993). Variability in ciliary beat frequency in normal subjects and in patients with bronchiectasis. *Thorax* 48(10), 1018-1020. doi: 10.1136/thx.48.10.1018.
- Verma, A., and Burns, D.L. (2007). Requirements for assembly of PtlH with the pertussis toxin transporter apparatus of *Bordetella pertussis*. *Infect Immun* 75(5), 2297-2306. doi: 10.1128/IAI.00008-07.
- Verma, A., Cheung, A.M., and Burns, D.L. (2008). Stabilization of the pertussis toxin secretion apparatus by the C terminus of PtlD. *J Bacteriol* 190(21), 7285-7290. doi: 10.1128/JB.01106-08.
- Villarino Romero, R., Hasan, S., Fae, K., Holubova, J., Geurtsen, J., Schwarzer, M., et al. (2016). *Bordetella pertussis* filamentous hemagglutinin itself does not trigger anti-inflammatory interleukin-10 production by human dendritic cells. *Int J Med Microbiol* 306(1), 38-47. doi: 10.1016/j.ijmm.2015.11.003.

- Vllasaliu, D., Fowler, R., Garnett, M., Eaton, M., and Stolnik, S. (2011). Barrier characteristics of epithelial cultures modelling the airway and intestinal mucosa: a comparison. *Biochem Biophys Res Commun* 415(4), 579-585. doi: 10.1016/j.bbrc.2011.10.108.
- Voegele, A., O'Brien, D.P., Subrini, O., Sapay, N., Cannella, S.E., Enguene, V.Y.N., et al. (2018). Translocation and calmodulin-activation of the adenylate cyclase toxin (CyaA) of *Bordetella pertussis*. *Pathog Dis* 76(8). doi: 10.1093/femspd/fty085.
- Vysoka, B. (1958). The epidemiology of pertussis and parapertussis. *J Hyg Epidemiol Microbiol Immunol* 2(2), 196-204.
- Wagner, B., Melzer, H., Freymuller, G., Stumvoll, S., Rendi-Wagner, P., Paulke-Korinek, M., et al. (2015). Genetic Variation of *Bordetella pertussis* in Austria. *PLoS One* 10(7), e0132623. doi: 10.1371/journal.pone.0132623.
- Wang, F., Su, Z., and Wang, L. (2000). [Effects of nitric oxide on ciliary beat frequency in the human nasal mucosa]. *Zhonghua Er Bi Yan Hou Ke Za Zhi* 35(6), 432-434.
- Wanner, A., Salathe, M., and O'Riordan, T.G. (1996). Mucociliary clearance in the airways. *Am J Respir Crit Care Med* 154(6 Pt 1), 1868-1902. doi: 10.1164/ajrccm.154.6.8970383.
- Warfel, J.M., Beren, J., and Merkel, T.J. (2012). Airborne transmission of *Bordetella pertussis*. *J Infect Dis* 206(6), 902-906. doi: 10.1093/infdis/jis443.
- Warfel, J.M., Zimmerman, L.I., and Merkel, T.J. (2014). Acellular pertussis vaccines protect against disease but fail to prevent infection and transmission in a nonhuman primate model. *Proc Natl Acad Sci U S A* 111(2), 787-792. doi: 10.1073/pnas.1314688110.
- Watanabe, M., Takimoto, H., Kumazawa, Y., and Amano, K. (1990). Biological properties of lipopolysaccharides from *Bordetella* species. *J Gen Microbiol* 136(3), 489-493. doi: 10.1099/00221287-136-3-489.
- Watkins, D.N., Peroni, D.J., Basclain, K.A., Garlepp, M.J., and Thompson, P.J. (1997). Expression and activity of nitric oxide synthases in human airway epithelium. *Am J Respir Cell Mol Biol* 16(6), 629-639. doi: 10.1165/ajrcmb.16.6.9191464.
- Weingart, C.L., and Weiss, A.A. (2000). *Bordetella pertussis* virulence factors affect phagocytosis by human neutrophils. *Infect Immun* 68(3), 1735-1739. doi: 10.1128/iai.68.3.1735-1739.2000.
- Weiss, A.A., and Falkow, S. (1984). Genetic analysis of phase change in *Bordetella pertussis*. *Infect Immun* 43(1), 263-269. doi: 10.1128/IAI.43.1.263-269.1984.
- Weiss, A.A., and Hewlett, E.L. (1986). Virulence factors of *Bordetella pertussis*. *Annu Rev Microbiol* 40, 661-686. doi: 10.1146/annurev.mi.40.100186.003305.
- Weiss, A.A., Hewlett, E.L., Myers, G.A., and Falkow, S. (1984). Pertussis toxin and extracytoplasmic adenylate cyclase as virulence factors of *Bordetella pertussis*. *J Infect Dis* 150(2), 219-222.

- Werman, A., Werman-Venkert, R., White, R., Lee, J.K., Werman, B., Krelin, Y., et al. (2004). The precursor form of IL-1alpha is an intracrine proinflammatory activator of transcription. *Proc Natl Acad Sci U S A* 101(8), 2434-2439. doi: 10.1073/pnas.0308705101.
- Weston, R. (2012). Whooping Cough: A Brief History to the 19th Century. *Can Bull Med Hist* 29(2), 329-349. doi: 10.3138/cbmh.29.2.329.
- White, S.R., Fischer, B.M., Marroquin, B.A., and Stern, R. (2008). Interleukin-1beta mediates human airway epithelial cell migration via NF-kappaB. *Am J Physiol Lung Cell Mol Physiol* 295(6), L1018-1027. doi: 10.1152/ajplung.00065.2008.
- Wiese, K.M., Coates, B.M., and Ridge, K.M. (2017). The Role of Nucleotide-Binding Oligomerization Domain-Like Receptors in Pulmonary Infection. *Am J Respir Cell Mol Biol* 57(2), 151-161. doi: 10.1165/rcmb.2016-0375TR.
- Willems, R., Paul, A., van der Heide, H.G., ter Avest, A.R., and Mooi, F.R. (1990). Fimbrial phase variation in *Bordetella pertussis*: a novel mechanism for transcriptional regulation. *EMBO J* 9(9), 2803-2809.
- Wilson, R., Read, R., Thomas, M., Rutman, A., Harrison, K., Lund, V., et al. (1991). Effects of *Bordetella pertussis* infection on human respiratory epithelium in vivo and in vitro. *Infect Immun* 59(1), 337-345. doi: 10.1128/IAI.59.1.337-345.1991.
- Winsnes, R., Lonnes, T., Mogster, B., and Berdal, B.P. (1985). Antibody responses after vaccination and disease against leukocytosis promoting factor, filamentous hemagglutinin, lipopolysaccharide and a protein binding to complement-fixing antibodies induced during whooping cough. *Dev Biol Stand* 61, 353-365.
- Yahalom, A., Davidov, G., Kolusheva, S., Shaked, H., Barber-Zucker, S., Zarivach, R., et al. (2019). Structure and membrane-targeting of a *Bordetella pertussis* effector N-terminal domain. *Biochim Biophys Acta Biomembr* 1861(12), 183054. doi: 10.1016/j.bbmem.2019.183054.
- Yamaoka, J., Kabashima, K., Kawanishi, M., Toda, K., and Miyachi, Y. (2002). Cytotoxicity of IFN-gamma and TNF-alpha for vascular endothelial cell is mediated by nitric oxide. *Biochem Biophys Res Commun* 291(4), 780-786. doi: 10.1006/bbrc.2002.6487.
- Yeh, S.H., and Mink, C.M. (2006). Shift in the epidemiology of pertussis infection: an indication for pertussis vaccine boosters for adults? *Drugs* 66(6), 731-741. doi: 10.2165/00003495-200666060-00001.
- Yeung, K.H.T., Duclos, P., Nelson, E.A.S., and Hutubessy, R.C.W. (2017). An update of the global burden of pertussis in children younger than 5 years: a modelling study. *Lancet Infect Dis* 17(9), 974-980. doi: 10.1016/S1473-3099(17)30390-0.
- Yonker, L.M., Mou, H., Chu, K.K., Pazos, M.A., Leung, H., Cui, D., et al. (2017). Development of a Primary Human Co-Culture Model of Inflamed Airway Mucosa. *Sci Rep* 7(1), 8182. doi: 10.1038/s41598-017-08567-w.
- Yoo, J.W., Kim, Y.S., Lee, S.H., Lee, M.K., Roh, H.J., Jhun, B.H., et al. (2003). Serially passaged human nasal epithelial cell monolayer for in vitro drug

- transport studies. *Pharm Res* 20(10), 1690-1696. doi: 10.1023/a:1026112107100.
- Yoon, B.N., Choi, N.G., Lee, H.S., Cho, K.S., and Roh, H.J. (2010). Induction of interleukin-8 from nasal epithelial cells during bacterial infection: the role of IL-8 for neutrophil recruitment in chronic rhinosinusitis. *Mediators Inflamm* 2010, 813610. doi: 10.1155/2010/813610.
- Yuk, M.H., Cotter, P.A., and Miller, J.F. (1996). Genetic regulation of airway colonization by *Bordetella* species. *Am J Respir Crit Care Med* 154(4 Pt 2), S150-154. doi: 10.1164/ajrccm/154.4_Pt_2.S150.
- Zacharia, I.G., and Deen, W.M. (2005). Diffusivity and solubility of nitric oxide in water and saline. *Ann Biomed Eng* 33(2), 214-222. doi: 10.1007/s10439-005-8980-9.
- Zaretsky, F.R., Gray, M.C., and Hewlett, E.L. (2002). Mechanism of association of adenylate cyclase toxin with the surface of *Bordetella pertussis*: a role for toxin-filamentous haemagglutinin interaction. *Mol Microbiol* 45(6), 1589-1598.
- Zech, J.C., Pouvreau, I., Cotinet, A., Goureau, O., Le Varlet, B., and de Kozak, Y. (1998). Effect of cytokines and nitric oxide on tight junctions in cultured rat retinal pigment epithelium. *Invest Ophthalmol Vis Sci* 39(9), 1600-1608.
- Zhang, J.S., Wang, H.M., Yao, K.H., Liu, Y., Lei, Y.L., Deng, J.K., et al. (2020). Clinical characteristics, molecular epidemiology and antimicrobial susceptibility of pertussis among children in southern China. *World J Pediatr* 16(2), 185-192. doi: 10.1007/s12519-019-00308-5.
- Zhang, N., Van Crombruggen, K., Gevaert, E., and Bachert, C. (2016). Barrier function of the nasal mucosa in health and type-2 biased airway diseases. *Allergy* 71(3), 295-307. doi: 10.1111/all.12809.
- Zhang, W.H. (2009). [Global pertussis epidemiology and immunization strategies]. *Zhongguo Yi Miao He Mian Yi* 15(5), 467-472.
- Zihni, C., Mills, C., Matter, K., and Balda, M.S. (2016). Tight junctions: from simple barriers to multifunctional molecular gates. *Nat Rev Mol Cell Biol* 17(9), 564-580. doi: 10.1038/nrm.2016.80.
- Zimmerman, L.I., Papin, J.F., Warfel, J., Wolf, R.F., Kosanke, S.D., and Merkel, T.J. (2018). Histopathology of *Bordetella pertussis* in the Baboon Model. *Infect Immun* 86(11). doi: 10.1128/IAI.00511-18.
- Zimna, K., Medina, E., Jungnitz, H., and Guzman, C.A. (2001). Role played by the response regulator Ris in *Bordetella bronchiseptica* resistance to macrophage killing. *FEMS Microbiol Lett* 201(2), 177-180. doi: 10.1111/j.1574-6968.2001.tb10753.x.
- Zlamy, M. (2016). Rediscovering Pertussis. *Front Pediatr* 4, 52. doi: 10.3389/fped.2016.00052.

Appendices

Appendix 1: mean concentration of inflammatory cytokine of

	Apical	Basal
	Mean Conc \pm SD (pg/ml)	Mean Conc \pm SD (pg/ml)
IL-1β(n=5)		
Control	7.86 \pm 5.94	11.30 \pm 4.41
TCT	10.32 \pm 7.76	10.10 \pm 5.58
LPS	11.43 \pm 1 0.23	11.26 \pm 5.41
TCT/LPS	5.81 \pm 3.32	16.06 \pm 12.99
IL-6 (n=3)		
Control	3097.53 \pm 2312.51	5649.74 \pm 6505.70
TCT	3306.83 \pm 1929.08	60028.79 \pm 69309.55
LPS	10807.25 \pm 8498.14	32684.65 \pm 47869.68
TCT/LPS	7418.80 \pm 5123.85	63969.40 \pm 62382.40
IL-8 (n=6)		
Control	18730.18 \pm 14789.57	92656.91 \pm 93830.22
TCT	21981.96 \pm 15533.16	144289.31 \pm 96409.01
LPS	46463.72 \pm 32639.59	120568.57 \pm 87677.80
TCT/LPS	42435.49 \pm 12790.09	125748.82 \pm 81826.63
IL-10 (n=6)		
Control	0.54 \pm 0.71	2.75 \pm 3.44
TCT	0.69 \pm 0.80	2.47 \pm 2.65
LPS	0.44 \pm 0.71	4.87 \pm 4.35
TCT/LPS	0.54 \pm 0.73	4.10 \pm 3.62

Appendix 2

Weekly calculated TEER of individual hTBM over 21 days of development

Day	4	11	18	21
A1	15,62	14,905	21,615	18,755
A2	18,81	22,495	21,065	21,725
A3	21,67	26,565	33,055	29,095
A4	25,63	26,895	29,205	21,615
B1	20,57	15,785	21,945	17,655
B2	20,57	19,305	28,215	19,305
B3	27,5	41,635	71,445	90,585
B4	28,16	35,035	44,055	43,505
C1	20,68	14,905	21,395	17,325
C2	20,24	17,875	22,055	17,985
C3	31,35	31,295	39,105	40,095
C4	25,63	32,175	33,715	36,685
A1	16,94	24,585	21,175	25,575
A2	25,08	36,245	65,285	109,175
A3	49,61	59,565	110,935	143,275
A4	62,15	131,065	180,455	138,325
B1	32,89	60,445	97,735	128,865
B2	25,52	38,115	54,615	115,445
B3	27,94	26,125	26,895	42,955
B4	30,03	35,035	45,375	131,615
C1	40,59	71,665	130,405	101,035
C2	33,99	53,185	97,515	145,145
C3	30,03	40,425	37,015	82,005
C4	30,8	39,105	33,825	39,105
A1	18,04	10,89	15,84	18,65
A2	23,65	25,63	26,07	25,58
A3	17,93	28,6	23,32	26,07
A4	21,12	19,69	23,65	28,05
B1	22,88	24,2	26,07	22,61
B2	17,93	12,21	34,32	27,06
B3	23,65	28,27	24,42	56,43
B4	29,15	26,18	29,26	29,7
C1	22,88	25,85	33,44	25,74
C2	6,16	-3,74	4,4	16,5
C3	17,49	23,21	28,71	29,04
Mean	25,80	32,44	44,50	53,78
SD	1,69	3,85	6,26	7,43

Appendix 3

Weekly calculated TEER of individual hNM over 21 days of development

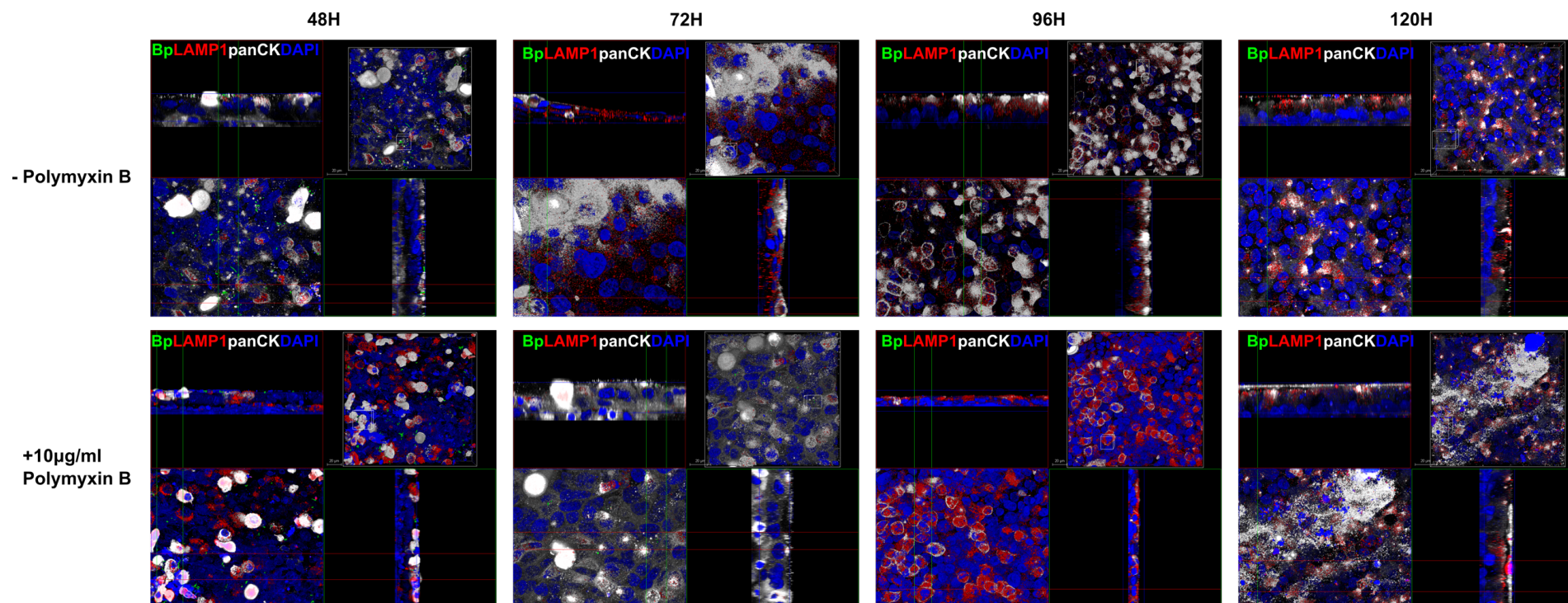
Day	4	11	18	21
A1	31,185	33,935	24,915	24,475
A2	32,065	33,715	23,485	22,935
A3	34,045	30,965	23,265	39,875
A4	32,945	35,475	21,175	28,875
B1	32,285	35,255	25,685	28,215
B2	35,365	41,085	28,655	36,795
B3	30,415	38,225	24,915	32,615
B4	41,415	34,375	32,285	36,245
C1	32,835	38,775	24,915	33,935
C2	32,175	40,205	27,995	32,945
C3	38,445	45,595	28,985	52,415
C4	34,705	37,455	25,575	33,825
A1	21,01	21,34	49,83	128,81
A2	18,37	16,72	23,98	20,57
A3	23,43	21,23	98,89	150,59
A4	15,4	16,5	42,24	48,73
B1	17,93	19,36	145,75	55,33
B2	14,85	17,49	35,42	39,93
B3	16,61	17,16	46,09	123,64
B4	19,25	15,84	35,09	102,85
C1	15,62	20,57	35,86	99,66
C2	16,06	18,26	35,31	117,48
C3	17,16	21,23	58,3	192,94
C4	18,92	15,29	23,76	62,7
Mean	25,9370833	27,7520833	39,2654167	64,4325
SD	1,77361611	2,05087985	5,73776341	9,71012805

Appendix 4

Weekly calculated TEER of individual hBM over 21 days of development

Day	4	11	18	21
A1	21,285	26,565	24,695	29,205
A2	17,765	25,575	28,765	28,985
A3	19,745	22,825	26,235	25,025
A4	19,415	22,605	26,235	38,885
B1	18,755	25,245	25,135	26,455
B2	23,375	27,995	26,125	28,765
B3	18,315	25,575	26,015	25,355
B4	20,625	26,015	25,245	26,675
C1	19,525	28,105	23,705	31,625
C2	21,285	28,545	26,345	28,325
C3	20,075	26,235	28,325	35,035
C4	21,945	28,215	26,675	25,135
A1	21,285	26,675	20,735	28,215
A2	19,635	23,485	18,975	24,365
A3	19,855	25,245	22,055	24,035
A4	19,305	31,185	26,895	29,865
B1	19,965	24,695	18,645	28,985
B2	21,835	27,335	18,535	28,215
B3	20,515	26,675	23,815	29,535
B4	17,875	24,585	22,495	24,915
C1	19,415	29,755	22,055	31,845
C2	19,965	25,795	20,075	27,995
C3	23,155	29,095	26,895	31,295
C4	19,855	29,645	21,505	24,915
A1	21,835	20,405	27,335	26,895
A2	25,465	26,015	27,775	27,885
A3	34,045	20,515	28,655	33,715
A4	25,245	19,635	25,135	25,795
B1	25,465	24,145	41,525	36,245
B2	27,555	19,745	24,475	26,015
B3	31,295	25,685	30,195	32,065
B4	30,965	23,155	28,215	30,965
C1	32,505	20,515	25,245	27,885
C2	34,155	21,725	23,045	27,445
C3	32,725	24,475	33,715	34,925
C4	19,855	13,695	22,825	25,245
Mean	22,9411111	24,9272222	25,3977778	28,8536111
SD	0,82119003	0,58636831	0,72290448	0,60327245

Appendix 5



Intracellular survival of *B. pertussis* in hTBM

Matured hTBMs were inoculated with GFP_ *B. pertussis* at a MOI50 for 24 hours. Extracellular bacteria were killed by culturing the models with 100µg/ml polymyxin B for 2 hours. The hTBM were then washed 2x with DPBS and incubated for 5 days. One set of hTBM were cultured for the 5 days without polymyxin B (upper panel) while the other set were cultured with 10µg/ml polymyxin B (lower panel). The hTBM were fixed with 4%PFA at 4°C overnight 48H, 72H, 96H and 120H after polymyxin B treatment, immunostained with LAMP1(Red) and panCK (white). Z-stack of whole model mounts through 25µm was imaged using TCS SP8 and 3D reconstructed. Viable bacteria were detected up to 72 hours after the initial 100µg/ml polymyxin B treatment in both setups according to cfu counts.

Curriculum Vitae

Kessie, David Komla

Personal Information

Email: davidkessie@icloud.com

Date of Birth: 04.02.1986

Birth

Nationality: Ghanaian

Education

- 06.2016 - **PhD** (Infection and Immunity)
present Julius-Maximilians-University of Wuerzburg, Germany.
- 10.2014 – **MSc** (FOKUS Life Science)
02.2016 Julius-Maximilians University of Wuerzburg, Germany
- 08.2010 – **MPhil** (Human Anatomy and Cell Biology)
06.2014 Kwame Nkrumah University of Science and Technology, Ghana
- 08.2005 – **BSc** (Biological Science)
05.2009 Kwame Nkrumah University of Science and Technology, Ghana

Research/Professional experience

Doctoral Researcher (06.2016 – present)

Chair of Microbiology, Biocentre, University of Wuerzburg

Advisor: Prof. Dr. Roy Gross

Major task: Analysis of the virulence mechanism of *Bordetella pertussis* using engineered 3D human airway mucosa models. Development a method for dissociation of the engineered 3D models for single cell RNA sequencing of infected tissues.

Master Research (07.2015 – 02.2016)

Institute of Anatomy and Cell Biology, University of Wuerzburg

Advisor: Prof. Dr. Frank Edenhofer

Major tasks: Assessment of the role of gap junctional communication through connexin channels in the development of the primitive endoderm using mouse embryonic stem cells.

Intern (03.2016)

Department of Bioinformatics, Biocenter, University of Wuerzburg, Germany
AG Dandekar

Major task: Development and analysis of an in silico gene regulatory networks involved in the differentiation of chondrocytes and osteocytes from stem cells.

Intern, 03.2015

Stem Cell and Regenerative Medicine, Institute of Anatomy, Julius - Maximilians University of Wuerzburg, Germany. AG Edenhofer

Major task: Premature aging induction in induced pluripotent stem cells to model late-onset diseases.

Intern, 01.2015

Developmental Neurobiology, University Clinic of Wuerzburg, Germany. AG Martini

Major task: Characterization of mouse models of juvenile neuronal ceroid lipofuscinosis and multiple sclerosis.

Fellowships/Awards

- | | |
|------|---|
| 2020 | Tutorenpreis, KOMPASS Tutoren and Mentorenprogram, University of Wuerzburg |
| 2016 | Graduate Research College (GRK2157) fellowship at the University of Wuerzburg, Germany. |
| 2014 | MountCrest University College, Ghana. Scholarship to pursue the MSc FOKUS Life Science at the University of Wuerzburg |
| 2009 | Dean's Honour Award, Faculty of Biological Sciences, KNUST, Ghana |
| 2001 | Ghana Commercial Bank, Scholarship for Staff Child in Senior Secondary School, |

Certification

- Rules of good scientific practice, University of Wuerzburg
- R statistical Programming, University of Wuerzburg
- Basic and advanced image processing using FIJI, Biovoxxel, University of Wuerzburg
- Project management, University of Wuerzburg

Skills and expertise

- Standard microbiological practices
- Advanced cell culture methods – primary cells, cell lines, iPSC, static and dynamic 3D cell culture
- Cell based assays including infection protocols, flow cytometry and fluorescence microscopy
- Statistical analysis using R

- Proficient in Advanced Microsoft office

Teaching experience

- Supervision of Master F1 research practical and thesis of Mr. Aby Anand, University of Wuerzburg, Germany (**2019**).
- Co-supervisor of Master thesis of Ms Deborah Ibukun Olufemi, University of Wuerzburg, Germany (**2019**)
- Teaching assistant for Basic microbiology practical course for 1st Semester, Bachelor of Science, University of Wuerzburg, Germany (**2019**)
- Teaching assistant for functional materials, BSc Material Science, University of Wuerzburg, Germany (**2017-2018**)
- Tutor for the MSc FOKUS Life Science program, University of Wuerzburg, Germany (**2015 – 2018**)

Languages:

- English: Native proficiency
- German: Limited working proficiency
- French: Elementary proficiency
- Ewe: Native proficiency
- Ashanti: Native proficiency

Wuerzburg, 18.01.20

Place, Date

Signature

List of publications and presentations

Research article

Activity of tracheal cytotoxin of *Bordetella pertussis* in a human tracheobronchial 3D tissue model

David K Kessie, Nina Lodes, Heike Oberwinkler, William E. Goldman, Thorsten Walles, Maria Steinke and Roy Gross; Front. Cell. Infect. Microbiol. (2020), doi:10.3389/fcimb.2020.614994

Posters

Characterisation of *Bordetella pertussis* virulence mechanisms using engineered human airway tissue models

David K Kessie, Maria Steinke, Roy Gross. Eureka! 12th International GSLS student symposium, University of Wuerzburg, Germany (2017)

Characterisation of *Bordetella pertussis* virulence mechanisms using engineered human airway tissue models

David K Kessie, Maria Steinke and Roy Gross. 3D Cell Culture Conference: How close to in vivo can we get? Models, Applications and translations, Freiburg, Germany (2018)

Characterisation of *Bordetella pertussis* virulence mechanisms with 3D airway models.

David K Kessie, Heike Walles, Maria Steinke, Roy Gross. 12th International conference and workshop on biological barriers, Helmholtz Institute for Pharmaceutical Research, University of Saarland, Saarbruecken, German (2018)

Activity of *Bordetella pertussis* cytotoxin in an engineered human airway model

David K. Kessie, Maria Steinke, Roy Gross. GRK2157:3DInfect: Tissue infection Symposium, University of Wuerzburg, Germany (2019)

Characterisation of *Bordetella pertussis* virulence mechanisms in 3D airway mucosa models

David K. Kessie, Maria Steinke, Roy Gross. 12th International *Bordetella* symposium. University of Brussels, Belgium (2019)

Oral presentation

Characterisation of *Bordetella pertussis* virulence mechanisms with 3D airway models. 12th International conference and workshop on biological barriers, Helmholtz Institute for Pharmaceutical Research, Saarbruecken, German (2018)

Affidavit

I hereby confirm that my thesis entitled Characterisation of the virulence mechanism of *Bordetella pertussis* using an engineered human airway tissue model is the result of my own work. I did not receive any help or support from commercial consults. All sources and/or materials applied are listed and specified in the thesis

Furthermore, I confirm that this thesis has not yet been submitted as part of another examination process neither in identical nor similar form.

Wuerzburg
Place, Date

Signature

Eidesstattliche Erklärung

Hiermit erkläre ich an Eides statt, die Dissertation Charakterisierung der Virulenzmechanismen von *Bordetella pertussis* mit humanen Gewebemodellen der Atemwege eigenständig, d.h. insbesondere selbständig und ohne Hilfe eines kommerziellen Promotionsberaters, angefertigt und keine anderen als die von mir angegebenen Quellen und Hilfsmittel verwendet zu haben.

Ich erkläre außerdem, dass die Dissertation weder in gleicher noch in ähnlicher Form bereits in einem anderen Prüfungsverfahren vorgelegen hat.

Würzburg
Ort, Datum

Unterschrift

Acknowledgements

I would like to first and foremost extend my sincere gratitude to my mentor, Prof. Dr. Roy Gross, for his guidance and advice and also for trusting me enough to allow me to explore as much as possible during the conduct of this thesis. I would also like to thank Dr. Maria Steinke who basically was my second primary supervisor. Thank you for adopting me as your PhD student and making time for both scientific and non-scientific discussions. My gratitude also goes to Prof. Thomas Rudel for the opportunity to work at the Chair of Microbiology.

I would also like to thank Prof. Dr. Thomas Dandekar for being part of my thesis committee and for making time for the discussions and to Prof. Dr. Markus Sauer for accepting to be the chairperson of my thesis. My gratitude also goes to Prof William Goldman for providing the Tracheal cytotoxin and to Prof. Dr. Thorsten Walles and Stephan Hackenberg for their immense contribution with the tissue biopsies. I am gracious to Prof. Dr. Peter Sebo for providing the GFP-Bordetella as well as all the scientific discussions and being a generous host on all the occasions we visited his lab. To Dr. Emmanuel Saliba, Oliver Dietrich and Tobias Krammer, I say thank you for your immense input during the tissue dissociation, FACS and scRNA-seq library preparation and your continuous support. I am also grateful to the Prof. Dr. Christian Stigloher, Claudia Gehring and Daniela Bunsen for helping with the Electron microscopy.

My gratitude also goes to Dr. Kathrin Stelzner and Franziska Solger for all their help running the FACS. I thank Susanne Bauer and Heike Oberwinkler for the great technical support and for helping out with my German. My profound appreciation also goes to my family especially to my Mom, Peace Dakla and Dad, the late SS. Kwame Kessie who have shaped my life and pushed me to be a better human. The load was lighter, and the journey was easy during my stay in Wuerzburg because of all the friends; Sanjana, Michaela, Xidi, Jonathan, Ana-Rita, Claudia, Jhi, Tobi, Rinu, Tom, Nadine, Max, Suleman, Tobias, who became my family.

Lastly, I would like to thank all past and present members of the Chair of Tissue Engineering for adopting me as one of their very own and members of the Chair of Microbiology for providing a conducive and friendly work atmosphere. I would like to especially thank Frau Simone Haninger, Elbert Oezlem and Ana Stefl for the amazing support regarding forms and documentation.